

Springer Protocols

Terry J. McGenity  
Kenneth N. Timmis  
Balbina Nogales *Editors*

# Hydrocarbon and Lipid Microbiology Protocols

Bioproducts, Biofuels, Biocatalysts  
and Facilitating Tools

 Springer

# Springer Protocols Handbooks

More information about this series at <http://www.springer.com/series/8623>

Terry J. McGenity · Kenneth N. Timmis · Balbina Nogales  
Editors

# Hydrocarbon and Lipid Microbiology Protocols

Bioproducts, Biofuels, Biocatalysts  
and Facilitating Tools

## **Scientific Advisory Board**

Jack Gilbert, Ian Head, Mandy Joye, Victor de Lorenzo,  
Jan Roelof van der Meer, Colin Murrell, Josh Neufeld,  
Roger Prince, Juan Luis Ramos, Wilfred Röling,  
Heinz Wilkes, Michail Yakimov

*Editors*

Terry J. McGenity  
School of Biological Sciences  
University of Essex  
Colchester, Essex, UK

Kenneth N. Timmis  
Institute of Microbiology  
Technical University Braunschweig  
Braunschweig, Germany

Balbina Nogales  
Department of Biology  
University of the Balearic Islands  
and Mediterranean Institute  
for Advanced Studies  
(IMEDEA, UIB-CSIC)  
Palma de Mallorca, Spain

ISSN 1949-2448

Springer Protocols Handbooks

ISBN 978-3-662-53113-6

DOI 10.1007/978-3-662-53115-0

ISSN 1949-2456 (electronic)

ISBN 978-3-662-53115-0 (eBook)

Library of Congress Control Number: 2016938230

© Springer-Verlag Berlin Heidelberg 2017

This work is subject to copyright. All rights are reserved by the Publisher, whether the whole or part of the material is concerned, specifically the rights of translation, reprinting, reuse of illustrations, recitation, broadcasting, reproduction on microfilms or in any other physical way, and transmission or information storage and retrieval, electronic adaptation, computer software, or by similar or dissimilar methodology now known or hereafter developed.

The use of general descriptive names, registered names, trademarks, service marks, etc. in this publication does not imply, even in the absence of a specific statement, that such names are exempt from the relevant protective laws and regulations and therefore free for general use.

The publisher, the authors and the editors are safe to assume that the advice and information in this book are believed to be true and accurate at the date of publication. Neither the publisher nor the authors or the editors give a warranty, express or implied, with respect to the material contained herein or for any errors or omissions that may have been made.

Printed on acid-free paper

This Springer imprint is published by Springer Nature  
The registered company is Springer-Verlag GmbH Berlin Heidelberg

# Preface to Hydrocarbon and Lipid Microbiology Protocols<sup>1</sup>

All active cellular systems require water as the principal medium and solvent for their metabolic and ecophysiological activities. Hydrophobic compounds and structures, which tend to exclude water, although providing *inter alia* excellent sources of energy and a means of biological compartmentalization, present problems of cellular handling, poor bioavailability and, in some cases, toxicity. Microbes both synthesize and exploit a vast range of hydrophobic organics, which includes biogenic lipids, oils and volatile compounds, geochemically transformed organics of biological origin (i.e. petroleum and other fossil hydrocarbons) and manufactured industrial organics. The underlying interactions between microbes and hydrophobic compounds have major consequences not only for the lifestyles of the microbes involved but also for biogeochemistry, climate change, environmental pollution, human health and a range of biotechnological applications. The significance of this “greasy microbiology” is reflected in both the scale and breadth of research on the various aspects of the topic. Despite this, there was, as far as we know, no treatise available that covers the subject. In an attempt to capture the essence of greasy microbiology, the *Handbook of Hydrocarbon and Lipid Microbiology* (<http://www.springer.com/life+sciences/microbiology/book/978-3-540-77584-3>) was published by Springer in 2010 (Timmis 2010). This five-volume handbook is, we believe, unique and of considerable service to the community and its research endeavours, as evidenced by the large number of chapter downloads. Volume 5 of the handbook, unlike volumes 1–4 which summarize current knowledge on hydrocarbon microbiology, consists of a collection of experimental protocols and appendices pertinent to research on the topic.

A second edition of the handbook is now in preparation and a decision was taken to split off the methods section and publish it separately as part of the Springer Protocols program (<http://www.springerprotocols.com/>). The multi-volume work *Hydrocarbon and Lipid Microbiology Protocols*, while rooted in Volume 5 of the Handbook, has evolved significantly, in terms of range of topics, conceptual structure and protocol format. Research methods, as well as instrumentation and strategic approaches to problems and analyses, are evolving at an unprecedented pace, which can be bewildering for newcomers to the field and to experienced researchers desiring to take new approaches to problems. In attempting to be comprehensive – a one-stop source of protocols for research in greasy microbiology – the protocol volumes inevitably contain both subject-specific and more generic protocols, including sampling in the field, chemical analyses, detection of specific functional groups of microorganisms and community composition, isolation and cultivation of such organisms, biochemical analyses and activity measurements, ultrastructure and imaging methods, genetic and genomic analyses, systems and synthetic biology tool usage, diverse applications, and

---

<sup>1</sup> Adapted in part from the Preface to *Handbook of Hydrocarbon and Lipid Microbiology*.

the exploitation of bioinformatic, statistical and modelling tools. Thus, while the work is aimed at researchers working on the microbiology of hydrocarbons, lipids and other hydrophobic organics, much of it will be equally applicable to research in environmental microbiology and, indeed, microbiology in general. This, we believe, is a significant strength of these volumes.

We are extremely grateful to the members of our Scientific Advisory Board, who have made invaluable suggestions of topics and authors, as well as contributing protocols themselves, and to generous *ad hoc* advisors like Wei Huang, Manfred Auer and Lars Blank. We also express our appreciation of Jutta Lindenborn of Springer who steered this work with professionalism, patience and good humour.

Colchester, Essex, UK  
Braunschweig, Germany  
Palma de Mallorca, Spain

Terry J. McGenity  
Kenneth N. Timmis  
Balbina Nogales

## Reference

Timmis KN (ed) (2010) Handbook of hydrocarbon and lipid microbiology. Springer, Berlin, Heidelberg

# Contents

<b>Introduction to Bioproducts, Biofuels, Biocatalysts and Facilitating Tools . . . . .</b>	<b>1</b>
Willy Verstraete	
<b>Genetic Enzyme Screening System: A Method for High-Throughput Functional Screening of Novel Enzymes from Metagenomic Libraries . . . . .</b>	<b>3</b>
Haseong Kim, Kil Koang Kwon, Eugene Rha, and Seung-Goo Lee	
<b>Functional Screening of Metagenomic Libraries: Enzymes Acting on Greasy Molecules as Study Case . . . . .</b>	<b>13</b>
Mónica Martínez-Martínez, Peter N. Golyshin, and Manuel Ferrer	
<b>Screening for Enantioselective Lipases . . . . .</b>	<b>37</b>
Thomas Classen, Filip Kovacic, Benjamin Lauinger, Jörg Pietruszka, and Karl-Erich Jaeger	
<b>Use of Bacterial Polyhydroxyalkanoates in Protein Display Technologies . . . . .</b>	<b>71</b>
Iain D. Hay, David O. Hooks, and Bernd H.A. Rehm	
<b>Bacterial Secretion Systems for Use in Biotechnology: Autotransporter-Based Cell Surface Display and Ultrahigh-Throughput Screening of Large Protein Libraries . . . . .</b>	<b>87</b>
Karl-Erich Jaeger and Harald Kolmar	
<b>Syngas Fermentation for Polyhydroxyalkanoate Production in <i>Rhodospirillum rubrum</i> . . . . .</b>	<b>105</b>
O. Revelles, I. Calvillo, A. Prieto, and M.A. Prieto	
<b>Genetic Strategies on Kennedy Pathway to Improve Triacylglycerol Production in Oleaginous <i>Rhodococcus</i> Strains . . . . .</b>	<b>121</b>
Martín A. Hernández and Héctor M. Alvarez	
<b>Production of Biofuel-Related Isoprenoids Derived from <i>Botryococcus braunii</i> Algae . . . . .</b>	<b>141</b>
William A. Muzika, Nymul E. Khan, Lauren M. Jackson, Nicholas Winograd, and Wayne R. Curtis	
<b>Protocols for Monitoring Growth and Lipid Accumulation in Oleaginous Yeasts . . . . .</b>	<b>153</b>
Jean-Marc Nicaud, Anne-Marie Crutz-Le Coq, Tristan Rossignol, and Nicolas Morin	
<b>Protocol for Start-Up and Operation of CSTR Biogas Processes . . . . .</b>	<b>171</b>

A. Schnürer, I. Bohn, and J. Moestedt

<b>Protocols for the Isolation and Preliminary Characterization of Bacteria for Biosulfurization and Bionitrogenation of Petroleum-Derived Fuels</b> . . . . .	201
--	-----

Marcia Morales and Sylvie Le Borgne

<b>Protocol for the Application of Bioluminescence Full-Cell Bioreporters for Monitoring of Terrestrial Bioremediation</b> . . . . .	219
--	-----

Sarah B. Sinebe, Ogonnaya I. Iroakasi, and Graeme I. Paton

<b>Protocols for the Use of Gut Models to Study the Potential Contribution of the Gut Microbiota to Human Nutrition Through the Production of Short-Chain Fatty Acids</b> . . . . .	233
---	-----

Andrew J McBain, Ruth Ledder, and Gavin Humphreys

## About the Editors



**Terry J. McGenity** is a Reader at the University of Essex, UK. His Ph.D., investigating the microbial ecology of ancient salt deposits (University of Leicester), was followed by postdoctoral positions at the Japan Marine Science and Technology Centre (JAMSTEC, Yokosuka) and the Postgraduate Research Institute for Sedimentology (University of Reading). His overarching research interest is to understand how microbial communities function and interact to influence major biogeochemical processes. He worked as a postdoc with Ken Timmis at the University of Essex, where he was inspired to investigate microbial

interactions with hydrocarbons at multiple scales, from communities to cells, and as both a source of food and stress. He has broad interests in microbial ecology and diversity, particularly with respect to carbon cycling (especially the second most abundantly produced hydrocarbon in the atmosphere, isoprene), and is driven to better understand how microbes cope with, or flourish in hypersaline, desiccated and poly-extreme environments.



**Kenneth N. Timmis** read microbiology and obtained his Ph.D. at Bristol University, where he became fascinated with the topics of environmental microbiology and microbial pathogenesis, and their interface pathogen ecology. He undertook postdoctoral training at the Ruhr-University Bochum with Uli Winkler, Yale with Don Marvin, and Stanford with Stan Cohen, at the latter two institutions as a Fellow of the Helen Hay Whitney Foundation, where he acquired the tools and strategies of genetic approaches to investigate mechanisms and causal relationships underlying microbial activities. He was subsequently appointed Head of an Independent Research Group at the Max Planck Institute for Molecular Genetics in Berlin, then Professor of Biochem-

istry in the University of Geneva Faculty of Medicine. Thereafter, he became Director of the Division of Microbiology at the National Research Centre for Biotechnology (GBF)/now the Helmholtz Centre for Infection Research (HZI) and Professor of Microbiology at the Technical University Braunschweig. His group has worked for many years, *inter alia*, on the biodegradation of oil hydrocarbons, especially the genetics and regulation of toluene degradation, pioneered the genetic design and experimental evolution of novel catabolic activities, discovered the new group of marine hydrocarbonoclastic bacteria, and conducted early genome sequencing of bacteria that

became paradigms of microbes that degrade organic compounds (*Pseudomonas putida* and *Alcanivorax borkumensis*). He has had the privilege and pleasure of working with and learning from some of the most talented young scientists in environmental microbiology, a considerable number of which are contributing authors to this series, and in particular Balbina and Terry. He is Fellow of the Royal Society, Member of the EMBO, Recipient of the Erwin Schrödinger Prize, and Fellow of the American Academy of Microbiology and the European Academy of Microbiology. He founded the journals *Environmental Microbiology*, *Environmental Microbiology Reports* and *Microbial Biotechnology*. Kenneth Timmis is currently Emeritus Professor in the Institute of Microbiology at the Technical University of Braunschweig.



**Balbina Nogales** is a Lecturer at the University of the Balearic Islands, Spain. Her Ph.D. at the Autonomous University of Barcelona (Spain) investigated antagonistic relationships in anoxygenic sulphur photosynthetic bacteria. This was followed by postdoctoral positions in the research groups of Ken Timmis at the German National Biotechnology Institute (GBF, Braunschweig, Germany) and the University of Essex, where she joined Terry McGenity as postdoctoral scientist. During that time, she worked in different research projects on community diversity analysis of polluted environments. After moving to her current position,

her research is focused on understanding microbial communities in chronically hydrocarbon-polluted marine environments, and elucidating the role in the degradation of hydrocarbons of certain groups of marine bacteria not recognized as typical degraders.

# Introduction to Bioproducts, Biofuels, Biocatalysts and Facilitating Tools

Willy Verstraete

## Abstract

In this volume, two main aspects are addressed. First, there is the enzymatic machinery dealing with hydrocarbons, fats, and oils. There is great progress in this domain and plenty of novel routes are still possible to explore and to upgrade to bring better microbial derived toolboxes to market implementation. Secondly there is the vast array of microbial lipid-associated molecules, ranging from volatile fatty acids to alkanolates and oils. Also in this domain, novel breakthroughs are at hand. The fact that enzymes capable of acting towards greasy molecules both in the bioconversion and the cleantech industry are of great importance is well recognized. The protocols provided in this chapter allow to screen for a panoply of empowered fat-modifying biocatalysts such as, e.g., esterases, lipases, phospholipases, and even dehalogenases and C-C metacleaveage product hydrolyses. Clearly, these approaches offer potential for a variety of environmental friendly removals/degradations/modifications of this important group of waxy-greasy types of natural and xenobiotic molecules.

**Keywords:** Gut simulators, Novel lipases and esterases, Oleaginous microbial strains, PHA as protein binder

The production of proteins of interest directly relates to the putative secretion of proteinaceous products. A special chapter describes the generation of protein libraries and library screening, using magnetic- and fluorescence-activated cell sorting technologies which can be of specific use in the development of new novel lipases and esterases.

Short chain fatty acids produced in the gut by fermentation of feed/food components are of crucial importance in terms of resorption by the colonic epithelium. The understanding of the gastro-intestinal microbiome has made great progress in the last decade. A major breakthrough has been the development of gut models of such as the well known TIM system [1] and the well accessible SHIME [2] and its further advanced developments [3]. The protocol describes the set-up of a do-it-yourself three-stage continuous culture system and the way next generation sequencing

will generate the potential to better understand the possible links between fatty acid metabolism of the gastro-intestinal microbiome and the health of the host.

The pictures of “obese” microbial cells full of polyhydroxybutyrate are well known. There are a multitude of potential applications already reported in the literature about poly hydroxyl alkanooates ranging from a substrate to make biodegradable plastic [4] over a putative carbon source for denitrification [5] being a powerful prebiotic [6]. Yet the application of PHA as a biocompatible and biodegradable carrier for immobilized microbial proteins is really a very startling development, the more because it apparently can easily be engineered in *E. coli*.

To immobilize functional proteins on a solid support material is common practice in the biotech industry. This has also led to various catalytic processes enhancements but also to progress in the biosensor and micro-array technologies. The fact that one can achieve inside the microbial cell, the in vivo production of a functional protein covalently attached to the surface of a bio-polyester by fusing the functional protein to the polyester synthase, is really a marvellous concept.

Microbial oil and handling oleaginous strains is a topic of long-standing interest. Bacterial triacylglycerides (TAGs) have applications in feeds, cosmetics, and lubricants. The protocol on genetic strategies to enhance the single cell oil levels is most welcome in the framework of upgrading simple carbon sources under specific conditions (often N limiting) and offers quite some perspectives.

## References

1. Jedidi H et al (2014) Effect of milk enriched with conjugated linoleic acid and digested in a simulator (TIM-1) on the viability of probiotic bacteria. *Int Dairy J* 37:20–25
2. Alander M et al (1999) The effect of prebiotic strains on the microbiota of the simulator of the human microbial ecosystem (SHIME). *Int J Food Microbiol* 46:71–79
3. Marzorati M et al (2014) The HMI (TM) module a new tool to study the host-microbiota interaction in the human gastrointestinal tract in vitro. *BMC Microbiol* 14(133). doi:[10.1186/1471-2180-14-133](https://doi.org/10.1186/1471-2180-14-133)
4. Jiang Y et al (2014) *Plasticumulans lactivorans* sp nov, a polyhydroxybutyrate-accumulating gammaproteobacterium from a sequencing-batch bioreactor fed with lactate. *Int J Syst Evol Microbiol* 64:33–38
5. Gutierrez-Wing MT et al (2012) Evaluation of polyhydroxybutyrate as a carbon source for recirculating aquaculture water denitrification. *Aquacult Eng* 51:36–43
6. Hung V et al (2015) Application of poly-beta-hydroxybutyrate (PHB) in mussel larviculture. *Aquaculture* 446:318–324

# Genetic Enzyme Screening System: A Method for High-Throughput Functional Screening of Novel Enzymes from Metagenomic Libraries

Haseong Kim, Kil Koang Kwon, Eugene Rha, and Seung-Goo Lee

## Abstract

This protocol describes a single-cell high-throughput genetic enzyme screening system (GESS) in which GFP fluorescence is used to detect the production of phenolic compounds from a given substrate by metagenomic enzyme activity. One of the important features of this single-cell genetic circuit is that it can be used to screen more than 200 different types of enzymes that produce phenolic compounds from phenyl group-containing substrates. The highly sensitive and quantitative nature of the GESS, combined with flow cytometry techniques, will facilitate rapid finding and directed evolution of valuable new enzymes such as glycosidases, cellulases, and lipases from metagenomic and other genetic libraries.

**Keywords:** Enzyme screening, Fluorescence-assisted cell sorting, Genetic enzyme screening system, High-throughput screening, Metagenomic library, Synthetic biology

---

## 1 Introduction

The success of biology-based industrial applications largely depends on how efficiently bio-industrial products can be manufactured using biocatalysts, which are currently used to manufacture over 500 industrial products [1, 2]. In uncultivated environmental bacteria, the metagenome, which is theoretically considered one of the richest available enzyme sources, contains a vast number of uncharacterized enzyme-encoding genes [3]. Therefore, screening novel enzymes from the metagenome is essential for sustainable, cost-effective bio-industrial applications. Despite the rapid accumulation of sequence-driven approaches from genetic resources [4, 5], function-based screening techniques allow us to identify novel enzymes by direct observation of enzyme activities. The majority of metagenome-derived enzymes, including many esterases and lipases, have been isolated by functional screening methods [6]. Prior to 2008, a total of 76 esterases and lipases were identified via

metagenomic functional screening; however, only 11 of these enzymes were characterized due to time and cost constraints associated with overexpression and purification of metagenomic genes [7]. The recent development of rapid screening techniques has addressed some of the limitations of functional screening methods [8–12]. In particular, substrate-/product-induced transcription systems coupled with flow cytometry have enabled high-throughput enzyme screening from metagenomic/mutant libraries [8–10]. However, these methods require specific metabolite-responsive or product-induced transcriptional systems, suggesting their applications with other enzymes will be limited.

Here, we provide a detailed protocol for the genetic enzyme screening system (GESS), which was originally published in 2014 [13]. GESS was designed to utilize phenol-dependent transcriptional activators to screen for phenol-producing enzymes, which are one of the most abundant compounds in nature. The mechanism of GESS is depicted in Fig. 1. The system consists of two AND logics, the first of which has two inputs: a target enzyme and its

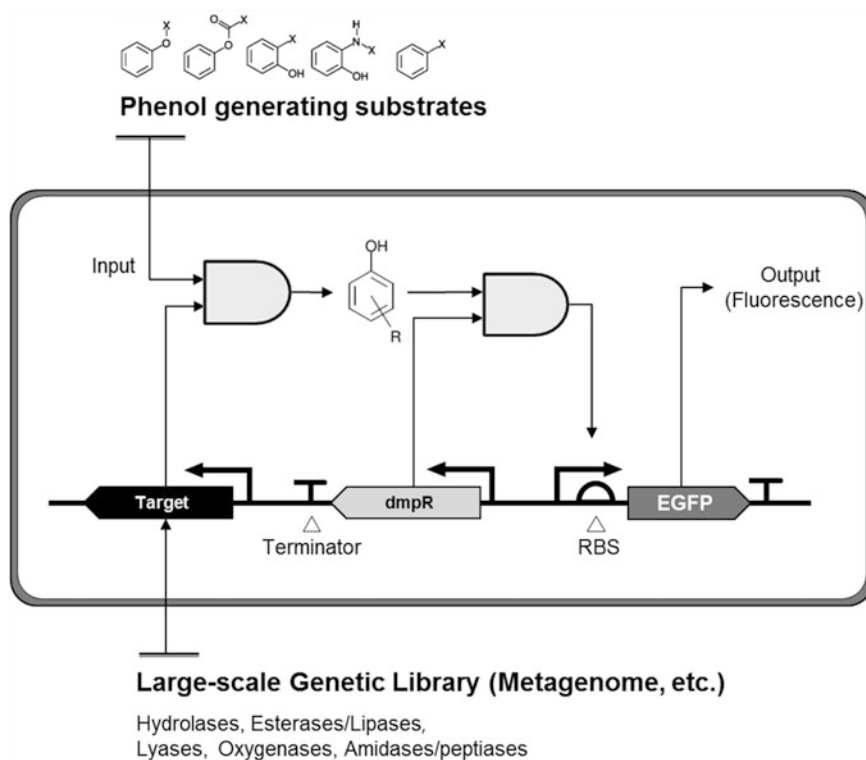


**Fig. 1** Schematic representation of the genetic enzyme screening system. Intracellular phenolic compounds are generated by various enzymatic reactions within the cell and visualized through enhanced green fluorescent protein (EGFP), expression of which is activated by the phenol–DmpR complex. X groups can be  $\alpha$ -/ $\beta$ -glycosidases, phosphates, alkyls, amines, amino acids, or halogens. R groups represent different substituents on the aromatic ring. Genes for target enzymes, such as hydrolases, esterases/lipases, lyases, oxygenases, and amidases/peptidases, are selected from genetic libraries based on fluorescence signals

substrate; the reaction between the enzyme and substrate is responsible for the accumulation of a phenol compound within the cell. In the other logic, the phenol compound and its inducible transcription factor activate the expression of a downstream reporter gene. Therefore, this system can detect the activity of any enzyme that produces phenolic compounds. In the BRENDA database (<http://www.brenda-enzymes.info>, 2013.7), 211 enzyme species have been reported to generate phenols or *p*-nitrophenol compounds as by-products of their catalytic reactions (Table 1). Intracellular phenol is specifically recognized by the transcription activator

**Table 1**  
**Enzymes that produce *p*-nitrophenol or phenol listed in the BRENDA database**

EC numbers	Description	No. of <i>p</i> -nitrophenol-producing enzymes (no. of reactions)	No. of phenol-producing enzymes (no. of reactions)
EC 1 Oxidoreductases	1.3 Acting on the CH–CH group of donors	–	1 (1)
	1.11 Peroxygenase	2 (2)	–
	1.14 Acting on paired donors, with incorporation or reduction of molecular oxygen	–	2 (4)
EC 2 Transferases	2.3 Acyltransferases	1 (30)	–
	2.4 Glycosyltransferases	8 (18)	–
	2.5 Transferring alkyl or aryl groups, other than methyl groups	1 (11)	1 (1)
	2.7 Transferring phosphorus-containing groups	1 (65)	1 (10)
	2.8 Transferring sulfur-containing groups	3 (111)	1 (2)
EC 3 Hydrolases	3.1 Act on ester bonds	67 (1,933)	16 (121)
	3.2 Glycosylases	75 (1,546)	21 (167)
	3.4 Act on peptide bonds – peptidase	26 (116)	4 (4)
	3.5 Act on carbon–nitrogen bonds, other than peptide bonds	5 (10)	3 (5)
	3.6 Act on acid anhydrides	4 (26)	–
	3.7 Act on carbon–carbon bonds	2 (3)	–
	EC 4 Lyases	4.1 Carbon–carbon lyases	–
4.2 Carbon–oxygen lyases		1 (32)	–
4.3 Carbon–nitrogen lyases		1 (4)	–
Subtotal number of enzymes (reactions)		197 (3,907)	53 (390)
Total number of enzymes (excluding overlapped enzymes)		211	

The first and second columns show EC numbers and class descriptions. All the enzymes in these classes could be primary candidates for GESS applications

DmpR, an NtrC family transcriptional regulator of the (methyl) phenol catabolic operon [14, 15]. We performed a sensitivity test of DmpR depending on the phenol concentration in Luria-Bertani (LB) media and minimal media with glucose. In addition, 21 phenolic compounds were tested for DmpR specificity [13]. DmpR (E135K), a mutant derivative of DmpR, can also be employed in GESS to detect *p*-nitrophenol; threefold more enzymes (197 enzymes) are responsible for *p*-nitrophenol production than for phenol production (53 enzymes) (Table 1). Cellulases, lipases, alkaline phosphatases, tyrosine phenol-lyases, and methyl parathion hydrolases have been screened by this high-throughput method [13, 16].

Lipases and hydrocarbons are one of the major enzyme-product pairs used in sustainable bio-industries. Lipases (EC 3.1.1.3) are particularly important biocatalysts in the biotechnological industry for their ability to hydrolyze insoluble triglycerides composed of long-chain fatty acids. *p*-Nitrophenol-mediated colorimetric assays are commonly used to determine lipase activity. Indeed, *p*-nitrophenyl esters, such as *p*-nitrophenyl butyrate, liberate *p*-nitrophenol via lipase activity, allowing for spectrophotometric activity measurements at 405–410 nm [17, 18]. GESS can also use *p*-nitrophenyl butyrate as a substrate; however, when combined with flow cytometry, our single-cell-based fluorescence-detection technique enables us to explore more than  $10^7$  library cells per day. Moreover, GESS can be used to screen for other types of lipases or esterases by simply changing substrates; Table 1 shows the possible candidates. Choosing a proper phenol-containing substrate is critical for successful identification of target enzyme activities from metagenomic DNA. Thus far, we have confirmed that two phenol-tagged substrates (phenyl phosphate and organophosphates) and three *p*-nitrophenol-tagged substrates (*p*-nitrophenyl butyrate, *p*-nitrophenyl cellotrioside, and methyl parathion) can be used to screen metagenomic enzymes [13, 16].

The vector map containing GESS (pGESS) is shown in Fig. 2, and a typical high-throughput screening protocol with pGESS is described below.

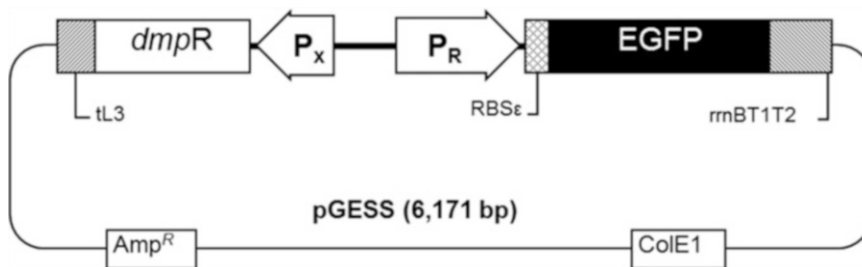


**Fig. 2** Plasmid pGESS, in which *dmpR* is under the control of its own promoter  $P_x$ , and EGFP is induced by the DmpR-regulated s54-dependent promoter  $P_R$ . The transcriptional terminator sequences *rrnBT1T2* and *tL3* are at the end of the EGFP and *dmpR* genes, respectively

---

## 2 Materials

### 2.1 Metagenomic DNA Library Preparation

1. Strains: *Escherichia coli* EPI300 (KO)
2. Plasmids: pGESS (*see Note 1*) and pCC1FOS™ (Epicentre, USA) metagenomic DNA library (*see Note 2*)
3. Growth media: Luria-Bertani (LB): 10 g tryptone, 5 g yeast extract, and 10 g NaCl per 1 L distilled water; super optimal broth with glucose (SOC): 2% (w/v) tryptone, 0.5% (w/v) yeast extract, 10 mM NaCl, 2.5 mM KCl, 10 mM MgCl<sub>2</sub>, 10 mM MgSO<sub>4</sub>, and 20 mM glucose per 1 L distilled water
4. Antibiotic stock solution: 50 mg/mL ampicillin and 34 mg/mL chloramphenicol
5. Cell storage media: 1× TY (8 g tryptone, 5 g yeast extract, and 2.5 g NaCl per 1 L distilled water) containing 15% (v/v) glycerol

### 2.2 Detection and Screening of Catalytic Activities Using Fluorescence-Assisted Cell Sorting (FACS)

1. Strains: *E. coli* EPI300 harboring the metagenomic DNA library and pGESS
2. Antibiotic stock solution: 50 mg/mL ampicillin and 34 mg/mL chloramphenicol
3. Flow cytometer: FACSAriaIII (BD Biosciences, USA) or equivalent
4. Microscope: AZ100M (Nikon, Japan) or equivalent epifluorescence instruments
5. Growth media: Luria-Bertani (LB): 10 g tryptone, 5 g yeast extract, and 10 g NaCl per 1 L distilled water
6. FACS sample buffer: phosphate-buffered saline (PBS), 8 g NaCl, 0.2 g KCl, 1.1 g Na<sub>2</sub>HPO<sub>4</sub>, and 0.2 g KH<sub>2</sub>PO<sub>4</sub> in distilled water, filtered through a 0.22- $\mu$ m filter is necessary

---

## 3 Methods

### 3.1 Preparation of a Metagenomic DNA Library for GESS

1. Construct a metagenomic library in *E. coli* EPI300 with the pCC1FOS vector using a CopyControl™ Fosmid Library Production Kit (Epicentre), according to the manufacturer's protocol (*see Note 2*). The library is stored at  $-70^{\circ}\text{C}$  with an optical density (OD<sub>600</sub>) of 100.
2. Thaw 100  $\mu$ L of the stock metagenomic library and inoculate in a 500-mL flask containing 50 mL LB and 12.5  $\mu$ g/mL chloramphenicol, and then incubate at  $37^{\circ}\text{C}$  for 2 h.
3. Harvest the cells in a 50-mL conical tube (BD Falcon, USA) by centrifugation at  $5,000\times g$  for 10 min at  $4^{\circ}\text{C}$ . Resuspend the pellet quickly in 50 mL ice-cold distilled water and centrifuge at

5,000×*g* for 10 min at 4°C. Resuspend the pellet in 50 µL ice-cold 10% (v/v) glycerol, which should reach an OD<sub>600</sub> of 100. This 50-µL cell aliquot is used as a source of electrocompetent cells.

4. Place the mixture of electrocompetent cells and pGESS DNA (10 ng) in an ice-cold electroporation cuvette, and electroporate (18 kV/cm, 25 µF; Gene Pulser Xcell, Bio-Rad, Hercules, CA, USA) the mixture. Quickly add 1 mL SOC medium, gently resuspend the cells, and allow them to recover at 37°C for 1 h.
5. Spread the cells on an LB agar plate containing 12.5 µg/mL chloramphenicol and 50 µg/mL ampicillin. Incubate at 30°C for 12 h (*see Note 3*).
6. Collect the bacterial colonies into a 50-mL conical tube using ice-cold cell storage media.
7. Centrifuge at 5,000×*g* for 10 min at 4°C. Resuspend the pellet in 20-mL ice-cold cell storage media.
8. Centrifuge at 5,000×*g* for 10 min at 4°C. Resuspend the pellet in ice-cold cell storage media to an OD<sub>600</sub> of 100.
9. Aliquot 20 µL of the cells for storage at -70°C.
10. For the negative control, prepare *E. coli* EPI300 containing empty pCC1FOS by standard transformation protocols and follow **steps 3–9**.

### **3.2 Detection and Screening of Catalytic Activities Using FACS**

1. Thaw the stock metagenomic library cells containing pCC1FOS and pGESS plasmids.
2. Inoculate 10 µL of the cells in 2 mL LB containing 50 µg/mL ampicillin and 12.5 µg/mL chloramphenicol in a 14-mL round-bottomed tube (BD Falcon). Incubate at 37°C with shaking at 200 rpm for 6 h.
3. Turn on the FACS machine and use the following settings: nozzle tip diameter, 70 µm; forward scatter (FSC) sensitivity, 300 V-logarithmic amplification; side scatter (SSC) sensitivity, 350 V-logarithmic amplification; fluorescein isothiocyanate (FITC) sensitivity, 450 V-logarithmic amplification; and threshold parameter, FSC value 500. For GFP fluorescence intensity measurement, fix the FITC photomultiplier tube voltage at the fluorescence intensity of the negative control (lower than 10<sup>1</sup>).
4. Place the diluted metagenomic library sample in the FACS sample tube, and adjust the event rate to 3,000–5,000 events/s (*see Note 4*).
5. Check the cell count versus the log-scaled FSC and log-scaled SSC histogram. The number of peaks should be one, and no

cutoff should be observed in the edges of the bell-shaped distribution. Plot the cell count versus the log-scaled FITC, and then adjust the FITC power such that the peak of the bell-shaped distribution is less than  $10^1$  for the FITC intensity.

6. Set a sample gate R1 around the bacterial population on the log-scaled FSC and log-scaled SSC plot. Set a sorting gate R2 on the cell count versus the log-scaled FITC plot.
7. Place a collection tube containing 0.2 mL LB at the outlet of the FACS instrument, and sort out  $10^7$  cells that show low FITC intensity (5% of the cells on the left side of the distribution) satisfying both the R1 and R2 gates. This step minimizes false-positive cells showing fluorescence in the absence of appropriate substrates (*see Note 5*).
8. Transfer the sorted cells to 2 mL LB containing 50  $\mu\text{g}/\text{mL}$  ampicillin and 12.5  $\mu\text{g}/\text{mL}$  chloramphenicol. Incubate at  $37^\circ\text{C}$  with shaking at 200 rpm to  $\text{OD}_{600}$  0.5.
9. Add 50  $\mu\text{M}$  phenol-containing substrates into the culture broth to activate GFP expression from pGESS when a putative enzyme in pCCIFOS releases phenol or phenol derivatives from the substrate. Add 5  $\mu\text{L}$  CopyControl induction solution (Epicentre) to amplify the intracellular fosmid copy number (*see Note 6*).
10. Incubate the cells at  $30^\circ\text{C}$  to  $\text{OD}_{600} \sim 2$  with vigorous shaking (*see Note 3*).
11. To prepare the FACS samples, dilute the cells by adding 5  $\mu\text{L}$  sample to a 5-mL round-bottomed tube (BD Falcon) containing 1 mL PBS (*see Note 4*).
12. Along with the metagenomic library sample, prepare a negative control by following the same procedure described in **steps 1, 2, and 9–11** with the negative control stock containing the empty pCCIFOS vector with pGESS.
13. Place the negative control in the FACS sample tube, and adjust the event rate to 3,000–5,000 events/s (*see Note 4*).
14. Set a sample gate R1 around the bacterial population on the log-scaled FSC and log-scaled SSC plot.
15. Set a sorting gate R2 on the cell count versus the log-scaled FITC plot so that less than 0.1% (10 out of 10,000 cells) of negative control cells is detected within this R2 gate.
16. Replace the negative control sample with the diluted metagenomic library sample, and adjust the event rate to 3,000–5,000 events/s.
17. Place a collection tube containing 0.2 mL LB at the outlet of the FACS instrument, and sort out 10,000 positive cells satisfying both the R1 and R2 gates.

18. Remove the collection tube, cap, and gently vortex after finishing the sorting procedure.
19. Spread the collected cells in a 0.2 mL volume on an LB agar plate containing 50 µg/mL ampicillin, 12.5 µg/mL chloramphenicol, and appropriate concentrations of the phenol-containing substrate. Incubate overnight at 37°C (*see Note 7*).
20. It is possible to perform additional rounds of sorting for enrichment by repeating **steps 17–19**. In each round, modify the sorting criteria of gate R2 as the FITC fluorescence is enriched.
21. Colonies that show higher fluorescence intensity than the negative control are picked as positives by observation under an AZ100M microscope (Nikon, Japan). The colonies can be observed using any epifluorescence instrument instead of the AZ100M microscope (*see Note 8*).
22. Inoculate the selected colonies in 2 mL LB containing 50 µg/mL ampicillin and 12.5 µg/mL chloramphenicol in a 14-mL round-bottomed tube (BD Falcon), and incubate overnight at 37°C with shaking at 200 rpm.
23. Test the in vitro enzyme activity or extract fosmid DNA using standard extraction procedures, and analyze the nucleotide sequence to identify the candidate enzyme.

---

## 4 Notes

1. pGESS can be constructed by referring to the vector map in Fig. 2. The *dmpR* gene can be replaced with *dmpR* (E135K) to construct a GESS detecting *p*-nitrophenol.
2. Metagenomic DNA can be isolated from a location of interest using a HydroShear machine (GeneMachines, Genomic Instrumentation Services, CA, USA). *E. coli* EPI300 is used for the library host, and the library can be constructed as described in the CopyControl Fosmid Library Production Kit (Epicentre). The average insert size of the pCC1FOS vector is 30 kb.
3. The library is incubated at 30°C rather than at 37°C to maintain library diversity by slowing the growth of *E. coli*.
4. The final concentration of the diluted cell solution depends on the event rate in FACS. If the event rate is less than 3,000 events/s, add more cells to the diluted sample; if the rate is more than 5,000, add more PBS to the sample. Note that the event rate can also be controlled by the flow rate parameter in the FACS software.

5. To minimize false positives, remove any cells that fluoresce in the absence of substrate (optional). The positivity rate of a GESS screen of a metagenome library is dependent on the substrate, metagenome sources, target enzymes, and user-defined screening criteria. In the original GESS paper [13], we defined false-positive hits as fluorescence less than 400 (log of FITC intensity) in the library without substrate, 1 mM phenyl phosphate. The positivity rate after treatment with phenyl phosphate was approximately 15% of the total cells, but only 0.5% of the total were sorted out as true positives for novel phosphatases.
6. The pCC1FOS vector contains both the *E. coli* F-factor single-copy origin of replication and the inducible high-copy oriV. CopyControl fosmid clones are typically grown at single copy to ensure insert stability and successful cloning of encoded and expressed toxic protein and unstable DNA sequences. The CopyControl induction solution can induce the fosmid clones up to 50 copies per cell. This step maximizes metagenomic enzyme activity while maintaining plasmid stability.
7. The number of recovered colonies is dependent on cell condition at the time of sorting. To maximize recovery and minimize cell damage, we add 0.2 mL LB to the collection tube prior to sorting (**Step 17**).
8. A light-emitting diode (LED) illuminator such as UltraSlim (Maestrogen, USA) may be used instead of the microscope to observe GFP fluorescence.
9. In conclusion, GESS is a practical and useful genetic circuit that turns enzyme activity into in vivo fluorescence intensity. The exceptional sensitivity, high-throughput, and analytical properties of this system enable us to detect diverse metagenomic enzymes including various types of lipase. Further development and characterization of the genetic parts of GESS will provide a high-throughput platform for screening and even evolutionary engineering of important industrial enzymes.

---

## Acknowledgment

This research was supported by grants from the Intelligent Synthetic Biology Center of Global Frontier Project (2011-0031944) and the KRIBB Research Initiative Program.

## References

1. Kumar A, Singh S (2013) Directed evolution: tailoring biocatalysts for industrial applications. *Crit Rev Biotechnol* 33(4):365–378
2. Jemli S, Ayadi-Zouari D, Hlima HB, Bejar S (2014) Biocatalysts: application and engineering for industrial purposes. *Crit Rev Biotechnol* 1–13
3. Lorenz P, Eck J (2005) Metagenomics and industrial applications. *Nat Rev Microbiol* 3(6):510–516
4. Simon C, Daniel R (2011) Metagenomic analyses: past and future trends. *Appl Environ Microbiol* 77(4):1153–1161
5. Iqbal HA, Feng Z, Brady SF (2012) Biocatalysts and small molecule products from metagenomic studies. *Curr Opin Chem Biol* 16(1):109–116
6. Ferrer M, Beloqui A, Timmis KN, Golyshin PN (2008) Metagenomics for mining new genetic resources of microbial communities. *J Mol Microbiol Biotechnol* 16(1–2):109–123
7. Steele HL, Jaeger K-E, Daniel R, Streit WR (2008) Advances in recovery of novel biocatalysts from metagenomes. *J Mol Microbiol Biotechnol* 16(1–2):25–37
8. Uchiyama T, Abe T, Ikemura T, Watanabe K (2004) Substrate-induced gene-expression screening of environmental metagenome libraries for isolation of catabolic genes. *Nat Biotechnol* 23(1):88–93
9. van Sint Fiet S, van Beilen JB, Witholt B (2006) Selection of biocatalysts for chemical synthesis. *Proc Natl Acad Sci U S A* 103(6):1693–1698
10. Dietrich JA, McKee AE, Keasling JD (2010) High-throughput metabolic engineering: advances in small-molecule screening and selection. *Annu Rev Biochem* 79:563–590
11. Lakhdari O, Cultrone A, Tap J, Gloux K, Bernard F, Ehrlich SD, Lefèvre F, Doré J, Blottière HM (2010) Functional metagenomics: a high throughput screening method to decipher microbiota-driven NF- $\kappa$ B modulation in the human gut. *PLoS One* 5(9):e13092
12. Jacquioud S, Demanèche S, Franqueville L, Ausec L, Xu Z, Delmont TO, Dunon V, Cagnon C, Mandic-Mulec I, Vogel TM (2014) Characterization of new bacterial catabolic genes and mobile genetic elements by high throughput genetic screening of a soil metagenomic library. *J Biotechnol* 190:18–29
13. Choi S-L, Rha E, Lee SJ, Kim H, Kwon K, Jeong Y-S, Rhee YH, Song JJ, Kim H-S, Lee S-G (2013) Toward a generalized and high-throughput enzyme screening system based on artificial genetic circuits. *ACS Synth Biol* 3(3):163–171
14. Shingler V, Bartilson M, Moore T (1993) Cloning and nucleotide sequence of the gene encoding the positive regulator (DmpR) of the phenol catabolic pathway encoded by pVII50 and identification of DmpR as a member of the NtrC family of transcriptional activators. *J Bacteriol* 175(6):1596–1604
15. Ng LC, O'Neill E, Shingler V (1996) Genetic evidence for interdomain regulation of the phenol-responsive 54-dependent activator DmpR. *J Biol Chem* 271(29):17281–17286
16. Jeong Y-S, Choi S-L, Kyeong H-H, Kim J-H, Kim E-J, Pan J-G, Rha E, Song JJ, Lee S-G, Kim H-S (2012) High-throughput screening system based on phenolics-responsive transcription activator for directed evolution of organophosphate-degrading enzymes. *Protein Eng Des Sel* 25(11):725–731
17. LESUISSE E, Schanck K, Colson C (1993) Purification and preliminary characterization of the extracellular lipase of *Bacillus subtilis* 168, an extremely basic pH-tolerant enzyme. *Eur J Biochem* 216(1):155–160
18. Salameh M, Wiegel J (2007) Lipases from extremophiles and potential for industrial applications. *Adv Appl Microbiol* 61:253–283

# Functional Screening of Metagenomic Libraries: Enzymes Acting on Greasy Molecules as Study Case

Mónica Martínez-Martínez, Peter N. Golyshin, and Manuel Ferrer

## Abstract

Greasy molecules such as aromatic and aliphatic hydrocarbons are ubiquitous and chemically heterogeneous microbial substrates that occur in the biosphere through human activities as well as natural inputs. Organic compounds consisting of one, two, or more fused aromatic rings are due to their toxicity considered as pollutants of a great concern; however, they are also important chemical building blocks of relevance for biology, chemistry, and materials sciences. Biological approaches are known to provide exquisite ecologically friendly methods, as compared to chemical ones, for their biodegradation or bioconversions. For that, ubiquitous yet specialized hydrocarbonoclastic bacteria and polycyclic aromatic hydrocarbons (PAH) degrading bacteria of the genera *Alcanivorax*, *Marinobacter*, *Oleispira*, *Thalassolituus*, *Oleiphilus*, *Cycloclasticus*, and *Neptunomonas* to name some, have developed a complex arsenal of catabolic genes involved in greasy oil component degradation. Oxidoreductases and hydrolases are the first enzymes initiating on their catabolism. The rapid evolution of next generation sequencing methods had a big impact on the identification of genes for metabolism of greasy molecules. But sequencing allows only the identification of enzymes with certain sequence similarity to those previously deposited in databases without functional information. Functional screening of expression libraries from pure cultures or microbial consortia is an alternative approach that solves the problem of sequence similarity and also ensures proper function assignation. Here we describe available screening methods to identify enzymes capable of acting towards greasy molecules that include not only oil components such as alkanes and PAH but also other types of greasy molecules of biotechnological relevance to produce fine chemicals and precursors in chemical industries.

**Keywords:** Dioxygenase, Esterase, Lipase, *Meta*-cleavage, Metagenomic, Monooxygenase, Screening

---

## 1 Introduction

Greasy molecules and, among them, polycyclic aromatic hydrocarbons (PAH) are a group of hydrophobic organic compounds consisting of two or more fused benzene rings in linear, angular, or cluster structural arrangements [1]. They are ubiquitous environmental chemicals owing to their abundance in crude oil and their widespread use in chemical manufacturing [2] and are considered as pollutants of great concern owing to their toxicity to living cells [3].

Because of their low aqueous solubility and their absorption to solid particles, most of them persist in the ecosystem for many years [4, 5]. They are introduced in the biosphere through human activities such as crude oil spillage, fossil fuel combustion, and gasoline leakage as well as natural inputs like forest fire smoke and natural petroleum seepage [6]. These chemicals can be removed from the environment through many processes including volatilization, photooxidation, chemical oxidation, bioaccumulation, adsorption, and microbial transformation and degradation [7]. Despite all the possible approaches, biological treatments should be considered as attractive methods as they present advantages such as the complete degradation of the pollutants, lower costs, greater safety, and less environmental alteration [8]. Although greasy molecules with lower complexity such as low-molecular-weight PAH are usually degraded by a number of bacteria under laboratory and in situ conditions, less is known about bacteria able to metabolize complex ones such as PAH containing five or more rings [9].

The rapid development of the functional sequencing technologies has the potential to dramatically impact the study of greasy molecules metabolism [10] by providing information about the genomic and enzymatic complements needed for their biodegradation. Oxidoreductases, including reductases, oxidases, dehydrogenases, peroxidases, and laccases, to cite some, are positioned among the first steps in the biodegradation pathways and usually are the first enzymes initiating their metabolism [10, 11]. Hydrolases, such as esterases, C–C *meta*-cleavage hydrolases, and dehalogenases, are among the second most abundant class of enzymes involved in bioremediation processes [11]. Ester formation is a common detoxification mechanism, but little is known about whether aromatics, including greasy molecule esters, occur naturally. Recently a novel esterase (CN1E1) has been described as the first efficient and catalytically active esterase from the  $\alpha/\beta$ -hydrolase family for PAH ester hydrolysis [12].

Nowadays as genomic sequencing is an increasingly cheaper and more accessible technique, the number of genomes of greasy molecule-degrading organisms is rapidly growing [13, 14]. But high-throughput sequencing only allows the identification of genes encoding enzymes involved in their degradation based on sequence similarity to those previously described and listed in databases. Furthermore amplifying annotation mistakes in databases are of great concern as they may drive to wrong functional assignments [15]. Functional screens guarantee the identification of enzymes from clone libraries with no sequence information and at the same time solve the problems related to sequence/activity inconsistencies in databases [15]. Functional screening might thus be considered as an advantageous method for proper annotation of enzymes, including those acting toward greasy molecules.

In fact, wrong annotation is particularly noticeable in case of enzymes acting toward such chemicals [3].

In the present chapter protocols for the functional screens for clones or microbes containing greasy molecules-modifying enzymes are provided. Special attention is given for mono- and dioxygenases, laccases, dehydrogenases, and hydrolases such as esterases, lipases, phospholipases, dehalogenases, and C–C *meta*-cleavage product hydrolases, among the most significant ones. Screens are valid for any kind of microbial cells and/or metagenomic libraries constructed using different types of vectors (e.g., plasmids, phagemids, fosmids, cosmids, and bacterial artificial chromosomes (BAC)) which are developed for the cloning of DNA inserts with different sizes (from few kbp to 300 kbp) and bacterial hosts [16, 17].

---

## 2 Materials (see Note 1)

Unlike otherwise stated, most of the described materials, needed for the different screens, can be used for clone or phage libraries prepared as clone arrays (e.g., individual clones arrayed in 96- or 384-well format) or pool of clones or phages. For a review of metagenomic library constructions using distinct type of vectors and hosts, see Vieites et al. [17].

### 2.1 Buffered (B) Solutions

1. B1: 50 mM phosphate buffer pH 7.5. This buffer must be prepared preferably the day of the assay by using ready-to-use stock solutions of 0.2 M  $\text{KH}_2\text{PO}_4$  and 0.2 M  $\text{Na}_2\text{HPO}_4$  (Panreac, Barcelona, Spain; <http://www.panreac.es>) that may be prepared and maintained at 4°C for several months. Mix 8 mL of 0.2 M  $\text{KH}_2\text{PO}_4$ , 42 mL of 0.2 M  $\text{Na}_2\text{HPO}_4$ , and 50 mL of sterile distilled water to prepare a 0.1 M phosphate buffer pH 7.5. The day of the assay dilute 0.1 M phosphate buffer pH 7.5 to 50 mM with sterile distilled water.
2. B2: 50 mM Tris–HCl pH 7.5.
3. B3: 20 mM 4-(2-hydroxyethyl) piperazine-1-ethanesulfonic acid (HEPES) pH 7.0.
4. B4: 50 mM HEPES pH 7.0.
5. B5: 5 mM 4-(2-hydroxyethyl)-1-piperazinepropanesulfonic acid (EPPS) pH 8.0 supplemented with 450  $\mu\text{M}$  phenol red. This buffer must be prepared preferably the day of the assay by using ready-to-use stock solutions of 100 mM EPPS buffer pH 8.0 and 0.9 mM phenol red solution in 5 mM EPPS pH 8.0, that may be prepared and maintained at 4°C for several months. The day of the assay mix equal volume of 5 mM EPPS buffer pH 8.0 and 5 mM EPPS buffer pH 8.0 containing 0.9 mM phenol red.

## 2.2 Agar-Containing Buffer Solutions (AB Buffers)

For activity screens in solid media, it is recommended to use solidified buffers. For that the utilization of agarose or, preferably, agar is recommended.

1. Add 0.4 g of agar (GibcoBRL, Life Technologies, Rockville, MD USA; <http://www.lifetechnologies.com>) to 100 mL Buffers B1 to B5 described in the previous section (Subheading 2.1) and dissolve it in a microwave at approximately 240 watts for 5–10 min. The final percentage of agar is 0.4% *w/v*. Once a homogeneous solution is achieved, cool the solution to 40–50°C before utilization. Agar-containing buffers (AB1 to AB5) must be prepared preferably the day of the assay and maintained at 40–50°C until use.

## 2.3 Substrate Solutions (SS) for Easy Screens (See Note 2)

The following substrate solutions are recommended for screen assays in which the microbes or clones are already cultured under appropriate conditions. The activity test is performed directly on grown single colonies with a diameter about 1 mm.

1. SS1: 10 mM 3-methyl-catechol in distilled water. Note that other substrates such as catechol, 4-methyl-catechol, or 4-chloro-catechol can be used instead of 3-methyl-catechol.
2. SS2: 10 mM 2,3-dihydroxybiphenyl in 10% *v/v* ethanol:H<sub>2</sub>O (Scharlab, Barcelona, Spain; <http://www.scharlab.com>).
3. SS3 [0.15 mM 6-oxo-6-phenylhexa-2,4-dienoate (HOPHD)] and SS4 [0.15 mM 2-hydroxy-6-oxohepta-2,4-dienoate (HOHD)], prepared as described elsewhere [18–20].
4. SS5: 1% *w/v* guaiacol or syringaldazine in water (*see Note 3*).
5. SS6: 100 mM 2,2'-azino-bis(3-ethylbenzothiazoline-6-sulfonic acid) (ABTS) in distilled water (*see Note 3*).
6. SS7: 15 mM 12-*para*-nitrophenoxydodecanoic acid (12-*p*NCA, Angene; <http://www.an-gene.com>) in dimethyl sulfoxide (DMSO).
7. SS8: 100 mg/mL C2 to C30 alkanes in acetonitrile.
8. SS9: pure 1,2-ethanediol or 2,3-butanediol, 1,2-propanediol or glycerol.
9. SS10: 20 mg/mL  $\alpha$ -naphthyl acetate in acetone (Scharlab, Barcelona, Spain; <http://www.scharlab.com>), prepared as described in Reyes-Duarte et al. [21].
10. SS11: 20 mg/mL indoxyl acetate (IA) or indoxyl laurate (IL) in acetone (Scharlab, Barcelona, Spain; <http://www.scharlab.com>), prepared as described in Beloqui et al. [22].
11. SS12: 100 mg/mL in acetonitrile of any esters for which hydrolytic activity should be checked. Full details of esters successfully tested and protocol for the preparation can be

seen in Martínez-Martínez et al. [12], Alcaide et al. [18], and Alcaide et al. [23].

12. SS13: 100 mg/mL in acetonitrile of any haloacids or haloalkanes, prepared as described in Beloqui et al. [22].
13. SS14: 4% *w/v* Remazol Brilliant Blue in distilled water. Dissolve 0.4 g of Remazol Brilliant Blue in 10 mL of distilled water (*see Note 3*).

#### **2.4 Substrate-Containing Culture Media (SCM) for Easy Screens**

In some cases it is preferably to add the substrate for activity screen in the culture medium. In this case, substrates are added to the standard culture media where clones are going to be cultivated.

1. SCM1: tributyrin emulsion (50% *v/v* tributyrin, 33 g/L gum arabic). Weigh 1.65 g of gum arabic and add 25 mL of tributyrin. Add distilled water to reach 50 mL. Dissolve using a homogenizer or blender. Add 22.5 mL of the emulsion to 500 mL of the appropriate agar medium (e.g., LB agar; Subheading 2.7) and sterilize by autoclaving.
2. SCM2: olive oil emulsion rhodamine agar medium. To 500 mL appropriate agar medium (e.g., LB agar; Subheading 2.7), add 15.625 mL of olive oil and 5 mL of reagent 3 (Subheading 2.5). Mix thoroughly using a homogenizer or blender.
3. SCM3: olive oil brilliant green agar emulsion (20% *v/v* olive oil and 4% *w/v* gum arabic). Add 2 g of gum arabic to a 100 mL Pyrex bottle containing 40 mL of distilled water, minimal medium or appropriate medium. Dissolve the gum arabic and add 10 mL of olive oil. Emulsify on ice by sonication using a pin sonicator (Sonicator<sup>®</sup> 3000; Misonix) (two pulses of 3 min each one). Let the emulsion stand at room temperature for 15–30 min and transfer the volume to a new bottle, avoiding the upper part (containing not emulsified oil). Sterilize by autoclaving (*see Note 4*). To each 500 mL of autoclaved solution, add 25 mL of autoclaved olive oil emulsion and 4 mL of reagent R4 (Subheading 2.5) (*see Note 5*).
4. SCM4: egg yolk agar plates. Add an egg yolk (circa 8% *v/v*) to each 500 mL of appropriate agar medium (e.g., LB agar; Subheading 2.7) cooled to less than 40°C after autoclaving. Then, add appropriate antibiotics and supplements such as autoinduction solution (Subheadings 2.5 and 2.6).
5. SCM5: 0.01% *w/v* guaiacol or syringaldazine agar medium. To each 500 mL of appropriate agar medium (e.g., LB agar; Subheading 2.7) cooled to less than 40°C after autoclaving, add 5 mL of SS5 (Subheading 2.3).
6. SCM6: 1 mM ABTS agar medium. To each 500 mL of appropriate agar medium (e.g., LB agar; Subheading 2.7) cooled to less than 40°C after autoclaving, add 5 mL of SS6 (Subheading 2.3).

7. SCM7: 0.01% *w/v* Remazol Brilliant Blue agar medium. To each 500 mL of appropriate agar medium (e.g., LB agar; Subheading 2.7) cooled to less than 40°C after autoclaving, add 5 mL of SS14 (Subheading 2.3).
8. SCM8: 100 mM benzyl alcohol, benzoylformate, mandelonitrile, or benzoin in acetonitrile. To each 500 mL of appropriate agar medium (e.g., LB agar; Subheading 2.7) cooled to less than 40°C after autoclaving add 50 mL of the previous substrate solution.

## 2.5 Reagents

1. Reagent 1 (R1): Schiff reagent in 96% *v/v* ethanol (Scharlab, Barcelona, Spain; <http://www.scharlab.com>). Dissolve 25 mg of *p*-rosaniline in 10 mL of 95% ethanol: distilled water. Add 125 mg of sodium bisulfite and dissolve (*see Note 2*).
2. R2: 80 mg/mL Fast Blue RR (or 4-benzoylamino-2,5-dimethoxyaniline, Azoic Diazo No. 24) in DMSO (*see Note 2*).
3. R3: 0.1% *w/v* rhodamine B in distilled water (*see Note 3*).
4. R4: 1% *w/v* brilliant green in distilled water (*see Note 3*).

## 2.6 Antibiotics and Additives

1. Chloramphenicol (Cm25): 25 mg/mL in 100% ethanol (*see Note 2*).
2. Ampicillin (Amp): 100 mg/mL in distilled water (*see Notes 2 and 3*).
3. CCFAS: CopyControl fosmid autoinduction solution (Epicentre Biotechnologies, Madison, WI; <http://www.epicentre.com>). Add 800  $\mu$ L to 400 mL of LB broth or LB agar to reach the appropriate final concentration.
4. Isopropyl- $\beta$ -D-galactopyranoside (IPTG): 1 M IPTG (Fisher Scientific, Madrid, Spain; <http://www.fishersci.com>) in distilled water (*see Notes 2 and 3*).
5. Tetracycline (Tc10): 10 mg/mL in ethanol stored at  $-20^{\circ}\text{C}$  (*see Note 2*).

## 2.7 Bacterial Growth Media

The culture media (sterilized by autoclaving at 120°C for 15 min) and strains to be used should be adapted to the different vectors used for library screens. For simplicity, we describe in this chapter the conditions used for screening clone libraries created in the pCCFOS fosmid that are also based on bacterial F factor and *E. coli* EPI300-T1<sup>R</sup> strain (Epicentre Biotechnologies; Madison, WI, USA) as a host and Luria Bertani (LB) as medium. The insert size cloned into fosmids can be as long as 25–40 Kb.

1. LBb: LB broth medium.
2. LBa: LB agar medium (Lennox formulation).

3. LBbCm: LBb containing 12.5 µg/mL Cm final concentration.
4. LbACmCCFAS: LbA containing 12.5 µg/mL Cm final concentration and 800 µL inducer (CCFAS) per each 400 mL of melted (<50°C) LbA.
5. M9 medium for functional screenings over pLAFR3 libraries in *Pseudomonas*.

## 2.8 Small Equipments

1. Heating water bath.
2. Microwave.
3. Probe sonicator (e.g., Pin Sonicator<sup>®</sup> 3000; Misonix).
4. Bacteriological incubators (to 37°C).
5. Refrigerated centrifuge.
6. Refrigerated incubator or chamber.
7. Ultraturrax homogenizer (e.g., Janke & Kunkel KG, Staufen, Germany) or Blender.

---

## 3 Methods

### 3.1 General Comments

The following protocols allow for the identification of clones containing genes encoding enzymes capable of modifying greasy molecules. For simplicity, methods for screening pool of clones based on pCC1FOS fosmid are described in this chapter. The pCC1FOS vector contains both a single copy origin and the high-copy *oriV* origin of replication. Initiation of replication from *oriV* requires *trfA* gene product. The Epi300 *E. coli* employed here to construct fosmid libraries possess a mutant *trfA* gene whose expression is under tight, regulated control inducible promoter. So, this system allows recovering from one (clone counting purposes) to 10–200 (fosmid DNA recovery, functional screening purposes) copies of recombinant fosmids per cell by adding the induction or autoinduction solution to the growth medium. The pCC1FOS vector contains a chloramphenicol (Cm) resistance gene to maintain selection pressure. A final concentration of 12.5 µg/mL Cm (Subheading 2.6) should be always added to supplement growth medium. To perform functional screening from the libraries, here we will describe the utilization of LB medium (Subheading 2.7).

As mentioned before, other types of libraries could be also used for functional screenings described below, as, for example, libraries based on the cosmid pLAFR3 or on BACs (pBac vectors) or libraries using the Lambda Zap<sup>®</sup> Express System (Stratagene, Agilent, Santa Clara, CA, USA; <http://www.genomics.agilent.com>). In each case growth medium has to be supplemented with the appropriate antibiotic and supplements and, when necessary, inducer molecules (e.g., CCFAS or IPTG; Subheading 2.6).

### **3.2 Preparation and Replication of pCCFOS Libraries for Functional Screening Purposes**

1. Prepare a 1/10 serial dilution of the clone library in LBbCm. Add 100  $\mu$ L of the working library to a 1.5 mL Eppendorf tube containing 900  $\mu$ L of LBbCm and vortex gently to mix. This will be the 1/10 dilution. Take 100  $\mu$ L of this dilution and transfer them to a new tube containing 900  $\mu$ L of LBbCm to make the 1/100 dilution. Vortex gently and repeat until reach 1/10,000 or 1/100,000 dilutions.
2. Seed 145 mm LB agar Petri dishes containing supplemented LBaCm with up to 100  $\mu$ L clone serial dilutions. Check several dilutions and use different volumes of each one (e.g., plate 20, 50, and 100  $\mu$ L of 1/1,000, 1/10,000, and 1/100,000 dilutions). In order to be able to uniformly distribute bacteria all over the medium surface, the final volume added to the Petri dish should be 100  $\mu$ L or higher.
3. Spread all the volume over the surface of the LBaCm using a digralsky spreader.
4. Once the liquid has been absorbed, turn the dishes upside down and incubate them overnight (12–15 h) at 37°C, if otherwise not stated, to produce single colonies with a diameter about 1 mm.
5. The plates containing grown clones are directly subjected to activity screens, following the methods described below. For functional screening purposes select the dilution and volume that correspond to the plates where a total number of colonies around 1,000–3,000 have grown separated enough to pick them easily.

In case clone libraries are arrayed in 96- or 384-well format, replicate the clones directly in Petri dishes containing LBaCmCC-FAS. Then turn the dishes upside down and incubate them overnight (12–15 h) at 37°C, if otherwise not stated, to produce single colonies with a diameter about 1 mm. It is highly recommended to use square Petri dishes (120  $\times$  120 mm), where about a total number of 2,304 clones might be directly screened by any of the methods described below.

### **3.3 Functional Screening for Extradiol Dioxygenases**

Biodegradation of aromatics by oxygenases requires the presence of molecular oxygen to initiate the enzymatic attack of benzene rings. The initial oxidation of arenes drives to the formation of dihydroxylated intermediates that may then be cleaved by intra or extradiol ring-cleaving dioxygenases through either an *ortho*-cleavage pathway or a *meta*-cleavage pathway leading to central intermediates that are further converted to tricarboxylic acid (TCA) intermediates [9]. The protocol described below aims to detect enzymes that catalyze ring cleavage of 2,3-dihydroxybiphenyl or 3-methyl-catechol yielding a yellow *meta*-cleavage product (6-oxo-6-phenylhexa-2,4-dienoate (HOPHD) and 2-hydroxy-6-oxohepta-2,4-dienoate (HOHD) respectively).

1. In a Falcon tube containing 24.5 mL of AB1 (Subheading 2.2), add 500  $\mu$ L of SS1 (Subheading 2.3). In a second Falcon tube containing 24.5 mL of Buffer AB1 (Subheading 2.2), add 500  $\mu$ L of the SS2 (Subheading 2.3). Mix gently by inverting the tubes several times. Final concentration of each substrate will be 0.2 mM. Higher concentrations are not recommended as they may cause substrate inhibition giving false-positive results.
2. Overlay the plates containing grown clones with the above solutions: one plate per substrate mix.
3. Positive clones will appear as intense or pale yellow colonies in 1–60 min (*see* **Note 6**).

The protocol can be also performed by spraying with filter-sterilized catechol (1% *w/v*) after 36 h of incubation [20]. Positive colonies turned yellow due to extradiol cleavage of catechol. As example, a total of 254 unique positive clones (corresponding to a hit rate of 1:240) were identified as active out of a total of 61,000 clones in two contaminated soil samples [24]. In some cases, screening for extradiol dioxygenase can be performed also in liquid assays [25], as follows.

1. Cells are grown in 96-well plates with vigorous agitation (1,200 rpm) at 37°C overnight in LBbCmCCFAS medium.
2. Harvest cells by centrifugation (3,000 rpm, 15 min, 4°C).
3. After removing the supernatant, re-suspend cells in 100  $\mu$ L of 50 mM phosphate buffer (pH 7.5).
4. Add 100  $\mu$ L filter-sterilized catechol (1% *w/v*) to each 100  $\mu$ L of cell suspension and the plates incubated with mild agitation (250 rpm) at 25°C.
5. Positive wells are identified by the presence of a yellow color, after incubation for 1 or 16 h.

Although this method has been proven successful, with the detection of up to a total of 91 positive clones (corresponding to a hit rate of 1:1,054) out of a total of 96,000 clones from activated sludge used to treat coke plant wastewater [25], it is more time consuming.

### **3.4 Functional Screening for Aromatic Ring Hydroxylases (Acting Toward Indigo/Indirubin)**

This assay attempts to detect the expression of oxygenases able to hydroxylate indole and thus other aromatic rings. Indole can be oxidized by mono- and dioxygenases to various 2- and 3-position hydroxyl and epoxide indoles. Upon exposure to air, the generated compounds further oxidize and dimerize to form indigo and indirubin, both intensely colored [26]. LB medium contains tryptophan that is converted to indole through tryptophanase from *E. coli*. If a clone from the library contains a gene for an oxygenase able to

hydrolyze indole, then this enzyme will transform indole to indigo or to indirubin and as a consequence positive clones will appear as dark blue/black- or red-colored colonies.

1. Incubate plates at 25°C (room temperature) for 2–4 days instead of overnight at 37°C.
2. After 2–4 days incubate the plates at 4°C during 1–3 h.
3. Look for dark blue colonies.

The protocol has been successfully applied for the screening of pigment-producing clones containing flavin monooxygenases from an effluent treatment plant sludge metagenomic library [27] (2 clones out of a total of 40,000 clones; hit rate of 1:20,000) and forest soil [28] (1 clone out of a total of 113,700 clones).

### **3.5 Functional Screening for C–C Hydrolase Activity (see Note 6)**

The aim of the following assay is to detect *meta*-cleavage product (MCP) hydrolases as well as recently described dual esterases – MCP hydrolases [18], both from the  $\alpha/\beta$ -hydrolase family. MCP hydrolases catalyze the hydrolysis of linear C–C bonds of vinylogous 1,5-diketones formed by the dioxygenative *meta*-cleavage of activated aromatic hydrocarbons [29]. In Subheading 3.3, it was described that 3-methyl-catechol can be hydroxylated to HOPHD by the action of catechol 2,3-dioxygenases and in the same way 2,3-dihydroxybiphenyl can be hydroxylated to HOHD by 2,2',3-trihydroxybiphenyl dioxygenase. MCP hydrolases are able to hydrolyze both colored products, and the reaction can be detected through the loss of yellow color.

1. In a Falcon tube containing 24.5 mL of AB1 (Subheading 2.2), add 500  $\mu$ L of SS3 or SS4 (Subheading 2.3). Mix gently by inverting the tubes several times.
2. Once an intense yellow color is produced due to substrates conversion, overlay the plates containing grown clones with the above solutions, one plate per substrate mix, and incubate for 1–60 min.
3. Positive clones will appear due to de formation of a colorless halo over a yellowish background.

### **3.6 Functional Screening for Laccase Activity**

Laccases (benzenediol-oxygen oxidoreductases) are copper-containing enzymes that catalyze the oxidative conversion of a variety of chemicals using oxygen as the final electron acceptor [30]. Although they play an important role in the carbon cycle due to their participation in the transformation of lignin and other polyphenols, these enzymes are especially attractive because their potential ability to transform aromatics and xenobiotic compounds. Laccases can oxidize a wide variety of substrates [31], and due to the broad substrate specificity, a wide range of chromogenic substrates has been proposed to measure their activity [32] as, for example, Remazol Brilliant Blue, guaiacol, and ABTS.

1. Replicate clone library in SCM5, SCM6, or SCM7 media (Subheading 2.4).
2. Incubate the plates overnight at 37°C.
3. Positive clones will be identified as a halo around an intense blue background when growing in SCM5 plates or as blue/dark brown colonies when growing in SCM6 or SCM7 plates.

A recent successful example of the application of such protocol is described in Beloqui et al. [33], where one positive clone has been identified by screening a bacteriophage  $\lambda$ -based metagenome library of bovine rumen microflora on indicator plates supplemented with syringaldazine.

### **3.7 Functional Screening for Monoxygenases Acting Toward 12-*p*NCA Acids**

Monoxygenases catalyze the insertion of molecular oxygen into non-activated C–H bonds, and thus they are of enormous biotechnological interest. While they naturally function in primary and secondary metabolism as well as in drug detoxification, these enzymes may also have a great industrial potential for the synthesis of fine chemicals or polymer building blocks and also for pollution management [34–37]. The protocol described below is based on a colorimetric assay using as substrate 12-*para*-nitrophenoxydodecanoic acid (12-*p*NCA), a carboxylic acid covalently bound to a nitrophenol group. Its oxygenation by a monoxygenase leads to an unstable intermediate which dissociates into an oxycarboxylate and *p*-nitrophenolate which results in yellow color formation. This substrate is commercially available, but the assay can be performed using other *p*-nitrophenoxycarboxylic acids with shorter or longer carbon chains that can be synthesized following a previously published protocol [38].

1. Add 10  $\mu$ L of SS7 (Subheading 2.3) to a Falcon tube containing 20 mL of buffer AB2 (Subheading 2.1) and mix by gently inverting the tube.
2. Overlay the plates containing grown clones with the above solution and incubate 1–24 h.
3. Positive clones will appear as yellow colonies.

Note that bacterial cell wall is not totally permeable to the substrate, so detection of monoxygenase activity can be quite difficult. Therefore, the performance of a complementary assay where colonies are grown in liquid media in microtiter plates, prior the assay, is highly recommended. A protocol based on cell wall permeabilization and cofactor regeneration facilitation, using also in 12-*p*NCA as a substrate, has been developed [39]. In that case, plates have to be replicated in liquid media in 96 multi-well plates under similar conditions as for the ones used in solid media.

Other assays to detect monoxygenases based on epoxidation of styroles [40] as well as in hydroxylation of carbon chains [41]

have been published. Both protocols can be performed using protein extracts from pCCFOS and other type of metagenomic libraries. The first assay is based on the use of the yellow chromophore *para*-nitrophenolate (*p*NTP). Monooxygenase drives the epoxidation of a styrol (e.g., styrene) to a styrol oxide that is attacked by the nucleophilic *p*NTP resulting in a colorless product. The activity can be monitored as a decrease in absorbance at 405 nm. The second protocol based on hydroxylation allows discrimination between terminal and subterminal hydroxylations of carbon chains using a two-step assay. Terminal and subterminal hydroxylation of alkanes drives to the formation of primary and secondary alcohols, respectively. Hydroxylation reaction implies NADPH consumption, which can be monitored as a decrease of absorbance at 340 nm. In the published method, hydroxylation reaction is coupled with an oxidation reaction catalyzed by a commercial alcohol dehydrogenase (ADH) that oxidizes only primary alcohols, resulting in NADP<sup>+</sup> reduction to NADPH that can be monitored as an increase in absorbance at 340 nm.

### **3.8 Functional Screening for Enzymes Catalyzing the Hydroxylation of Alkanes (Toward *Pseudomonas putida* KT2440 Libraries)**

Several enzymes are potentially useful to degrade alkanes. The method described below is based on the use of the bacterial strain *P. putida* KT2440 which can grow with C10 to C22 fatty alcohols but not with alkanes as a sole carbon and energy source. Then to perform this assay, it is necessary to use a metagenomic library based on pLAFR3 cosmid which is a vector with a broad host range, being able to replicate in different Gram-negative species [42] including *P. putida*. The library will be grown in a minimal media (e.g., M9) supplemented with the desired alkane, so only clones carrying the genes that codify for the enzymatic activities required to convert the substrate into fatty acids will grow in the supplemented minimal medium.

1. Prepare M9 agar plates (Subheading 2.7) supplemented with the desired alkane (SS8, Subheading 2.3). Prepare one plate for each alkane to be tested. Add 560 µL of 100 mg/mL alkane to each 35 mL of M9 agar (1.6 mg/mL alkane final concentration) supplemented with Tc10 (Subheading 2.6). Plate into 120 × 120 mm squared Petri dishes.
2. Replicate the clone library from the *P. putida* pLAFR3 library in the plates prepared in step 1.
3. Grow plates at 30°C for 48 h.
4. Positive clones will be those that are able to grow in each plate.

### **3.9 Functional Screening for Alcohol Dehydrogenase Activity**

Interconversion of alcohols, aldehydes, and ketones is involved in an astonishingly wide range of essential metabolic reactions in microorganisms. These redox reactions are catalyzed by oxidoreductases, including dehydrogenases [43]. Alcohol dehydrogenases catalyze

the reaction  $\text{alcohol} + \text{NAD(P)}^+ \leftrightarrow \text{aldehyde} + \text{NAD(P)H} + \text{H}^+$ . Carbonyl group from the aldehyde product drives to an intensely red Schiff base formation.

1. Add the appropriate volume of the desired substrate SS9 (Subheading 2.3) to reach a final concentration of 100 mM to 20 mL of Buffer AB3 (Subheading 2.2) supplemented with reagent R1 (Subheading 2.5) and mix by inverting the tube/bottle.
2. Overlay the agar plates containing individual clones with 20 mL of the mix from step 1.
3. Positive clones will appear like intensely red colonies surrounded by a zone of dye diffusion.

The protocol has been successfully applied for the screening of alcohol/aldehyde dehydrogenases capable to act toward glycerol and 1,2-propanediol from a sugar beet field [43]: 24 clones out of a total of 100,000 clones; hit rate of 1:4,170).

### **3.10 Functional Screening for Enzymes Catalyzing the Synthesis of Greasy Enantiomers (Using Libraries Created in *P. putida* KT2440)**

Several enzymes are potentially useful for the conversion of greasy molecules that can be used to synthesize pure enantiomers (e.g., alcohol dehydrogenases, hydroxynitrile lyases, benzoylformate decarboxylases, benzaldehyde lyases). Recently a growth selection method to identify new benzoylformate decarboxylases has been developed [44]. This method is based on the use of the strain *P. putida* KT2440, which can grow with benzaldehyde as a sole carbon and energy source. At the same time, this strain lacks the enzymes necessary to form benzaldehyde from several precursors (e.g., benzyl alcohol, benzoylformate, mandelonitrile, or benzoin). So, as explained in Subheading 3.8, when a metagenomic DNA is cloned in pLAFR3 cosmid, the library can be developed into *P. putida*. Then the published method can be applied to *P. putida* recombinant colonies from the generated metagenomic library. Clone library will be grown in minimal media (e.g., M9) supplemented with the mentioned precursors of benzaldehyde to detect alcohol dehydrogenase, hydroxynitrile lyase, benzoylformate decarboxylase, and benzaldehyde lyase activities.

1. Plate M9 agar medium (Subheading 2.7), supplemented with Tc10 (Subheading 2.6) and the desired benzaldehyde precursor substrate (at a final concentration of 10 mM from a stock solution of 100 mM in acetonitrile) into 120 × 120 mm squared Petri dishes. Prepare one plate for each enzymatic activity to be tested.
2. Replicate the clones from a *P. putida* pLAFR3 library in the plates prepared in step 1.
3. Grow plates at 30°C for up to 16–48 h.
4. Positive clones will be those that are able to grow in each plate.

A recent successful example of the application of such protocol is described in Henning et al. [44], where one positive clone, containing benzoylformate decarboxylase activity, was identified by screening 14,000 clones whose genomic material was transferred to *P. putida* KT2440, on an agar plate containing benzoylformate selective medium.

### **3.11 Functional Screening for General Esterase/Lipase Activity (Toward Greasy $\alpha$ -Naphthyl Acetate)**

This protocol is based on the use of the substrate  $\alpha$ -naphthyl acetate that is enzymatically hydrolyzed by esterases, liberating a free naphthol product [21]. This then couples with a diazonium compound (4-benzoylamino-2,5-dimethoxyaniline, Azoic Diazo No. 24; also known as Fast Blue RR solution), forming brown-colored deposits at sites of general esterase activity. Then positive clones will appear due to the formation of a dark brown precipitate.

1. Add 320  $\mu$ L of the substrate solution SS10 (Subheading 2.3) and 320  $\mu$ L of the reagent R2 (Subheading 2.5) to a Falcon tube containing 20 mL of Buffer AB4 and mix by inverting the tube.
2. Overlay the plates containing individual clones with 20 mL of the mix.
3. Positive clones will appear as dark brown colonies after 30 s to 60 min (*see* Note 8).

The protocol has been successfully applied for the screening of esterase and lipases from the  $\alpha/\beta$ -fold hydrolase superfamily from bacteriophage  $\lambda$ -based metagenome libraries of deep hypersaline anoxic basins in the Eastern Mediterranean Sea [45] (5 positives) and bovine rumen microflora (22 positives) [46].

### **3.12 Functional Screening for General Esterase/Lipase Activity (Toward Greasy Indoxyl Substrates)**

Indoxyl esters are aromatic compounds which can be hydrolyzed by an organophosphate-sensitive enzyme. The hydrolysis of indoxyl esters yields indoxyl, which react with molecular oxygen to form indigo that as explained before is a blue-colored compound.

1. Add 320  $\mu$ L of SS11 (Subheading 2.3) to a Falcon tube containing 20 mL of AB4 (Subheading 2.2) and mix by inverting the tube/bottle.
2. Overlay the plates containing individual clones with 20 mL of the mix.
3. Positive clones will appear as blue colonies after 30 s to 60 min.

A recent successful example of the application of such protocol is described in Alcaide et al. [18], where two positive clones have been identified by screening a bacteriophage  $\lambda$ -based metagenome library (14,000 phage particles) of crude oil-enriched seawater sample.

### **3.13 Functional Screening for General Lipase Activity (Toward Greasy Tributyrin)**

The following protocol is based on a published method for detection of lipolytic microorganisms in foodstuffs and other materials [47]. The assay is based on the use of tributyrin as substrate and on the ability of the secreted lipases to diffuse in the medium and to hydrolyze the tributyrin. That hydrolysis results in a clear halo formation surrounding lipolytic colonies.

1. Replicate clone library into SCM1 agar plates (Subheading 2.4).
2. Incubate the plates for 16 h at 37°C.
3. Positive clones will appear as colonies surrounded by a clear halo.

This protocol, that uses a common noncommercially valuable substrate (tributyrin), has been proven successful for the identification of esterase/lipase-like enzymes with interesting properties. Thus, recently a lipolytic enzyme from the cutinase family with polyethylene terephthalate-degrading activity has been identified from a fosmid library of a leaf-branch compost metagenome by functional screening using tributyrin agar plates [48].

### **3.14 Functional Screening for General Lipase Activity (Toward Rhodamine and Olive Oil)**

The protocol described below is based on previously published methods [49–51] and it uses the ability of rhodamine B to form colored compounds when reacting with acidic materials. When olive oil is hydrolyzed by a lipase, free fatty acids are completely ionized. Then the resulting liberated protons react with rhodamine B producing its cationic form. This cationic form reacts with the free fatty acids forming the colored compounds. In the following protocol, agar plates are pink. Clones expressing lipases are detected due to the observation of an orange fluorescent halo surrounding the colonies after UV light irradiation (350 nm).

1. Replicate clone library into SCM2 agar plates (Subheading 2.4).
2. Incubate the plates for 16 h at 37°C.
3. Place the plates under UV light (350 nm) and positive clones will appear as colonies surrounded by an orange fluorescent halo.

A recent successful example of the application of such protocol is described in Zheng et al. [52], where six positive clones were identified by screening 20,000 clones.

### **3.15 Functional Screening for General Lipase Activity (Toward Brilliant Green and Olive Oil)**

The following protocol is based on the method described by Svendsen and collaborators [53], modified in order to be applied over colonies growth in agar plates. This method is based on the formation of blue spots after hydrolysis of olive oil by a lipase. Thus, positive clones will appear as green/blue colonies surrounded by a clear halo.

1. Replicate clone library into SCM3 green agar plates (Subheading 2.4).
2. Incubate the plates for 24–96 h at 37°C.
3. Positive clones will appear as blue/green colonies.

### **3.16 Functional Screening for Phospholipase Activity**

The protocol described below is based in a previously published method [54] that uses the phospholipids from egg yolk to detect phospholipase activity. Hydrolysis of phospholipids drives to the liberation of fatty acids. Calcium forms a complex with the free fatty acids resulting in the formation of a precipitation halo around the colonies.

1. Replicate clone library into SCM4 agar plates (Subheading 2.4).
2. Incubate the plates for 16 h at 37°C.
3. Positive clones will appear as colonies surrounded by a precipitation halo.

### **3.17 Functional Screening for Hydrolases Using pH Indicator and General Greasy Esters**

When an ester conjugated molecule is hydrolyzed by an esterase/lipase or other hydrolase, acetic acid is liberated occurring acidification of the medium. In the protocol described below, pH indicator phenol red will turn yellow as a consequence of that acetic acid formation, so positive clones will appear as yellow clones. This protocol has been successfully applied to different substrates such as short-to-long acetyl, propionyl, and butyryl esters of long fatty acids, triglycerides, and cinnamic esters as well as a broad range of enantiomeric esters (Subheading 2.3). This method can be applied also to detect dehalogenases using halo acids or halo alkanes as substrates. Dehalogenases are hydrolases that remove a halogen atom from a substrate, like an acid or an alkane molecule. They are thus of potential interest for the production of modified halogenated chemicals for industrial applications and represent important tools for bioremediation [55]. During the dehalogenation a proton is liberated at the expense of a single water molecule so the enzymatic reaction can be followed because of the protons produced, which, in turn, can be monitored by a pH indicator.

1. Add 320–1,000  $\mu\text{L}$  of the desired substrate (from SS12 or SS13 list; (Subheading 2.3) at 100 mg/mL (*see Note 9*) to 20 mL of buffer AB5 and mix by inverting the tube/bottle.
2. Overlay the plates containing individual clones with 20 mL of the mix (*see Note 10*).
3. Positive clones will appear as yellow colonies on a red background.

A recent successful example of the application of such protocol is described in Beloqui et al. [22], where an esterase-haloacid dehalogenase-positive clone was identified by screening a

bacteriophage  $\lambda$ -based metagenome library of crude oil-enriched seawater sample. Recently, a clone (hit rate 1:1,375) versatile esterase (CNIE1) from the  $\alpha/\beta$ -hydrolase family able to act toward greasy molecules such as polyaromatic hydrocarbon (phenanthrene, anthracene, naphthalene, benzoyl, protocatechuate, and phthalate) esters has been identified by using naphthalene carboxylic acid methyl ester as substrate [12].

### **3.18 Functional Screening for Enzymes Catalyzing the Formation of Unsaturated Fatty Acids**

Fatty acid-modifying enzymes are of great biotechnological interest, especially those catalyzing the production of unsaturated fatty acids (UFA). These fatty acids are widely sought as food or health additives, as valuable precursor molecules, and for applications in petrol chemistry. Several systems are known for UFA production in bacteria. For instance, fatty acid desaturases are capable of introducing double bonds into existing fatty acids of various chain lengths. UFAs can also be produced by de novo biosynthesis. Most bacteria produce C18:1 UFAs using an alternate function of the standard fatty acid synthesis pathway. Some bacteria from deep-sea environments, however, are known to produce long chain, polyunsaturated fatty acids (e.g., eicosapentaenoic acid (C20:5) and docosahexaenoic acid (C22:6)) to cope with the low temperatures of those habitats. The production of those fatty acids involves enzymes which share similarities with polyketide synthases and fatty acid synthases [56]. The genes involved in known systems of this type are usually located in a single cluster of about 20 kb in size. Enzymes involved in UFA formation mainly function as part of an adaptive mechanism to enhance cold tolerance [57]. Thus a temperature-based screening method to identify such enzymes could be established. *E. coli* cells containing a metagenomic library will be grown at low temperatures to identify faster growing colonies with increased cold tolerance. While the focus of this screening system is on UFA-forming enzymes, it is also possible to identify other types of proteins that enhance cell growth at low temperatures. Several fatty acid desaturases originating from *Arthrospira platensis*, *Synechocystis*, *Bacillus subtilis*, and *Stappia* aggregate were already heterologously expressed in *E. coli* BL21(DE3) to confirm the functionality of the screening method. *E. coli* BL21(DE3) containing expression vectors harboring putative desaturase genes are incubated at low temperatures (5–25°C) and their growth is compared to *E. coli* BL21(DE3) cells harboring the empty expression vector.

1. Replicate the clone library in LBaCmCCFAS (Subheading 2.7).
2. Incubate the plates at different temperatures between 5 and 25°C for several days.
3. Select the clones that grow faster at each temperature.

The applicability of other *E. coli* strains including *E. coli* M5, M8, and PAM155 which are unable to grow at low temperatures due to a mutation in the genes *fabA* (M8, PAM155) or *fabB* (M5) which are vital for UFA synthesis [58, 59] has been also investigated. At restrictive temperatures, these strains can only grow in culture medium supplemented with exogenous UFAs. Hence, heterologous expression of genes or gene clusters encoding desaturating activities should relieve this phenotype resulting in growth of such cold-sensitive *E. coli* expression strains.

### 3.19 Screening Method Statistics: Summary

Table 1 summarizes the list of target enzymes, cost time, and hit rates for the different substrate-detection methods (e.g., color change, growth ability) described above. The table contains information regarding different enzymatic activities and different substrates within them to screen. For comparative purposes, statistics are also provided for the utilization of other enzyme activities and substrates. For references and detailed description, see above and information reported in the table.

---

## 4 Notes

1. Unless otherwise stated, chemicals, biochemicals, and solvents were purchased from Sigma Chemical Co. (St. Louis, MO, USA), Aldrich (Oakville, ON), or Fluka (Oakville, ON) and were of p.a. (pro-analysis) quality.
2. Substrate solutions must be prepared preferably the day of the assay, although they can be stored for up to 24 h at 4°C. In case of ester substrates, they can be stored at -20°C for longer incubations. For antibiotics and IPTG solutions, store them at -20°C.
3. Sterilize by filtering through a 0.22 µm syringe filter.
4. Olive oil substrate is an emulsion of olive oil in gum arabic so to get the emulsion, vigorous agitation or sonication should be applied. To avoid emulsion disruption, the autoclaved substrate should be used on the day of preparation.
5. To ensure uniform distribution of olive oil substrate in each plate, mix vigorously the bottle containing LB olive oil brilliant green agar before plating every 4–5 plates or as many times as necessary.
6. To be sure that all positive clones have been detected, once positive clones have been identified, mark them with a permanent marker and leave the plates in the bench at room temperature till next day. Look again for new yellow clones and pick them in a new 96 multi-well plate.

**Table 1**  
**List of target enzymes, cost time, and hit rates for the different substrate-detection methods**

<b>Panel A: statistics for enzyme activities</b>				
<b>Enzymatic activity</b>	<b>Positive incidence range (mean)</b>	<b>Detection method</b>	<b>Assay time</b>	<b>Reference</b>
Esterases-lipases	1:11 to 1:193,200 (1:17,321)	Color/halo	1 min to 48 h	See below and in the text
Oxidoreductases	1:32 to 1: 20,000 (1:6,671)	Color/ growth	1 min to 96 h	
Penicillin G acylases	1:333	Color	1 min to 96 h	
Phosphatases	1:2,843	Color	1 min to 48 h	
Proteases	1:833 to 1:30,000 (1:9,318)	Halo	24–48 h	
Glycosidases	1:43 to 1:700,000 (1:31,189)	Color/halo	1 min to 96 h	
<b>Panel B: statistics for substrate-dependent hydrolytic (e.g., esterase and lipase-like) activity</b>				
<b>Substrate</b>	<b>Positive incidence range (mean)</b>	<b>Detection method</b>	<b>Assay time</b>	<b>Reference</b>
$\alpha$ -NA	1:1,375 to 1:77,600 (1:19,924)	Color	1–60 min	[21]
Indoxyl acetate	1:700	Color	1–60 min	[18]
Olive oil	1:1,000 to 1:50,000 (1:25,500)	Color/Halo	16–48 h	[52, 53]
Tributyrin	1:11 to 1:100,000 (1:13,289)	Halo	16–48 h	[60–64]
Tricaprylin	1:3,937 to 1:193,200 (1:68,279)	Halo	16–48 h	[60–64]
Triolein	1:7,680 to 1:36,000 (1:19,768)	Halo	16–48 h	[52]
Esters	1:191 to 1:30,000 (1:20,064)	Color	1–300 min	[12, 22]
Tween-20 and 80	1:500 to 1: 26,496 (1:13,498)	Halo	16–48 h	[65, 66]
5-Bromo-4-chloro-3-indolylcaprylate	1:7,000 to 1:93,000 (1:50,000)	Halo	1–300 min	[67]
pNP-dodecanoate	1:706	Color	1–300 min	[68]
Polyethylene terephthalate	1:21,400	Halo	16–48 h	[48]
Poly (DL-lactic acid)	1:13,333	Halo	16–48 h	[66, 69]
Egg yolk	1:833 to 1: 30,000 (9,318)		16–48 h	[54]

(continued)

**Table 1**  
(continued)

<b>Panel C: statistics for substrate-dependent oxidoreductase activity</b>				
<b>Substrate</b>	<b>Positive incidence range (mean)</b>	<b>Detection method</b>	<b>Assay time</b>	<b>Reference</b>
Catechol	1:111 to 1:1,842 (1:946)	Color	1–60 min	[25]
Guaiacol	1:8,000	Color	1–60 min	[33]
Indigo	1:6,000 to 1:20,000 (1:10,889)	Color	48–96 h	[27, 28]
Phenol	1:32	Color	16–48 h	[70]
Alkanes (e.g., hexadecane)	1:69	Growth	48 h	[71]
Glycerol/1,2-propanediol	1:4,170	Color	24 h	[43]
Benzaldehyde	1:14,000	Growth	16–48 h	[44]
12-pNCA	n.d.	Color	1–60 min	[38–40]
HOHD:HOPHD	n.d.	Color	1–60 min	[18]
Syringaldazine	n.d.	Color	1–60 min	[33]
UFA synthesis	n.d.	Growth	24–48 h	[56–59]
ABTS	n.d.	Color	16 h	[32, 33]

Incidence rate (clones with the desired activity referred to the total number of clones screened) is reported for studies in which metagenomic clone libraries were subjected to functional naïve screens. Note that to avoid biases due to the type of libraries, only studies considering the screen of fosmid clones have been considered. Statistics for general enzyme-dependent screens (A), for screening hydrolytic activity using different substrates (B), and for screening oxidoreductase activity using different substrates (C) are shown

*n.d.* not determined before the number of total screened clones was not described

7. Substrates for *meta*-cleavage product hydrolases are stable for at least 4–5 h but it is preferably to use them immediately.
8. Don't leave the plates for more than 10 min as at the end all the colonies will turn brown, but it doesn't mean that the clones are necessarily esterase positive.
9. For some substrates, particularly esters (SS12), or haloacids, and haloalkanes (SS13), higher initial concentrations up to 200 mg/mL could be necessary to reach positive clones. Such concentrations are needed as the functional screens based on pH indicators require accumulation of acid (after hydrolysis of an ester) before color change is observed.
10. In this case, in order to save substrate, and depending on the number of individual clones to be checked, you can perform the functional screening pipetting the substrate drop by drop over each individual clone.

## Acknowledgments

The authors gratefully acknowledge the financial support provided by the European Community project MAMBA (FP7-KBBE-2008-226977), MAGIC-PAH (FP7-KBBE-2009-245226), ULIXES (FP7-KBBE-2010-266473), KILL-SPILL (FP7-KBBE-2012-312139), and MicroB3 (FP7-OCEAN.2011-2-287589). We thank EU Horizon 2020 Program for the support of the Project INMARE H2020-BG-2014-2634486. This work was further funded by grants BIO2011-25012, PCIN-2014-107, and BIO2014-54494-R from the Spanish Ministry of Economy and Competitiveness. The present investigation was also funded by the Spanish Ministry of Economy and Competitiveness within the ERA NET IB2, grant number ERA-IB-14-030. The authors gratefully acknowledge the financial support provided by the European Regional Development Fund (ERDF).

## References

1. Bamforth SM, Singleton I (2005) Bioremediation of polycyclic aromatic hydrocarbons: current knowledge and future directions. *J Chem Technol Biotechnol* 80:723–736
2. Kästner M (2000) Degradation of aromatic and polyaromatic compounds. In: Rehm HJ, Reed G (eds) *Biotechnology*. Wiley-VCH, Weinheim, pp 211–239
3. Guazzaroni ME, Herbst FA, Lores I, Javier Tamames J, Peláez AI, López-Cortés N, Alcaide M, Del Pozo MV, Vieites JM, von Bergen M, Gallego JLR, Bargiela R, López-López A, Pieper DH, Ramon Rossello-Mora R, Sánchez J, Seifert J, Ferrer M (2013) Metaproteogenomic insights beyond bacterial response to naphthalene exposure and biostimulation. *ISME J* 7:122–136
4. Volkering F, Breure AM, van Adel JG (1993) Effect of microorganisms on the bioavailability and biodegradation of crystalline naphthalene. *Appl Microbiol Biotechnol* 40:535–540
5. Bosma TNP, Middeldorp PJM, Scraa G, Zender AJB (1997) Mass transfer limitation of biotransformation: quantifying bioavailability. *Environ Sci Technol* 31:248–252
6. Dolfing J, Xu A, Gray ND, Larter SR, Head IM (2009) The thermodynamic landscape of methanogenic PAH degradation. *Microbiol Biotechnol* 2:566–574
7. Moscoso F, Ferreira L, Deive FJ, Morán P, Sanromán MA (2013) Viability of phenanthrene biodegradation by an isolated bacterial consortium: optimization and scale-up. *Bioprocess Biosyst Eng* 36:133–141
8. Habe H, Omori T (2003) Genetic of polycyclic aromatic hydrocarbon metabolism in diverse aerobic bacteria. *Biosci Biotechnol Biochem* 67:225–243
9. Peng RH, Xiong AS, Xue Y, Fu XY, Gao F, Zhao W, Tian YS, Yao QH (2008) Microbial biodegradation of polyaromatic hydrocarbons. *FEMS Microbiol Rev* 32:927–955
10. Singleton DR, Hu J, Aitken DA (2012) Heterologous expression of polycyclic aromatic hydrocarbon ring-hydroxylating dioxygenase genes from a novel pyrene-degrading Betaproteobacterium. *Appl Environ Microbiol* 78:3552–3559
11. Shah V, Jain K, Desai C, Madamwar D (2012) Molecular analyses of microbial activities involved in bioremediation. In: Satyanarayana T, Johri BN, Prakash A (eds) *Microorganisms in environmental management: microbes and environment*. Springer, Berlin, pp 221–247
12. Martínez-Martínez M, Lores I, Peña-García C, Bargiela R, Reyes-Duarte D, Guazzaroni ME, Peláez AI, Sánchez J, Ferrer M (2014) Biochemical studies on a versatile esterase that is most catalytically active with polyaromatic esters. *Microbiol Biotechnol* 7:184–191
13. Bergmann F, Selesi D, Weinmaier T, Tischler P, Rattei T, Meckenstock RU (2011) Genomic insights into the metabolic potential of the

- polycyclic aromatic hydrocarbon degrading sulfate-reducing *Deltaproteobacterium* N47emi\_2391. *Environ Microbiol* 13:1125–1137
14. Chauhan A, Layton AC, Williams DE, Smartt AE, Ripp S, Karpinets TV, Brown SD, Saylor GS (2011) Draft genome sequence of the polycyclic aromatic hydrocarbon-degrading, genetically engineered bioluminescent bioreporter *Pseudomonas fluorescens* HK44. *J Bacteriol* 193:5009–5010
  15. Fernández-Arrojo L, Guazzaroni ME, López-Cortés N, Beloqui A, Ferrer M (2010) Metagenomic era for biocatalyst identification. *Curr Opin Biotechnol* 21:725–733
  16. Shizuya H, Birren B, Kin UJ, Mancino V, Slepak T, Tachiiri Y, Simon M (1992) Cloning and stable maintenance of 300-kilobase-pair fragments of human DNA in *Escherichia coli* using an F factor-based vector. *Proc Natl Acad Sci* 89:8794–8797
  17. Vieites JM, Guazzaroni ME, Beloqui A, Golyshin PN, Ferrer M (2010) Molecular methods to study complex microbial communities. In: Streit WR, Daniel R (eds) *Metagenomics. Methods and protocols*. Humana, Totowa, pp 1–37
  18. Alcaide M, Tornes J, Stogios PJ, Xu X, Gertler C, Di Leo R, Bargiela R, Lafraya A, Guazzaroni ME, López-Cortés N, Chernikova TN, Golyshina OV, Nechitaylo TY, Plumeier I, Pieper DH, Yakimov MM, Savchenko A, Golyshin PN, Ferrer M (2013) Single residues dictate the co-evolution of dual esterases: MCP hydrolases from the  $\alpha/\beta$  hydrolase family. *Biochem J* 454:157–166
  19. Happe B, Eltis LD, Poth H, Hedderich R, Timmis KN (1993) Characterization of 2,2',3-trihydroxybiphenyl dioxygenase, an extradiol dioxygenase from the dibenzofuran- and dibenzo-p-dioxin-degrading bacterium *Sphingomonas* sp. strain RW1. *J Bacteriol* 175:7313–7320
  20. Junca H, Plumeier I, Hecht HJ, Pieper DH (2004) Difference in kinetic behaviour of catechol 2,3-dioxygenase variants from a polluted environment. *Microbiology* 150:4181–4187
  21. Reyes-Duarte D, Ferrer M, Garcia-Arellano H (2012) Functional-based screening methods for lipases, esterases and phospholipases in metagenomic libraries. In: Sandoval G (ed) *Lipases and phospholipases: methods and protocols*. Springer, New York, pp 101–113
  22. Beloqui A, Polaina J, Vieites JM, Reyes-Duarte D, Torres R, Golyshina OV, Chernikova TN, Waliczek A, Aharoni A, Yakimov MM, Timmis KN, Golyshin PN, Ferrer M (2010) Novel hybrid esterase-haloacid dehalogenase enzyme. *Chembiochem* 11:1975–1978
  23. Alcaide M, Tchigvintsev A, Martínez-Martínez M, Popovic A, Reva ON, Lafraya A, Bargiela R, Nechitaylo TY, Matesanz R, Cambon-Bonavita MA, Jebbar M, Yakimov MM, Savchenko A, Golyshina OV, Yakunin AF, Golyshin PN, Ferrer M (2015) Identification and characterization of carboxyl esterases of gill chamber-associated microbiota in the deep-sea shrimp *Rimicaris exoculata* using functional metagenomics. *Appl Environ Microbiol* 81(6):2125–2136
  24. Brennerova MV, Josefičova J, Brenner V, Pieper DH, Junca H (2009) Metagenomics reveals diversity and abundance of meta-cleavage pathways in microbial communities from soil highly contaminated with jet fuel under air-sparging bioremediation. *Environ Microbiol* 11:2216–2227
  25. Suenaga H, Ohnuki T, Miyazaki K (2007) Functional screening of a metagenomic library for genes involved in microbial degradation of aromatic compounds. *Environ Microbiol* 9:2289–2297
  26. Johannes TW, Woodyer RD, Zhao H (2006) High-throughput screening methods developed for oxidoreductases. In: Raymond JL (ed) *Enzyme assays: high-throughput screening, genetic selection and fingerprinting*. Wiley-VCH, Weinheim, pp 77–93
  27. Singh A, Singh Chauhan N, Thulasiram HV, Taneja V, Sharma R (2010) Identification of two flavin monooxygenases from an effluent treatment plant sludge metagenomic library. *Bioresour Technol* 101:8481–8484
  28. Lim HK, Chung EJ, Kim JC, Choi GJ, Jang KS, Chung YR, Cho KY, Lee SW (2005) Characterization of a forest soil metagenome clone that confers indirubin and indigo production on *Escherichia coli*. *Appl Environ Microbiol* 71:7768–7777
  29. Hernández MJ, Andújar E, Ríos JL, Kaschabek SR, Reineke W, Santero E (2000) Identification of a serine hydrolase which cleaves the alicyclic ring of tetralin. *J Bacteriol* 182:5448–5453
  30. Thurston CF (1994) The structure and function of fungal laccases. *Microbiology* 140:19–26
  31. Baldrian P (2006) Fungal laccases – occurrence and properties. *FEMS Microbiol Rev* 30:215–242
  32. Eichlerová I, Šnajdr J, Baldrian P (2012) Laccase activity in soils: considerations for the measurement of enzyme activity. *Chemosphere* 88:1154–1160

33. Beloqui A, Pita M, Polaina J, Martínez-Arias A, Golyshina OV, Zumárraga M, Yakimov MM, García-Arellano H, Alcalde M, Fernández VM, Elborough K, Andreu JM, Ballesteros A, Plou FJ, Timmis KN, Ferrer M, Golyshin PN (2006) Novel polyphenol oxidase mined from a metagenome expression library of bovine rumen: biochemical properties, structural analysis, and phylogenetic relationships. *J Biol Chem* 28:22933–22942
34. Stegeman JJ, Lech JJ (1991) Cytochrome P-450 monooxygenase systems in aquatic species: carcinogen metabolism and biomarkers for carcinogen and pollutant exposure. *Environ Health Perspect* 90:101–109
35. Juchau MR (1990) Substrate specificities and functions of the P450 cytochromes. *Life Sci* 47:2385–2394
36. Guengerich FP, Gillam EM, Shimada T (1996) New applications of bacterial systems to problems in toxicology. *Crit Rev Toxicol* 26:551–583
37. Schneider S, Wubbolts MG, Sanglard D, Witholt B (1998) Biocatalyst engineering by assembly of fatty acid transport and oxidation activities for *In vivo* application of cytochrome P-450BM-3 monooxygenase. *Appl Environ Microbiol* 64:3784–3790
38. Schwaneberg U, Schmidt-Dannert C, Schmitt J, Schmid RD (1999) A continuous spectrophotometric assay for P450 BM-3, a fatty acid hydroxylating enzyme, and its mutant F87A. *J Biotechnol* 269:359–366
39. Schwaneberg U, Otey C, Cirino PC, Farinas E, Arnold FH (2001) Cost-effective whole-cell assay for laboratory evolution of hydroxylases in *Escherichia coli*. *J Biomol Screen* 6:111–117
40. Tee KL, Schwaneberg U (2006) A screening system for the directed evolution of epoxigenases: importance of position 184 in P450BM3 for stereoselective styrene epoxidation. *Angew Chem Int Ed* 45:5380–5383
41. Lentz O, Feenstra A, Habicher T, Hauer B, Schmid RD, Urlacher VB (2006) Altering the regioselectivity of cytochrome P450 CYP102A3 of *Bacillus subtilis* by using a new versatile assay system. *ChemBioChem* 7:345–350
42. Guazzaroni ME, Golyshin PN, Ferrer M (2010) Analysis of complex microbial communities through metagenomic survey. In: Marco D (ed) *Metagenomics: theory, methods and applications*. Caister Academic Press, Norfolk, pp 55–77
43. Knietsch A, Waschowitz T, Bowien S, Henne A, Daniel R (2003) Construction and screening of metagenomic libraries derived from enrichment cultures: generation of a gene bank for genes conferring alcohol oxidoreductase activity on *Escherichia coli*. *Appl Environ Microbiol* 69:1408–1416
44. Henning H, Leggewie C, Pohl M, Müller M, Eggert T, Jaeger KE (2006) Identification of novel benzoylformate decarboxylases by growth selection. *Appl Environ Microbiol* 72:7510–7517
45. Ferrer M, Golyshina OV, Chernikova TN, Khachane AN, Martins Dos Santos VA, Yakimov MM, Timmis KN, Golyshin PN (2005) Microbial enzymes mined from the Urania deep-sea hypersaline anoxic basin. *Chem Biol* 12:895–904
46. Ferrer M, Golyshina OV, Chernikova TN, Khachane AN, Reyes-Duarte D, Santos VA, Strompl C, Elborough K, Jarvis G, Neef A, Yakimov MM, Timmis KN, Golyshin PN (2005) Novel hydrolase diversity retrieved from a metagenome library of bovine rumen microflora. *Environ Microbiol* 7:1996–2010
47. Anderson JA (1940) The use of tributyrin agar in dairy bacteriology. *Rept Proc Int Congr Microbiol* 3:726
48. Sulaiman S, Yamato S, Kanaya E, Kim JJ, Koga Y, Takano K, Kanaya S (2012) Isolation of a novel cutinase homolog with polyethylene terephthalate-degrading activity from leaf-branch compost by using a metagenomic approach. *Appl Environ Microbiol* 78:1556–1562
49. Kouker G, Jaeger KE (1987) Specific and sensitive plate assay for bacterial lipases. *Appl Environ Microbiol* 53:211–213
50. Mackenzie RD, Blohm TR, Auxier EM, Luther AC (1967) Rapid colorimetric micromethod for free fatty acids. *J Lipid Res* 8:589–597
51. Höfelmann M, Kittsteiner-Eberle R, Schreier P (1983) Ultrathin-layer agar gels: a novel print technique for ultrathin-layer isoelectric focusing of enzymes. *Anal Biochem* 128:217–222
52. Zheng J, Liu C, Liu L, Jin Q (2013) Characterisation of a thermo-alkali-stable lipase from oil-contaminated soil using a metagenomic approach. *Syst Appl Microbiol* 36:197–204
53. Svendsen A, Clausen IG, Okkels JS, Thellersen M (1995) A method of preparing a variant of a lipolytic enzyme. Patent: Novo Nordisk, WO 95/22615
54. Price MF, Wilkinson ID, Gentry LO (1982) Plate method for detection of phospholipase activity in *Candida albicans*. *Sabouraudia* 20:7–14

55. Chang CH, Schindler JF, Unkefer CJ, Vanderberg LA, Brainard JR, Terwilliger TC (1999) In vivo screening of haloalkane dehalogenase mutants. *Bioorg Med Chem* 7(2175):2181
56. Mansilla MC, Banchio CE, de Mendoza D (2008) Signalling pathways controlling fatty acid desaturation. *Subcell Biochem* 49:71–99
57. Okuyama H, Orikasa Y, Nishida T, Watanabe K, Morita N (2007) Bacterial genes responsible for the biosynthesis of eicosapentaenoic and docosahexaenoic acids and their heterologous expression. *Appl Environ Microbiol* 73:665–670
58. Broekman JH, Steenbakkers JF (1974) Effect of the osmotic pressure of the growth medium on *fabB* mutants of *Escherichia coli*. *J Bacteriol* 117:971–977
59. Johnson BF, Greenberg J (1975) Mapping of *sul*, the suppressor of *lon* in *Escherichia coli*. *J Bacteriol* 122:570–574
60. Glogauer A, Martini VP, Faoro H, Couto GH, Müller-Santos M, Monteiro RA, Mitchell DA, de Souza EM, Pedrosa FO, Krieger N (2011) Identification and characterization of a new true lipase isolated through metagenomic approach. *Microb Cell Fact* 10:54–68
61. Song JK, Chung B, Oh YH, Rhee JS (2002) Construction of DNA-shuffled and incrementally truncated libraries by a mutagenic and unidirectional reassembly method: changing from a substrate specificity of phospholipase to that of lipase. *Appl Environ Microbiol* 68:6146–6151
62. Liu K, Wang J, Bu D, Zhao S, McSweeney C, Yu P, Li D (2009) Isolation and biochemical characterization of two lipases from a metagenomic library of China Holstein cow rumen. *Biochem Biophys Res Commun* 385:605–611
63. Tirawongsaroj P, Sriprang R, Harnpicharnchai P, Thongaram T, Champreda V, Tanapongpipat S, Pootanakit K, Eurwilaichitr L (2008) Novel thermophilic and thermostable lipolytic enzymes from a Thailand hot spring metagenomic library. *J Biotechnol* 133:42–49
64. Colin DY, Deprez-Beauclair P, Silva N, Infantes L, Kerfelec B (2010) Modification of pancreatic lipase properties by directed molecular evolution. *Protein Eng Des Sel* 23:365–373
65. Heravi KM, Eftekhari F, Yakhchali B, Tabandeh F (2008) Isolation and Identification of a Lipase producing *Bacillus* sp. from soil. *Pak J Biol Sci* 11:740–745
66. Okamura Y, Kimura T, Yokouchi H, Meneses-Osorio M, Katoh M, Matsunaga T, Takeyama H (2010) Isolation and characterization of a GDSL esterase from the metagenome of a marine sponge associated bacteria. *Mar Biotechnol* 12:395–402
67. Li G, Wang K, Liu YH (2008) Molecular cloning and characterization of a novel pyrethroid hydrolyzing esterase originating from the metagenome. *Microb Cell Fact* 7:38–47
68. Dror A, Shemesh E, Dayan N, Fishman A (2014) Protein engineering by random mutagenesis and structure-guided consensus of *Geobacillus stearothermophilus* lipase T6 for enhanced stability in methanol. *Appl Environ Microbiol* 80:1515–1527
69. Akutsu-Shigeno Y, Teeraphatpornchai T, Teamtisong K, Nomura N, Uchiyama H, Nakahara T, Nakajima-Kambe T (2003) Cloning and sequencing of a poly(DL-lactic acid) depolymerase gene from *Paenibacillus amylolyticus* strain TB-13 and its functional expression in *Escherichia coli*. *Appl Environ Microbiol* 69:2498–2504
70. Choi SL, Rha E, Lee SJ, Kim H, Kwon K, Jeong YS, Rhee YH, Song JJ, Kim HS, Lee SG (2014) Toward a generalized and high-throughput enzyme screening system based on artificial genetic circuits. *ACS Synth Biol* 3:163–171
71. Xu M, Xiao X, Wang F (2008) Isolation and characterization of alkane hydroxylases from a metagenomic library of Pacific deep-sea sediment. *Extremophiles* 12:255–262

# Screening for Enantioselective Lipases

Thomas Classen, Filip Kovacic, Benjamin Lauinger, Jörg Pietruszka,  
and Karl-Erich Jaeger

## Abstract

Many lipolytic enzymes are enantioselective thus being able to distinguish between two enantiomers of a given racemic substrate. This property together with ample availability and comparatively easy handling makes lipolytic enzymes the most widely used class of biocatalysts in the chemical and pharmaceutical industries. However, lipase activity as well as selectivity is often negligible towards typical industrial substrates which usually do not resemble natural ones. Therefore, suitable enzymes must first be identified, usually by activity-based screening methods which, however, differ in reliability, throughput and surrogate function. Here, we describe important parameters determining the reliability and reproducibility of such screening systems for five different assays in detail. Moreover, comprehensive protocols for the synthesis of enantiopure lipase substrates and their use for screening of enantioselective lipases are provided.

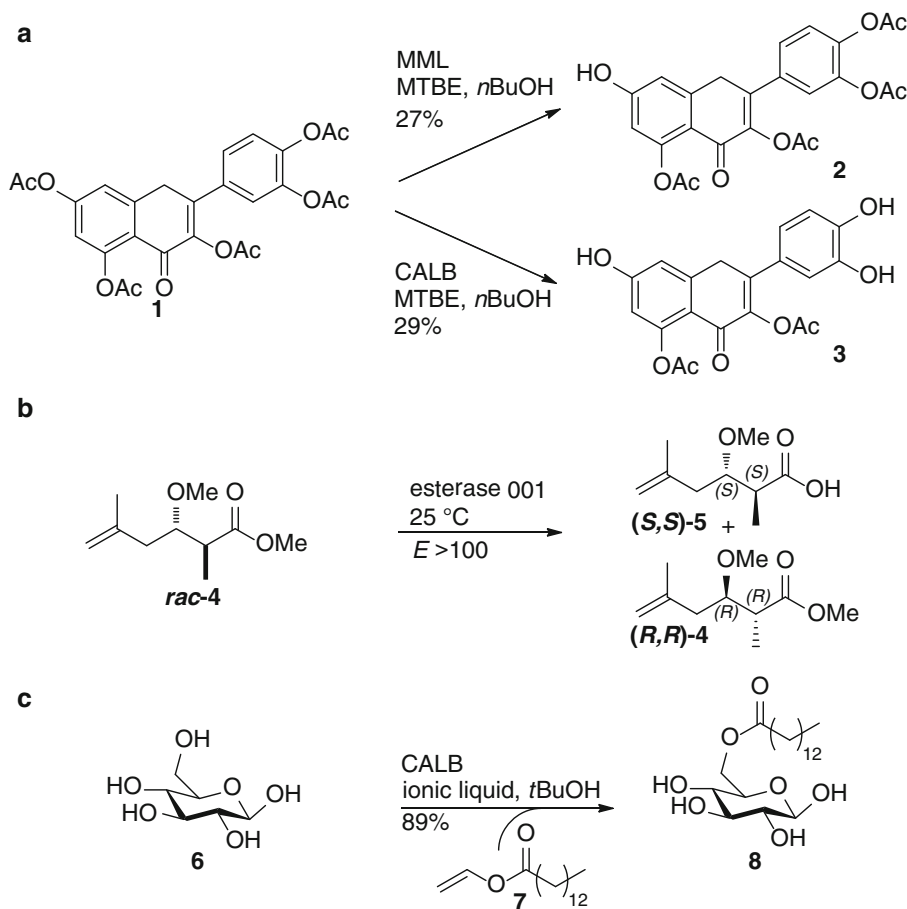
**Keywords:** Adrenaline assay, Agar plate assay, Colorimetric assay, Fluorometric assay, Quick E assay

---

## 1 Introduction

The application of lipases (EC 3.1.1.3) at an industrial scale was driven by the fact that these enzymes do not require costly cofactors for activity and they are considerably stable at high temperatures as well as in organic solvents, i.e. under biotechnological process conditions [1, 2]. The physiological function of lipases is the hydrolysis of lipidic ester substrates although they catalyse the synthesis of esters under low water conditions as well [3]. Complete or partial substitution of water by an organic solvent increases the solubility of hydrophobic substrates, on the one hand, and shifts the thermodynamic equilibrium of a lipase reaction towards the product side, on the other hand.

Both hydrolytic and synthetic lipase reactions are used in organic chemistry mainly due to the regio- and stereoselectivity of lipases [4, 5], e.g. for the regioselective synthesis of sugar fatty acid ester derivatives [6], regioselective deacetylation of quercetin pentaacetate [7, 8] or the enantioselective synthesis of pycnimeric acid



**Scheme 1** (a) Regioselective deprotection of quercetin pentaacetate (**1**) by *Mucor miehei* lipase (MML) and *Candida antarctica* lipase B (CALB) to the flavones **2** and **3** [7, 8]. (b) Kinetic resolution for the enantioselective synthesis of psymberic acid (**5**) from its racemic ester (**4**) [9]. (c) Selective synthesis of myristic acid ester (**8**) from glucose (**6**) and vinyl myristate (**7**) using CALB [25]. These reactions can be carried out chemically only by labour-intensive reaction sequences including many steps and with much lower final yields. Yields (%) and enantioselectivity (% *ee*) are given; *MTBE* methyl *tert*-butyl ether, *nBuOH* *n*-butanol, *tBuOH* *tert*-butanol, *nPrOH* *n*-propanol

by kinetic resolution [9] (Scheme 1). While regioselectivity can be harnessed for precise (de-)protections or acylations allowing a target-oriented processing of the very molecule, kinetic resolutions are an easy way to obtain enantiopure compounds. However, substrate specific transformations require identification of highly selective enzymes. Typically, most lipases lack selectivity for industrial substrates; therefore, suitable enzymes must be identified. To this end, three conceptually different approaches were developed: (1) screening of commercially available enzymes [10, 11]; (2) screening of rationally or randomly generated libraries obtained from a specific enzyme [12, 13]; or (3) screening of libraries constructed

with DNA isolated from uncultured microorganisms (so-called metagenomic libraries) [14–18]. Molecular biological methods for the construction of large libraries based on error-prone polymerase chain reaction (PCR), degenerate oligonucleotides, mutator strains, DNA shuffling and direct or indirect methods for the extraction and cloning of environmental DNA were successfully applied in the quest for isolating enzymes with increased enantioselectivity [19–21]. Recently developed novel approaches for the generation of combinatorial libraries using solid-phase gene synthesis showed clear advantages over conventional PCR methods [22].

Obviously, the identification of enantioselective biocatalysts from large libraries requires efficient screening techniques. The respective screening systems should provide reliable analytic outputs for about 1,000–100,000 variants, ideally within a day. Furthermore, screening substrates should be derivatives or analogues of the substrate of interest, so-called surrogate substrates. In addition to our previously published detailed protocols for determination of lipase activities [23, 24], we describe here protocols for the synthesis of chromogenic and fluorogenic lipase substrates and screening methods to identify enantioselective lipases developed in our laboratory.

### **1.1 Methods to Determine the Stereopreference of an Enzyme**

By definition, enantiomers do not behave different from each other in an achiral environment. Unfortunately, most routine analytics such as chromatography methods (GC, HPLC, TLC), spectroscopy (UV/Vis, IR) or mass spectrometry are achiral themselves and thus do not differentiate between enantiomers. Three strategies to overcome this problem have been successfully developed. Firstly, achiral methods can be converted into chiral ones. Prominent examples are GC or HPLC which can be carried out using chiral stationary phases to separate enantiomers (Fig. 1a; [26]). As a more sophisticated attempt, NMR-spectroscopy has been used for enantiomeric analysis using chiral solvents or adding chiral ligands to the compound of interest [27, 28]. The aforementioned strategy – analysing the enantiomers directly by diastereomeric interactions – is the only way to analyse reactions where stereogenic information is generated by asymmetric synthesis from a prochiral compound. The strategies only work when the stereogenic information is already present in the substrate, which is true for most lipase substrates. In the second approach, the enantiomers are chemically converted into pseudo-enantiomers to make them inherently distinguishable (Fig. 1b), often by isotope labelling of one enantiomer using deuterium or  $^{13}\text{C}$  [29–32]. The tested enzyme ignores the difference between these enantiomers and converts the substrate according to its natural stereopreference, but the products or the residual substrate can be easily analysed and distinguished with standard mass spectrometric, NMR- and IR-spectroscopic methods



enantiomers separately (Fig. 1c). Although the ratio of these rates reflects the stereoselectivity of the particular enzyme, only an apparent stereoselectivity can be calculated because reaction conditions are non-competitive, i.e. the enzyme cannot differentiate between the two enantiomers at the same time as only one of them is available in the reaction mixture. Thus, inhibiting effects or lower conversion rates of one enantiomer, which might occur in a competitive fashion, can hardly be detected. Only if the conversion rate of the racemic mixture is similar to the arithmetic mean of both individual conversion rates, the apparent stereoselectivity is most likely similar to the effective one. This approach allows using simple spectroscopic or chromatographic methods without the need for any previous chiral modifications.

## 1.2 The Screening System

Three main criteria characterise the systems used to screen for enantioselectivity, namely their **throughput**, **reliability** and the use of **surrogate substrates**. A comparison of various screening methods with respect to these criteria is shown in Table 1 and Fig. 2.

**Throughput:** The more enzyme variants need to be tested, the faster a screening system has to be. Usually, NMR spectroscopy or chromatographic techniques are restricted in throughput, although they deliver very accurate data. Due to the efforts of the groups of Reetz and Trapp, the throughput of various chromatographic methods could significantly be increased [26, 34]. Ultraviolet–visible (UV–vis) and fluorescence spectroscopy using 96- or 384-microtiter plate photometers allow for high throughput analysis, and the fluorescence activated cell sorting (FACS) technique is an ultra-high throughput method with the ability to analyse ten thousands of cells per minute [35].

**Reliability:** The identification of active and enantioselective enzymes by screening may be affected by the presence of interfering compounds. This is an important issue for qualitative agar plate assays with growing microbial colonies (e.g. the tributyrin and rhodamine B assays) [36, 37] or quantitative microtiter plate assays with crude cell lysates or supernatants (colorimetric or fluorometric assays). Variations in protein expression levels and thus yield of active enzymes may also prevent positive results and exact reproducibility. A single amino acid exchange in an enzyme can already significantly alter the essential cellular processes of transcription, translation, folding and transport.

Usually, pre-screening on agar plates of lipase-producing clones is the method of choice using either the tributyrin agar plate assay [33] identifying esterases and lipases or the rhodamine B agar plate assay [37] for the detection of true lipases. Positive colonies are transferred from agar plates into microtiter plates containing growth medium followed by cultivation. Preferably 500–1,000 colonies should be obtained for convenient handling of assays.

**Table 1**  
**Screening assays**

<b>Nr.</b>	<b>Assay, substrate</b>	<b>Format, throughput</b>	<b>Method</b>	<b>Strengths</b>	<b>Weaknesses</b>	<b>Ref.</b>
1	Agar plates, tributyrin	Agar plate, >100 k/day	Qualitative densitometry	Rapid identification of lipases and esterases, native substrate	No enantioselectivity, preference for extracellular hydrolases	[36]
2	Agar plates, triolein, rhodamine B	Agar plate, >100 k/day	Qualitative fluorometry	Rapid identification of lipases, native substrate	No enantioselectivity, preference for extracellular hydrolases	[37]
3	Liquid assay, <i>p</i> -nitrophenyl ester	Microtiter plate, 1–10 k/day	Photometry	Linear read-out on wide concentration scale	Non-competitive selectivity, moderate sensitivity, artificial substrate	[41]
4	Liquid assay, umbelliferyl ester	Microtiter plate, 1–10 k/day	Fluorometry	High sensitivity, suitable for weak activities	Non-competitive selectivity, artificial substrate	[42, 43] <sup>a</sup>
5	Liquid Quick E assay, <i>p</i> -nitrophenyl ester and resorufine tetradecanoate	Microtiter plate, 1–10 k/day	Photometry	Quasi-competitive assay, linear read-out on wide concentration scale	Evaluation of the screening results with real substrates necessary	[33]
6	Liquid adrenaline assay, polyol acetate esters	Microtiter plate, 1–10 k/day	Photometry	Native substrates, detailed substrate spectrum	Non-competitive selectivity, specific substrate required	[44]

7 <sup>b</sup>	In vivo covalent attachment of products via enzyme display, biotin-tyramide ester, streptavidin and R-phycoerythrin	Cell sorter, >1,000 k/day	Fluorometry	Ultra-high throughput, high sensitivity, competitive assay	Technically challenging [35]
8 <sup>b</sup>	Liquid assay with isotope-labelled pseudo-enantiomers, any ester	Autosampler, 100-10 k/day	NMR spectroscopy	Precise quantification, analysis of multiple products, competitive assays	Low throughput, low sensitivity, abstractness of the pseudo-enantiomer (cf. Fig. 1b) [32]
9 <sup>b</sup>	Liquid assay with deuterium-labelled pseudo-enantiomers, any ester	Autosampler, 1-10 k/day	Mass spectrometry	Precise quantification, high sensitivity, analysis of multiple products, competitive assays	Degree of abstraction of the pseudo-enantiomer (see Fig. 1b) [29]
10 <sup>b</sup>	Liquid HPLC and GC assay, liquid and volatile esters	Autosampler, 10-700/day	HPLC, GC	Precise quantification, high sensitivity, analysis of multiple products, competitive assays	Low throughput, reference compounds needed [26, 45]

<sup>a</sup>The basis has been set by achiral substrates; the enantioselectivity assay is described in this book chapter

<sup>b</sup>These methods are not described in detail in this chapter

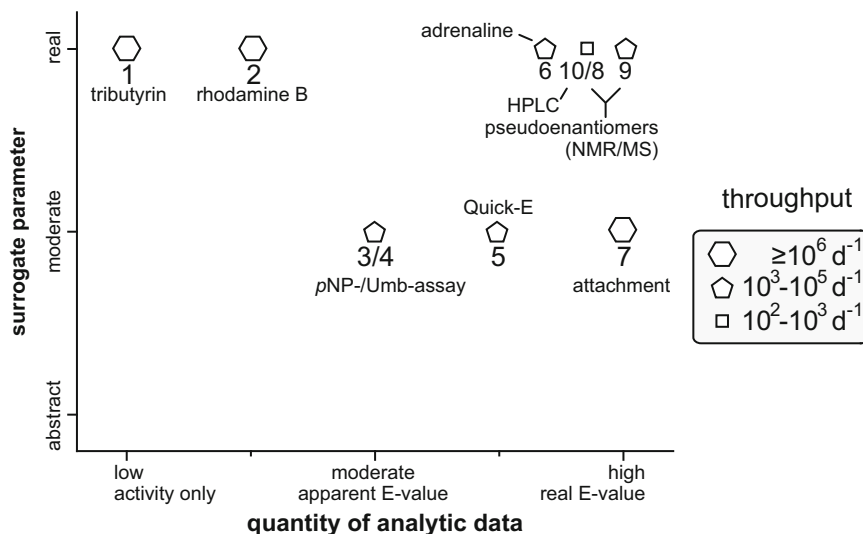


**Fig. 2** Schematic classification of various assays; numbers refer to the entries in Table 1. Throughput per day is indicated by size and shape, respectively, of polygons shown in the insert

Growth temperature, incubation time, volume of growth medium and agitation speed are common parameters to be optimised to achieve detectable enzymatic activity. Microtiter master plates containing a library of variants producing enzymatically active enzymes may be stored at  $-80^\circ\text{C}$  in the presence of 15% (v/v) glycerol.

**Surrogate Substrates:** Several high throughput screening methods are based on the hydrolysis of chromogenic or fluorogenic surrogate substrates. Researchers should be aware that these substrates allow easy handling of assays, but the results may not be transferable to the biocatalytic conversion of ‘real’ substrates, i.e. the enantioselectivities of enzymes determined with surrogate substrates may not be relevant for industrial substrates.

Therefore, microtiter plate assays were developed allowing for screening with label-free substrates which may represent real substrates of interest. For screening of lipases, available methods include measuring pH changes due to released carboxylic acids using indicators [38] or measuring NADH production in reactions coupled to the oxidation of released carboxylic acid [39].

Surrogate parameters may be defined as well for the reaction conditions used for screening. If a biocatalytic conversion needs defined pH, temperature or the presence of organic solvents, the screening system should mimic these conditions, too. For example, an enzyme variant identified by screening for enhanced enantioselectivity might have lost the temperature or pH stability of the respective wild-type enzyme and consequently, will not be applicable for the desired process. The problem of considering surrogate

### 1.3 Calculating Stereoselectivity

parameters during screening is best illustrated by Frances Arnold's statement 'you get what you screen for' [40].

Usually, two parameters describe enantioselectivity: the enantiomeric excess (ee) and the *E*-value. The ee-value indicates the composition of a mixture of two enantiomers which is calculated as the difference of the concentrations (*c*) of both enantiomers divided by the sum of both concentrations [here: (*R*)-enantiomer assumed to be the major component]:

$$ee = \frac{c_R - c_S}{c_R + c_S} 100\%$$

The rationale behind this formula is depicted by an example shown in Fig. 3a. Having a mixture of 75% of the (*R*)-enantiomer and 25% of the (*S*)-enantiomer, all molecules of the (*S*)-enantiomer do find a pendant within the amount of the (*R*)-enantiomer. Thus, one can assume that 50% (25% *R* plus 25% *S*) of the mixture are racemic. Consequently, the remaining 50% must consist of the (*R*)-enantiomer corresponding to an ee-value of 50%. From a practical point of view, the ee-value is used rather than a simple ratio of both enantiomers, because this value behaves linear over all possible compositions ranging from 0% to 100% ee (the value is by definition always positive).

The *E*-value is defined as the ratio between the conversion rate constant of the faster converted enantiomer and the conversion rate constant for the slower converted enantiomer. Two types of reactions can be envisaged (see Fig. 3b): for an asymmetric synthesis, a prochiral compound (*P*) is converted to a chiral one (*R/S*); for a kinetic resolution, an enantiomeric starting material (*A/B*) is converted to the respective enantiopure products (*R/S*). In both cases, the catalysed reaction is described by the kinetic rate constants *k*<sub>1</sub> and *k*<sub>2</sub>. Hence, the *E*-value is defined as:

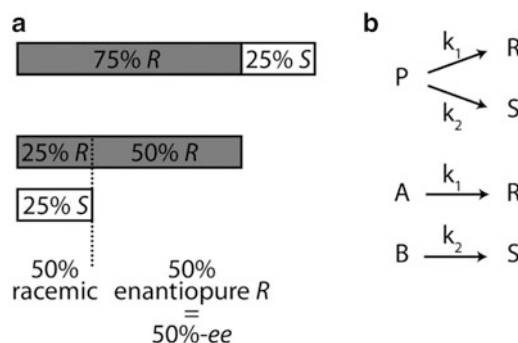


**Fig. 3** The rationales behind enantiomeric excess *ee* (a) and the enantioselectivity *E* (b)

$$E = k_1 / k_2 = \frac{k_{\text{cat},1}}{K_{\text{m},1}} \bigg/ \frac{k_{\text{cat},2}}{K_{\text{m},2}}$$

For an asymmetric synthesis, the  $E$ -value gives the ratio between the measured concentrations of both enantiomers and this value is independent of the conversion.

In contrast, the conversion rates for A and B, respectively, (Fig. 3b) strongly depend on the enantiomeric excess and the conversion. Thus, the determination of conversion rate constants ( $k_1/k_2$ ) is more sophisticated. A detailed description of the analysis of such cases can be found in reference [46]. The rate constants can be determined from steady-state kinetics, where the ratio of the turnover number  $k_{\text{cat}}$  and the Michaelis-constant  $K_{\text{m}}$  equals the conversion rate constant  $k$ .

In the context of screening, you won't survey a steady-state kinetic for each and every library member. Usually, simplifications are used to get a good idea of what could be the real  $E$ -value (e.g. measurements at substrate saturation concentration). Distinct assumptions and simplifications will be mentioned in the paragraphs describing the screening methods. However, the difference between apparent and effective  $E$ -value should be discussed here shortly. The effective (or real)  $E$ -value is defined under competitive conditions, i.e. the non-preferred enantiomer is present while the other is converted. This could cause competitive inhibition or even allosteric effects. In screenings, the rates for both enantiomers are often determined individually and then, the  $E$ -value is calculated according to the mentioned equation. Such apparent  $E$ -values might be different from real enantioselectivities. The strength of an enantioselectivity screening is measured by its ability to predict or estimate the real  $E$ -value under simplified conditions.

---

## 2 Materials

All chemicals and solvents are commercially available (for company web-sites, see <http://www.sigmaaldrich.com>; <http://www.tcichemicals.com/> and <http://www.alfa.com/>; for laboratory equipment and glass ware, see <http://www.carlroth.com> and <https://de.vwr.com/>). Prepare all buffer solutions using analytical grade reagents and ultrapure water with electrical resistivity of 18 M $\Omega$  cm. The accuracy of any activity assay strongly depends on the careful preparation of all solutions; therefore, pay attention when weighing small amounts of substrates and pipetting small volumes of solutions. We recommend to freshly prepare buffers needed for activity assays rather than to add toxic sodium azide for conservation. Buffers can usually be stored for up to 2 weeks at

room temperature or up to one month at 8°C. Warm up the assay buffers to the temperature chosen for the assays and ensure that pH is adjusted at this same temperature (**Note 1**).

## 2.1 Agar Plate Assays

Luria-Bertani (LB) agar medium [44]: 10 g/L bacto-tryptone, 10 g/L sodium chloride, 5 g/L bacto-yeast extract, 15 g/L agar. Add distilled water, dissolve the components, adjust to pH 7 with NaOH and autoclave.

### 2.1.1 Tributyrin Emulsion Assay [36]

Tributyrin emulsion: 50% (v/v) tributyrin, sterilised by filtration through 0.22 µm membranes, 50 g/L sterile gum arabic dissolved in sterile distilled water. Mix the emulsion for 1 min using a homogeniser (e.g. Ultra Turrax, IKA Labortechnik, Germany) rinsed with 70% (v/v) ethanol.

### 2.1.2 Rhodamine B Assay [37]

Rhodamine B solution: 1 mg/mL dissolved in sterile distilled water; sterilise by filtration through 0.22 µm membranes.

Olive oil emulsion: mix 25 g/L olive oil with sterile distilled water, sterilise by filtration and emulsify by mixing for 1 min with a homogeniser rinsed with 70% (v/v) ethanol.

## 2.2 Synthesis of Chiral 4-Methylumbelliferyl Esters and Fluorimetric Screening

### 2.2.1 General Materials

1. Dewar vessel
2. Dry ice
3. Low-temperature thermometer
4. Acetone
5. Heat gun
6. Schlenk flasks (10 mL, 25 mL, 50 mL, 100 mL)
7. Rubber septa
8. Magnetic stir bars
9. Magnetic stirrer
10. Schlenk line for providing dry nitrogen (**Note 2**) and vacuum
11. Brine (saturated sodium chloride solution)
12. Erlenmeyer flasks
13. Anhydrous magnesium sulphate
14. Funnels with Celite™ filter material or filter paper
15. Round bottom flasks
16. B. Braun Injekt® 5 mL Luer Solo syringes
17. B. Braun Injekt® 20 mL Luer Solo syringes
18. B. Braun Injekt® 2 mL Luer Solo syringes
19. B. Braun Sterican® 0.80 × 120 mm BL/LB (21G × 4 3/4") hypodermic-needles
20. Ethyl acetate

21. Petroleum ether (bp 40–60°C)
22. Chromatography column
23. Silica gel (230–400 mesh)
24. Separation funnels

2.2.2 *Synthesising (R)- and (S)-2-Methyldecanoic Acid (12) in Three Steps [47]*

Synthesis of (R)- and (S)-4-Benzyl-3-Decanoyloxazolidin-2-One

1. Anhydrous tetrahydrofuran (THF)
2. (R)-4-Benzylloxazolidin-2-one
3. (S)-4-Benzylloxazolidin-2-one
4. *n*-Butyl lithium (2.5 M in hexane)
5. Decanoyl chloride
6. Saturated aqueous ammonium chloride solution
7. Dichloromethane (CAUTION: Dichloromethane is toxic and suspected of causing cancer!)
8. Aqueous potassium carbonate solution (1.0 M)

Synthesis of (4*R*,2'*R*)- and (4*S*,2'*S*)-3-(2'-Methyldecanoyl)-4-Benzylloxazolidin-2-One

1. Sodium bis(trimethylsilyl)amide (1.0 M in THF, 3.3 mL, 3.3 mmol)
2. (R)-4-Benzyl-3-decanoyloxazolidin-2-one
3. (S)-4-Benzyl-3-decanoyloxazolidin-2-one
4. Iodomethane (EXTREME CAUTION: Iodomethane is toxic and suspected of causing cancer!)
5. Saturated aqueous ammonium chloride solution
6. Dichloromethane (CAUTION: Dichloromethane is toxic and suspected of causing cancer!)
7. Aqueous sodium sulphite solution (1.0 M)

Synthesis of (*R*)- and (*S*)-2-Methyldecanoic Acid

1. (4*R*,2'*R*)-3-(2'-methyldecanoyl)-4-benzylloxazolidin-2-one
2. (4*S*,2'*S*)-3-(2'-methyldecanoyl)-4-benzylloxazolidin-2-one
3. THF
4. Ice bath (0°C)
5. Deionized water
6. Aqueous hydrogen peroxide solution (30%)
7. Lithium hydroxide hydrate
8. Aqueous HCl solution (1.0 M)
9. pH indicator paper
10. Dichloromethane (CAUTION: Dichloromethane is toxic and suspected of causing cancer!)
11. Aqueous sodium sulphite solution (1.5 M)

2.2.3 *Coupling of the Fluorophore Methylumbelliferone to 2-Methyldecanoic Acid* [48]

1. (*R*)-2-Methyldecanoic acid in a small (10–25 mL) *Schlenk* flask
2. (*S*)-2-Methyldecanoic acid in a small (10–25 mL) *Schlenk* flask
3. Ice bath (0°C)
4. *N*-(3-Dimethylaminopropyl)-*N'*-ethylcarbodiimide hydrochloride (EDC · HCl)
5. Anhydrous *N,N*-dimethylformamide (DMF)
6. 4-Methylumbelliferone (4-MU)
7. 4-(Dimethylamino)pyridine (4-DMAP, EXTREME CAUTION: 4-DMAP may be fatal in contact with skin!)
8. Saturated aqueous sodium bicarbonate (sodium hydrogen carbonate) solution

2.3 **Screening for Enantioselectivity of Lipases/Esterases Using (*R*)- and (*S*)-Methylumbelliferyl 2-Methyldecanoate**

2.3.1 *Performing the Enantioselectivity Assay*

1. Screening buffer: mixture of 50 mM Na<sub>2</sub>HPO<sub>4</sub> and 50 mM KH<sub>2</sub>PO<sub>4</sub> adjusted to pH 8.0, add 50 mM sodium deoxycholate and 0.1% (w/v) gum Arabic
2. Substrate stock solutions 1 mM in DMSO (*see* Sect. 3.2.4.1)
3. 4-MU stock solutions in DMSO (0.125 mM, 0.25 mM, 0.5 mM, 0.75 mM, 1.0 mM and 1.25 mM, *see* 3.2.4.1)
4. 1.5 mL or 2.0 mL Eppendorf Safe Lock Tubes™ or 15 mL vessels
5. Black 96-well microtiter plate (flat bottom, e.g. from Greiner Bio-One)
6. DMSO
7. Multiwell-spectrofluorometer (Infinite® M1000Pro, Tecan)
8. Lipase/esterase stock solution

2.4 **Synthesis of *p*-Nitrophenyl Esters and Colorimetric Screening**

2.4.1 *Synthesis of (*R*)- and (*S*)-2-Methyldecanoic Acid* [47]

2.4.2 *Coupling of *p*-Nitrophenol to 2-Methyldecanoic Acid* [48]

1. For the synthesis of (*R*)- and (*S*)-2-methyldecanoic acid, *see* the materials described in Sects. 2.2.1 and 2.2.2
1. (*R*)-2-Methyldecanoic acid in a small (10–25 mL) *Schlenk* flask
2. (*S*)-2-Methyldecanoic acid in a small (10–25 mL) *Schlenk* flask
3. Ice bath (0°C)
4. EDC · HCl
5. DMF
6. *para*-nitrophenol (*p*-NP)

7. 4-DMAP (EXTREME CAUTION: 4-DMAP may be fatal in contact with skin!)
8. Saturated aqueous sodium bicarbonate (sodium hydrogen carbonate) solution

**2.4.3 *p*-Nitrophenyl  
2-Methyldecanoate (*p*-NP  
2-MD) Substrates [41]**

1. Substrate stock: 10 mg/mL (*R*)-*p*-NP 2-MD in acetonitrile (**Note 3**).
2. Substrate stock: 10 mg/mL (*S*)-*p*-NP 2-MD in acetonitrile (**Note 3**).
3. Assay buffer: 100 mM Tris-HCl pH 7.5
4. *p*-NP standard stock solution: 10 mg/ml *p*-nitrophenol in assay buffer.
5. Microplate reader: Vis spectrophotometer for measurements in 96-well microplates (e.g. SpectraMax 250, Molecular Devices Corp.).
6. 96-well microplates.

**2.5 Adrenaline  
Assay [44]**

1. Substrates: 10 mM of compounds listed in the Table 2 dissolved in acetonitrile.
2. Titrant 1: 10 mM NaIO<sub>4</sub> in water (**Note 4**).
3. Titrant 2: 15 mM L-adrenaline hydrochloride in water.
4. Enzyme in 50 mM aqueous borate buffer pH 8.0 (**Note 5**).
5. 96-well microplates.
6. Microplate reader: Vis spectrophotometer for measurements in 96-well microplates (e.g. SpectraMax 250, Molecular Devices Corp.).

**2.6 Quick E Assay**

1. Assay buffer: 50 mM Tris-HCl pH 8; 4.5 g/L Triton X-100
2. (*S*)-*p*-NP 2-PP substrate solution S: 7.8 mM (*S*)-*p*-nitrophenyl 2-phenylpropanoate [(*S*)-*p*-NP 2-PP] dissolved in acetonitrile.
3. (*R*)-*p*-NP 2-PP substrate solution R: 7.8 mM *p*-nitrophenyl-(*R*)-2-phenylpropanoate [(*R*)-*p*-NP 2-PP] dissolved in acetonitrile.
4. Reference substrate solution: 1.6 mM resorufine tetradecanoate dissolved in acetonitrile.
5. 96-well microplates.
6. Plate reader.

---

## 3 Methods

**3.1 Agar Plate  
Assays**

LB-agar is the most widely used solid medium for the growth of bacteria. It can be supplemented with antibiotics to maintain expression plasmids and with inducers of gene expression, e.g. isopropyl-β-D-galactopyranoside (IPTG). Substrates should be

**Table 2**  
**Commercially available polyol acetate substrates used for adrenaline lipase assays [49]**

Substrate name	CAS number	Supplier
Ethylene glycol diacetate	111-55-7	Sigma Aldrich
Diacetin, glycerol $\alpha,\alpha'$ -diacetate	5395-31-7	TCI Europe
Propylene glycol diacetate	623-84-7	Sigma Aldrich
Triacetin	102-76-1	Sigma Aldrich
( <i>R</i> )-(+)-Dihydro-5-(hydroxymethyl)-2(3H)-furanone	52813-63-5	Sigma Aldrich
( <i>S</i> )-(+)-Dihydro-5-(hydroxymethyl)-2(3H)-furanone	32780-06-6	Sigma Aldrich
(1 <i>R</i> ,2 <i>R</i> )-2-(Acetyloxy)cyclohexyl acetate	1759-71-3	Sigma Aldrich
$\beta$ - <i>D</i> -Ribofuranose 1,2,3,5-tetraacetate	13035-61-5	AK Scientific
$\alpha$ - <i>D</i> -Mannose pentaacetate	4163-65-9	Sigma Aldrich
$\beta$ - <i>D</i> -Ribopyranose 1,2,3,4-tetraacetate	4049-34-7	Sigma Aldrich
<i>D</i> -(+)-Sucrose octaacetate	126-14-7	Sigma Aldrich
4- <i>O</i> -(2,3,4,6-Tetra- <i>O</i> -acetyl- $\alpha$ - <i>D</i> -mannopyranosyl)- <i>D</i> -mannopyranose tetraacetate	123809-59-6	TRC
$\beta$ - <i>D</i> -Galactose pentaacetate	4163-60-4	Sigma Aldrich
$\beta$ - <i>D</i> -Ribopyranose 1,2,3,4-tetraacetate	4049-34-7	Sigma Aldrich
Lactose octaacetate	6291-42-5	TRC
<i>D</i> -(+)-Cellobiose octaacetate	3616-19-1	TRC
Mannitol hexaacetate	5346-76-9	MP Biomedicals
<i>D</i> -Sorbitol hexaacetate	7208-47-1	Sigma Aldrich
$\beta$ - <i>L</i> -Glucose pentaacetate	66966-07-2	TRC
1,2,3,4-Tetra- <i>O</i> -acetyl- $\alpha$ - <i>L</i> -fucopyranoside	64913-16-2	TCI Europe
$\beta$ - <i>D</i> -Ribopyranose 1,2,3,4-tetraacetate	4049-34-7	Sigma Aldrich

TRC Toronto Research Chemicals, TCI Europe Tokyo Chemical Industry Europe

freshly emulsified before adding to the agar medium to obtain an emulsion with optimal properties. It is recommended to use fresh agar plates to increase assay sensitivity and reproducibility (**Note 6**). The agar plates are usually incubated for 1 day at optimal growth temperature for enzyme production followed by incubation at 4°C up to 50°C required for detection of an enzymatic activity. When assaying lipases secreted into culture medium, enzymatic activity may be detected even before colonies are formed. For assay of intracellular lipases, strains should be grown to form colonies

followed by assaying enzymatic activities at growth suppressing temperature (usually in the refrigerator for psychrophilic and mesophilic enzymes). Not more than 500 clones per standard Petri dish (90 mm diameter) should be plated to achieve good spatial resolution of clones and allow identification of single enzyme-producing clones.

### 3.1.1 Tributyrin Agar Plate Assay [36]

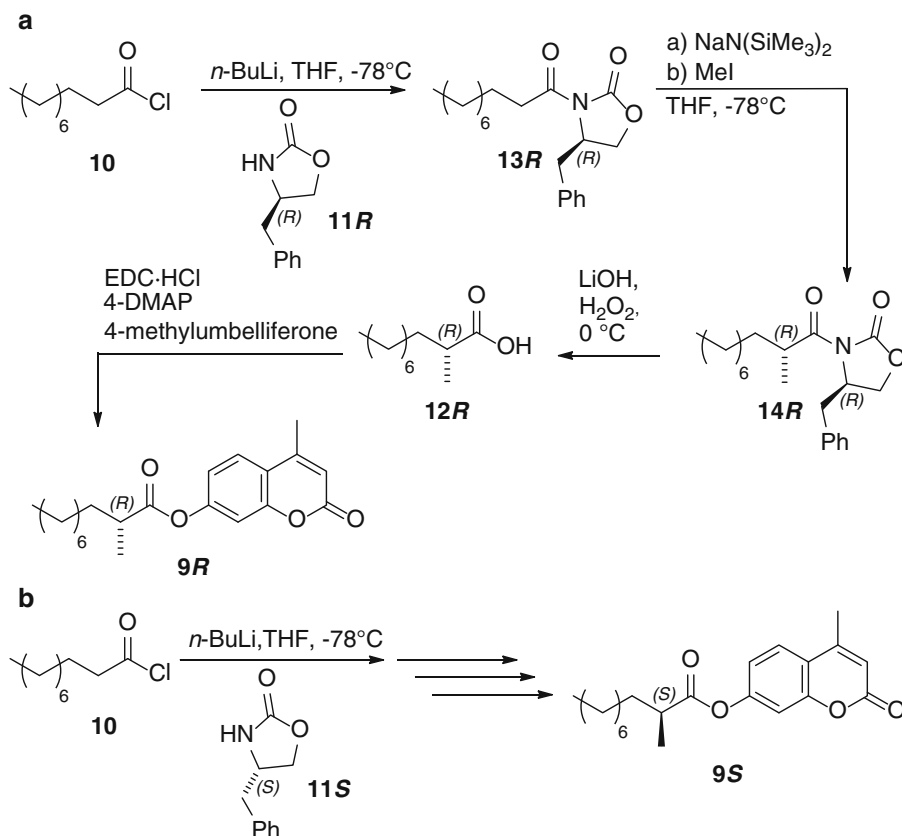
The most common agar plate assay to detect extracellular and intracellular lipases uses tributyrin which is a natural lipase substrate. However, tributyrin is a triglyceride ester with short chain (C4) fatty acids which is hydrolysed by lipases and esterases as well. Clear zones appearing around the bacterial colonies indicate the production of catalytic active lipolytic enzymes.

1. Add 30 mL of tributyrin emulsion, the respective antibiotic and (if required) inducer (e.g. IPTG) to 1 L of melted LB agar medium cooled to a temperature of about 60°C and mix thoroughly.
2. Pour 20 mL medium into appropriate Petri plates and let it solidify for at least 20 min.
3. Plate bacterial clones and incubate at optimal growth temperature for at least 16 h.
4. Positive clones are identified after overnight growth or after prolonged (2–4 days) incubation in refrigerator for clones expressing low amounts of active enzymes (**Note 7**).

### 3.1.2 Rhodamine B (RB) Agar Plate Assay [37]

This assay is specific for true lipases because it uses triolein as a substrate, which is a triglyceride ester containing long chain (C-18:1) fatty acids. Released fatty acids form fluorescent complexes with the cationic rhodamine B resulting in fluorescent halos around lipase-positive clones after irradiation of the agar plate with UV light at 350 nm. Clones which do not produce lipases appear pink coloured, but non-fluorescent (**Note 8**).

1. Add 31.25 mL of olive oil emulsion, 10 mL RB solution, respective antibiotic and inducer (e.g. IPTG) to 1 L of melted LB agar medium at a temperature of about 60°C and mix thoroughly.
2. Pour 20 mL medium into appropriate plates and let it solidify. Normally, plates are pink coloured and have opaque appearance.
3. Plate the clones and incubate at optimal growth temperature for at least 16 h.
4. Positive clones are identified under UV light (e.g. hand lamp at 350 nm) by fluorescent halos around colonies (**Note 9**).



**Scheme 2** (a) Synthesis of the screening substrate (*R*)-methylumbelliferyl 2-methyldecanoate (**9R**). The stereoselectivity of the alkylation (step 2) is controlled by the Evans auxiliary 4-benzyloxazolidin-2-one (**11R**). Using (*R*)-4-benzyloxazolidin-2-one (**11R**) yields the (*R*)-methylumbelliferyl 2-methyldecanoate (**9R**). (b) To obtain (*S*)-methylumbelliferyl 2-methyldecanoate (**9S**) the synthesis has to be performed starting with (*S*)-4-benzyloxazolidin-2-one (**11S**)

### 3.2 Fluorimetric Screening with Chiral Methylumbelliferyl (*R*)- and (*S*)-2-Methyldecanoate

In this section, the synthesis of (*R*)-methylumbelliferyl 2-methyldecanoate (**9R**) and (*S*)-methylumbelliferyl 2-methyldecanoate (**9S**) will be described starting from decanoyl chloride (**10**) and the Evans auxiliary (*R*)-4-benzyloxazolidin-2-one (**11R**) or (*S*)-4-benzyloxazolidin-2-one, respectively (Scheme 2) [47].

Determining the activity of a lipase or esterase towards both 4-methylumbelliferyl 2-methyldecanoate enantiomers under non-competitive conditions in separate reactions enables a fast estimation of the enantioselectivity of the tested enzyme in a 96-well plate scale. Hydrolysis of 4-MU esters by lipases can be followed continuously by monitoring the increase of fluorescence intensity due to the production of highly fluorescent 4-methylumbelliferone (4-MU) with an emission spectra maximum at 460 nm. In contrast to emission maxima the fluorescence excitation maxima of 4-MU is pH dependent and varies from 330 nm at pH 4.6 to 385 nm at

pH 10.4 [43]. For activity calculations, it is necessary to correct for spontaneous hydrolysis of the substrates and background fluorescence of the protein sample. Enzyme activity is defined as the amount of released 4-MU per minute, and can be calculated with a standard curve obtained by measuring the fluorescence of 4-MU under assay conditions. The reported assay is based on the conditions described by Winkler and Stuckmann [51].

### 3.2.1 General Procedures

1. Fill a Dewar vessel halfway with acetone and carefully add dry ice until a temperature of  $-78^{\circ}\text{C}$  is reached (**Note 10**).
2. Preparation of an inert *Schlenk* flask: Connect a *Schlenk* flask of appropriate size to the *Schlenk* line, add a magnetic stir bar, seal it with a rubber septum and evacuate the flask. Heat the evacuated flask carefully all-over with a heat gun while the flask is connected to the vacuum. (CAUTION: DO NOT HEAT A CLOSED FLASK!). Let the *Schlenk* flask chill and flush it with dry nitrogen (**Note 11**). Repeat this evacuation, heating, chilling and flushing cycle two times.

### 3.2.2 Synthesising (*R*)- and (*S*)-2- Methyldecanoic Acid (12) in Three Steps [47]

#### Synthesis of (*R*)- and (*S*)-4-Benzyl-3- Decanoyloxazolidin-2- One (13)

1. Transfer 20 mL of anhydrous THF to the nitrogen flushed 100 mL *Schlenk* flask under inert conditions by using a 20 mL syringe with a hypodermic-needle.
2. Dissolve (*R*)-4-benzyloxazolidin-2-one (1.0 g, 5.6 mmol) in THF under inert conditions by stirring.
3. Cool the reaction mixture to  $-78^{\circ}\text{C}$  using a dry ice/acetone cooling bath.
4. Add *n*-butyl lithium (2.5 M in hexane, 2.3 mL, 5.7 mmol) under inert conditions drop wise at  $-78^{\circ}\text{C}$  during 15 min using a 5 mL syringe with a hypodermic-needle.
5. Add decanoyl chloride (1.18 g, 1.28 mL, 6.2 mmol) under inert conditions drop wise at  $-78^{\circ}\text{C}$  by using a 2 mL syringe with a hypodermic-needle.
6. Allow the solution to warm to  $0^{\circ}\text{C}$  during 1 h by slowly lifting the flask out of the acetone/dry ice cooling bath and dipping it into an ice bath.
7. Let the solution stir for further 1 h.
8. Quench the reaction by slowly adding 10 mL of saturated aqueous ammonium chloride solution with a 20 mL syringe coupled to hypodermic-needle.
9. Transfer the reaction mixture to a separation funnel (use a funnel without filter paper if necessary) and rinse the *Schlenk* flask with dichloromethane. Add the dichloromethane used for rinsing to the separation funnel (CAUTION: Dichloromethane is toxic and suspected of causing cancer!).

10. Extract the reaction mixture with dichloromethane three times and collect the organic layers.
11. Wash the combined organic layers with aqueous potassium carbonate solution (1.0 M). CAUTION: Residual ammonium chloride can react with potassium carbonate and release carbon dioxide. To avoid high pressures in the separation funnel slew it slowly before closing with the plug.
12. Wash the combined organic layers with brine.
13. Transfer the combined organic layers to an Erlenmeyer flask and add anhydrous magnesium sulphate for drying.
14. Filter and transfer the combined organic layers by using a funnel with Celite™ or filter paper to a round bottom flask.
15. Remove the solvent under reduced pressure by using a rotary evaporator.
16. Purify the crude product by column chromatography using silica gel and a mixture of petroleum ether/ethyl acetate (9:1). Removing the solvent under reduced pressure by using a rotary evaporator gives (*R*)-4-benzyl-3-decanoyloxazolidin-2-one as colourless oil (1.17 g, 62%) that crystallises on standing to a colourless solid.
17. Transfer the product to a small (10 or 25 mL) round bottom or *Schlenk* flask (**Note 11**).
18. Analytical data [47]: mp 37–39°C; optical rotatory power:  $[\alpha]_{\text{D}}^{20} = -60.6$  ( $c = 1.0$ ,  $\text{CH}_2\text{Cl}_2$ );  $^1\text{H}$  NMR  $\delta = 0.87$  (t,  $J = 6.7$  Hz, 3H, 10-H), 1.15–1.34 (m, 12H, 6×  $\text{CH}_2$ ), 1.56–1.68 (m, 2H, 3-H), 2.74 (dd,  $J = 13.4, 9.6$  Hz, 1H, *CHHPh*), 2.79–2.94 (m, 2H, 2-H), 3.28 (dd,  $J = 13.4, 3.2$  Hz, 1H, *CHHPh*), 4.08–4.16 (m, 2H, 5'-H), 4.57–4.64 (m, 1H, 4'-H), 7.12–7.28 (m, 5H, Ph-H);  $^{13}\text{C}$  NMR  $\delta = 14.45, 22.70, 24.31$  (decanoyl C-3), 29.17, 29.31, 29.44, 29.48, 31.91, 35.57 (decanoyl C-2), 37.97, 55.19, 66.17, 127.36, 128.97, 129.45, 135.38, 153.49, 173.45 (decanoyl C-1).
19. Using (*S*)-4-benzoyloxazolidin-2-one as starting material in the step 4 yields (*S*)-4-benzyl-3-decanoyloxazolidin-2-one as a colourless oil (1.72 g, 93%) (mp 37–39°C); optical rotatory power:  $[\alpha]_{\text{D}}^{20} = +63.7$  ( $c = 1.0$ ,  $\text{CH}_2\text{Cl}_2$ ); the NMR data corresponds to (*R*)-4-benzyl-3-decanoyloxazolidin-2-one [47].

Synthesis of (4*R*,2'*R*)- and (4*S*,2'*S*)-3-(2'-Methyldecanoyl)-4-Benzyloxazolidin-2-One (14)

1. Prepare a 25 mL and a 50 mL *Schlenk* flask for working under inert conditions and a dry ice/acetone cooling bath as described in Sect. 3.2.1.
2. Transfer sodium bis(trimethylsilyl)amide (1.0 M in tetrahydrofuran, 3.3 mL, 3.3 mmol) under inert conditions to the nitrogen flushed 50 mL *Schlenk* flask by using a 5 mL syringe with a hypodermic-needle.

- Cool the reaction mixture to  $-78^{\circ}\text{C}$  by using the dry ice/acetone cooling bath.
- Flush the round bottom or *Schlenk* flask containing (*R*)-4-benzyl-3-decanoyloxazolidin-2-one (1.0 g, 3.0 mmol) with dry nitrogen and seal it with a rubber septum.
- Transfer 5–10 mL of anhydrous THF under inert conditions to the (*R*)-4-benzyl-3-decanoyloxazolidin-2-one containing flask and dissolve the (*R*)-4-benzyl-3-decanoyloxazolidin-2-one. Cool the solution to  $0^{\circ}\text{C}$ .
- Add the pre-cooled (*R*)-4-benzyl-3-decanoyloxazolidin-2-one in THF solution under inert conditions drop wise to the sodium bis(trimethylsilyl)amide solution at  $-78^{\circ}\text{C}$ .
- Let the reaction mixture stir for 1 h at  $-78^{\circ}\text{C}$ .
- Transfer 5 mL anhydrous THF under inert conditions to the empty nitrogen flushed 25 mL *Schlenk* flask by using a 5 mL syringe with a hypodermic-needle.
- Bend a new hypodermic-needle carefully by  $90^{\circ}$  close to the plastic Luer lock.
- Fill an empty 2 mL syringe equipped with the bend hypodermic-needle with iodomethane (0.9 mL, 15 mmol). EXTREME CAUTION: Iodomethane is volatile, toxic and suspected of causing cancer! Wear proper gloves and work in a well-ventilated fume hood!
- Take up 0.5 mL of anhydrous THF from the 25 mL *Schlenk* flask (filled with 5 mL of THF) with the iodomethane containing syringe equipped with the bend hypodermic-needle. Hold the syringe with the plunger pointing down to avoid the loss of iodomethane.
- A homogeneous solution is formed shaking the syringe with THF and iodomethane carefully with its plunger fully extended. Hold the syringe with the plunger pointing down to avoid the loss of iodomethane and THF.
- Add the iodomethane in THF solution drop wise to the reaction mixture at  $-78^{\circ}\text{C}$  under inert conditions and let it stir for further 3 h.
- Stop the reaction by adding saturated aqueous ammonium chloride solution (10 mL) using a 5 mL syringe with a hypodermic-needle.
- Allow the reaction mixture to warm to room temperature.
- Transfer the reaction mixture carefully into a separation funnel (use a funnel if necessary). EXTREME CAUTION: The reaction mixture contains an excess of iodomethane! Rinse the

*Schlenk* flask with dichloromethane and transfer the dichloromethane to the separation funnel as well.

17. Extract the reaction mixture thrice with dichloromethane and collect the organic layers. EXTREME CAUTION: IODOMETHANE!
18. Transfer the combined organic layers to a clean separation funnel and wash with aqueous sodium sulphite (1.0 M) solution EXTREME CAUTION: IODOMETHANE!
19. Transfer the combined organic layers to an Erlenmeyer flask and add anhydrous magnesium sulphate for drying. EXTREME CAUTION: IODOMETHANE!
20. Filter and transfer the combined organic layers by using a funnel with filter paper to a round bottom flask. EXTREME CAUTION: IODOMETHANE!
21. Remove the solvent *in vacuo* by using a rotary evaporator. EXTREME CAUTION: IODOMETHANE! Use a rotary evaporator placed in a well-ventilated fume hood!
22. Purify the crude product by column chromatography using silica gel and a mixture of petroleum ether/ethyl acetate (95:5).
23. Removing the solvent under reduced pressure by using a rotary evaporator gives (4*R*,2'*R*)-3-(2-methyldecanoyl) 4-benzyloxazolidin-2-one (650 mg, 1.9 mmol, 63%) as colourless oil.
24. Transfer the product to 100 mL round bottom flask.
25. Analytical data [47]: optical rotatory power:  $[\alpha]_{\text{D}}^{20} = -73.5$  ( $c = 1.0$ ,  $\text{CH}_2\text{Cl}_2$ );  $^1\text{H NMR } \delta = 0.86$  (t,  $J = 6.7$  Hz, 3H, 10-H), 1.20 (d,  $J = 6.9$  Hz, 3H, 2- $\text{CH}_3$ ), 1.16–1.26 (m, 12H, 6  $\times$  decanoyl  $\text{CH}_2$ ), 1.30–1.38 (m, 1H, 3- $\text{H}_a$ ), 1.62–1.70 (m, 1H, 3- $\text{H}_b$ ), 2.75 (dd, 1H,  $J = 13.2, 9.5$  Hz,  $\text{CHHPh}$ ), 3.26 (dd,  $J = 13.4, 3.2$  Hz, 1H,  $\text{CHHPh}$ ), 3.60–3.66 (m, 1H, 2-H), 4.07–4.15 (m, 2H, 5'-H), 4.58–4.63 (m, 1H, 4'-H), 7.11–7.28 (m, 5H, Ph-H);  $^{13}\text{C NMR } \delta = 14.09, 17.35$  (decanoyl 2- $\text{CH}_3$ ), 22.64, 27.25, 29.24, 29.46, 29.65, 31.85, 33.46 (decanoyl 3-C), 37.71 (decanoyl 2-C), 37.90, 55.36, 65.99, 127.32, 128.92, 129.44, 135.35, 153.05, 177.37.
26. Using (*S*)-4-benzyl-3-decanoyloxazolidin-2-one as starting material in the step 24 yields (4*S*,2'*S*)-3-(2-methyldecanoyl)-4-benzyloxazolidin-2-one as a colourless oil (68%). Optical rotatory power:  $[\alpha]_{\text{D}}^{20} = +76.6$  ( $c = 1.0$ ,  $\text{CH}_2\text{Cl}_2$ ); the NMR data are identical to its enantiomer (4*R*,2'*R*)-3-(2-methyldecanoyl)-4-benzyloxazolidin-2-one [47].

## Synthesis of (R)- and (S)-2-Methyldecanoic Acid (12)

1. Dissolve (4*R*,2'*R*)-3-(2'-methyldecanoyl) 4-benzyloxazolidin-2-one (650 mg, 1.9 mmol) in THF (27 mL) in a 100 mL round bottom flask with stirring.
2. Add 9 mL of deionized water.
3. Cool the reaction mixture with an ice bath to 0°C.
4. Add 1.4 mL aqueous hydrogen peroxide (30%), 150 mg (3.8 mmol) lithium hydroxide hydrate and stir at 0°C for 3 h (Note 12).
5. Stop the reaction by adding aqueous sodium sulphite solution (1.5 M, 13 mL, 20 mmol).
6. Acidify the reaction mixture with aqueous HCl (1.0 M) to pH 1 (check with pH indicator paper).
7. Transfer the reaction mixture to a separation funnel (use a funnel without filter paper if necessary) and rinse the round bottom flask with dichloromethane. Add the dichloromethane used for rinsing to the separation funnel.
8. Extract the reaction mixture with dichloromethane thrice and collect the organic layers.
9. Transfer the combined organic layers to an Erlenmeyer flask and add anhydrous magnesium sulphate for drying.
10. Filter and transfer the combined organic layers by using a funnel with filter paper to a round bottom flask.
11. Remove the solvent under reduced pressure by using a rotary evaporator.
12. Purify the crude product by column chromatography using silica gel and a mixture of petroleum ether/ethyl acetate 75:25 (Note 13).
13. Removing the solvent *in vacuo* by using a rotary evaporator gives (R)-2-methyldecanoic acid (320 mg, 1.7 mmol, 91%) as colourless oil.
14. Transfer the product to a small (10–25 mL) round bottom or *Schlenk* flask.
15. Analytical data [47]: optical rotatory power:  $[\alpha]_{\text{D}}^{20} = -16.3$  ( $c = 1.0$ , methanol),  $[\alpha]_{\text{D}}^{20} = -15.8$  (neat);  $[\alpha]_{\text{D}}^{20} = -15.4$  ( $c = 0.84$ , methanol);  $^1\text{H NMR } \delta = 0.86$  (t, 3H,  $J = 6.7$ , 10-H), 1.16 (d, 3H,  $J = 6.9$  Hz, 2-CH<sub>3</sub>), 1.22–1.48 (m, 13H, 6 × CH<sub>2</sub> + 3-H<sub>a</sub>), 1.65–1.72 (m, 1H, 3-H<sub>b</sub>), 2.42–2.49 (m, 1H, 2-H);  $^{13}\text{C NMR } \delta = 14.09$ , 16.80, 22.65, 27.13, 29.25, 29.42, 29.50, 31.85, 33.50, 39.38, 183.49.
16. Using (4*S*,2'*S*)-3-(2'-methyldecanoyl)-4-benzyloxazolidin-2-one as starting material in the step 47 yields (S)-2-methyldecanoic acid as a colourless oil (260 g, 1.4 mmol, quant.). Optical rotatory power:  $[\alpha]_{\text{D}}^{20} = +15.8$  ( $c = 1.0$ , methanol); the NMR data are identical to its enantiomer (R)-2-methyldecanoic acid [47].

3.2.3 Coupling of the  
Fluorophore  
Methylumbelliferone to  
(*R*)-2-Methyldecanoic Acid

1. Flush the *Schlenk* flask containing (*R*)-2-methyldecanoic acid (279 mg, 1.5 mmol) with dry nitrogen.
2. Dissolve the 2-methyldecanoic acid in anhydrous DMF (2–5 mL) under a dry nitrogen atmosphere using a 5 mL syringe with a hypodermic-needle.
3. Prepare an inert 100 mL *Schlenk* flask as described in Sect. 3.2.1.
4. Transfer the 2-methyldecanoic acid in anhydrous DMF under inert conditions to the dry, nitrogen flushed 100 mL *Schlenk* flask using a 5 mL syringe with a hypodermic-needle.
5. Add additional anhydrous DMF up to a final volume of 10 mL under inert conditions using a 10 mL syringe with a hypodermic-needle.
6. Cool the solution to 0°C using an ice bath.
7. Add 4-DMAP (32 mg, 260 μmol, 0.17 eq.) under inert conditions. EXTREME CAUTION: 4-DMAP may be fatal in contact with skin!
8. Add EDC · HCl (359 mg, 1.8 mmol, 1.3 eq.) under inert conditions.
9. Add 4-MU (317 mg, 1.8 mmol, 1.2 eq.) under inert conditions.
10. Let the reaction stir for 1 h at 0°C.
11. Allow the reaction to warm to room temperature and let it stir over night.
12. Dilute the reaction mixture with 30 mL ethyl acetate.
13. Transfer the reaction mixture to a separation funnel (use a funnel without filter paper if necessary) and rinse the *Schlenk* flask with ethyl acetate. Add the ethyl acetate used for rinsing to the separation funnel.
14. Wash the organic layer with saturated aqueous sodium bicarbonate solution thrice.
15. Wash the organic layer with deionized water thrice.
16. Transfer the organic layer to an Erlenmeyer flask and add anhydrous magnesium sulphate for drying.
17. Filter and transfer the organic layer by using a funnel with filter paper to a round bottom flask.
18. Remove the solvent under reduced pressure by using a rotary evaporator.
19. Purify the crude product by column chromatography using silica gel and a mixture of petroleum ether/ethyl acetate 77:23. Removing the solvent under reduced pressure using a rotary evaporator gives methylumbelliferyl (*2R*)-

methyldecanoate (0.299 g, 58%) as a white solid. Optical rotatory power: mp 37.0–38.5°C;  $[\alpha]_{\text{D}}^{20} = -28.0$  ( $c = 1.0$ ,  $\text{CHCl}_3$ ); TLC:  $R_f = 0.38$  (petroleum ether/ethyl acetate, 7:3);  $^1\text{H NMR}$  (600 MHz,  $\text{CDCl}_3$ )  $\delta = 0.89$  (t,  $J = 6.8$  Hz, 3H, 10-H), 1.21–1.47 (m, 12H, 6 × decanoyl  $\text{CH}_2$ ) 1.31 (d,  $J = 6.9$  Hz, 3H, 2- $\text{CH}_3$ ), 1.53–1.64 (m, 1H, 3- $\text{H}_a$ ), 1.77–1.86 (m, 1H, 3- $\text{H}_b$ ), 2.44 (s, 3H, 4'- $\text{CH}_3$ ), 2.71 (ddq,  $J = 7.0, 7.0, 6.9$  Hz, 1H, 2-H), 6.27 (s, 1H, 3'-H), 7.05 (dd,  $J = 8.7, 2.3$  Hz, 1H, 6'-H), 7.09 (d,  $J = 2.3$  Hz, 1H, 8'-H), 7.60 (d,  $J = 8.6$  Hz, 1H, 5'-H);  $^{13}\text{C NMR}$  (151 MHz,  $\text{CDCl}_3$ )  $\delta = 14.11$  (C-10), 16.89 (2- $\text{CH}_3$ ), 18.74 (4'- $\text{CH}_3$ ), 22.67 (decanoyl  $\text{CH}_2$ ), 27.21 (decanoyl  $\text{CH}_2$ ), 29.25 (decanoyl  $\text{CH}_2$ ), 29.46 (decanoyl  $\text{CH}_2$ ), 29.50 (decanoyl  $\text{CH}_2$ ), 31.85 (decanoyl  $\text{CH}_2$ ), 33.68 (C-3), 39.68 (C-2), 110.43 (C-8'), 114.46 (C-3'), 117.72 (arom. C), 118.11 (C-6'), 125.31 (C-5'), 151.91 (arom. C), 153.36 (arom. C), 154.21 (arom. C), 160.50 (2'), 174.71 (1); IR (ATR film):  $\tilde{\nu} = 2,959, 2,920, 2,853, 1,758, 1,725, 1,616, 1,573, 1,501, 1,466, 1,440, 1,418, 1,387, 1,368, 1,327, 1,261, 1,227, 1,145, 1,129, 1,116, 1,102, 1,066, 1,039, 1,018, 981, 939, 924, 896, 876, 860, 800, 748, 721, 705, 683, 664, 605, 580, 535, 520$ ; GC-MS (EI, 70 eV):  $m/z$  (%) = 344 (10%), 177 (100%), 148 (50%), 112 (20%), 85 (45%), 57 (40%)

20. Using (*S*)-2-methyldecanoic acid as starting material in a step 1 yields methylumbelliferyl 2-(*S*)-methyldecanoate as a white solid (66%): mp 38.5–39.0°C; Optical rotatory power:  $[\alpha]_{\text{D}}^{20} = +26.7$  ( $c = 1.0$ ,  $\text{CHCl}_3$ ); HRMS (ESI-TOF): calcd for  $(\text{C}_{21}\text{H}_{28}\text{O}_4\text{K})^+$  ( $[\text{M} + \text{K}]^+$ ) 383.1625, found 383.1628; the NMR, IR and GC-MS data are identical to its enantiomer (*R*)-methylumbelliferyl 2-methyldecanoate.

### 3.2.4 Fluorimetric Screening with Chiral Methylumbelliferyl 2-Methyldecanoate

#### Preparation of Substrate Stock Solutions

1. Dissolve 3.4 mg of methylumbelliferyl 2-(*R*)-methyldecanoate in 1 mL DMSO to obtain a 10 mM stock solution. Use a 1.5 mL Eppendorf Safe Lock Tube™ as vessel.
2. Transfer 100  $\mu\text{L}$  of the 10 mM methylumbelliferyl 2-(*R*)-methyldecanoate stock solution to an empty 1.5 mL Eppendorf Safe Lock Tube™ and add 900  $\mu\text{L}$  of DMSO to obtain a 1 mM stock solution.
3. Dissolve 3.4 mg of methylumbelliferyl 2-(*S*)-methyldecanoate in 1 mL DMSO to obtain a 10 mM stock solution. Use a 1.5 mL Eppendorf Safe Lock Tube™ as vessel.
4. Transfer 100  $\mu\text{L}$  of the 10 mM methylumbelliferyl 2-(*S*)-methyldecanoate stock solution to an empty 1.5 mL Eppendorf Safe Lock Tube™ and add 900  $\mu\text{L}$  of DMSO to obtain a 1 mM stock solution.

Performing the  
Enantioselectivity Assay

5. Prepare six 4-MU in DMSO stock solutions with a concentration of 0.125 mM, 0.25 mM, 0.5 mM, 0.75 mM, 1.0 mM and 1.25 mM in 1.5 mL Eppendorf Safe Lock Tubes™.
6. All stock solutions can be stored at -20°C for at least 2 months.

1. Pre-mix 100 µL screening buffer, 15 µL DMSO (**Note 14**) and 5 µL of (*R*)-methylumbelliferyl 2-methyldecanoate 1 mM stock solution per reaction in, e.g., a 1.5 mL, 2 mL or 15 mL tube and vortex thoroughly.
2. Pre-mix 100 µL screening buffer, 15 µL DMSO (**Note 14**) and 5 µL of (*S*)-methylumbelliferyl 2-methyldecanoate 1 mM stock solution per reaction in, e.g., a 1.5 mL, 2 mL or 15 mL tube and vortex thoroughly.
3. Set up the temperature of the spectrofluorometer at 30°C (**Note 15**).
4. Transfer 120 µL of each pre-mixed reaction mixture to separate wells of a black 96-well microtiter plate.
5. Prepare standard curve samples using 100 µL screening buffer, 15 µL DMSO and each with 5 µL of the particular 4-MU stock solutions in DMSO (0.0 mM [DMSO only], 0.125 mM, 0.25 mM, 0.5 mM, 0.75 mM, 1.0 mM and 1.25 mM).
6. Start the separate reactions with both (*R*)-methylumbelliferyl 2-methyldecanoate and (*S*)-methylumbelliferyl 2-methyldecanoate by adding 30 µL enzyme stock solution or buffer in which the enzyme is dissolved (as blank) to the respective reaction mixtures and standard curve mixtures (**Note 16**). Mix thoroughly.
7. Follow the reaction for 30 min at 360 nm/465 nm (excitation/emission).
8. Calculate the standard curve by plotting the fluorescence versus the final 4-MU concentrations in the wells. Ensure that there is a linear correlation.
9. Calculate the initial reaction velocity (linear range) by subtracting the blank and using the standard curve. Estimate the apparent *E*-value for each enzyme by dividing the initial velocity of the fast enantiomer by the initial velocity of the slow enantiomer:  $E_{\text{app}} = \frac{v_{\text{fast enantiomer}}}{v_{\text{slow enantiomer}}}$  (**Note 17**).

**3.3 Colorimetric  
Screening with Chiral  
*p*-Nitrophenol (*R*)-  
and (*S*)-2-  
Methyldecanoate**

The following synthesis can be carried out as described for chiral 4-methylumbelliferyl esters, but substituting 4-MU by *p*-NP to obtain the substrates for photometric screening [52]. These compounds have already been used in a high throughput fashion for the screening of enantioselective lipases [41]. This method is based on the quantification of *p*-nitrophenolate (*p*-NP) released during the

hydrolysis of *p*-nitrophenyl acyl esters by lipolytic enzymes. The artificial *p*-NP substrate analogues are suitable for routine and accurate quantification of lipase activity using standard equipment usually available in biochemical laboratories. The *p*-NP is chromogenic with an absorption maximum at 410 nm and it can be quantified continuously using a spectrophotometer. The *p*-NP ester substrates are not water-soluble, therefore, they are dissolved in organic solvents and then diluted with assay buffer. These lipidic substrates form micelles in solution the properties of which may be drastically affected by the temperature and the preparation procedure. Therefore, it is recommended to prepare substrate emulsions identically for the purpose of reproducibility which is a critical issue when thousands of variants are compared. The major disadvantage of *p*-NP acyl ester substrates is their spontaneous hydrolysis under assay conditions requiring careful control of assay conditions (temperature and pH).

### 3.3.1 Synthesis of (*R*)- and (*S*)-2-Methyldecanoic Acid

1. The synthesis procedure for (*R*)- and (*S*)-2-methyldecanoic acid is described in Sect. 3.2.2.

### 3.3.2 Coupling of *p*-NP to 2-Methyldecanoic Acid

1. 2-Methyldecanoic acid can also be esterified with *p*-NP using the same conditions as described for 4-MU (*see* Sect. 3.2.2). Instead of 4-methylumbelliferone use *p*-nitrophenol (250 mg, 1.8 mmol, 1.2 eq.).
2. Analytical data: (*R*)-MU 2-MD: optical rotary power  $[\alpha]_{\text{D}}^{20} = -28.0$  ( $c = 0.95$ ,  $\text{CHCl}_3$ ,  $ee > 99\%$ );  $^1\text{H}$  NMR (600 MHz,  $\text{CDCl}_3$ )  $\delta = 0.88$  (t, 3H,  $J = 6.9$  Hz, 10-H), 1.31 (d, 3H,  $J = 7.0$  Hz, 2- $\text{CH}_3$ ), 1.22–1.46 (m,  $6 \times \text{CH}_2$ ), 1.52–1.62 (m, 1H, 3- $\text{H}_a$ ), 1.75–1.86 (m, 1H, 3- $\text{H}_b$ ), 2.72 (ddq, 1H,  $J = 7.0, 7.0, 7.0$  Hz, 2-H), 7.24–7.29 (m, 2H), 8.25–8.29 (m, 2H);  $^{13}\text{C}$  NMR (151 MHz,  $\text{CDCl}_3$ )  $\delta = 14.10, 16.86, 22.67, 27.20, 29.24, 29.44, 29.48, 31.85, 33.63, 39.72, 122.42, 125.18, 145.24, 155.69, 174.39$ ; GC-MS (EI, 70 eV):  $m/z$  (%) = 195 (18%), 169 (80%), 139 (25%), 109 (43%), 85 (90%), 71 (75%), 57 (100%); IR (ATR film):  $\bar{\nu} = 3,120, 3,080, 2,925, 2,855, 1,763, 1,615, 1,593, 1,523, 1,490, 1,462, 1,378, 1,345, 1,206, 1,159, 1,097, 1,012, 882, 861, 746, 723, 689, 658$ ; (*S*)-MU 2-MD: optical rotary power  $[\alpha]_{\text{D}}^{20} = +28.0$  ( $c = 0.94$ ,  $\text{CHCl}_3$ ,  $ee > 99\%$ ), NMR, IR and GC-MS data are identical to its enantiomer.

### 3.3.3 Colorimetric Screening with Chiral *p*-Nitrophenyl-2-Methyldecanoate Substrates [41, 50–53]

1. Dilute (*R*)-*p*-NP 2-MD substrate stock solution 20 fold with the 12 assay buffer and vortex for 2 min.
2. Dilute (*S*)-*p*-NP 2-MD substrate stock solution 20 fold with the assay buffer and vortex for 2 min.
3. Pipette enzyme sample into microplates (10–30  $\mu\text{L}$ ). The same enzyme sample should be pipetted into two wells, one for

assaying with (*R*)- and second for assaying with (*S*)-enantiomer. Prepare the blank (non-enzymatic control) by adding buffer in which the enzyme is dissolved to the reaction tube or microplate well.

4. Set up the temperature of Vis spectrometer at 30°C (**Note 18**).
5. Fill one half of the microplate with (*R*)- and second half with (*S*)-substrate (100–200 μL) (**Note 19**). Place the plate into VIS microplate spectrophotometer (plate reader). Set up a 5 s mixing step prior measurements, start and record  $A_{410\text{nm}}$  each 10–30 s over the time course of 30 min.
6. Prepare at least six standard solution of *p*-NP by diluting standard stock solution of *p*-NP in the assay buffer in a range of 0.05–0.5 mg/mL under the assay conditions. Measure the  $A_{410\text{nm}}$  of *p*-NP dilutions. Prepare the standard curve by plotting the  $A_{410\text{nm}}$  versus the *p*-NP concentration. Ensure that there is a linear correlation.
7. Subtract the absorbance of the blank from the measured values for the enzyme samples and convert the  $A_{410\text{nm}}$  into enzyme activity using the standard curve.
8. Estimate the apparent *E*-value for each enzyme by dividing the initial velocity of the fast enantiomer by the initial velocity of the slow enantiomer:  $E_{\text{app}} = \frac{v_{\text{fast enantiomer}}}{v_{\text{slow enantiomer}}}$  (**Note 17**).

### 3.4 Adrenaline Assay [44]

The adrenaline assay is used for the simultaneous lipase activity measurement towards a range of different commercially available esters substrates (Table 2). This assay may also be used for high throughput screening, if suitable substrates are available. The products released by the hydrolytic activity of lipases initiate a sequence of chemical reactions that finally result in the formation of a chromogenic compound which can be quantified spectrophotometrically in a 96-well microtiter plate format.

In general, natural lipase substrates can be used for the adrenaline assay, but they should be polyols, so that the lipolytic activity results in the formation of 1,2-diols which are subsequently oxidised with periodate. The remaining periodate is then back-titrated with adrenaline to give a red coloured adrenochrome product with an absorption maximum at 490 nm. If both enantiomers of a polyol acetate substrate are available [as, e.g., for (*R*)-(+)-dihydro-5-(hydroxymethyl)-2(3H)-furanone and (*S*)-(+)-dihydro-5-(hydroxymethyl)-2(3H)-furanone (Table 2)], this assay can also be used for screening of enantioselective lipases.

1. Set up the temperature of VIS spectrometer at 37°C.
2. Mix 10 μL (*R*)-substrate with 10 μL NaIO<sub>4</sub> and 80 μL of enzyme solution in microplate and incubate for 60 min at

- 37°C. Prepare the blank (non-enzymatic control) by adding buffer in which the enzyme is dissolved to the reaction tube or microplate well.
- Mix 10  $\mu\text{L}$  (*S*)-substrate with 10  $\mu\text{L}$   $\text{NaIO}_4$  and 80  $\mu\text{L}$  of enzyme solution in a microplate and incubate for 60 min at 37°C. Prepare the blank (non-enzymatic control) by adding buffer in which the enzyme is dissolved in the reaction tube or in the microplate well.
  - Add 10  $\mu\text{L}$  adrenaline solution into each well and incubate for 5 min at 26°C.
  - Measure the absorbance at 490 nm.
  - Subtract the absorbance of the blank from the measured values.
  - Estimate the apparent *E*-value for each enzyme by dividing the initial velocity of the fast enantiomer by the initial velocity of the slow enantiomer:  $E_{\text{app}} = \frac{v_{\text{fast enantiomer}}}{v_{\text{slow enantiomer}}}$  (Note 17).

### 3.5 Quick E Method [33]

The Quick E method was developed for the fast determination of enantioselectivity of lipases. It is based on the hydrolysis of a pure enantiomer substrate in the presence of a reference substrate that must not be enantiomerically pure [54]. The pure enantiomer substrate and the reference substrate must be detectable simultaneously in the same solution. Colorimetric assays with pure (*S*)- and (*R*)-*p*-NP 2-phenylpropanoate, and resorufine tetradecanoate as a reference substrate, were performed with several lipases [54]. The *p*-nitrophenolate and resorufine can be detected spectrophotometrically at 404 nm and 572 nm, respectively, thus providing initial rates of hydrolysis of each enantiomer. Principally, by performing two measurements, one with a mixture of (*S*)-*p*-NP 2-PP and resorufine tetradecanoate and the second one with (*R*)-*p*-NP 2-PP and resorufine tetradecanoate, the enantioselectivity for both reactions can be calculated using Eqs. (1) and (2) [33]. By dividing these two enantioselectivities, a Quick *E*-value can be calculated (Eq. (3); [33]). Such simulated competition between enantiomeric and reference substrates results in better agreement of Quick *E*-values with true *E*-values than estimated *E*-values with true *E*-values, as demonstrated, e.g., for lipases of *Pseudomonas cepacia* (true and Quick *E*-values = 29) and *Candida rugosa* (true and Quick *E*-values = 3.5) [33]. By combining the pH indicator and a resorufine acetate ester as the reference substrate, the Quick E method was successfully used for measuring diastereoselectivity of lipases with methyl *trans*-2-benzyloxy-1,3-dioxolane-4-carboxylate isomers [33].

$$E1 = \frac{(R)\text{-substrate}}{\text{reference}} \text{selectivity} = \frac{\frac{\text{reaction rate } (R\text{-enantiomer})}{\text{concentration } (R\text{-enantiomer})}}{\frac{\text{reaction rate (reference substrate)}}{\text{concentration (reference substrate)}}} \quad (1)$$

$$E2 = \frac{(S)\text{-substrate}}{\text{reference}} \text{selectivity} = \frac{\frac{\text{reaction rate } (S\text{-enantiomer})}{\text{concentration } (S\text{-enantiomer})}}{\frac{\text{reaction rate } (\text{reference substrate})}{\text{concentration } (\text{reference substrate})}} \quad (2)$$

$$\begin{aligned} E_{\text{Quick}} &= \frac{E1}{E2} = \frac{\frac{(R)\text{-substrate}}{\text{reference}} \text{selectivity}}{\frac{(S)\text{-substrate}}{\text{reference}} \text{selectivity}} \\ &= \frac{(R)\text{-substrate}}{(S)\text{-substrate}} \text{selectivity} \end{aligned} \quad (3)$$

1. Add 0.5 mL of (*S*)-*p*-NP 2-PP substrate solution and 0.5 mL of reference substrate solution into 9 mL of assay buffer drop wise and vortex 2–3 min until emulsion is clear (**Note 20**).
2. Add 0.5 mL of (*R*)-*p*-NP 2-PP substrate solution and 0.5 mL of reference substrate solution into 9 mL of assay buffer drop wise and vortex 2–3 min until emulsion is clear.
3. Pipette enzyme sample into microplates (10–30  $\mu\text{L}$ ). The same enzyme sample should be pipetted into two wells, one for assaying with (*R*)- and second for assaying with (*S*)-enantiomer. Prepare the blank (non-enzymatic control) by adding the buffer in which enzyme sample is dissolved to the microplate. Add the assay buffer only (without the substrate) to the microplate well with the enzyme sample and measure the intrinsic absorbance.
4. Set up the temperature of spectrophotometer at 25°C.
5. Add 180  $\mu\text{L}$  substrate emulsion [containing (*S*)- and reference substrates] in microplate and measure the increase in absorbance at 404 nm and 572 nm at 25°C for 30 min with steps of 15 s.
6. Add 180  $\mu\text{L}$  substrate emulsion (containing (*R*)- and reference substrates) in microplate and measure the increase in absorbance at 404 nm and 572 nm at 25°C for 30 min with steps of 15 s.
7. Subtract the absorbance of the blank and intrinsic enzyme absorbance from the sample. Enantiomeric ratio for (*R*)- and (*S*)-enantiomer separately is calculated using Eqs. (1) and (2), respectively. Quick E enantiomeric ratio is calculated using Eq. (3).

---

## 4 Notes

1. pH of buffers may change with temperature; hence, for measuring temperature optima, use buffers having their pH adjusted accordingly.

2. Alternatively, dry argon can be used instead of dry nitrogen.
3. Stock solution is stable at  $-20^{\circ}\text{C}$  for at least 2 months
4.  $\text{NaIO}_4$  solution in water should be prepared freshly.
5. Sodium phosphate buffer may be used depending on optimal stability and activity of enzyme. Do not use buffer that is oxidised with  $\text{NaIO}_4$ , e.g. Tris or triethanol amine buffers.
6. The spontaneous hydrolysis of substrates can result in its decreased concentration upon long term storage of plates.
7. To increase the probability to find lipase-producing clones one can prepare several tributyrin agar plate replicas from one master plate after overnight incubation. Each replica plate may then be incubated at a different temperature, for example,  $4^{\circ}\text{C}$ ,  $37^{\circ}\text{C}$  and  $50^{\circ}\text{C}$  in order to detect lipases with different temperature optima.
8. Bacteria take up and accumulate pink coloured rhodamine B which is not fluorescent in the absence of free fatty acids.
9. To prevent damaging effects of UV light, apply UV radiation only for a short time (a few sec) if you want to propagate the clones from the same plate afterwards.
10. CAUTION: When adding the dry ice too fast, acetone will be spilled due to the released carbon dioxide.
11. Since the following step has to be carried out under inert conditions, a *Schlenk* flask can facilitate flushing with dry nitrogen.
12. Check the conversion of the starting material by thin layer chromatography.
13. 2-Methyldecanoic acid can hardly be visualised by using cerium ammonium molybdate stain [10 g  $\text{Ce}(\text{SO}_4)_2 \cdot 4 \text{H}_2\text{O}$ , 25 g molybdophosphoric acid, 60 mL conc.  $\text{H}_2\text{SO}_4$ , 940 mL  $\text{H}_2\text{O}$ ] for thin layer chromatography. For identifying fractions containing 2-methyldecanoic acid, GC-MS analysis can be useful.
14. We could observe a higher stability of different *p*-nitrophenyl and methylumbelliferyl esters in buffer in presence of DMSO.
15. Adjust the temperature to the enzymes to be tested. For high temperatures it is suitable to incubate the reactions in an incubator and interrupt the incubation for short measurements at lower temperatures. We incubated reactions at temperatures up to  $65^{\circ}\text{C}$ .
16. By adding enzyme solution to the standard curve mixtures the fluorescence of the enzyme will be included in the measurements. If the fluorescence of the enzyme is low also the enzyme solution buffer can be added in order to save enzyme. Furthermore, please consider that the fluorescence of 4-MU is pH-dependent. Ensure not to have high pH deviations.

17. The  $E$ -value is defined as  $E = \frac{(k_{\text{cat}}/K_M)_{\text{ent-1}}}{(k_{\text{cat}}/K_M)_{\text{ent-2}}}$  under competitive conditions, while the apparent  $E$ -value is determined under non-competitive conditions. The mere quotient of the initial conversion rates for both enantiomers is a simplification, which does not take into account effects occurring from concentration effects or competition (see Sect. 1.3).
18. The assay can be performed at temperatures up to 80–90°C, although the spontaneous hydrolysis of the substrate at higher temperatures is significant.
19. For the sake of reproducibility the same variant should be assayed with both enantiomers in the same plate.
20. Such an emulsion remains stable for 2–3 h.

## References

1. Jaeger K-E, Dijkstra BW, Reetz MT (1999) Bacterial biocatalysts: molecular biology, three-dimensional structures, and biotechnological applications of lipases. *Annu Rev Microbiol* 53:315–351
2. Jaeger K-E, Eggert T (2002) Lipases for biotechnology. *Curr Opin Biotechnol* 13 (4):390–397
3. Hausmann S, Jaeger K-E (2010) Lipolytic enzymes from bacteria. In: Timmis KN (ed) *Handbook of hydrocarbon and lipid microbiology*. Springer, Heidelberg, pp 1099–1126
4. Barbayanni E, Kokotos G (2012) Biocatalyzed regio- and chemoselective ester cleavage: synthesis of bioactive molecules. *ChemCatChem* 4 (5):592–608
5. Fischer T, Pietruszka J (2010) Key building blocks via enzyme-mediated synthesis. *Top Curr Chem* 297:1–43
6. Chang SW, Shaw JF (2009) Biocatalysis for the production of carbohydrate esters. *N Biotechnol* 26(3–4):109–116
7. Lambusta D et al (2003) Application of lipase catalysis in organic solvents for selective protection–deprotection of bioactive compounds. *J Mol Catal B: Enzym* 22(5):271–277
8. Nicolosi G et al (1999) Biocatalytic process for the preparation of 3-O-acyl-flavonoids. *WO Patent* 9966062
9. Pietruszka J, Simon RC (2009) Chemoenzymatic synthesis of (protected) psymberic acid. *Eur J Org Chem* 2009(21):3628–3634
10. Bódalo A et al (2009) Screening and selection of lipases for the enzymatic production of polyglycerol polyricinoleate. *Biochem Eng J* 46 (2):217–222
11. Steenkamp L, Brady D (2003) Screening of commercial enzymes for the enantioselective hydrolysis of R,S-naproxen ester. *Enzym Microb Technol* 32(3–4):472–477
12. Jaeger KE et al (2001) Directed evolution and the creation of enantioselective biocatalysts. *Appl Microbiol Biotechnol* 55(5):519–530
13. Liebeton K et al (2000) Directed evolution of an enantioselective lipase. *Chem Biol* 7 (9):709–718
14. Handelsman J (2004) Metagenomics: application of genomics to uncultured microorganisms. *Microbiol Mol Biol Rev* 68(4):669–685
15. Lorenz P et al (2002) Screening for novel enzymes for biocatalytic processes: accessing the metagenome as a resource of novel functional sequence space. *Curr Opin Biotechnol* 13(6):572–577
16. Voget S et al (2003) Prospecting for novel biocatalysts in a soil metagenome. *Appl Environ Microbiol* 69(10):6235–6242
17. Chow J et al (2012) The metagenome-derived enzymes LipS and LipT increase the diversity of known lipases. *PLoS One* 7(10), e47665
18. Liebl W et al (2014) Alternative hosts for functional (meta)genome analysis. *Appl Microbiol Biotechnol* 98(19):8099–8109
19. Chusacultanachai S, Yuthavong Y (2004) Random mutagenesis strategies for construction of large and diverse clone libraries of mutated DNA fragments. *Methods Mol Biol* 270:319–334
20. Reigstad LJ, Bartossek R, Schleper C (2011) Preparation of high-molecular weight DNA and metagenomic libraries from soils and hot springs. *Methods Enzymol* 496:319–344

21. Bornscheuer UT (2002) Methods to increase enantioselectivity of lipases and esterases. *Curr Opin Biotechnol* 13(6):543–547
22. Hoebenreich S et al (2015) Speeding up directed evolution: combining the advantages of solid-phase combinatorial gene synthesis with statistically guided reduction of screening effort. *ACS Synth Biol* 4:317–331
23. Franken B, Jaeger KE, Pietruszka J (2010) Screening for enantioselective enzymes. In: Timmis KN (ed) *Handbook of hydrocarbon and lipid microbiology*. Springer, Heidelberg, pp 2860–2876
24. Jaeger KE, Kovacic F (2014) Determination of lipolytic enzyme activities. *Methods Mol Biol* 1149:111–134
25. Ganske F, Bornscheuer UT (2005) Lipase-catalyzed glucose fatty acid ester synthesis in ionic liquids. *Org Lett* 7(14):3097–3098
26. Reetz MT et al (2001) A GC-based method for high-throughput screening of enantioselective catalysts. *Catal Today* 67(4):389–396
27. Pirkle WH, Hoover DJ (1982) NMR chiral solvating agents. *Top Stereochem* 13:263–331
28. Goering HL, Eikenberry JN, Koermer GS (1971) Tris [3-(trifluoromethylhydroxymethylene)-D-camphorato] europium (III). Chiral shift reagent for direct determination of enantiomeric compositions. *J Am Chem Soc* 93(22):5913–5914
29. Reetz MT et al (1999) A Method for high-throughput screening of enantioselective catalysts. *Angew Chem Int Ed Engl* 38(12):1758–1761
30. Schrader W et al (2002) Second-generation MS-based high-throughput screening system for enantioselective catalysts and biocatalysts. *Can J Chem* 80(6):626–632
31. Tielmann P et al (2003) A practical high-throughput screening system for enantioselectivity by using FTIR spectroscopy. *Chem Eur J* 9(16):3882–3887
32. Reetz MT et al (2002) A practical NMR-based high-throughput assay for screening enantioselective catalysts and biocatalysts. *Adv Synth Catal* 344(9):1008–1016
33. Kazlauskas RJ (2006) Quantitative assay of hydrolases for activity and selectivity using color changes. In: Reymond J (ed) *Enzyme assays*. Wiley-VCH Verlag GmbH & Co. KGaA, pp 15–39
34. Trapp O (2007) Boosting the throughput of separation techniques by “multiplexing”. *Angew Chem Int Ed Engl* 46(29):5609–5613
35. Becker S et al (2005) A generic system for the *Escherichia coli* cell-surface display of lipolytic enzymes. *FEBS Lett* 579(5):1177–1182
36. Kugimiya W et al (1986) Molecular cloning and nucleotide sequence of the lipase gene from *Pseudomonas fragi*. *Biochem Biophys Res Commun* 141(1):185–190
37. Kouker G, Jaeger K-E (1987) Specific and sensitive plate assay for bacterial lipases. *Appl Environ Microbiol* 53(1):211–213
38. Janes LE, Löwendahl AC, Kazlauskas RJ (1998) Quantitative screening of hydrolase libraries using pH indicators: identifying active and enantioselective hydrolases. *Chem Eur J* 4(11):2324–2331
39. Bottcher D, Bornscheuer UT (2006) High-throughput screening of activity and enantioselectivity of esterases. *Nat Protoc* 1(5):2340–2343
40. Arnold FH (1998) Design by directed evolution. *Acc Chem Res* 31(3):125–131
41. Reetz MT et al (1997) Creation of enantioselective biocatalysts for organic chemistry by in vitro evolution. *Angew Chem Int Ed Engl* 36(24):2830–2832
42. Dolinsky VW et al (2004) Regulation of the enzymes of hepatic microsomal triacylglycerol lipolysis and re-esterification by the glucocorticoid dexamethasone. *Biochem J* 378(Pt 3):967–974
43. Jacks TJ, Kircher HW (1967) Fluorometric assay for the hydrolytic activity of lipase using fatty acyl esters of 4-methylumbelliferone. *Anal Biochem* 21(2):279–285
44. Fluxá VS, Wahler D, Reymond J-L (2008) Enzyme assay and activity fingerprinting of hydrolases with the red-chromogenic adrenaline test. *Nat Protoc* 3(8):1270–1277
45. Reetz MT et al (2000) Circular dichroism as a detection method in the screening of enantioselective catalysts. *Chirality* 12(5–6):479–482
46. Faber K (2011) *Biotransformations in organic chemistry: a textbook*. Springer
47. Darley DJ et al (2009) Synthesis and use of isotope-labelled substrates for a mechanistic study on human  $\alpha$ -methylacyl-CoA racemase 1A (AMACR; P504S). *Org Biomol Chem* 7(3):543–552
48. Neises B, Steglich W (1978) Simple method for the esterification of carboxylic acids. *Angew Chem Int Ed Engl* 17(7):522–524
49. Wahler D et al (2004) Adrenaline profiling of lipases and esterases with 1,2-diol and carbohydrate acetates. *Tetrahedron* 60(3):703–710
50. Reetz MT (2006) High-throughput screening systems for assaying the enantioselectivity of enzymes. In: Reymond J (ed) *Enzyme assays*. Wiley-VCH Verlag GmbH & Co. KGaA, pp 41–76

51. Winkler UK, Stuckmann M (1979) Glycogen, hyaluronate, and some other polysaccharides greatly enhance the formation of exolipase by *Serratia marcescens*. J Bacteriol 138 (3):663–670
52. Franken B, Jaeger KE, Pietruszka J (2010) Protocols to screen for enantioselective lipases. In: Timmis KN (ed) Handbook of hydrocarbon and lipid microbiology. Springer, Heidelberg, pp 4581–4586
53. Reetz MT et al (2007) Learning from directed evolution: further lessons from theoretical investigations into cooperative mutations in lipase enantioselectivity. ChemBiochem 8(1):106–112
54. Janes LE, Kazlauskas RJ (1997) Quick E. A fast spectrophotometric method to measure the enantioselectivity of hydrolases. J Org Chem 62(14):4560–4561

# Use of Bacterial Polyhydroxyalkanoates in Protein Display Technologies

Iain D. Hay, David O. Hooks, and Bernd H.A. Rehm

## Abstract

Protein display and immobilization are powerful tools used in industrial biocatalysts, bioremediation, biomolecule screening and purification, as well as biosensor applications. Immobilization can aid in the stability and function of a protein and can allow its recovery and potential reuse. Traditional protein immobilization techniques involving entrapment or non-covalent interactions between the protein and support materials are susceptible to leaching and often require additional cross-linking steps; which may be costly, potentially toxic and may negatively affect the function of the protein. All of these approaches require multiple steps to produce, isolate, and immobilize the protein of interest. Here we present protocols for the *in vivo* production of a protein of interest covalently immobilized on the surface of a bio-polyester resin in a single step. The steps involved in vector construction, protein/bead production, and isolation are explained and outlined.

**Keywords:** Polyhydroxyalkanoate, Protein immobilization

---

## 1 Introduction

Over the past few decades, the immobilization of functional proteins to solid support materials has become a powerful technique used in various medical and industrial applications. Enzyme immobilization is widely employed to increase the stability and/or kinetics of enzymes for use in industrial biocatalyst applications as well as bioremediation applications. The immobilization of ligand-binding domains allows the simple purification of, or removal of diverse molecules through affinity chromatography. Furthermore the immobilization of functional proteins often allows their recovery and reuse. More recently the immobilization of enzymes and binding domains has led to various emerging biosensor and microarray technologies [1–5].

The manufacture of these immobilized proteins typically involves multiple discrete steps: the production of the functional protein by conventional cell-based techniques; the purification of

the functional protein from the unwanted cellular material (potentially followed by a refolding step if the protein is produced as inclusion bodies); the production and preparation of the support material; and finally the immobilization of the protein to the support. Typically a covalent attachment is desirable to prevent leaching or enzyme loss, this generally involves chemical cross-linking [4, 6, 7]. This conventional method has several potential drawbacks, primarily the cost and duration of the discrete steps as well as the potentially costly and toxic chemicals used in the cross-linking/immobilization step. Furthermore, although some immobilization techniques can allow for a more defined orientation of a protein, many of the commonly used techniques result in a random distribution of protein orientations, which can potentially result in a population of the proteins having occluded binding/catalytic sites and hence decreased functionality [8].

Here we present a technique for the *in vivo* production of functional protein covalently attached to the surface of a sub-micrometer (50–500 nm diameter) bio-polyester (polyhydroxyalkanoate, PHA) beads (Fig. 1). The protein production, support material (PHA) production, and immobilization occur in a single bacterial fermentation step. The functional bio-polyester bead can be isolated from the bacteria by straightforward lysis, centrifugation, and washing steps. This technique exploits a naturally occurring process used by many bacterial species for carbon storage. Many bacteria can deposit PHA as spherical inclusions in the cytoplasm; the key enzyme involved in this accumulation, the polyester synthase, remains covalently attached to the emerging polyester chain and the enzyme-polyester molecules self-assemble into growing PHA beads inside the cell [9, 10]. By fusing functional proteins to the polyester synthase (at the genetic level), it is possible to immobilize proteins on these PHA beads *in vivo*. The entire metabolic pathway can be easily implemented in the industrial

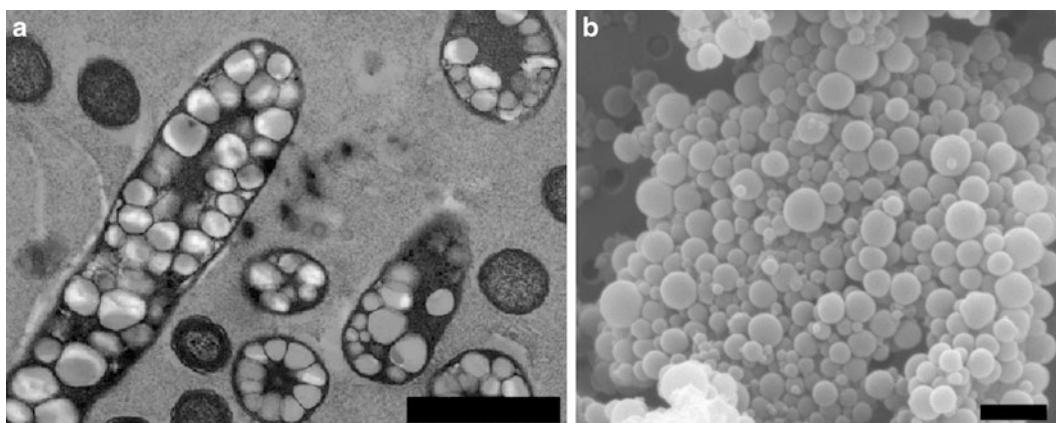


**Fig. 1** (a) Transmission electron microscopy of *E. coli* cells producing polyester beads. (b) Scanning electron microscopy of purified PHA beads. The *black bar* represents 1  $\mu\text{m}$

workhorse *Escherichia coli* through the addition of only three genes from the natural PHA-producing *Ralstonia eutropha* (*Cupriavidus necator*): *phaA*, encoding a  $\beta$ -ketothiolase; *phaB*, encoding an acetoacetyl-CoA reductase; and *phaC*, the PHA-polyester synthase to which the protein of interest is genetically fused. PhaA and PhaB divert acetyl-CoA from the central metabolism to generate (*R*)-3-hydroxybutyryl-CoA which is subsequently polymerized by PhaC into PHA [11–13].

This technique has successfully been used for the immobilization of various enzymes, binding domains, other functional proteins [14–28, 33], as well as various proprietary proteins (IDH and BHAR unpublished results). An advantage of this technique is that PHA is a biodegradable and biocompatible material [29, 30]. Where the potential for trace levels of endotoxin in the final product is a concern, a Gram-positive host can be used [23, 31].

---

## 2 Vector Construction

### 2.1 Notes Before Commencing

- The vectors used for the generation of PhaC fusion proteins can be obtained from PolyBatics Ltd. (pPOLY-N and pPOLY-C) or are available to academic research labs from the following sources: pET14b:ZZ-PhaC [14] for fusion to the N-terminus of PhaC and pET-14b:PhaC-linker-GFP [20] for fusion to the C-terminus of PhaC.
- In order to produce protein-displaying beads, use the *NdeI* and *SpeI* sites to add your protein-coding region to the N-terminus of the polyester synthase (i.e., fusion via the C-terminus of your protein) (Fig. 1) (NB. If using pET14b:ZZ-PhaC, only *NdeI* should be used and the direction of the ligated insert will need to be checked) and *XhoI* and *BamHI* to add your protein-coding region to the C-terminus of the polyester synthase (i.e., fusion via the N-terminus of your protein). Utilizing the *NdeI* site allows you to use the ATG site within the CATATG recognition site as the start codon. If you plan to attach to the C-terminus of the synthase (i.e., via the N-terminus of the antigen), it is recommended to integrate a stop codon (TAA) before the *BamHI* site when amplifying or synthesizing your target antigen. Although there is a stop codon immediately after the *BamHI* site on the plasmid, utilizing this results in an additional Gly-Ser on the C-terminus.
- To generate a “dual fusion” (i.e., fusion to both the N- and C-termini of PhaC), the antigen should be cloned into the pPOLY-N and pPOLY-C (or pET14b:ZZ-PhaC and pET-14b:PhaC-linker-GFP) vectors independently and then the C-terminal encoding region of the fusion cut from the pPOLY-C (pET-14b:PhaC-linker-GFP) derived plasmid encoding your protein

via *NotI* and *BamHI* and ligated into the corresponding sites of the pPOLY-N (or pET14b:ZZ-PhaC) derived plasmid encoding your protein (*see* Fig. 2c).

- It is recommended to confirm all final constructs by sequencing the region of the plasmid containing the inserted antigen-coding region. Commonly available “T7 promoter” and “T7 terminator” primers will sequence the N-terminal encoding and C-terminal encoding regions, respectively.

## 2.2 Reagents and Equipment Required

- Plasmids containing *phaC* under the control of a T7 (or similar) promoter and restriction sites to allow ligation of your gene of interest in frame (see Sect. 2.1 for details)
- T4 DNA ligase and associated buffer(s)
- Restriction enzymes and associated buffers (*NdeI*, *SpeI*, *XhoI*, *BamHI*)
- Equipment for DNA agarose gel electrophoresis
- Commercial kit (or alternative) to isolate DNA fragments from agarose gels
- Commercial plasmid isolation kit or any alternative
- Competent cells – general-purpose *E. coli* “cloning strain” (e.g., XL1Blue, Top10, DH5 $\alpha$ <sup>TM</sup>)
- DNA encoding your protein of interest (commercially synthesized or amplified via PCR with appropriate restriction sites)
- LB agar plates with 75  $\mu$ g/ml ampicillin

## 2.3 Protocol (Fig. 2)

1. Linearize 1–4  $\mu$ g of the *phaC* containing vector with appropriate restriction enzymes.
  - *NdeI* and *SpeI* for pPOLY-N (fusion to the N-terminus of PhaC via the C-terminus of your protein)
  - *NdeI* for pET14b:ZZ-PhaC (fusion to the N-terminus of PhaC via the C-terminus of your protein)
  - *XhoI* and *BamHI* for pPOLY-C or pET-14b:PhaC-linker-GFP (fusion to the C-terminus of PhaC via the N-terminus of your protein)
2. Gel purify the linearized vector (according to kit manufacturer’s instructions).
3. Prepare your gene of interest by hydrolysis with the same enzymes as above (gel purify if necessary).

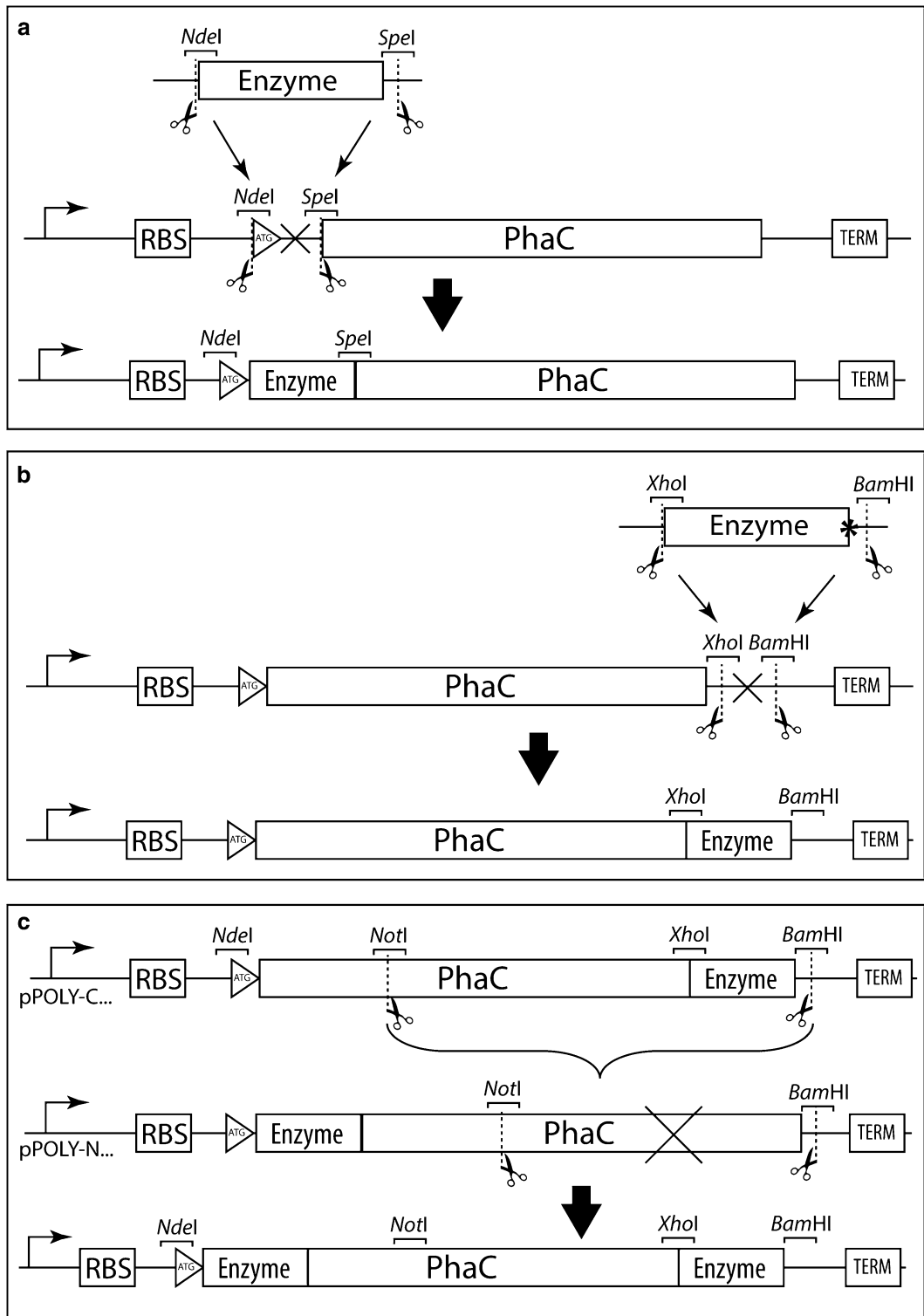


**Fig. 2** (a) Schematic representation of the cloning strategy to generate genetic fusions of enzymes (or other proteins) to the N-terminus of PhaC using the pPOLY-N vector backbone (if using pET14b:ZZ-phaC, then only the *NdeI* site should be used and the direction of the insert will need to be confirmed). (b) Schematic description of the cloning strategy to generate genetic fusions to the C-terminus of PhaC using pPOLY-C or pET14b:PhaC-linker-GFP as backbones. (c) Schematic description of the cloning strategy to generate genetic dual antigenic fusions to PhaC from the constructs generated in A and B

4. Ligate your protein-encoding fragment into the vector according to the ligase manufacturer's instructions or use the following:
  - 20 ng DNA of interest
  - 50 ng of vector from step 1
  - 400 cohesive end units of T4 DNA ligase
  - T4 DNA ligase buffer diluted to 1×
  - H<sub>2</sub>O to final volume 20 µl
  - Incubate for at least 2 h at 16°C
5. Transform 2–10 µl of the ligation mixture into competent cells (general cloning strain) following the manufacturer's instructions.
6. Plate transformed cells on LB agar plates containing 75 µg/ml ampicillin and incubate at 37°C overnight.
7. Screen colonies for correct ligation by restriction analysis, colony PCR, or sequencing.
8. Create a stock of correct strains and isolate plasmids with a commercial plasmid isolation kit.

---

### 3 Protein and PHA Bead Production

#### 3.1 Reagents and Equipment Required

- Plasmid containing *phaA* and *phaB*: pMCS69 [32] or pPOLY-HELP available from PolyBatics Ltd.
- Competent *E. coli* cells – production strains must be lysogenic for λ-DE3, which encodes T7 RNA polymerase under the control of the lac UV5 promoter (e.g., BL21(DE3), T7 Express)
- Buffers for making competent or electrocompetent cells (any common method will work)
- LB agar plates with 34 µg/ml chloramphenicol
- LB agar plates with 75 µg/ml ampicillin, 34 µg/ml chloramphenicol, and 1% glucose
- 1 M IPTG
- 75 mg/ml ampicillin and 34 mg/ml chloramphenicol
- LB liquid medium
- Conical flasks (the total volume of the flask should be approximately 5 times the volume of media contained in the flask to allow sufficient aeration)
- Orbital shaker at 25 °C
- Spectrophotometer for OD<sub>600nm</sub> measurement

### 3.2 Protocol: Creating Your Competent Production Host

1. Transform competent cells (production strain, DE3) with the *phaA* and *phaB* containing plasmid.
2. Plate transformants on LB agar containing 34 µg/ml chloramphenicol and incubate at 37°C overnight.
3. Isolate a single colony, confirm it contains the appropriate plasmid, and make a stock of this colony for long-term storage.
4. Make competent cells with this strain (remembering to include chloramphenicol when growing the cells).

### 3.3 Protocol: Protein and PHA Bead Production

1. Transform the competent cells harboring the *phaA* and *phaB* containing plasmid with your PhaC fusion protein-encoding vector generated in Sect. 2.
2. Plate on LB agar plates with 75 µg/ml ampicillin, 34 µg/ml chloramphenicol, 1% glucose and incubate overnight.
3. Select a few colonies and inoculate several precultures (LB containing 75 µg/ml ampicillin, 34 µg/ml chloramphenicol, and 1% glucose); incubate with shaking overnight at 37°C.
4. Inoculate new flasks (100 ml LB containing 75 µg/ml ampicillin, 34 µg/ml chloramphenicol, and 1% glucose in a 500 ml flask) with 1% of the overnight cultures. Incubate these flasks with shaking (200–250 rpm) at 25°C.
5. When cultures reach an OD<sub>600nm</sub> of 0.3–0.5, induce them with the addition of 1 mM IPTG (final concentration in the flask) and return to the 25°C shaker for an additional 40–48 h.

---

## 4 Bead Isolation (Fig. 3)

### 4.1 Notes Before Commencing

- Several methods can be used for cell lysis. Mechanical methods such as French press or microfluidizer based systems tend to yield the best results, though sonication and chemical methods such as BugBuster<sup>®</sup> or B-Per<sup>®</sup> have been used successfully.
- The addition of 0.5 mg/ml lysozyme and DNase to the lysis buffer followed by a 30-min incubation before disruption can help with cell lysis and separation of beads from cell debris.
- If PBS is not compatible with your protein of interest, then PBS can be substituted by most common buffers (though buffers containing strong reducing agents such as DTT should be avoided).
- If possible, best results are obtained by separating polyester beads from cellular debris over a glycerol step gradient centrifuged at 100,000 × *g* for 2 h. If this high-speed centrifugation is not feasible (lack of ultracentrifuge), then satisfactory results

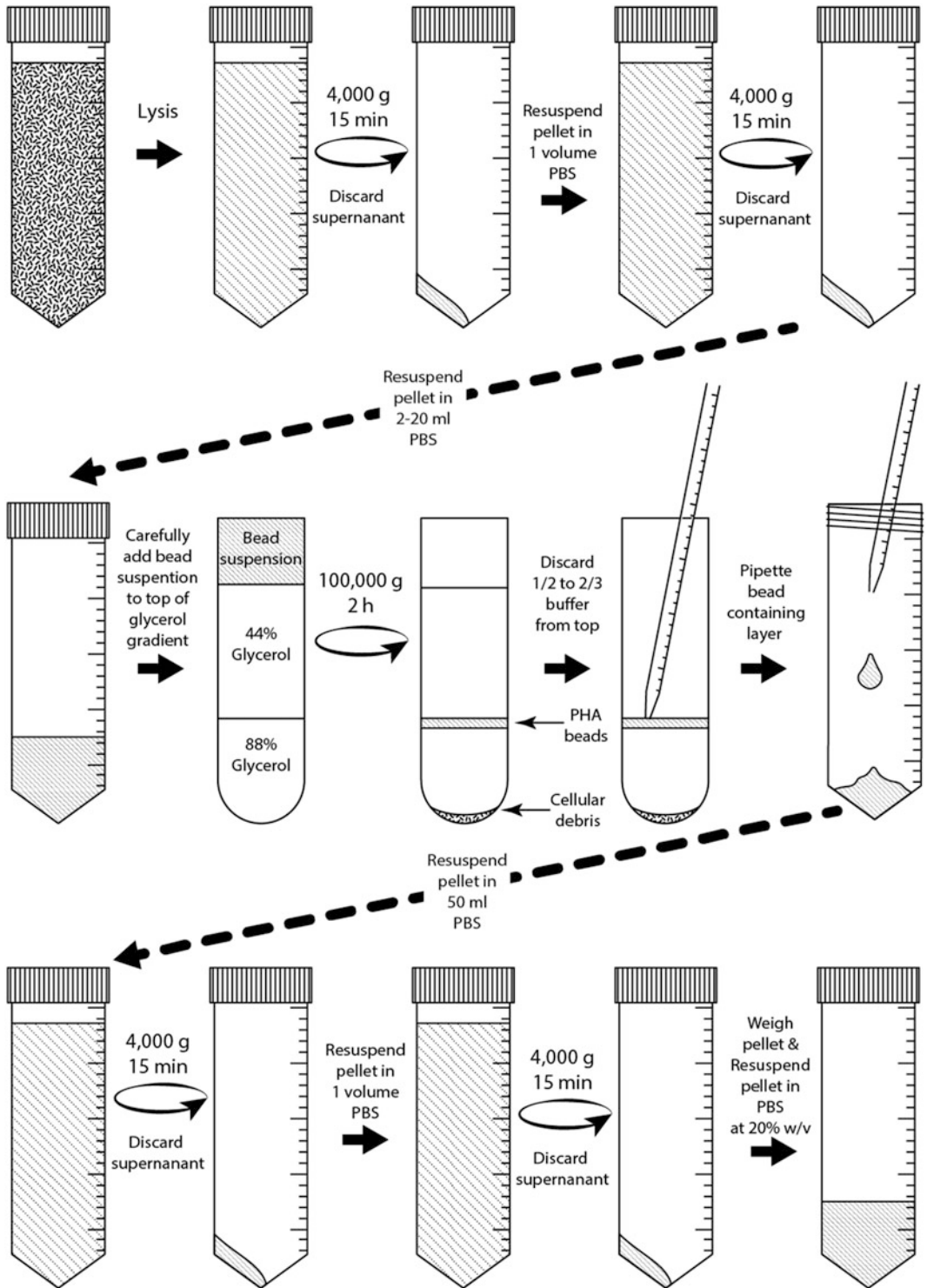


**Fig. 3** Schematic representation of the bead isolation strategy

have been obtained by using centrifugation at  $40,000\text{--}50,000 \times g$  for 4–5 h. Beads will concentrate between the two glycerol layers.

#### **4.2 Reagents and Equipment Required**

- Centrifuge capable of spinning 100 ml at 5,000 g
- $10\times$  phosphate buffered saline (PBS) (1.37 M NaCl, 27 mM KCl, 100 mM  $\text{Na}_2\text{HPO}_4$ , 18 mM  $\text{KH}_2\text{PO}_4$ )
- $1\times$  PBS – sterilize by autoclaving
- 88% glycerol – 88% (v/v) glycerol, 10%  $10\times$  PBS, 2%  $\text{H}_2\text{O}$
- 44% glycerol – 44% (v/v) glycerol, 10%  $10\times$  PBS, 46%  $\text{H}_2\text{O}$
- Equipment for bacterial cell disruption (*see* Sect. 4.1)
- Centrifuge capable of spinning 10–30 ml at  $100,000 \times g$  (and tubes capable of sustaining  $100,000 \times g$ )

#### **4.3 Protocol: Bead Isolation**

1. Harvest cells by centrifugation at  $5,000 \times g$ .
2. Resuspend cells in 0.5 volumes of PBS and lyse cells by your preferred method (*see* Sect. 4.1).
3. Centrifuge cell lysate at  $4,000 \times g$  for 30 min.
4. Discard supernatant (may be slightly cloudy).
5. Wash insoluble pellet in 40 ml PBS and centrifuge again at  $4,000 \times g$  for 15 min.
6. Discard supernatant (may be slightly cloudy) and suspend PHA bead containing pellet into PBS to an approximately 10–20% slurry of PHA beads.
7. Fill  $1/3$  of a centrifuge tube with 88% glycerol and carefully add another  $1/3$  of 44% glycerol on top of the 88% layer (you should see a distinct interface between the layers).
8. Carefully add the bead suspension to the top of the glycerol. NB. To achieve maximum purity, it is advised that you split your crude bead suspension between several tubes (less beads per tube generally results in cleaner beads).
9. Centrifuge at  $100,000 \times g$  for 2 h (sufficient separation has also been achieved at  $50,000 \times g$  for 3 h, *see* Sect. 4.1).
10. You should see a layer of beads at the interface between the 44% and 88% glycerol layer and possibly a layer of un-lysed cells and cellular debris at the bottom of the tube.
11. Carefully pipette or scoop out the bead containing interphase between the 44% and 88% layer and add to a new tube.

12. Resuspend the beads (vortex or pipette) in ~50 ml of PBS and centrifuge at  $4,000 \times g$  for 20 min. Discard the supernatant (it may be slightly cloudy) and repeat this step twice more.
13. Weigh the resulting bead pellet and resuspend in sufficient PBS to achieve a 20% (w/v) bead suspension.
14. Store at 4°C.

## 5 Analysis of the Protein-Displaying Beads

### 5.1 SDS Polyacrylamide Gel Electrophoresis of Beads and Protein Densitometry (Fig. 4)

The amount of proteins on the beads can be routinely assessed by subjecting the beads to conventional SDS polyacrylamide gel electrophoresis. Typically loading a few microliters of a 5% bead suspension on SDS-PAGE should provide a good indication of the relative amount of fusion protein (and contaminating proteins) on the beads. Determining the specific immobilized PhaC fusion protein concentration is challenging due to the immobilized nature of the proteins and the light-scattering effect of PHA granules during spectroscopy; additionally the potential number of co-purified granule-associated proteins can complicate this.

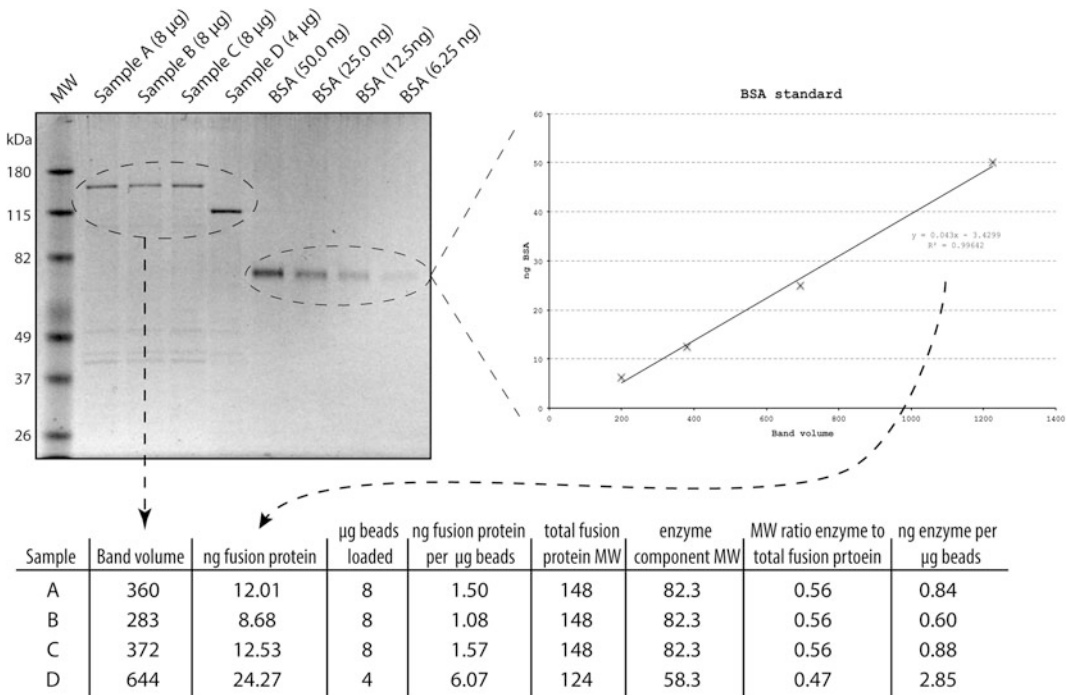


**Fig. 4** An example of an SDS-PAGE analysis of isolated enzymes displaying PHA beads and the subsequent densitometry, BSA standard, and calculations to determine how much enzyme is present on the beads (bead weights reported here are in wet weight; if dry weights are required, the representative sample can be freeze dried and weighed)

Densitometry on protein bands resolved by SDS-PAGE allows for precise measurement of the PhaC fusion protein mass. As immobilization of an enzyme to a solid support matrix often has an effect on its activity (beneficial or deleterious), it is important to assess enzymatic properties of an immobilized form to the soluble form of the enzyme. Determining an accurate concentration of PhaC fusion protein allows for calculation of specific enzyme activity which can then be directly compared to the activity of the free enzyme.

#### 5.1.1 Reagents and Equipment Required

- 3× protein denaturing solution (800 mg SDS, 3.7 mg EDTA, 0.5 mg bromophenol blue all dissolved in 2 ml of β-mercaptoethanol, 4 ml of glycerol, and 4 ml of 100 mM Tris-HCl, pH 6.8) – most common SDS-PAGE loading dyes should also work
- BSA stock solution (10 mg of BSA in 1 ml of PBS)
- Equipment for SDS-PAGE
- SDS-PAGE gels (typically 4% stacking and 10% separating gels though this can be modified to suit the MW of your fusion protein)
- Coomassie blue stain (2.5 g Coomassie Brilliant Blue R-250, in 450 ml methanol, 100 ml of acetic acid, and 450 ml H<sub>2</sub>O)
- Destaining solution (10% (v/v) acetic acid and 45 % (v/v) methanol, 45% (v/v) H<sub>2</sub>O)
- 7% v/v acetic acid in water
- Equipment to capture images of SDS-PAGE gels and software to analyze gel images (e.g., Bio-Rad's Gel Doc™ and Image Lab™)

#### 5.1.2 Protocol: SDS-PAGE and Densitometry

1. Produce the PHA beads displaying the immobilized enzyme of interest and resuspend in PBS at a known concentration, typically 20% (w/v) or 200 mg/ml (wet bead mass).
2. Dilute the PHA bead sample to a final concentration of 0.9 mg/ml (wet bead mass) in PBS.
3. Serially dilute BSA stock solution with protein denaturing buffer (1×) to concentrations of 5, 2, 1, and 0.5 ng/μl BSA. These standards can be stored at -20°C until required.
4. Add protein denaturing buffer (3×) at a ratio of 1:3 to the diluted PHA beads. Then heat PHA bead samples and BSA standards at 95°C for 15 min to denature surface proteins and dissociate them from the PHA beads.
5. Pipette 10 μl samples containing 2–10 μg of PHA granules (wet weight) into a vertical SDS polyacrylamide mini gel. The amount of protein on the granules can vary markedly according to the fusion partner; highly produced proteins will

need fewer beads (more dilutions) on the gel, whereas low levels of production will need more materials.

6. Pipette 10  $\mu\text{l}$  of 5, 2, 1, and 0.5 ng/ $\mu\text{l}$  BSA standards into separate wells.
7. Run the SDS-PAGE at 150 V for 1 h.
8. Stain the gel with Coomassie blue stain for at least 30 min and subsequently destain with destaining solution.
9. To ensure sufficient destaining for accurate densitometry, the gel should be further incubated overnight in 7% acetic acid.
10. Capture the gel image.
11. Measure the protein band intensity of the BSA standards and PhaC fusion protein bands using appropriate imaging software.
12. Create a standard curve of the BSA band intensities and use it to determine PhaC fusion protein concentration. A typical example may contain 24 ng protein from 6  $\mu\text{g}$  of beads leading to a protein density of 4  $\mu\text{g}/\text{mg}$  beads. If only the amount of the functional protein is required, then the ratio of the molecular weight of the functional protein component to the total molecular weight of the fusion protein (functional protein + PhaC (64.3 kDa)) should be used for the calculation.

**5.2 Protocol:**  
**Determining Enzyme**  
**Activity**

1. Weigh enough 1.7 ml tubes for all samples.
2. Transfer 500  $\mu\text{l}$  of 20% (w/v) PHA beads into 1.7 ml tubes and centrifuge ( $3,400 \times g$ , 4 min).
3. Discard the supernatant.
4. Briefly centrifuge (up to  $3,400 \times g$ ) and discard residual supernatant.
5. Reweigh the tubes and calculate wet PHA bead mass.
6. Multiply the wet PHA bead mass by the fusion protein proportion figure to calculate the fusion protein mass present in each sample.
7. Samples of the free enzyme can be set up to correspond with the amount of fusion protein present in the PHA bead samples.
8. Perform the appropriate enzyme activity assay and determine activity ( $\mu\text{mol}/\text{min}$ ) for both the free and immobilized enzyme (NB. The immobilized enzyme will typically need some kind of shaking or mixing to prevent the beads from settling).
9. The amount of protein as determined by densitometry (remembering to factor in the molecular weight ratio of enzyme to enzyme + PhaC) can then be used to determine the amount of only the fusion partner, i.e., only the enzyme, in order to determine the specific activity. This can be directly compared to the free enzyme activity.

### 5.3 Assessing the Levels of PHA Production and Yield

Fusing additional protein sequence to the N- and/or C-termini of PhaC can have an effect on the quantity of PHB synthesized by the production host. GCMS allows the measurement of PHB production down to trace amounts. Quantifying the amount of PHA *in vivo* is a useful indication of PhaC activity and PHA yield.

#### 5.3.1 Reagents and Equipment Required

- Methanolic sulfuric acid: Measure 85 ml of methanol and place in a beaker on ice to cool. Measure 15 ml of sulfuric acid and slowly add to the methanol while it is on ice. *Caution:* this reaction is extremely exothermic.
- Chloroform (containing 105 µg/ml undecane as an internal standard): Add 14.2 µl of undecane to 100 mL of chloroform and mix.
- Screw-capped glass tubes. The tube, lid, and gasket must be able to sustain the chloroform and methanolic sulfuric acid at 100°C without any leakage.
- 100°C oil bath or similar.
- Equipment for GCMS analysis. An example setup would be a Shimadzu GC-17A gas chromatograph equipped with a Restek Rxi-5ms GC column (30 m × 0.25 mm ID × 0.25 µm film thickness) and a QP5050A quadrupole mass spectrometer to detect the PHA methyl esters. Injection volume is 1 µl, split is 20:1, and helium (1 ml/min) is used as the carrier gas. The temperature of the injector is set at 220°C and the detector temperature is 250°C. The temperature program used is 35°C for 5 min, a temperature ramp of 5°C/min to 100°C, and finally a ramp of 15°C/min to 285°C. In these conditions the retention time of β-hydroxybutyric acid methyl ester is 9.10 min.

#### 5.3.2 Protocol: Assessing the Levels of PHA Production and Yield

1. Prepare 50 ml of bacterial PHA bead culture, and after 48 h of cultivation, pellet the cells by centrifugation ( $5,000 \times g$ , 20 min).
2. Resuspend the cell pellet in 5 ml PBS (pH 7.4) and freeze for at least 12 h at  $-80^{\circ}\text{C}$  or for 10 min in liquid nitrogen.
3. Freeze dry the frozen cell suspension for at least 12 h.
4. Grind the dry cell pellet into a fine powder.
5. Weigh 10–30 mg of the powdered cell pellet into a screw cap glass test tube recording the exact weight.
6. Prepare the PHB standards of 1, 2, 5, 10, and 15 mg in the same way.
7. Add 2 ml chloroform containing internal standard and 2 ml 15% methanolic sulfuric acid and vortex mix for 1 min.
8. Place the samples in a 100°C oil bath for 5 h and then cool in an ice bath to room temperature. This reaction breaks down the PHB into β-hydroxybutyric acid methyl ester.

9. Add 2 ml water and vortex mix for 1 min and then leave to sit for 5 min allowing the phases to separate.
10. Use a glass Pasteur pipette to remove the lower, organic phase. Expel the pipette as it is inserted through the upper layer to ensure the aqueous phase does not enter the pipette tip.
11. Filter the collected organic phase containing  $\beta$ -hydroxybutyric acid methyl ester through cotton wool to remove any remaining particulates.
12. At this point the sample can be stored at  $-80^{\circ}\text{C}$  until required for analysis.
13. Subject the samples to GCMS analysis using the method described above or similar.
14. Position the standards at the beginning, middle, and end of the GCMS analysis runs.
15. Divide all PHB values by undecane internal standard peak area to account for differences in sample evaporation.
16. Average the standard runs and create a standard curve.
17. Calculate the PHB amount in each of the unknown samples using the standard curve and then divide by the initial dry cell weight to determine PHB as a percent of dry cell weight.
18. The deduced level of PHA in your cells can then be related to the amount of material you recovered to give an idea of the yield of the bead isolation.

---

## 6 Troubleshooting

### **6.1 Excessive Contaminating Bands on SDS-PAGE**

The immobilization of some proteins can cause cellular proteins to “co-purify” with the beads more than others. In these cases, changing the buffer used for lysis and washing can be beneficial; increasing the salt concentration and changing the pH are good starting points. The addition of low levels (0.05%) of Tween 20 can also be beneficial in these cases.

### **6.2 Low Enzyme Activity/Protein Function**

Each protein fused to the beads may perform differently. Some proteins will tolerate fusion to one terminus and not the other; thus switching the fusion site (i.e., via the protein’s N- or C-terminus) can often have beneficial effects on function of the immobilized protein. Structural information (if known) about the protein can often be used to guide decisions about the optimal fusion point. The addition of polypeptide linkers between the polyester synthase and the protein of interest may help in optimizing the level of protein function.

### 6.3 No Beads/ Inclusion Bodies at the Bottom of the Glycerol Gradient

Occasionally some proteins are so prone to aggregation during production that the formation of inclusion bodies occurs before the immobilization of the proteins on growing PHA beads. In these cases the proteins will typically form a proteinaceous inclusion body pellet at the bottom of the glycerol gradient (this is easily identified due to its typically gray color compared to the typically white color of the PHA beads). This can often be combated by lowering the temperature during growth and/or modifying the time of IPTG induction. Changing the strain of *E. coli* used for the production can also help in these cases (though the strain must still be lysogenic for  $\lambda$ -DE3 to allow T7 expression). This is particularly useful when the protein of interest has disulfide bonds, which will typically not form in the *E. coli* cytosol. In these cases it is often beneficial to use strains engineered to have more oxidizing cytosols (e.g., Origami™ or SHuffle®) for bead production [33].

### References

1. Cretich M, Damini F, Pirri G, Chiari M (2006) Protein and peptide arrays: recent trends and new directions. *Biomol Eng* 23:77–88. doi:10.1016/j.bioeng.2006.02.001
2. Mateo C, Palomo JM, Fernandez-Lorente G, Guisan JM, Fernandez-Lafuente R (2007) Improvement of enzyme activity, stability and selectivity via immobilization techniques. *Enzyme Microb Technol* 40:1451–1463. doi:10.1016/j.enzmictec.2007.01.018
3. Sheldon RA (2007) Enzyme immobilization: the quest for optimum performance. *Adv Synt Catal* 349:1289–1307. doi:10.1002/adsc.200700082
4. Brena B, Gonzalez-Pombo P, Batista-Viera F (2013) Immobilization of enzymes: a literature survey. *Methods Mol Biol* 1051:15–31. doi:10.1007/978-1-62703-550-7\_2
5. Putzbach W, Ronkainen NJ (2013) Immobilization techniques in the fabrication of nanomaterial-based electrochemical biosensors: a review. *Sensors (Basel)* 13:4811–4840. doi:10.3390/s130404811
6. Hanefeld U, Gardossi L, Magner E (2009) Understanding enzyme immobilisation. *Chem Soc Rev* 38:453–468. doi:10.1039/b711564b
7. Sheldon RA, van Pelt S (2013) Enzyme immobilisation in biocatalysis: why, what and how. *Chem Soc Rev* 42:6223–6235. doi:10.1039/c3cs60075k
8. Secundo F (2013) Conformational changes of enzymes upon immobilisation. *Chem Soc Rev* 42:6250–6261. doi:10.1039/c3cs35495d
9. Grage K, Jahns AC, Parlani N, Palanisamy R, Rasiah IA, Atwood JA, Rehm BH (2009) Bacterial polyhydroxyalkanoate granules: biogenesis, structure, and potential use as nano-/micro-beads in biotechnological and biomedical applications. *Biomacromolecules* 10:660–669. doi:10.1021/bm801394s
10. Draper JL, Rehm BH (2012) Engineering bacteria to manufacture functionalized polyester beads. *Bioengineered* 3:203–208. doi:10.4161/bioe.19567
11. Rehm BH (2006) Genetics and biochemistry of polyhydroxyalkanoate granule self-assembly: the key role of polyester synthases. *Biotechnol Lett* 28:207–213. doi:10.1007/s10529-005-5521-4
12. Rehm BH (2010) Bacterial polymers: biosynthesis, modifications and applications. *Nat Rev Microbiol* 8:578–592. doi:10.1038/nrmicro2354
13. Hooks DO, Venning-Slater M, Du J, Rehm BH (2014) Polyhydroxyalkanoate synthase fusions as a strategy for oriented enzyme immobilisation. *Molecules* 19:8629–8643. doi:10.3390/molecules19068629
14. Brockelbank JA, Peters V, Rehm BH (2006) Recombinant *Escherichia coli* strain produces a ZZ domain displaying biopolyester granules suitable for immunoglobulin G purification. *Appl Environ Microbiol* 72:7394–7397. doi:10.1128/AEM.01014-06
15. Backstrom BT, Brockelbank JA, Rehm BH (2007) Recombinant *Escherichia coli* produces tailor-made biopolyester granules for applications in fluorescence activated cell sorting: functional display of the mouse interleukin-2 and myelin oligodendrocyte glycoprotein. *BMC Biotechnol* 7:3. doi:10.1186/1472-6750-7-3

16. Grage K, Rehm BH (2008) In vivo production of scFv-displaying biopolymer beads using a self-assembly-promoting fusion partner. *Bioconjug Chem* 19:254–262. doi:[10.1021/bc7003473](https://doi.org/10.1021/bc7003473)
17. Jahns AC, Haverkamp RG, Rehm BH (2008) Multifunctional inorganic-binding beads self-assembled inside engineered bacteria. *Bioconjug Chem* 19:2072–2080. doi:[10.1021/bc8001979](https://doi.org/10.1021/bc8001979)
18. Peters V, Rehm BH (2008) Protein engineering of streptavidin for in vivo assembly of streptavidin beads. *J Biotechnol* 134:266–274. doi:[10.1016/j.jbiotec.2008.02.006](https://doi.org/10.1016/j.jbiotec.2008.02.006)
19. Atwood JA, Rehm BH (2009) Protein engineering towards biotechnological production of bifunctional polyester beads. *Biotechnol Lett* 31:131–137. doi:[10.1007/s10529-008-9836-9](https://doi.org/10.1007/s10529-008-9836-9)
20. Jahns AC, Rehm BH (2009) Tolerance of the *Ralstonia eutropha* class I polyhydroxyalkanoate synthase for translational fusions to its C terminus reveals a new mode of functional display. *Appl Environ Microbiol* 75:5461–5466. doi:[10.1128/AEM.01072-09](https://doi.org/10.1128/AEM.01072-09)
21. Rasiah IA, Rehm BH (2009) One-step production of immobilized alpha-amylase in recombinant *Escherichia coli*. *Appl Environ Microbiol* 75:2012–2016. doi:[10.1128/AEM.02782-08](https://doi.org/10.1128/AEM.02782-08)
22. Grage K, Peters V, Rehm BH (2011) Recombinant protein production by in vivo polymer inclusion display. *Appl Environ Microbiol* 77:6706–6709. doi:[10.1128/AEM.05953-11](https://doi.org/10.1128/AEM.05953-11)
23. Parlane NA, Grage K, Lee JW, Buddle BM, Denis M, Rehm BH (2011) Production of a particulate hepatitis C vaccine candidate by an engineered *Lactococcus lactis* strain. *Appl Environ Microbiol* 77:8516–8522. doi:[10.1128/AEM.06420-11](https://doi.org/10.1128/AEM.06420-11)
24. Blatchford PA, Scott C, French N, Rehm BH (2012) Immobilization of organophosphohydrolase OpdA from *Agrobacterium radiobacter* by overproduction at the surface of polyester inclusions inside engineered *Escherichia coli*. *Biotechnol Bioeng* 109:1101–1108. doi:[10.1002/bit.24402](https://doi.org/10.1002/bit.24402)
25. Parlane NA, Grage K, Mifune J, Basaraba RJ, Wedlock DN, Rehm BH, Buddle BM (2012) Vaccines displaying mycobacterial proteins on biopolyester beads stimulate cellular immunity and induce protection against tuberculosis. *Clin Vaccine Immunol* 19:37–44. doi:[10.1128/CVI.05505-11](https://doi.org/10.1128/CVI.05505-11)
26. Hooks DO, Blatchford PA, Rehm BH (2013) Bioengineering of bacterial polymer inclusions catalyzing the synthesis of N-acetylneuraminic acid. *Appl Environ Microbiol* 79:3116–3121. doi:[10.1128/AEM.03947-12](https://doi.org/10.1128/AEM.03947-12)
27. Robins KJ, Hooks DO, Rehm BH, Ackerley DF (2013) *Escherichia coli* NemA is an efficient chromate reductase that can be biologically immobilized to provide a cell free system for remediation of hexavalent chromium. *PLoS One* 8:e59200. doi:[10.1371/journal.pone.0059200](https://doi.org/10.1371/journal.pone.0059200)
28. Chen S, Parlane NA, Lee J, Wedlock DN, Buddle BM, Rehm BH (2014) New skin test for detection of bovine tuberculosis on the basis of antigen-displaying polyester inclusions produced by recombinant *Escherichia coli*. *Appl Environ Microbiol* 80:2526–2535. doi:[10.1128/AEM.04168-13](https://doi.org/10.1128/AEM.04168-13)
29. Chen GQ, Wu Q (2005) The application of polyhydroxyalkanoates as tissue engineering materials. *Biomaterials* 26:6565–6578. doi:[10.1016/j.biomaterials.2005.04.036](https://doi.org/10.1016/j.biomaterials.2005.04.036)
30. Rehm BH (2007) Biogenesis of microbial polyhydroxyalkanoate granules: a platform technology for the production of tailor-made bioparticles. *Curr Issues Mol Biol* 9:41–62
31. Mifune J, Grage K, Rehm BH (2009) Production of functionalized biopolyester granules by recombinant *Lactococcus lactis*. *Appl Environ Microbiol* 75:4668–4675. doi:[10.1128/AEM.00487-09](https://doi.org/10.1128/AEM.00487-09)
32. Amara AA, Rehm BH (2003) Replacement of the catalytic nucleophile cysteine-296 by serine in class II polyhydroxyalkanoate synthase from *Pseudomonas aeruginosa*-mediated synthesis of a new polyester: identification of catalytic residues. *Biochem J* 374:413–421. doi:[10.1042/BJ20030431](https://doi.org/10.1042/BJ20030431)
33. Hay ID, Du J, Chen S, Burr N, Rehm BH (2015) Bioengineering bacteria to assemble custom-made polyester affinity resins. *Appl Environ Microbiol*. doi:[10.1128/AEM.02595-14](https://doi.org/10.1128/AEM.02595-14)

# Bacterial Secretion Systems for Use in Biotechnology: Autotransporter-Based Cell Surface Display and Ultrahigh-Throughput Screening of Large Protein Libraries

Karl-Erich Jaeger and Harald Kolmar

## Abstract

In recent years, continuous progress was made in our understanding of bacterial secretion pathways and the application of protein secretion for biotechnology. Efficient protein export is a prerequisite for cost-effective downstream processing, and secretion of a protein of interest may also be useful for certain enzyme assays, for biotransformation reactions, and, in particular, for screening enzyme variants in libraries generated by directed evolution. Cells that display a particular enzyme variant can be exposed to a broad spectrum of different chemical environments, can sustain a broad pH range, and can therefore allow one to probe the desired target protein under defined conditions. In recent years, fluorescent-activated cell sorting (FACS) in combination with cell surface display has become a powerful tool for the activity-based ultrahigh-throughput screening of mutant proteins from large libraries. The below protocol provides the detailed description for the generation of protein libraries, *E. coli* cell surface display, and library screening using magnetic- and fluorescence-activated cell sorting technologies with an emphasis on activity and selectivity screening of lipases and esterases.

**Keywords:** Autodisplay, Cell surface display, Esterases, High-throughput screen, Lipases, Protein secretion, Type V secretion pathway

---

## 1 Introduction

At present, numerous bacterial secretion pathways are known, which illustrate the impressive variety of molecular mechanisms underlying protein transport. Although they all fulfil the same function – secretion of at least one protein across the bacterial cell membrane(s) – protein export machineries significantly differ in structural complexity and the number of proteins they are composed of (for review, *see* [1–4]). In this article, we will focus on the so-called two-step secretion pathways in Gram-negative bacteria, which have been mainly characterized in pathogenic bacteria such as *Pseudomonas aeruginosa*. Two-step secretion pathways are highly

efficient and catalyse two distinct protein translocation events: one across the inner membrane to the periplasmic space and the second from the periplasmic space into the culture medium across the outer membrane. Inner membrane translocation is mediated by the Sec or Tat pathway depending on whether the target protein needs to be folded or provided with co-factors from the cytoplasm prior to its secretion [5, 6]. Efficient direction of the target to the translocation machinery in the inner membrane requires specific signal peptides which share some conserved features. They are located at the *N*-terminus of the secreted protein and are specifically recognized by components of the secretion complex [7, 8]. For example, the PelB- or PhoA-leader sequences originating from the highly abundant enzymes pectate lyase from *Erwinia carotovora* and the alkaline phosphatase of *Escherichia coli* are highly efficient in mediating secretion. The PelB-leader sequence is used in pET vectors of the commercial Novagen T7-expression system (Novagen, [www.novagen.com](http://www.novagen.com)) and has proved its potential in directing transport of a variety of recombinant proteins [9]. The PhoA signal sequence has also been successfully used in *E. coli* for secreting homologous and heterologous proteins out of the cytoplasm [10, 11]. Interestingly, in Gram-positive bacteria with only a single membrane, *N*-terminal signal sequences are already sufficient to direct export into the culture medium. Several authors reported the production and secretion of recombinant proteins in Gram-positive hosts [12–16]. Unfortunately, the efficiency of secretion of a heterologously expressed protein even in industrial production strains like *B. subtilis* is still difficult to predict. At this point, the choice of suitable signal peptide for a particular target protein needs to be evaluated on a case-by-case basis [7, 17, 18].

In contrast to the Sec and Tat pathways, almost nothing is known about the signals directing proteins through the type II secretion apparatus. It has repeatedly been proposed that the signal probably lies in the three-dimensional structure of the exoprotein and not in a simple amino acid sequence [19–24]. Type II secretion machineries are highly specific, not only for a certain subgroup of periplasmic proteins but also in terms of ‘species’ specificity. This is reflected by the fact that only proteins of closely related bacterial species are recognized and secreted by the type II system. The type II secretion machinery of *P. aeruginosa* is a complex of 12 different, so-called Xcp proteins [25]. The complex is anchored in the inner membrane, spans the periplasm, and forms a gated channel in the outer membrane. The machinery from *P. aeruginosa* was successfully expressed in *P. putida* and used to co-express and efficiently secrete a *P. aeruginosa* lipase [26]. Despite a few successes, the use of the type II secretion system for biotechnological applications in general is still limited, due to the complexity and the lack of knowledge on the nature of the secretion signal.

In contrast, the type V secretion pathway has found its way into biotechnological applications. This ‘autotransporter’ pathway

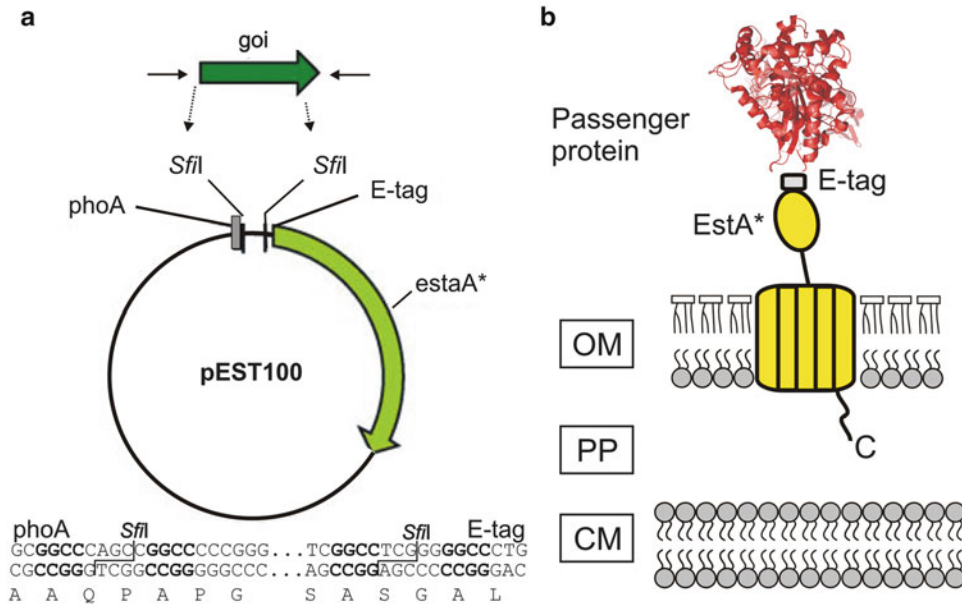


**Fig. 1** (a) Map of the plasmid pEst100. *phoA* coding sequence for the signal sequence of alkaline phosphatase of *Escherichia coli*, *E-tag* coding sequence for the E-epitope (GAPVPYPDPLEPR), and *EstA\** coding sequence of the inactive, truncated esterase A from *Pseudomonas aeruginosa*. The cloning site for the gene of interest (*goi*) and the recognition sequences for *SfiI* endonuclease, which are important to design primers for *goi* amplification and cloning, are shown below the plasmid map. For more details, see notes. (b) Schematic representation of the resulting cell surface display construct. *OM* outer membrane, *PP* periplasm, *CM* cytoplasmic membrane

is widely used to display polypeptides on the surface of Gram-negative bacterial cells [10, 27–32]. Autotransporter proteins position themselves in the outer membrane where they produce a complex-specific pore which is formed by the protein's own pore-forming domain and mediates secretion (Fig. 1b) [33, 34]. With a molecular mass of about 30 kDa (corresponding to 300–350 aa), the pore-forming domains of autotransporters are relatively constant in size, whereas the size of the translocated passenger proteins can vary largely [35]. The lesson to learn from this is that the size of the passenger protein, which one would like to have secreted by the autotransporter, probably is not a limiting factor in this type of secretion. In the PFAM database (PF03797; <http://pfam.xfam.org>) currently over 8,000 sequences of potential autotransporter protein encoding genes can be found, which originate from approximately 1,520 bacterial genera, most of them belonging to the *Proteobacteria* [36].

The most thoroughly investigated autotransporters for biotechnological applications are the IgA autotransporter from *Neisseria gonorrhoeae* [30, 37–39], AIDA-I (adhesion involved in diffuse adherence) and related autotransporters from *E. coli* strains [37, 40, 41], and EstA from *P. aeruginosa* [28, 35, 37, 42].

Autotransporter proteins consist of three functional parts: an amino terminal leader sequence that directs protein translocation through the inner membrane, a passenger domain, and a C-terminal  $\beta$ -barrel domain (also known as translocator domain) that directs the passenger domain through the outer membrane. In this process, the passenger domain remains at least partially unfolded in the periplasm in a complex with periplasmic chaperones [43, 44]. The  $\beta$ -barrel likely acts as a pore with a hydrophilic channel through which the passenger protein can pass [45].

After secretion, the passenger protein is typically cleaved off proteolytically from the autotransporter at the cell surface, either by autoprolytic cleavage or by an additional protease located in the outer membrane [46, 47], and is either released from the surface or remains attached to the  $\beta$ -domain via non-covalent interactions [43]. By contrast, the members of a small subfamily of autotransporter proteins with the outer membrane esterase EstA from *P. aeruginosa* being the prototype protein are not cleaved and remain attached to the autotransporter moiety on the bacterial surface [48]. The enzymatically active N-terminal domain of this esterase belongs to the GDSL-hydrolase family motif [49] and is thought to represent an ancient type of hydrolytic enzymes. The GDSL autotransporters group currently consists of about 1,270 proteins (Pfam 00657) in 550 bacterial species. Although it is not clear why these proteins remain intact after translocation without being processed, this unique property is an obvious intrinsic advantage for surface display applications, as described below.

A major application of cell surface display of a passenger protein is the screening of functional protein variants in libraries generated by directed evolution. This requires the construction of a gene library (genotype), the establishment of a linkage between a protein and its encoding gene, and the selection of proteins of the desired function (phenotype) from the library. One elegant way of achieving phenotype/genotype coupling is to anchor the target protein directly on the surface of the producer cells of *E. coli*, e.g. by genetic fusion to an autotransporter. Various autotransporters with a wide range of sizes and functions were used for the display of recombinant protein passengers [35, 50]. Examples include single-chain antibody domains [51], metal-binding proteins [52], toxins [53, 54], engineering binding proteins [37, 55], enzyme inhibitors [56], and enzymes [10, 57]. Because *E. coli* is easily amenable to genetic manipulation and large-scale library generation, it provides a promising system for large-scale clone production and functional screenings, e.g. for enzyme activity or protein-protein interactions using single-cell analysis methods as fluorescence-activated cell sorting (FACS).

In this article, we describe a robust surface display and high-throughput screening method based on the autotransporter EstA, which allows one to present proteins on the *E. coli* cell surface with

high efficiency [10]. We provide detailed guidelines for the generation of peptide/protein libraries via the construction of variants fused to esterase A, *E. coli* cell surface display, and library screening using magnetic (MACS) and fluorescence-activated cell sorting (FACS).

---

## 2 Materials

### 2.1 Strains and Vectors

*Escherichia coli* JM109 [F' *traD36 proA<sup>+</sup>B<sup>+</sup> lacI<sup>q</sup> Δ(lacZ)M15/Δ(lac-proAB) glnV44 e14<sup>-</sup> gyrA96 recA1 relA1 endA1 thi hsdR17*] [58]

Plasmid: pEst100 – the construction of pEst100 has been described in detail in [10] (see also Fig. 1).

### 2.2 Media and Buffers

1. Chloramphenicol stock solution: 25 mg/ml in 96% (v/v) ethanol.
2. 2YT medium: 1% (w/v) yeast extract; 1.6% (w/v) Bacto tryptone; 0.5% (w/v) NaCl.
3. 2YT-Cm<sup>25</sup> medium: 2YT medium supplemented with chloramphenicol to a final concentration of 25 µg/ml (added after autoclaving).
4. 2YT-Cm<sup>25</sup> plates: 2YT-Cm<sup>25</sup> medium supplemented with 1.5% (w/v) agar.
5. M9 minimal medium plates: 0.7% (w/v) Na<sub>2</sub>HPO<sub>4</sub> · 2H<sub>2</sub>O, 0.3% (w/v) KH<sub>2</sub>PO<sub>4</sub>, 0.1% (w/v) NH<sub>4</sub>Cl, and 1.5% agar. After autoclaving, add the following sterilized solutions: 25 ml 20% (w/v) glucose, 1 ml 100 mM CaCl<sub>2</sub>, 1 ml 1 M MgSO<sub>4</sub>, 5 ml 0.1 mM FeCl<sub>3</sub>, and 1 ml thiamine solution (1 mg/ml).
6. SOB medium: 2% (w/v) Bacto tryptone, 0.5% (w/v) yeast extract, and 0.05% (w/v) NaCl.
7. SOC medium: 2% (w/v) Bacto tryptone, 0.5% (w/v) yeast extract, 10 mM NaCl, and 2.5 mM KCl. After autoclaving, add the following sterilized solutions at the final concentration indicated: 10 mM MgCl<sub>2</sub>, 10 mM MgSO<sub>4</sub>, and 20 mM glucose.
8. PBS buffer: 140 mM NaCl, 10 mM KCl, 6.4 mM Na<sub>2</sub>HPO<sub>4</sub> · 2H<sub>2</sub>O, and 2 mM KH<sub>2</sub>PO<sub>4</sub>.
9. Reaction buffer: 90 mM potassium phosphate buffer, pH 7.2, 9 mM MgSO<sub>4</sub>; 100 mM imidazole, 0.001% (v/v) H<sub>2</sub>O<sub>2</sub>.
10. Sodium borate buffer: 100 mM sodium tetraborate, pH 9.1
11. Sucrose gradient buffer: 100 mM Tris-HCl, pH 8.0, 10 mM EDTA, and 100 mM NaCl.

### 2.3 Biological and Chemical Materials

1. Anti-DNP Alexa Fluor 488 antibody conjugate (Life Technologies) (<http://www.lifetechnologies.com/>).

2. IPTG stock, 100 mM in sterile water.
3. Anti-mouse IgG (whole molecule)–biotin conjugate (Sigma-Aldrich, B-7264) (<http://www.sigmaaldrich.com>).
4. Anti-rabbit IgG (whole molecule)–biotin conjugate (Sigma-Aldrich, B-7389) (<http://www.sigmaaldrich.com>).
5. Anti-E-epitope antibody (1 mg/ml) (GE Healthcare Life Sciences) (<http://www.gelifesciences.com/>).
6. Bovine serum albumin, BSA 100×, 10 mg/ml (New England Biolabs) (<http://www.NEB.com>).
7. Streptavidin-coated super-paramagnetic microbeads (Miltenyi Biotec) (<http://www.miltenyibiotec.com/>).
8. Streptavidin, R-phycoerythrin conjugate, 1 mg/ml (Life Technologies) (<http://www.lifetechnologies.com/>).
9. T4 DNA Ligase HC (high concentration), 30 u/ml (MBI Fermentas) (<http://www.fermentas.com>).
10. Horseradish peroxidase (Sigma-Aldrich) (<http://www.sigmaaldrich.com>).
11. NAP-5 column of Sephadex G-25 (GE Healthcare Life Sciences) (<http://www.gelifesciences.com/>).

#### 2.4 Equipment

1. Epifluorescence microscope (e.g. Zeiss Axioskop)
2. Gene Pulser<sup>®</sup> (Bio-Rad) (<http://www.biorad.com>).
3. MidiMACS columns – MultiStand and separation unit (Miltenyi Biotec) (<http://www.miltenyibiotec.com/>).
4. MoFlo FACS (Beckman Coulter) or similar sorter (<http://www.beckmancoulter.com>).
5. SW 40 Ti Rotor, Swinging Bucket (Beckmann Coulter) (<http://www.beckmancoulter.com>).
6. Tube, Thinwall, Ultra-Clear<sup>™</sup>, 14 ml (Beckmann Coulter) (<http://www.beckmancoulter.com>).

---

## 3 Methods

### 3.1 Examination of Cell Surface Exposition of the Passenger Protein by Immunofluorescence Staining of *E. coli* Cells

It is mandatory to check successful cell surface display of the protein of interest since rate of success is unpredictable and depends on several factors (*see Note 1*).

1. Inoculate an Erlenmeyer flask containing 50 ml 2YT-Cm<sup>25</sup> medium with 50 µl of a fresh overnight culture of *E. coli* strain JM109 carrying the pEst100 plasmid that contains the gene encoding for the protein to be displayed (see also ‘Notes’ section for cloning considerations). Shake the culture flask at 37°C.
2. At an O.D.<sub>600</sub> of 0.5, add 250 µl of IPTG stock solution to the culture medium. Shake at 37°C for another 60 min.

3. Pellet cells (200–500  $\mu\text{l}$ ) by centrifugation in a tabletop centrifuge for 2 min.
4. Remove supernatant, resuspend the cell pellet in 10  $\mu\text{l}$  PBS, and add 1  $\mu\text{l}$  (1 mg/ml) of an antibody directed against the protein to be displayed, or if not available, use an anti-E-tag antibody. Leave on ice for 10 min.
5. Wash the cells by the addition of 180  $\mu\text{l}$  PBS and centrifugation as in **step 3**.
6. Remove the supernatant and resuspend the cells in 10  $\mu\text{l}$  PBS containing anti-mouse- or anti-rabbit IgG–biotin conjugate as required (1:10 dilution). Leave on ice for 10 min and wash the cells by the addition of 180  $\mu\text{l}$  PBS and centrifugation.
7. Resuspend the cell pellet in 10  $\mu\text{l}$  of PBS containing streptavidin and *R*-phycoerythrin conjugate (1:10 dilution) and incubate on ice again for 10 min.
8. Wash the cells by the addition of 180  $\mu\text{l}$  PBS; centrifuge and resuspend the pellet in 10  $\mu\text{l}$  PBS.
9. Analyse by fluorescence microscopy (Zeiss filter number 15 absorption, 565 nm; emission, 578 nm) or by flow cytometry [e.g. MoFlo cell sorter. Parameters are set as follows: side scatter, 730 (LIN mode, amplification factor 6); FL1 (FITC), 600 (LOG mode); FL2 (PE), 600 (LOG mode); trigger parameter, side scatter. No forward scatter measurement is necessary. The sample flow rate is adjusted to an event rate of approximately 10,000  $\text{s}^{-1}$ , with similar settings for other cell sorters].

### **3.2 Preparation of Vector DNA for Library Construction**

For isolation of pEst100 plasmid DNA (for vector details and cloning considerations, *see* **Notes 2** and **3**), any convenient mid-prep purification system (e.g. Qiagen<sup>®</sup> Plasmid Midi Kit (<http://www.qiagen.com>)) can be used. It is advisable to extract the purified DNA once with phenol/chloroform and once with chloroform and precipitate the DNA by the addition of 1/10 volume of 7 M ammonium acetate and three volumes of 96% ethanol. Dissolve the DNA in  $\text{H}_2\text{O}$  at approximately 1  $\mu\text{g}/\text{ml}$  for further use. The vector DNA should preferably be purified by sucrose gradient centrifugation (*see* **Note 4**).

1. Digest 50–100  $\mu\text{g}$  pEst100 vector DNA in a total volume of 200  $\mu\text{l}$  with 5 units of *Sfi*I per  $\mu\text{g}$  DNA at 50°C for 5 h or overnight in the manufacturer's recommended buffer.
2. Control *Sfi*I cleavage by agarose gel electrophoresis.
3. Prepare solutions of 40%, 30%, and 10% sucrose (w/v) in sucrose gradient buffer. Fill 500  $\mu\text{l}$  of 40% sucrose solution into a 14 ml ultra centrifuge tube. Layer a gradient ranging

from 10% to 30% sucrose on top of the 40% cushion using a gradient mixer.

4. Layer the DNA solution from the restriction digest on top of the sucrose gradient. Balance with 10% sucrose solution.
5. Centrifuge at 30,000 rpm for 21 h in a type SW40Ti (Beckmann, swing-out) or equivalent at 15°C.
6. Fractionate the gradient in 500 µl aliquots by puncturing the bottom of the tube with a needle and collecting drops after removal of the needle.
7. Analyse the fractions by agarose gel electrophoresis. Combine the fractions containing the vector fragment and precipitate DNA with 1/10 volume of 7 M ammonium acetate and three volumes of 96% (v/v) ethanol.

### **3.3 Insert Generation for Library Construction**

The procedures for generating gene libraries of a given protein to be displayed are well established. For example, DNA shuffling [59], error-prone PCR [60], saturation mutagenesis, or CASTing [61] techniques can be used to generate a variant gene population. The basic condition is that the gene library should contain DNA ends compatible with *Sfi*I-restricted pEst100.

### **3.4 Ligation for Library Construction**

Ligation of digested vector and insert DNA is performed using standard procedures. For creating large libraries, it is advisable to set up several ligation reactions in parallel.

1. Set up 12 ligation reactions each containing the following: 300 ng of digested vector DNA, threefold molar excess of insert DNA, 2 µl 10 × T4 DNA ligase buffer, 0.2 ml BSA (100×), 1 µl T4 DNA ligase, and H<sub>2</sub>O to 20 µl.
2. Incubate overnight at 15°C.
3. Inactivate ligase by incubation at 65°C for 10 min.
4. Pool the 12 reactions and extract once with one volume of phenol/chloroform and once with one volume of chloroform. Precipitate DNA with 1/10 vol of 7 M ammonium acetate and 3 vol of 96% (v/v) ethanol. Incubate for at least 30 min at -20°C and then centrifuge in a tabletop centrifuge for 15–30 min at 13,000 rpm.
5. Discard the supernatant and resuspend the DNA pellet in 240 µl H<sub>2</sub>O and either store at -20°C or use directly for electroporation.

### **3.5 Electroporation for Library Construction**

Transformation is done by electroporation of cells. The use of chemical competent cells is not recommended because it gives much lower yields of transformants.

The following materials have to be prepared in advance: 2 l of sterile bidistilled H<sub>2</sub>O, precooled on ice; 36 SOC-Cm<sup>25</sup> agar plates

using large petri dishes (15 cm in diameter); 10 SOC-Cm<sup>25</sup> agar plates using small petri dishes (9.2 cm in diameter); and two 1 l Erlenmeyer flasks each containing 400 ml SOB medium, one flask containing 100 ml SOC medium and one flask containing 100 ml SOB medium.

1. For preparation of electrocompetent cells, inoculate 5 ml SOB medium with cells grown on a M9 minimal medium plate and shake overnight at 37°C.
2. Inoculate each of the two flasks containing 400 ml SOB medium with 2 ml of the overnight culture. Shake at 37°C until an O.D.<sub>600</sub> of 0.5 has been reached (2–3 h).
3. Partition the cell culture into 50 ml plastic tubes and centrifuge at 4,000 rpm for 10 min at 4°C (Eppendorf 5810R or equivalent). Discard the supernatant.
4. Carefully resuspend the cell pellets each in 50 ml precooled H<sub>2</sub>O (on ice). Incubate on ice for 1 h.
5. Centrifuge at 4,000 rpm for 10 min at 4°C. Discard the supernatant.
6. Resuspend cells in 25 ml precooled H<sub>2</sub>O. Incubate on ice for 1 h and centrifuge as before. Discard the supernatant.
7. Wash with 10 ml precooled H<sub>2</sub>O. Distribute the cell suspensions equally into 12 tubes. Leave on ice for 1 h and centrifuge as before. Discard the supernatant. Place the tubes on ice for another 10 min and resuspend the cells in the remaining liquid which should not exceed 200 µl.
8. For electroporation, add 20 µl of the ligation reaction to each of the 12 aliquots of competent cells and incubate for at least 30 min on ice, and then transfer into prechilled electroporation cuvettes.
9. Set up a Gene Pulser to give a 2,500 V pulse, using a 25 µF capacitor and adjust the resistance to 200 Ω. Place the cuvette in the electroporation chamber and pulse once.
10. Immediately add 800 µl SOC medium and transfer the cell suspension into a test tube. Rinse the cuvette twice with 800 ml SOC medium and incubate the cells with agitation at 37°C for 45–60 min.
11. Pool the contents of all 12 tubes. Remove 50 µl aliquot and make a serial dilution (add to 450 µl PBS per dilution step) over seven dilution steps. Plate out 250 µl of each dilution. Plate the dilutions on small SOC-Cm<sup>25</sup> agar plates. Streak the remaining cell suspension on 36 large SOC-Cm<sup>25</sup> agar plates and incubate overnight at 37°C.
12. Count the colonies on dilution plates with an appropriate number of colonies the following day to determine the total

number of transformants ( $10^6$ – $10^9$  can be expected when setting up 12 ligation reactions). Harvest the library cells by flooding each of the 36 plates with 4 ml SOC medium and detach cells by scraping off under sterile conditions. Pool the cell suspension and add DMSO to a final concentration of 9% (v/v). Store at  $-70^\circ\text{C}$  in 2 ml aliquots or use directly for library screening.

### **3.6 Screening of Hydrolases Using the ESCAPED Technology**

The identification and isolation of cell-surface-exposed enzyme variants that are able to catalyse a particular reaction requires the identification of enzymatically proficient cells from inactive ones, preferably by covalent attachment of an easily detectable label to the cell surface [10]. The tyramide signal amplification (TSA) reaction makes use of the fact that horseradish peroxidase (HRP) can react with hydrogen peroxide and the phenolic part of biotin tyramide to produce a radical. HRP has to be coupled to the cell surface in order that the short-lived peroxidase-generated tyramide radical covalently attaches to tyrosine residues in close vicinity to HRP. Ideally, attachment occurs onto tyrosine residues of cell-surface-exposed proteins [62]. The phenolic hydroxyl group of tyramide is blocked by esterification and can be activated in situ by cell-surface-exposed lipases and esterases. Using biotin tyramide ester as substrate, only those cells become labelled with biotin, which displayed esterolytic activity on their cell surface. These cells can then be easily isolated from a very large background of inactive cells by using magnetic labelling with biotin-binding streptavidin-coated paramagnetic microbeads (MACS) or by using biotin-binding streptavidin coupled to a fluorescent dye via fluorescence-assisted cell sorting (FACS) [63].

#### **3.6.1 Preparation of HRP**

Conjugation of periodate-oxidized horseradish peroxidase (HRP) to *E. coli* cells is performed as follows:

1. Glycosylated horseradish peroxidase (Sigma) (200  $\mu\text{g}$ ) is dissolved in water (200  $\mu\text{l}$ ).
2. The terminal sugar residues of HRP are oxidized to aldehydes by adding 20  $\mu\text{l}$  of sodium periodate (0.088 M) and incubate for 1 h in the dark. HRP changes colour from brown to green.
3. Pre-equilibrate a size exclusion NAP-5 column of Sephadex G-25 (GE Healthcare Life Sciences) with 5 ml sodium borate buffer.
4. Load the sample to the column and elute the oxidized enzyme with sodium borate buffer by collecting the colored fractions.
5. Green fraction in a final volume of 2 ml.
6. Store if necessary at  $-20^\circ\text{C}$  in the dark.

### 3.6.2 Coupling

The aldehydes of activated HRP can react with amino groups on the cell surface to form imines and are thereby covalently coupled:

1. *E. coli* cells containing the respective plasmid expressing the corresponding fusion protein are grown at 37°C in dYT medium to an O.D.<sub>600</sub> of 0.5.
2. Add IPTG to a final concentration of 0.5 mM to induce the expression and incubate for another 60 min.
3. Determine the cell density at O.D.<sub>600</sub> and adjust the culture to an O.D.<sub>600</sub> of 0.5.
4. Pellet cells (1 ml) by centrifugation in a tabletop centrifuge at 13,000 rpm for 2 min.
5. Wash the cells in 500 µl PBS buffer and centrifuge again.
6. Resuspend the cells in 150 µl activated HRP and incubate for 1 h in the dark at room temperature.
7. Remove unreacted peroxidase by washing the cells three times in PBS buffer (500 µl).

### 3.7 Cell Staining with Tyramide Esters for Monitoring Carboxyl Ester Hydrolase Activity

For the chemical synthesis of tyramide esters, *see* [63]:

1. HRP-decorated cells are resuspended in 500 µl reaction buffer (90 mM potassium phosphate buffer, pH 7.2, 9 mM MgSO<sub>4</sub>; 100 mM imidazole, 0.001% (v/v) H<sub>2</sub>O<sub>2</sub>) containing the desired biotin tyramide ester, for example, biotin tyramide caprylate (2.9 nmol) (*see* also **Note 5**) [63].
2. Incubate cells for 15 min at room temperature in the dark.
3. Collect cells by centrifugation in a tabletop centrifuge at 13,000 rpm for 2 min.
4. Wash cells with 500 µl PBS

#### 3.7.1 Fluorescence Analysis and Sorting

1. For fluorescence analysis, resuspend cells in 10 µl streptavidin and (R)-phycoerythrin conjugate (1:10 dilution in PBS) and incubate on ice for 10 min.
2. Again, harvest the cells, wash with 500 µl PBS, resuspend finally in 10 µl PBS, and subject the sample to microscopy or FACS analysis.

#### 3.7.2 Magnetic Cell Sorting (MACS)

1. Resuspend the cells in 200 µl PBS plus 20 µl streptavidin microbeads (Miltenyi Biotec) and incubate on ice for 10 min.
2. Collect cells by centrifugation in a tabletop centrifuge at 13,000 rpm for 1 min.
3. Wash with 500 µl PBS and resuspend cells finally in 1 ml PBS. Take a sample of the cells (1 µl) and determine the cell count by plating different dilutions (10<sup>-6</sup>–10<sup>-8</sup>) on selective dYT.

4. Equilibrate a MACS LS column (Miltenyi Biotec) three times with 3 ml PBS when stacking in the magnet (Midi MACS). Apply the cells to the column and add immediately 3 ml PBS.
5. Let the column flow by gravitation and wash three times with 3 ml PBS to discard unbound cells.
6. Take the column out of the magnet and elute bound cells with 1 ml PBS under pressure.
7. After magnetic sorting, take again a sample of the cells (1  $\mu$ l) and determine the cell counts by plating different dilutions ( $10^{-4}$ – $10^{-6}$ ) on selective dYT.
8. Calculate the enrichment factor.
9. For further selection rounds, grow the enriched cells again and repeat the steps described above.
10. Check the enrichment by activity or binding assays as required.

### **3.8 Discrimination Between (R)- and (S)-Enantioselectivity of Esterases**

When enantiomeric tyramide conjugates are used for HRP-mediated conjugation, for example, the tyramide ester of (*R*)- or (*S*)-2-methyl decanoate, it is possible to correlate the enantioselectivity of an esterase variant displayed on the cell surface with the extent of fluorophore labelling (*see* also **Note 6**). As a consequence, cells with enhanced enantioselectivity can be identified and isolated by FACS [27, 63].

1. HRP-decorated cells (*see* above) are resuspended in 1 ml reaction buffer containing 1.14 nmol (*S*)-2-MDA-biotin-tyramide ester or (*R*)-2-MDA 2,4 DNP tyramide ester (for synthesis, *see* [27, 63]) individually or a 1:1 mixture of both.
2. Cells are incubated for 5 min at room temperature.
3. The conjugation reaction is terminated by the addition of 100  $\mu$ l 500 mM tyramine.
4. Harvest the cells in a tabletop centrifuge at 13,000 rpm for 2 min and wash with 500  $\mu$ l PBS and centrifuge again.
5. Cells are resuspended in 10  $\mu$ L PBS containing 100  $\mu$ g/ml streptavidin, *R*-phycoerythrin conjugate, and/or anti-DNP Alexa Fluor 488 antibody conjugate.
6. Incubate the mixture for 5 min at room temperature.
7. Add PBS (300  $\mu$ l) and pellet the cells.
8. Resuspend in PBS (1 ml) for flow cytometry analysis.
9. *E. coli* cells are analysed/sorted on a MoFlo cell sorter. Parameters are set as follows: side scatter: 730 (LIN mode, amplification factor 6); FL1 (FITC), 600 (LOG mode); FL2 (PE), 600 (LOG mode); and trigger parameter, side scatter. No forward scatter measurement is necessary. The sample flow rate is adjusted to an event rate of approximately 15,000–30,000 s<sup>-1</sup>, with similar

settings for other cell sorters. Make two-dimensional plots with FL1 as X-axis and FL2 as Y-axis. Cells displaying no enantioselectivity are expected to be represented as dots along a diagonal. Cells presenting enzyme variants with enhanced enantioselectivity are expected to display enhanced FL1 compared with FL2 (indicative of preferred cleavage of (*R*)-2-MDA) or enhanced FL2 compared with FL1 (indicative of preferred cleavage of (2)-2-MDA), respectively, and should therefore appear off-diagonal.

---

## 4 Notes

1. It is mandatory to check successful cell surface display (*see* Sect. 3.1) of the target protein. The protein of interest has to be translocated through two membranes, the inner and the outer membranes, and for both translocation processes, the passenger protein has to be at least partially unfolded. Hence, for fast folding proteins, cell surface display may be hampered [64]. In these cases, optimization of bacterial growth conditions by reducing growth temperature or addition of compounds that interfere with target protein folding (low concentrations of detergent, chelator, reducing agents) may improve export yields [64]. For passenger proteins that contain disulphide bonds, surface display may be enhanced in an *E. coli* strain lacking the periplasmic disulphide isomerase DsbA [54, 64]. One should also check whether the protein of interest contains a cleavage site for the *E. coli* OmpT protease, an outer membrane protein of *E. coli* that efficiently cleaves at two adjacent basic residues [54, 55, 65]. In this case, an OmpT-deficient *E. coli* strain as UT5600 [54] or an *E. coli* B strain as BL21 should be considered, since *E. coli* B strains generally lack this protease [55]. For detection of successful cell surface display of the protein of interest, fluorescence staining methods should be applied, since the labelling compounds (antibodies, streptavidin, *R*-phycoerythrin conjugate, etc.) are unable to enter intact *E. coli* cells. Surface display can be verified by fluorescence staining of the cells using (a) an antibody directed against the protein to be displayed or (b) an antibody directed against the E-epitope of the EstA fragment (Fig. 1).
2. For cloning the gene of interest into the expression vector pEST100 (*see* Sect. 3.1), a pair of *Sfi*I recognition sites is used (Fig. 1a). The recognition sequence of *Sfi*I comprises 13 nucleotides and contains five variable nucleotides in its center. The length of this sequence qualifies the enzyme as a true rare cutter, and, as a consequence of the variable region, directed cloning can be achieved by changing the variable sequence at the corresponding positions while using only a single enzyme.

Therefore, special care is required in designing the respective primers to be used to maintain the reading frame.

3. In expression vector pEST100 a naturally occurring *Sfi*I recognition sequence within the *estA* gene was deleted by truncation of *estA* (Fig. 1). This generates the so-called *estA*\* variant, which produces an esterase inactive protein. Inactivation of EstA was necessary to exclude background esterase activity, which would disturb screening for heterologous hydrolytic and lipolytic enzymes. Expression of the resulting gene fusion is under *lac* P/O control in pEst100 and can be induced by the addition of IPTG. The plasmid is replicated from its ColE1 origin and carries the chloramphenicol acyl transferase gene (*cat*) [10].
4. For library generation, sucrose gradient purification of the vector fragment is recommended (Sect. 3.2). Alternatively, the vector fragment can be isolated from a preparative agarose gel using commercially available extraction kits. In our hands, yields are lower and transformation efficiencies compared to DNA purification by sucrose gradient centrifugation may be reduced due to co-purification of ionic impurities of the agarose that negatively influence ligation and/or transformation.
5. For application of the ESCAPED technology (Sect. 3.6) for hydrolase-mediated cell staining, it may be required to optimize the concentration of biotin-tyramide conjugate. We have occasionally observed that higher substrate concentrations result in the lack of cell staining.
6. For discrimination between (*R*)- and (*S*)-enantioselectivities of esterases (Sect. 3.8), it is recommended to use a 1:1 mixture of two enantiomeric substrates that lead to different types of cell surface conjugation, as, e.g. biotin and 2,4-DNP [63]. For the subsequent fluorescent labelling, pairs of fluorophores with nonoverlapping excitation/emission spectra should be preferably used, as, e.g. Alexa Fluor 488<sup>®</sup>-labelled streptavidin and an allophycocyanin-conjugated anti-DNP antibody that can be selectively excited by a green and a red laser, respectively [66].

## References

1. Holland IB (2010) The extraordinary diversity of bacterial protein secretion mechanisms. *Methods Mol Biol* 619:1–20
2. Ma Q, Zhai Y, Schneider JC et al (2003) Protein secretion systems of *Pseudomonas aeruginosa* and *P fluorescens*. *Biochim Biophys Acta* 1611:223–233
3. Rosenau F, Jaeger KE (2000) Bacterial lipases from *Pseudomonas*: regulation of gene expression and mechanisms of secretion. *Biochimie* 82:1023–1032
4. Saier MH Jr (2006) Protein secretion and membrane insertion systems in gram-negative bacteria. *J Membr Biol* 214:75–90
5. Natale P, Bruser T, Driessen AJ (2008) Sec- and Tat-mediated protein secretion across the bacterial cytoplasmic membrane—distinct translocases and mechanisms. *Biochim Biophys Acta* 1778:1735–1756
6. Kudva R, Denks K, Kuhn P et al (2013) Protein translocation across the inner membrane of Gram-negative bacteria: the Sec and Tat

- dependent protein transport pathways. *Res Microbiol* 164:505–534
7. Brockmeier U, Caspers M, Freudl R et al (2006) Systematic screening of all signal peptides from *Bacillus subtilis*: a powerful strategy in optimizing heterologous protein secretion in Gram-positive bacteria. *J Mol Biol* 362:393–402
  8. Clerico EM, Maki JL, Gierasch LM (2008) Use of synthetic signal sequences to explore the protein export machinery. *Biopolymers* 90:307–319
  9. Sletta H, Tondervik A, Hakvag S et al (2007) The presence of N-terminal secretion signal sequences leads to strong stimulation of the total expression levels of three tested medically important proteins during high-cell-density cultivations of *Escherichia coli*. *Appl Environ Microbiol* 73:906–912
  10. Becker S, Theile S, Heppeler N et al (2005) A generic system for the *Escherichia coli* cell-surface display of lipolytic enzymes. *FEBS Lett* 579:1177–1182
  11. Oka T, Sakamoto S, Miyoshi K et al (1985) Synthesis and secretion of human epidermal growth factor by *Escherichia coli*. *Proc Natl Acad Sci U S A* 82:7212–7216
  12. Anne J, Vrancken K, Van Mellaert L et al (2014) Protein secretion biotechnology in Gram-positive bacteria with special emphasis on *Streptomyces lividans*. *Biochim Biophys Acta* 1843:1750–1761
  13. Fu LL, Xu ZR, Li WF et al (2007) Protein secretion pathways in *Bacillus subtilis*: implication for optimization of heterologous protein secretion. *Biotechnol Adv* 25:1–12
  14. Harwood CR, Cranenburgh R (2008) *Bacillus* protein secretion: an unfolding story. *Trends Microbiol* 16:73–79
  15. Tjalsma H, Bolhuis A, Jongbloed JD et al (2000) Signal peptide-dependent protein transport in *Bacillus subtilis*: a genome-based survey of the secretome. *Microbiol Mol Biol Rev* 64:515–547
  16. Westers L, Westers H, Quax WJ (2004) *Bacillus subtilis* as cell factory for pharmaceutical proteins: a biotechnological approach to optimize the host organism. *Biochim Biophys Acta* 1694:299–310
  17. Degering C, Eggert T, Puls M et al (2010) Optimization of protease secretion in *Bacillus subtilis* and *Bacillus licheniformis* by screening of homologous and heterologous signal peptides. *Appl Environ Microbiol* 76:6370–6376
  18. Kang Z, Yang S, Du G et al (2014) Molecular engineering of secretory machinery components for high-level secretion of proteins in *Bacillus* species. *J Ind Microbiol Biotechnol* 41:1599–1607
  19. Hausmann S, Wilhelm S, Jaeger KE et al (2008) Mutations towards enantioselectivity adversely affect secretion of *Pseudomonas aeruginosa* lipase. *FEMS Microbiol Lett* 282:65–72
  20. Hazes B, Frost L (2008) Towards a systems biology approach to study type II/IV secretion systems. *Biochim Biophys Acta* 1778:1839–1850
  21. Johnson TL, Abendroth J, Hol WG et al (2006) Type II secretion: from structure to function. *FEMS Microbiol Lett* 255:175–186
  22. Korotkov KV, Sandkvist M, Hol WG (2012) The type II secretion system: biogenesis, molecular architecture and mechanism. *Nat Rev Microbiol* 10:336–351
  23. Pineau C, Guschinskaya N, Robert X et al (2014) Substrate recognition by the bacterial type II secretion system: more than a simple interaction. *Mol Microbiol* 94:126–140
  24. Sandkvist M (2001) Biology of type II secretion. *Mol Microbiol* 40:271–283
  25. Filloux A (2004) The underlying mechanisms of type II protein secretion. *Biochim Biophys Acta* 1694:163–179
  26. Rosenau F, Jaeger KE (2003) Design of systems for overexpression of *Pseudomonas* lipases. In: Sevendsen A (ed) *Enzyme functionality: design, engineering, and screening*. Marcel Dekker, New York, pp 617–631
  27. Becker S, Höbenreich H, Vogel A et al (2008) Single-cell high-throughput screening to identify enantioselective hydrolytic enzymes. *Angew Chem Int Ed Engl* 47:5085–5088
  28. Becker S, Schmoldt HU, Adams TM et al (2004) Ultra-high-throughput screening based on cell-surface display and fluorescence-activated cell sorting for the identification of novel biocatalysts. *Curr Opin Biotechnol* 15:323–329
  29. Grijpstra J, Arenas J, Rutten L et al (2013) Autotransporter secretion: varying on a theme. *Res Microbiol* 164:562–582
  30. Jose J, Meyer TF (2007) The autodisplay story, from discovery to biotechnical and biomedical applications. *Microbiol Mol Biol Rev* 71:600–619
  31. van Ulsen P, Rahman S, Jong WS et al (2014) Type V secretion: from biogenesis to biotechnology. *Biochim Biophys Acta* 1843:1592–1611
  32. Wilhelm S, Rosenau F, Becker S et al (2007) Functional cell-surface display of a lipase-specific chaperone. *Chembiochem* 8:55–60
  33. Dautin N, Bernstein HD (2007) Protein secretion in gram-negative bacteria via the

- autotransporter pathway. *Annu Rev Microbiol* 61:89–112
34. Henderson IR, Navarro-Garcia F, Nataro JP (1998) The great escape: structure and function of the autotransporter proteins. *Trends Microbiol* 6:370–378
  35. van Bloois E, Winter RT, Kolmar H et al (2011) Decorating microbes: surface display of proteins on *Escherichia coli*. *Trends Biotechnol* 29:79–86
  36. Finn RD, Bateman A, Clements J et al (2014) Pfam: the protein families database. *Nucleic Acids Res* 42:D222–D230
  37. Binder U, Matschiner G, Theobald I et al (2010) High-throughput sorting of an Anticalin library via EspP-mediated functional display on the *Escherichia coli* cell surface. *J Mol Biol* 400:783–802
  38. Mistry D, Stockley RA (2006) IgA1 protease. *Int J Biochem Cell Biol* 38:1244–1248
  39. Pyo HM, Kim IJ, Kim SH et al (2009) *Escherichia coli* expressing single-chain Fv on the cell surface as a potential prophylactic of porcine epidemic diarrhea virus. *Vaccine* 27:2030–2036
  40. Jose J (2006) Autodisplay: efficient bacterial surface display of recombinant proteins. *Appl Microbiol Biotechnol* 69:607–614
  41. Jose J, Maas RM, Teese MG (2012) Autodisplay of enzymes—molecular basis and perspectives. *J Biotechnol* 161:92–103
  42. Yang TH, Kwon MA, Song JK et al (2010) Functional display of *Pseudomonas* and *Burkholderia* lipases using a translocator domain of EstA autotransporter on the cell surface of *Escherichia coli*. *J Biotechnol* 146:126–129
  43. Jong WS, Sauri A, Luirink J (2010) Extracellular production of recombinant proteins using bacterial autotransporters. *Curr Opin Biotechnol* 21:646–652
  44. Jong WS, ten Hagen-Jongman CM, den Blaauwen T et al (2007) Limited tolerance towards folded elements during secretion of the autotransporter Hbp. *Mol Microbiol* 63:1524–1536
  45. Sauri A, Oreshkova N, Soprova Z et al (2011) Autotransporter beta-domains have a specific function in protein secretion beyond outer-membrane targeting. *J Mol Biol* 412:553–567
  46. van Ulsen P, van Alphen L, ten Hove J et al (2003) A Neisserial autotransporter NalP modulating the processing of other autotransporters. *Mol Microbiol* 50:1017–1030
  47. Yen YT, Kostakioti M, Henderson IR et al (2008) Common themes and variations in serine protease autotransporters. *Trends Microbiol* 16:370–379
  48. Wilhelm S, Tommassen J, Jaeger KE (1999) A novel lipolytic enzyme located in the outer membrane of *Pseudomonas aeruginosa*. *J Bacteriol* 181:6977–6986
  49. Upton C, Buckley JT (1995) A new family of lipolytic enzymes? *Trends Biochem Sci* 20:178–179
  50. Rutherford N, Mourez M (2006) Surface display of proteins by gram-negative bacterial autotransporters. *Microb Cell Fact* 5:22
  51. Veiga E, de Lorenzo V, Fernandez LA (1999) Probing secretion and translocation of a beta-autotransporter using a reporter single-chain Fv as a cognate passenger domain. *Mol Microbiol* 33:1232–1243
  52. Valls M, Atrian S, de Lorenzo V et al (2000) Engineering a mouse metallothionein on the cell surface of *Ralstonia eutropha* CH34 for immobilization of heavy metals in soil. *Nat Biotechnol* 18:661–665
  53. Klauser T, Pohlner J, Meyer TF (1990) Extracellular transport of cholera toxin B subunit using *Neisseria* IgA protease beta-domain: conformation-dependent outer membrane translocation. *EMBO J* 9:1991–1999
  54. Maurer J, Jose J, Meyer TF (1997) Autodisplay: one-component system for efficient surface display and release of soluble recombinant proteins from *Escherichia coli*. *J Bacteriol* 179:794–804
  55. Fleetwood F, Andersson KG, Stahl S et al (2014) An engineered autotransporter-based surface expression vector enables efficient display of Affibody molecules on OmpT-negative *E. coli* as well as protease-mediated secretion in OmpT-positive strains. *Microb Cell Fact* 13:985
  56. Jose J, Zangen D (2005) Autodisplay of the protease inhibitor aprotinin in *Escherichia coli*. *Biochem Biophys Res Commun* 333:1218–1226
  57. Yang TH, Pan JG, Seo YS et al (2004) Use of *Pseudomonas putida* EstA as an anchoring motif for display of a periplasmic enzyme on the surface of *Escherichia coli*. *Appl Environ Microbiol* 70:6968–6976
  58. Yanisch-Perron C, Vieira J, Messing J (1985) Improved M13 phage cloning vectors and host strains: nucleotide sequences of the M13mp18 and pUC19 vectors. *Gene* 33:103–119
  59. Stemmer WP (1994) DNA shuffling by random fragmentation and reassembly: in vitro recombination for molecular evolution. *Proc Natl Acad Sci U S A* 91:10747–10751
  60. Cadwell RC, Joyce GF (1992) Randomization of genes by PCR mutagenesis. *PCR Methods Appl* 2:28–33

61. Reetz MT, Carballeira JD, Peyralans J et al (2006) Expanding the substrate scope of enzymes: combining mutations obtained by CASTing. *Chemistry* 12:6031–6038
62. McCormick ML, Gaut JP, Lin TS et al (1998) Electron paramagnetic resonance detection of free tyrosyl radical generated by myeloperoxidase, lactoperoxidase, and horseradish peroxidase. *J Biol Chem* 273:32030–32037
63. Becker S, Michalczyk A, Wilhelm S et al (2007) Ultrahigh-throughput screening to identify *E. coli* cells expressing functionally active enzymes on their surface. *Chembiochem* 8:943–949
64. Adams TM, Wentzel A, Kolmar H (2005) Intimin-mediated export of passenger proteins requires maintenance of a translocation-competent conformation. *J Bacteriol* 187:522–533
65. Gustavsson M, Backlund E, Larsson G (2011) Optimisation of surface expression using the AIDA autotransporter. *Microb Cell Fact* 10:72
66. Doerner A, Rhiel L, Zielonka S et al (2014) Therapeutic antibody engineering by high efficiency cell screening. *FEBS Lett* 588:278–287

# Syngas Fermentation for Polyhydroxyalkanoate Production in *Rhodospirillum rubrum*

O. Revelles, I. Calvillo, A. Prieto, and M.A. Prieto

## Abstract

Bioconversion of organic waste into value-added products by a process called syngas fermentation is gaining considerable interest during the last years. Syngas is a gaseous mixture composed mainly of hydrogen and carbon monoxide and smaller quantities of other gases like CO<sub>2</sub> that can be fermented by *Rhodospirillum rubrum*, a natural producer of polyhydroxybutyrate (PHB). *R. rubrum* is a highly versatile, purple, non-sulfur bacterium that can grow in a broad range of anaerobic and aerobic conditions. In anaerobiosis, it can utilize CO as carbon and energy source in the presence or absence of light. When exposed to CO, CO dehydrogenase, which catalyzes oxidation of CO into CO<sub>2</sub>, is induced. Part of the CO<sub>2</sub> produced is assimilated into cell material and the remaining CO<sub>2</sub>, along with the H<sub>2</sub>, is released into the environment. The protocol below provides detailed information of PHB production during syngas fermentation by *R. rubrum* at lab scale.

**Keywords:** Anaerobic culture, Gas analysis, Polyhydroxyalkanoates (PHA), Syngas, Syngas fermentation

---

## 1 Introduction

The rapid urban growth and modern lifestyle are generating an enormous amount of municipal and industrial wastes. In developing countries, urban agglomerations are growing at twice the rate of population growth. Organic waste provides a significant resource of biomass that can be utilized for generating commodity products such as chemicals, biofuels, or bioplastics [1, 2] by a bacterial fermentative process. Hence, valorizing and reusing wastes via their bioconversion into value-added products offer an interesting strategy with a high impact in bio-economy. Although some wastes might be homogeneous, many others (e.g., municipal waste) present a very complex composition. In this context, one of the processing methods that can be used in biorefineries is the gasification of organic materials to synthesis gas [3], or syngas, followed by microbial fermentation. Gasification is generally defined as a

thermochemical conversion (750–850°C) of carbonaceous compounds including biomass and organic wastes into gas mixtures consisting of carbon monoxide (CO), hydrogen (H<sub>2</sub>), carbon dioxide (CO<sub>2</sub>), methane (CH<sub>4</sub>), nitrogen (N<sub>2</sub>), usually named syngas, and smaller liquid (tar) and solid (char) fractions. Basically, tar fraction consists of a mixture of high molecular weight hydrocarbons and char is mainly charcoal and ashes [2]. Further, syngas is an important intermediate product in chemical industry, being of special interest for the ammonia industry. Additionally, it is also the intermediate energy carrier for the production of second-generation biofuels like methanol, DME (dimethyl ether), cellulosic ethanol, and Fischer-Tropsch diesel. Furthermore, such gaseous mixture could potentially be used by bacteria as carbon and energy sources and converted into fuel and biochemicals, in a process known as syngas fermentation. Using bacteria as biocatalysts for syngas fermentation offers several advantages over traditional mineral-based catalysts used for syngas transformation: (i) it can operate at temperatures and pressures which are closer to standard environmental conditions than traditional chemical catalysts; (ii) it is less sensitive to the ratio of CO to H<sub>2</sub> in syngas compared to traditional/commercial catalysts, and (iii) it is less sensitive to trace amounts of contaminants in the syngas, such as char and tar, chlorine, and sulfur [4]. Although syngas is mainly used in the chemical industry for the production of chemical compounds, its fermentation offers an economic alternative for biofuel and biochemical synthesis [1, 5].

Gasification allows for the processing of virtually all types of organic waste (e.g., industrial or municipal) into syngas, which in turn can be fermented to produce a diversity of compounds such as hydrogen, methane, alcohols, carboxylic acids, and specially the bioplastics polyhydroxyalkanoates (PHAs) [6–9]. The potential of syngas fermentation is evident by the advent of large-scale projects. LanzaTech is working with steel manufacturers and coal producers to make liquid fuels in China (<http://www.lanzatech.com>). Coskata (<http://www.coskata.com>) is commercializing the production of fuels using a wide variety of biomass sources through syngas fermentation, among others. BioMCN is converting glycerine to syngas to be further fermented into bio-methanol (<http://www.biomcn.eu>).

PHAs are interesting products obtained from bioconversion of syngas via fermentation process. *Rhodospirillum rubrum* is an organism particularly attractive for the bioconversion of syngas into H<sub>2</sub> and PHAs, mainly polyhydroxybutyrate (PHB), the prototype of the short-chain-length PHAs (Fig. 1) [7, 10]. It is one of the most versatile bacterial species in terms of metabolism, capable of growing autotrophically or heterotrophically, phototrophically, or chemotrophically, in the presence or absence of oxygen.



**Fig. 1** Pictures of *R. rubrum* growing in medium syn with and without syngas (a), a TEM (transmission electron microscopy) image of *R. rubrum* containing PHB granules (b), and optical microscopy image of *R. rubrum*'s spiral-shaped rods (c)

*R. rubrum* metabolism makes it an ideal bacterium for many industrial processes.

Under anaerobic conditions, regardless of the presence of light or other carbon sources, CO induces the synthesis of several proteins, including CO dehydrogenase (CODH) [11, 12]. Part of the CO<sub>2</sub> produced is assimilated into cell material, and the remaining CO<sub>2</sub> along with the H<sub>2</sub> is released into the environment [13, 14].



Here in this chapter, we provide detailed information about the syngas fermentation process to produce PHAs using *R. rubrum* as biocatalyst; growth conditions and medium for syngas fermentation are detailed. Moreover, the procedure to study the kinetics of growth during this process is also given. The chapter finishes with the extraction and quantification of the final value-added product of syngas fermentation, such as PHB.

## 2 Materials

**2.1 Bacterial Strain** *R. rubrum* DSMZ 467T type strain (ATCC 11170) (DSMZ collection: <http://www.dsmz.de>) (see **Note 1**).

**2.2 Bacterial Culture Media** These may be individually purchased from any supplier of common bacterial growth components or as pre-prepared media. In our lab all products are provided by Sigma (<http://www.sigmaldrich.com>). The components and amounts for 1 L of medium are given below:

1. 112 *Van Niel's* yeast agar medium (ATCC medium: <http://www.atcc.org>): K<sub>2</sub>HPO<sub>4</sub> 1 g, MgSO<sub>4</sub> 0.5 g, yeast extract 10 g, and agar 20 g. pH 7.0–7.2.
2. Syn medium: MgSO<sub>4</sub> × 7H<sub>2</sub>O 250 mg, CaCl<sub>2</sub> × 2H<sub>2</sub>O 132 mg, NH<sub>4</sub>Cl 1 g, NiCl<sub>2</sub> 20 μM, MOPS 2.1 g and biotin 2 μg, and 10 mL of a chelated iron-molybdenum aqueous solution (H<sub>3</sub>BO<sub>3</sub> 0.28 g/L, Na<sub>2</sub>EDTA 2 g/L, ferric citrate 0.4 g/L, and Na<sub>2</sub>MoO<sub>4</sub> 0.1 g/L) adjusting pH to 7.1. Following autoclaving and degasification, the medium was supplemented with the subsequent anaerobic solutions: 0.05 mL of potassium phosphate buffer 1.91 M (pH 7.0), 0.1 mL of Na<sub>2</sub>S<sub>x</sub>9H<sub>2</sub>O 1% and 0.25 mL of NaHCO<sub>3</sub> 0.5 M (pH 8.0) [15], and the carbon source (15 mM fructose or 10 mM acetate).
3. Gassing station for dispensing anoxic gases is needed. Syringes from 1 to 5 mL (Plastipak BD: <http://www.bd.com>).

**2.3 Culture Preparation for Anaerobic Growth**

1. Nitrogen gas cylinder provided with a gas regulator (Air Liquide: <http://www.airliquide.com>). Serum bottles (Wheaton glass serum bottle (<http://www.sigmaldrich.com>)), lyophilization stopper chlorobutyl 20 mm (Wheaton W224100-202: <http://www.wheaton.com>), and lyophilization clamps with center disk tear-out (<http://www.wheaton.com>) (Fig. 2).

**2.4 Syngas Fermentation** Start the culture and syngas feeding. Parameter monitoring.

1. *R. rubrum* anaerobic culture in Syn-Fructose OD<sub>600</sub> 1.
2. Vacuum pump device (Fisher Scientific vacuum pump: <http://www.fishersci.com>).
3. CO gas detector (MX6 iBrid-Industrial Scientific: <http://www.indsci.com>). Syngas cylinder (Air Liquide: <http://www.airliquide.com>). A personalized syngas mixture was prepared from the provider. Its composition (purity; percentage (v/v) and ppm) is 40% CO, 40% H<sub>2</sub>, 10% N<sub>2</sub>, and 10% CO<sub>2</sub> (see **Note 2**). ATTENTION. Due to its CO content, syngas is toxic by inhalation and must be carefully handled.



**Fig. 2** Bottles and tools used to prepare anaerobic cultures; bottles for culturing anoxygenic *R. rubrum*, chorobutyl rubber stoppers, and aluminum clamps (a) and hand crimper for crimping aluminum caps on vessels (b). Gas supply equipment. (c) Oxygen purging with nitrogen while putting the needle connected to the gas nozzle directly into the liquid. (d) Vacuum is done inside the bottle for 1 min prior to adding the syngas mixture. (e) The headspace of the vial is refilled with syngas

### 2.5 Measurement of Cell Dry Weight (CDW)

1. Filter 0.4  $\mu\text{m}$   $\text{\O}$  (<http://www.millipore.com>); filtering flask and water aspirator device for cell dry weight determination (Fisher Scientific: <http://www.fishersci.com>).
2. NaCl solution 0.9% as washing cell solution.

3. Oven at 55°C (Mettler: <http://www.mettler.com>).
4. Precision balance (Denver instrument, now Sartorius: <http://www.sartorius.us>).

**2.6 HPLC Analyses to Determine Biomass Specific Rate of Acetate Consumption (Qs)**

1. HPLC system (GILSON: <http://www.gilson.com>) equipped with an Aminex HPX-87H column (<http://www.bio-rad.com>). Mobile phase: aqueous 2.5 mM H<sub>2</sub>SO<sub>4</sub> solution. Data were recorded and analyzed using KARAT 32 software (<http://www.beckmancoulter.com>).
2. Syringe filter 0.2 µm for chromatography (Whatman GD/X syringe filters: <http://www.sigmaaldrich.com>).
3. Screw caps and autosampler vials (<http://www.chem.agilent.com>).
4. Acetate stock solutions of 0.1 mM, 0.5 mM, 1 mM, 5 mM, and 10 mM to calculate acetate standard curve (*see* **Note 3**).

**2.7 Gas Analysis**

1. Headspace (HS) sampler. Our instrument is the Agilent 7697A (<http://www.chem.agilent.com>) that comprises a 12-vial carousel for 10 or 20 mL vials inside an oven, a 1 mL injection loop, and a 1 m transfer line. Vials are independently pressurized and leak-checked before injection and automatically purged after analysis using the control software (7697A Headspace Control MSD Data System rev. B.01.0X).
2. Gas chromatograph (GC) equipped with a ten-port valve and a thermal conductivity detector (TCD). Our instrument is the Agilent 7890A (<http://www.chem.agilent.com>). Data were recorded and analyzed using the instrument's software GC ChemStation rev. B.04.03-SP1 (87) from Agilent Technologies, Inc.
3. Stainless steel columns: 80/100 Porapak Q (6 ft, 1/8 in. 2 mm) and 60/80 MolSieve 13X (6 ft, 1/8 in. 2 mm). The two columns are connected in series.
4. 10 mL beveled-neck flat bottom headspace vials, 20 mm aluminum crimp caps, crimper for seals, and 20 mm PTFE/silicon septa (PTFE, polytetrafluoroethylene) (<http://www.agilent.com>).
5. Helium N50 gas cylinder (Air Liquide: <http://www.airliquide.com>).
6. Gas-tight syringes of different volumes (<http://www.sge.com>) and disposable needles (25G, 0.5 × 16 mm) (<http://www.bd.com>).

**2.8 PHB****Quantification:****Lyophilization,  
Methanolysis, and Gas  
Chromato-  
graphy–Mass  
Spectrometry (GC–MS)**

1. Lyophilizer at  $-56^{\circ}\text{C}$  and  $10^{-2}$  mbar (Cryodos-50 Telstar: <http://www.telstar.com>).
2. Chloroform-methanol solution containing 15% sulfuric acid and 0.5 mg/mL of 3-methylbenzoic acid (IS) (<http://www.sigmaaldrich.com>).
3. Thermoblock at  $80^{\circ}\text{C}$  (Fisher Scientific dry bath: <http://www.fishersci.com>).
4. Standard curve from 0.5 to 2 mg of PHB from Sigma (Cat: 36,350-2) (<http://www.sigmaaldrich.com>) (*see Note 3*).
5. Screw caps and autosampler vials (<http://www.chem.agilent.com>).
6. Gas chromatograph (GC) with split/splitless injector and quadrupole mass detector (MS) equipped with a HP-5MS capillary column ( $30\text{ m} \times 0.25\text{ mm} \times 0.25\text{ }\mu\text{m}$ ). Our system is the Agilent 7890A/5975C (<http://www.chem.agilent.com>), and data are acquired and processed with the software MSD ChemStation E.02.00.493 from Agilent Technologies, Inc.

**2.9 General  
Equipment**

1. Centrifuge (Eppendorf Centrifuge 5810R: <http://www.eppendorf.com>).
2. Spectrophotometer (Shimadzu: <http://www.shimadzu.com>).
3. Shaker at  $30^{\circ}\text{C}$  (Innova 44: <http://www.eppendorf.com>).
4. Phase contrast microscope (DM 4000B: <http://www.leica-microsystems.com>).
5. Gassing station for dispensing anoxic gases.

---

**3 Methods****3.1 Culture****Preparation for  
Anaerobic Growth  
and Syngas****Fermentation: Tricks  
for Keeping Anaerobic  
Conditions While  
Feeding Syngas**

Bottles of any convenient shape are used to cultivate anaerobic bacteria on an intermediate-size scale (from 15 mL up to 100 mL). The air must be removed from the culture. Further, the use of anaerobe culture tubes and serum bottles requires proper sealing by special chlorobutyl rubber stoppers that can be punctured without causing leaks, purging of the headspace with appropriate oxygen-free gases, and proper sealing of the bottles with aluminum crimp caps.

1. Dissolve all the ingredients in distilled water, except heat-sensitive components (biotin), precipitate-causing materials (e.g., carbonate), reducing agents ( $\text{Na}_2\text{S} \times 9\text{H}_2\text{O}$ ), and buffer phosphate. Adjust pH to 7.0, and bring the volume up to 1 L with water. Heat the mixture to its boiling point and dispense it into the culture bottles (20 mL medium/100 mL bottle).

2. Oxygen removal is done by directly bubbling nitrogen into the medium in order to exclude dissolved oxygen (*see Note 4*). To do so, a needle connected to the end of the gas nozzle is immersed into the liquid for 30 min (Fig. 2c). To avoid bubbling over the bottle, the nitrogen pressure supplied is regulated with the gas regulator. Keep the rubber stopper on top of the bottle during gassing. The bottle is rapidly sealed with hand crimper while removing the nozzle, leaving no chance for oxygen to enter. Finally, the bottle is tightened sealed with aluminum clamp (Fig. 2a, b).
3. The bottles with the culture medium are autoclaved at 121°C for 20 min.
4. After autoclaving and prior to inoculation, the medium is supplemented with the rest of anoxic solutions, and carbon source different to syngas when needed (e.g., acetate or fructose). Before being added, the supplements and reducing agents should be sterilized by filtration and then oxygen-purged with nitrogen under sterile conditions. The reducing agent ( $\text{Na}_2\text{S} \times 9\text{H}_2\text{O}$ ) should be added last. Sterile needles and syringes are used to add these solutions to the medium through the rubber stopper. Be sure that no bubbles trapped in the syringe are injected into the medium.
5. To assure an aseptic and anaerobic handle, the top of the bottle should be sterilized by wiping with 70% ethanol and flaming.

### 3.2 Inoculum Preparation for Syngas Fermentation

1. With an inoculating needle, take a single colony of *R. rubrum* from a fresh agar plate and transfer it into a screw-capped test tube of 10 mL filled with 5 mL of 112 *Van Niel's* yeast medium and close it (Fig. 3).
2. Incubate shaking at 250 rpm and 30°C. After 4–7 days the growth is evident by turbidity. When examined microscopically, the cells appear as spiral-shaped rods, singles, and in chains (Fig. 1c).
3. Put at least 200  $\mu\text{L}$  of the culture suspension into a 100 mL bottle with 20 mL Syn medium, yeast extract 1 g/L, and 15 mM fructose, oxygen-free.
4. Incubate the broth culture at 30°C and 250 rpm. Subsequent growth should be detected within 48–72 h (Fig. 3).

### 3.3 Syngas Fermentation: Start the Culture and Syngas Feeding

Syngas fermentation was carried out in 100 mL bottles containing 20 mL of Syn medium supplemented with syngas and 10 mM acetate. The complete medium is prepared as follows:

1. Inoculate the bottles for syngas fermentation to an initial  $\text{OD}_{600}$  of 0.05 from the well-grown ( $\text{OD}_{600} = 1\text{--}2$ ) syn-Fructose-grown *R. rubrum* (see above). Prior to its

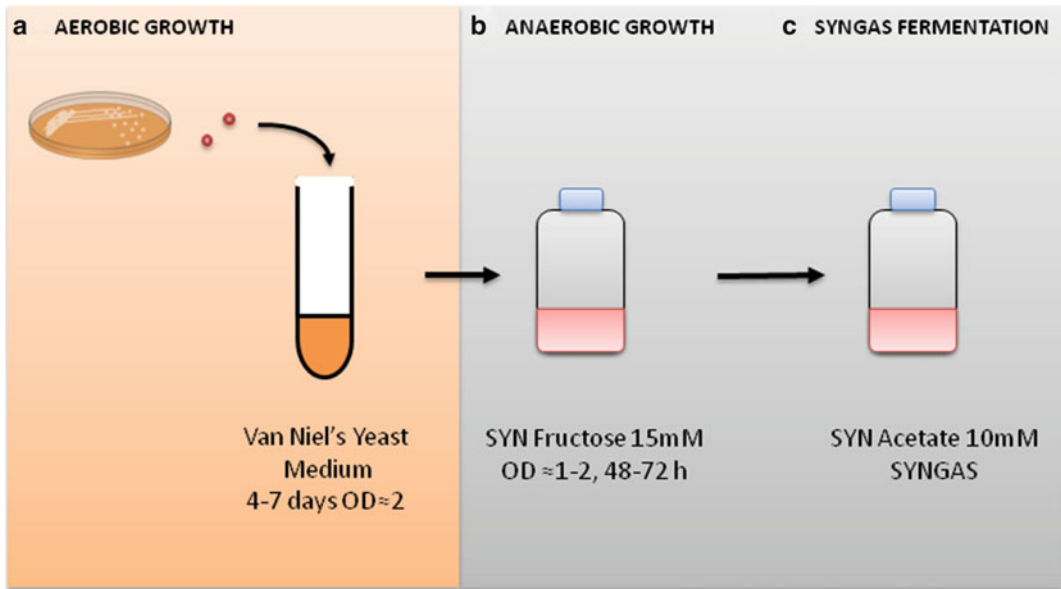


**Fig. 3** Scheme describing the different steps to perform syngas fermentation. (a) Aerobic growth, (b) anaerobic growth, and (c) syngas fermentation

inoculation, centrifuge and wash out the medium. After washing the culture cells, resuspend the pellet in 0.5 mL of fresh medium.

2. Purge the headspace gas of the bottle by making vacuum for 1 min with the vacuum pump (Fig. 2d).
3. Saturate the headspace of the bottle with syngas to 1 atmosphere of pressure (Fig. 2e). This step was repeated every day for syngas feeding (*see Note 5*).
4. Grow shaking (250 rpm) at 30°C (*see Note 6*).
5. Take 1 mL sample every 12 h monitoring the OD<sub>600</sub>.
6. Spin down the cells by centrifugation at 8,000 × *g* for 10 min at 4°C, discard the pellet, and store the supernatant at -20°C for further analysis (*see Subheading 3.5*).

### 3.4 Measurement of CDW

Measurement of CDW is an important parameter for estimating biomass concentration, productivity, and percentages of cell components. This experiment involves taking aliquots of the culture suspension, drying samples to a constant weight, and expressing this value as the weight of the dry cell matter per sample volume:

1. Dry overnight in an oven an empty cellulose acetate filter membrane, 47 mm in diameter and 0.45 μm in pore size. Weigh and store them in a desiccator lined with Drierite (anhydrous CaSO<sub>4</sub>).

2. Measure OD<sub>600</sub> (*see Note 7*) of a syngas-growing fermentation culture in exponential phase. Take out 10 mL of the same cultures and filter them applying vacuum to pull the liquid through the membrane. Rinse the filter with 10 mL of NaCl 0.9%. Three independent biological replicates of all determinations shall be performed. From each culture just one point at mid-exponential phase will be taken.
3. Dry overnight in an oven the filters containing the cell paste and weigh them (*see Note 8*). Calculate the weight difference, normalize to the measured OD<sub>600</sub>, and express the dry weight in g/L per OD<sub>600</sub> unit to obtain the conversion factor.
4. Convert the OD<sub>600</sub> values to CDW using the conversion factor.

### 3.5 HPLC Analysis to Determine Acetate (Qs) [16]

During syngas fermentation *R. rubrum* is consuming acetate and syngas. In this section the Qs for acetate will be determined along the growth. It is important to stress that PHB production reaches its maximum when all the acetate is consumed and thus the importance of this parameter.

1. Prepare standard solutions 0.1 mM, 0.5 mM, 1 mM, 5 mM, and 10 mM of sodium acetate to determine the retention time of acetate, as well as to make a standard calibration curve (*see Note 3*).
2. Filter the standard solutions or the sample supernatants (*see Subheading 3.3.6*) through 0.2 μm syringe filters into 1.8 mL autosampler vials prior to HPLC analysis. A minimum volume of 500 μL is needed.
3. Analyze the standards and samples by HPLC (*see Subheading 2.6.1*) at 40°C with a mobile phase flow rate of 0.6 mL/min.
4. Determine peak areas by using the integration software of your system.
5. Using the standard curve and the measured areas for the acetate peak in samples, deduce the acetate concentration.
6. Determine the acetate consumption rate(s) as the slope of acetate consumption curve.
7. Biomass specific rate of substrate consumption, in our case acetate (Qs), can be calculated from the substrate consumption and biomass production rate (mmol.g.DW<sup>-1</sup>h<sup>-1</sup>).
8. Acetate uptake rate is the slope of the plot of acetate consumption versus time.

### 3.6 Gas Analysis [6]

1. Instrument configuration (HS-GC-TCD). The whole system comprised the 7697A HS sampler, coupled to a 7890A GC with TCD. The GC is equipped with a ten-port valve, used to address the carrier flow through the columns in the right path at different steps of the analytical method. Two stainless steel

columns, 80/100 Porapak Q (6 ft, 1/8 in. 2 mm) and 60/80 Molesieve 13X (6 ft, 1/8 in. 2 mm) are connected in series inside the oven to achieve separation of all components of the gas mixture (*see Note 9*). The carrier gas (He) is maintained at constant pressure (45 psi).

## 2. Chromatographic parameters:

1. HS sampler: The loop and transfer line temperatures are fixed at 100°C and the HS oven at 70°C. The times for vial equilibration and injection are 1 min and 0.5 min, respectively. Using the HS sampler software, the vial size (10 mL) is selected and the vials are programmed to be filled with He to a final pressure of 14 psi (1 atmosphere). Then, 1 mL of sample is injected (single extraction mode) and each vial is automatically purged after injection. The complete GC cycle was set to 20 min.
2. GC: The initial oven temperature is isothermal for 5 min at 30°C and then programmed to rise from 30 to 180°C at 25°C min<sup>-1</sup>. The detector is set to 250°C and the valve box at 100°C. The ten-port valve is initially set up in the ON position, programmed to commute to OFF at 2.2 min from injection and again to ON at 10.9 min (*see Note 10* and Fig. 4). The GC run time is 11 min.

Under these experimental conditions, the elution order of the potential analytes expected is H<sub>2</sub> (detected as a negative peak), CO<sub>2</sub>, N<sub>2</sub>, H<sub>2</sub>O, and CO (*see Note 11*)

## 3. Preparation and analysis of syngas standards:

1. Fill with syngas (*see Note 6*) a 100 mL glass bottle with 20 mL of fresh Syn medium closed with a rubber stopper. This bottle will be used as syngas stock.

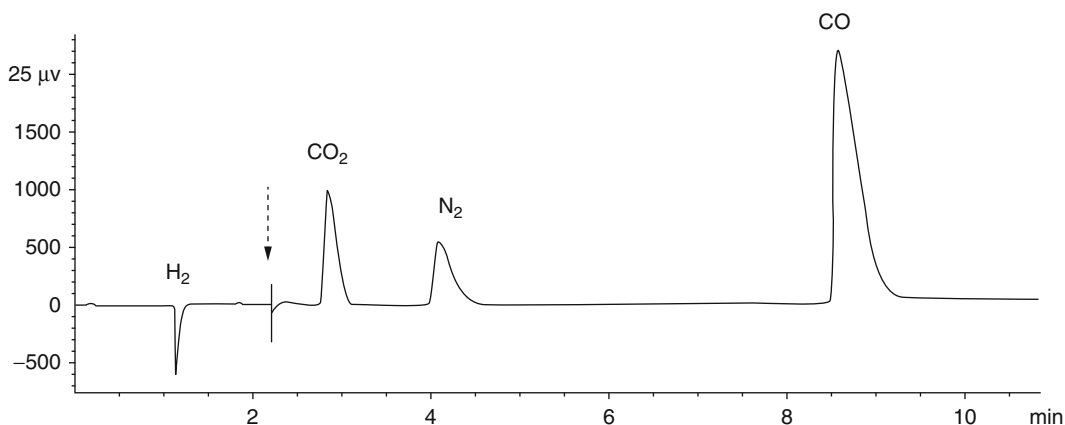


**Fig. 4** Elution profile of a syngas standard using HS-GC-TCD. The elution order of the expected analytes is H<sub>2</sub> (detected as a negative peak), CO<sub>2</sub>, N<sub>2</sub>, H<sub>2</sub>O, and CO. The broken arrow indicates the change in the ten-port valve position, initially set up in ON, and it is commuted to OFF at minute 2

2. Degasified closed empty HS vials and purge with He (*see Note 12*) for 2 min to ensure complete removal of air.
3. Withdraw known volumes (0.1, 0.25, 0.5, 1, 2, 5, and 10 mL) of the bottle containing the syngas stock using the gas-tight syringe, and add each volume to one of the HS vials prepared. All standards are prepared and analyzed in duplicate.
4. Place the HS vials containing syngas standards in the carousel of the HS sampler and analyze standards by HS-GC-TCD to make the calibration curve (*see* Subheading 3.6.2., Chromatographic parameters).
5. Using the GC data analysis software, integrate the chromatograms corresponding to different calibration points. For each component of the standards mixture, plot concentration vs. peak area to build its calibration curve. Concentration is calculated by the ideal gas law  $PV = nRT$ , where the letters denote pressure ( $P$ ) of the system is 1 atmosphere, volume ( $V$ ), amount ( $n$ ), ideal gas constant ( $R$ ), and temperature of the gas ( $T$ ), respectively. Assess response linearity in the concentration range assayed for every standard.
4. Preparation and analysis of samples:
  1. Using a gas-tight syringe, extract 0.5 mL samples extracted from the headspace of cultures, from 0 to up to 7 days.
  2. Inject the sample in HS vials filled with He. Samples are prepared and analyzed in duplicate.
  3. Place the sample vials in the carousel of the HS sampler and analyze by HS-GC-TCD (*see* Subheading 3.6.2., Chromatographic parameters).
  4. Using the GC data analysis software, integrate the chromatograms. From the peaks areas, calculate the concentration of each sample's component using the calibration curve.

### 3.7 PHB Quantification [17, 18]

The most widely used approach for PHB quantification comprises biomass lyophilization, polymer methanolysis followed by GC-MS analysis of the methylated monomers.

1. Centrifuge at  $8,000 \times g$  for 15 min at 4°C. Wash the cells twice using MilliQ water.
2. Froze the cells at -80°C for at least 1 h and lyophilize them at -56°C and  $10^{-2}$  mbar. We use a Cryodos-50 Telstar lyophilizer.
3. Weigh the dry cell pellet to estimate the CDW, expressed in mg/L.

4. Suspend from 5 to 10 mg of lyophilized cells into 0.5 mL of chloroform and 2 mL of methanol containing 15% sulfuric acid and 0.5 mg/mL of 3-methylbenzoic acid (internal standard).
5. Vortex properly the mixture and incubate the sample at 100°C for 4 h in an oil bath.
6. Chill the samples on ice for 5 min.
7. Add 1 mL of MilliQ water and 1 mL of chloroform and vortex the samples.
8. Centrifuge at 3,500 rpm (Eppendorf Centrifuge 5810R).
9. Recover the organic phase where the methyl esters are and proceed to analyze it by GC-MS as explained in Subheading 2.8.6.
10. Apply the previously described procedure on known quantities of a commercial PHB standard to prepare a standard curve from 0.5 to 2 mg of PHB (*see Note 3*).
11. For quantification of the sample components, integrate sample peak areas by using the integration method of your system, and interpolate these values in the PHB calibration curve.

---

## 4 Notes

1. *R. rubrum* can be stored at -80°C in 15% glycerol (viable for >5 years) or at 4°C on Petri agar plate of Van Niel's yeast agar medium (viable for 1 week).
2. Syngas mixture composition (purity; percentage (v/v) and ppm) is H<sub>2</sub> (Alphagaz range 1; 40%, 400 ppm), N<sub>2</sub> (Alphagaz range 1; 10%, 100 ppm), CO (N37; 40%, 20,000 ppm), and CO<sub>2</sub> (N38; 10%, 5,000 ppm).
3. A calibration curve should be generated for each analyte in the sample, and the concentrations of the standards should be chosen on the basis of the concentration range expected in the study. Therefore, to prepare a good calibration curve, a blank and at least six samples covering the expected range must be prepared and analyzed.
4. A redox sensitive dye, for instance, resazurin, can be included in the culture media to monitor the redox potential. Resazurin is commonly used because it is not toxic and very low concentrations (0.5 to 1 mg/L) are needed. It turns pink when oxygen is present.
5. Invert the bottle upside down and introduce the needle connected to the nozzle of gas in the medium through the stopper. Adjust the gas regulators to 1 atm and fill the bottle until bubbling ceases.

6. A high ratio of gas-to-liquid volume and vigorous stirring of the cell suspension are needed to enhance gas-liquid mass transfer throughout the growth period.
7. Volume must be adapted to the amount of biomass. We suggest to do a linear regression curve OD versus CDW and estimating the conversion factor from the lineal range of the curve.
8. Depending on the oven temperature and the thickness of the cellpaste, it can take between 6 and 24 h to dry the sample. To ensure complete sample dryness, weigh the filters periodically until constant weight.
9. CO<sub>2</sub> and water are retained and separated in Porapak and permanent gases (H<sub>2</sub>, O<sub>2</sub>, N<sub>2</sub>, and CO) in the MolSieve column.
10. The ten-port valve was initially set up in the ON position, allowing the carrier gas and sample to flow through the columns in the direction Porapak-MolSieve-TCD. After 2.2 min from injection, before CO<sub>2</sub> and water enter the molecular sieve column, the valve is programmed to commute to the OFF position, which changes the carrier and sample path flow to MolSieve-Porapak-TCD. Doing this, the entrance of CO<sub>2</sub> and water inside the second column, which would cause their irreversible retention and then the impossibility of detecting them, is avoided. Just before the end of the chromatographic run (10.9 min), the valve is reset to its initial position.
11. Notice that if the sample is contaminated with air, the order of analytes will be H<sub>2</sub> (detected as a negative peak), O<sub>2</sub>, CO<sub>2</sub>, N<sub>2</sub>, H<sub>2</sub>O, and CO.
12. Vials are purged with He via two disposable needles stuck through the cap. One is connected through PTFE tubing to the gas cylinder, and the additional needle allows venting of the gas excess.

---

## Acknowledgments

The design of this protocol was supported by the project European Commission SYNPOL no. 311815 [<http://www.sympol.org>]. We are indebted to Prof. Jose Luis García, the SYNPOL coordinator, for the helpful discussions about this technology.

## References

1. Latif H, Zeidan AA, Nielsen AT, Zengler K (2014) Trash to treasure: production of biofuels and commodity chemicals via syngas fermenting microorganisms. *Curr Opin Biotechnol* 27:79–87
2. Munasinghe PC, Khanal SK (2010) Biomass-derived syngas fermentation into biofuels: opportunities and challenges. *Bioresour Technol* 101(13):5013–5022

3. Belgiorno V, De Feo G, Della Rocca C, Napoli RMA (2003) Energy from gasification of solid wastes. *Waste Manag* 23(1):1–15
4. Munasinghe PC, Khanal SK (2010) Syngas fermentation to biofuel: evaluation of carbon monoxide mass transfer coefficient (kLa) in different reactor configurations. *Biotechnol Prog* 26(6):1616–1621
5. Beneroso D, Bermúdez JM, Arenillas A, Menéndez JA (2015) Comparing the composition of the synthesis-gas obtained from the pyrolysis of different organic residues for a potential use in the synthesis of bioplastics. *J Anal Appl Pyrolysis* 111:55–63
6. Younesi H, Najafpour G, Mohamed AR (2005) Ethanol and acetate production from synthesis gas via fermentation processes using anaerobic bacterium, *Clostridium ljungdablii*. *Biochem Eng J* 27(2):110–119
7. Do YS, Smeenk J, Broer KM et al (2007) Growth of *Rhodospirillum rubrum* on synthesis gas: conversion of CO to H<sub>2</sub> and poly-beta-hydroxyalkanoate. *Biotechnol Bioeng* 97(2):279–286
8. Najafpour GD, Younesi H (2007) Bioconversion of synthesis gas to hydrogen using a light-dependent photosynthetic bacterium *Rhodospirillum rubrum*. *World J Microbiol Biotechnol* 23(2):275–284
9. Kim Y-K, Park SE, Lee H, Yun JY (2014) Enhancement of bioethanol production in syngas fermentation with *Clostridium ljungdablii* using nanoparticles. *Bioresour Technol* 159:446–450
10. Klasson KT, Gupta A, Clausen EC, Gaddy JL (1993) Evaluation of mass-transfer and kinetic parameters for *Rhodospirillum rubrum* in a continuous stirred tank reactor. *Appl Biochem Biotechnol* 39–40(1):549–557
11. Kerby RL, Hong SS, Ensign SA et al (1992) Genetic and physiological characterization of the *Rhodospirillum rubrum* carbon monoxide dehydrogenase system. *J Bacteriol* 174(16):5284–5294
12. Uffen RL (1976) Anaerobic growth of a *Rhodospseudomonas* species in the dark with carbon monoxide as sole carbon and energy substrate. *Proc Natl Acad Sci U S A* 73(9):3298–3302
13. Buchanan BB, Evans MC (1965) The synthesis of alpha-ketoglutarate from succinate and carbon dioxide by a subcellular preparation of a photosynthetic bacterium. *Proc Natl Acad Sci U S A* 54(4):1212–1218
14. Buchanan BB, Evans MC, Arnon DI (1967) Ferredoxin-dependent carbon assimilation in *Rhodospirillum rubrum*. *Arch Mikrobiol* 59(1):32–40
15. Kerby RL, Ludden PW, Roberts GP (1995) Carbon monoxide-dependent growth of *Rhodospirillum rubrum*. *J Bacteriol* 177(8):2241–2244
16. Revelles O, Millard P, Nougayred JP et al (2013) The carbon storage regulator (Csr) system exerts a nutrient-specific control over central metabolism in *Escherichia coli* strain Nissle 1917. *PLoS One* 8(6):e66386
17. Lageveen RG, Huisman GW, Preusting H, Ketelaar P, Eggink G, Witholt B (1988) Formation of polyesters by *Pseudomonas oleovorans*: effect of substrates on formation and composition of poly-(R)-3-hydroxyalkanoates and poly-(R)-3-hydroxyalkenoates. *Appl Environ Microbiol* 54:2924–2932
18. de Eugenio LI, Escapa IF, Dinjaski N et al (2010) The turnover of medium-chain-length polyhydroxyalkanoates in *Pseudomonas putida* KT2442 and the fundamental role of PhaZ depolymerase for the metabolic balance. *Environ Microbiol* 12(1):207–221

# Genetic Strategies on Kennedy Pathway to Improve Triacylglycerol Production in Oleaginous *Rhodococcus* Strains

Martín A. Hernández and Héctor M. Alvarez

## Abstract

During the last years, microorganisms (yeasts, fungi, microalgae, and bacteria) have been receiving increasing attention as alternative lipid sources (also called single cell oils). Some lipid-accumulating bacteria, in particular those belonging to actinomycetes, are able to synthesize remarkably high amounts of triacylglycerides (TAGs) (up to 70% of the cellular dry weight) from simple carbon sources such as glucose, which are accumulated as intracellular lipid bodies. The applied potential of bacterial TAG may be similar to that of vegetable oil sources, such as additives for feed, cosmetics, oleochemicals, lubricants, and other manufactured products. In addition, bacterial oils have been recently considered as alternative sources for biofuel production. Because the development of an industrial and commercially significant process depends on the optimization of engineered cells and the technological procedures, several efforts to improve the natural accumulation of microbial lipids have been performed around the world. This chapter focuses on some genetic strategies for improving TAG accumulation in bacteria using oleaginous *Rhodococcus* strains as model. Particularly, protocols focus on the two last enzymatic steps of the Kennedy pathway by over-expression of *ro00075* gene and 2 *atf* genes coding for a phosphatidic acid phosphatase type 2 (PAP2) and diacylglycerol acyltransferase (WS/DGAT) enzymes, respectively.

**Keywords:** Biofuels, PAP2, *Rhodococcus*, Triacylglycerols, WS/DGAT

---

## 1 Introduction

Triacylglycerides (TAGs) are neutral lipids commonly found in eukaryotic organisms, including animals, plants, yeasts, and fungi, which constitute an important storage material, used as energy and/or carbon sources. In addition, TAGs also occur frequently in certain groups of prokaryotes as storage lipids. Although some Gram-negative bacteria are able to accumulate neutral lipids such as wax esters (WEs) and TAG, the ability to synthesize and accumulate significant amounts of these last is mainly common in members of actinobacteria, such as *Rhodococcus*, *Mycobacterium*, *Nocardia*, and *Streptomyces*, among other genera (Table 1) [1–6]. These

**Table 1**  
**Occurrence of TAG and WE accumulation in bacteria**

Bacteria	Type of storage lipids <sup>a</sup>
<i>Gram positive</i>	
<i>Rhodococcus opacus</i>	<b>TAG</b> /WE
<i>Rhodococcus jostii</i>	<b>TAG</b> /WE
<i>Rhodococcus fascians</i>	<b>TAG</b> /WE
<i>Rhodococcus erythropolis</i>	<b>TAG</b> /WE
<i>Rhodococcus ruber</i>	<b>TAG</b> /WE
<i>Nocardia asteroides</i>	<b>TAG</b>
<i>Nocardia globerula</i>	<b>TAG</b>
<i>Nocardia restricta</i>	<b>TAG</b>
<i>Mycobacterium tuberculosis</i>	<b>TAG</b>
<i>Mycobacterium smegmatis</i>	<b>TAG</b>
<i>Mycobacterium ratisbonense</i>	<b>TAG</b> /WE
<i>Streptomyces coelicolor</i>	<b>TAG</b>
<i>Streptomyces avermitilis</i>	<b>TAG</b>
<i>Gordonia</i> sp.	<b>TAG</b>
<i>Dietzia</i> sp.	<b>TAG</b>
<i>Gram negative</i>	
<i>Acinetobacter baylyi</i>	WE/ <b>TAG</b>
<i>Alcanivorax borkumensis</i>	WE/ <b>TAG</b>
<i>Marinobacter hydrocarbonoclasticus</i>	WE

<sup>a</sup>The occurrence of main neutral lipid is highlighted in bold letter

microorganisms produce variable amounts of TAG during cultivation with different carbon sources, and some species are able to accumulate these neutral lipids at very high levels. This is the case of some *Rhodococcus* strains, such as *R. opacus* PD630 and *R. jostii* RHA1, which are able to accumulate TAG up to 60% by cellular dry weight with gluconate, glucose, and other carbon sources when grown under nitrogen-limiting conditions (media with low concentration or in the absence of the nitrogen source) or in culture media with high C/N ratio [1–3, 7]. For this reason, such oleaginous microorganisms can be considered good candidates for single cell oil production. In this context, bacterial oils may be useful for the production of feed additives, cosmetics, oleochemicals, lubricants, and other manufactured products. In addition, bacterial lipids have been proposed as a source for biofuel production (biodiesel) by a chemical process of transesterification [8, 9]. Lipid production by bacteria provides some advantage over using vegetable sources, such as the high variability of fatty acid composition in lipids, according to the use of diverse carbon sources for cell cultivation, as well as the better accessibility of bacterial cells for genetic manipulations.

In the last years, several research efforts have been focused on the culture conditions, biochemistry, and genetics of oil-accumulating bacteria, for designing a scalable and commercially

viable oil-producing system from inexpensive feedstocks. Particularly, in oleaginous *Rhodococcus* species, several genes involved in TAG metabolism have been identified and characterized [10–16]. Additionally, several cloning/expression vectors for such actinobacteria have been designed or adapted from related microorganisms as genetic tools for basic studies or biotechnological purposes (Table 2).

**Table 2**  
**Genetic tools used in *Rhodococcus* species**

Plasmid	Description	Reference(s)
<i>Replicative cloning vectors</i>		
pNC9503	<i>E. coli/Rhodococcus</i> shuttle vector, Km <sup>R</sup> , Thio <sup>R</sup>	[17, 18]
pNC9501	<i>E. coli/Rhodococcus</i> shuttle vector, Km <sup>R</sup> , Thio <sup>R</sup>	[17–19]
pRHBR71/171	<i>E. coli/Rhodococcus</i> shuttle vector, Ap <sup>R</sup> , Tet <sup>R</sup>	[20]
pFAJ2574	<i>E. coli/Rhodococcus</i> shuttle vector, Cm <sup>R</sup>	[21]
pMVS301	<i>E. coli/Rhodococcus</i> shuttle vector, Ap <sup>R</sup> , Thio <sup>R</sup>	[22]
pBS305	<i>E. coli/Rhodococcus</i> shuttle vector, Ap <sup>R</sup> , Thio <sup>R</sup>	[23]
pDA21	<i>E. coli/Rhodococcus erythropolis</i> shuttle vectors, As <sup>R</sup>	[24]
pDA71	<i>E. coli/Rhodococcus erythropolis</i> shuttle vectors, Ap <sup>R</sup> , Cm <sup>R</sup>	[25]
pRE-1	<i>E. coli/Rhodococcus equi</i> shuttle vector, Ap <sup>R</sup> , Km <sup>R</sup>	[26]
pAL281/pAL298	<i>E. coli/Rhodococcus</i> shuttle vectors, Gm <sup>R</sup>	[27]
pSRK21	<i>E. coli/Rhodococcus erythropolis</i> shuttle vector, Km <sup>R</sup>	[28]
pIAM1484	<i>E. coli/Rhodococcus</i> shuttle vector, Ap <sup>R</sup> , Km <sup>R</sup>	[29]
pRF37	<i>E. coli/Rhodococcus fascians</i> shuttle vector, Ap <sup>R</sup> , Bl <sup>R</sup>	[30]
pK4	<i>E. coli/Rhodococcus</i> shuttle vector, Km <sup>R</sup>	[31]
pRESQ	<i>E. coli/Rhodococcus</i> shuttle vector, Km <sup>R</sup>	[32]
pAL358	<i>E. coli/Rhodococcus</i> shuttle vector, Gm <sup>R</sup>	[33, 34]
pAL307	<i>E. coli/Rhodococcus</i> shuttle vector, Spc <sup>R</sup>	[34]
<i>Expression vectors</i>		
pJAM2	<i>Mycobacterium/Rhodococcus/E. coli</i> shuttle vector with P <sub>acc</sub> , Km <sup>R</sup>	[35–37]
pTip series vectors	<i>Rhodococcus/E. coli</i> shuttle vector with P <sub>tipA</sub> , Cm/Tet <sup>R</sup> , Thio <sup>R</sup>	[38, 39]
pNit series vectors	<i>Rhodococcus/E. coli</i> shuttle vector with P <sub>nit</sub> , Cm/Tet <sup>R</sup> , Thio <sup>R</sup>	[39]
pDEX	<i>Rhodococcus</i> dual-expression vector with P <sub>tipA</sub> and P <sub>nit</sub> , Ap <sup>R</sup> , Cm <sup>R</sup> , Thio <sup>R</sup>	[40]
pPR27 <sub>acc</sub>	<i>Mycobacterium</i> -based vector with P <sub>acc</sub> , Gm <sup>R</sup>	[41, 11]
pSM846	<i>Rhodococcus/E. coli</i> shuttle vector with a constitutive P <sub>amy</sub>	[42]
pDPM70	<i>Saccharomyces/Rhodococcus/E. coli</i> shuttle vector with P <sub>smyc</sub> , Gm <sup>R</sup>	[14, 16]

(continued)

**Table 2**  
**(continued)**

Plasmid	Description	Reference(s)
<i>Integrative/transposable vectors</i>		
pMV306/pMV <sub>acc</sub>	Integrative plasmid containing the attachment site (attP) and integrase gene (int) of the L5 mycobacteriophage	[43–45], this chapter
pSET152	Integrative plasmid containing the attachment site (attP) and integrase gene (int) of the phiC31 actinophage, Ap <sup>R</sup>	[46]
pBP5	Integrative plasmid containing the attachment site (attP) and integrase gene (int) of the L1 mycobacteriophage	[47]
pTO1	Integrative plasmid containing the attachment site (attP) and integrase gene (int) of the phiC31 actinophage	[48, 49]
pTNR-KA/pTNR-TA	Transposon-based vectors used as protein expression systems in <i>Rhodococcus</i> species	[50]
pTip-istAB-sacB/ pRTSK-sacB system	Transposon-based vectors for random integration of multiple copies of DNA into the <i>Rhodococcus</i> genome	[51]

The biosynthesis and accumulation of TAG is a complex process that involves several catalytic enzymes participating at different metabolic levels. In rhodococci, the main biosynthetic pathway for TAG biosynthesis, known as Kennedy pathway (Kennedy 1961), involves the sequential esterification of glycerol-3-phosphate producing phosphatidic acid (PA) (Fig. 1). PA, a key molecule for the biosynthesis of membrane glycerophospholipids in bacteria [52, 53], is dephosphorylated by a phosphatidic acid phosphatase type 2 enzyme (PAP, EC 3.1.3.4) to yield diacylglycerol (DAG). The occurrence of this enzyme in actinobacteria and its role in TAG metabolism have been recently reported [12, 54]. The produced DAG is then condensed with an acyl-CoA molecule to form TAG during the last reaction of Kennedy pathway. This reaction is catalyzed by the bifunctional wax ester synthase/diacylglycerol acyltransferase (WS/DGAT) enzymes encoded by the so-called *atf* genes. Interestingly, in Gram-positive actinomycete group, a high genetic redundancy of these enzymes is found, including 15 putative *atf* genes in *Mycobacterium tuberculosis* [5], 14 *atf* genes in *Rhodococcus jostii* RHA1 [7], three in *Streptomyces coelicolor* [55], and at least 16 in *Rhodococcus opacus* PD630 [9, 11]. Because PAP and WS/DGAT could catalyze the rate-limiting steps in the TAG formation in oleaginous actinobacteria, the identification of those genes encoding for both types of enzymes is an important aspect not only to understand the glycerolipid metabolism but also as a key point to manipulate TAG accumulation in such microorganisms.

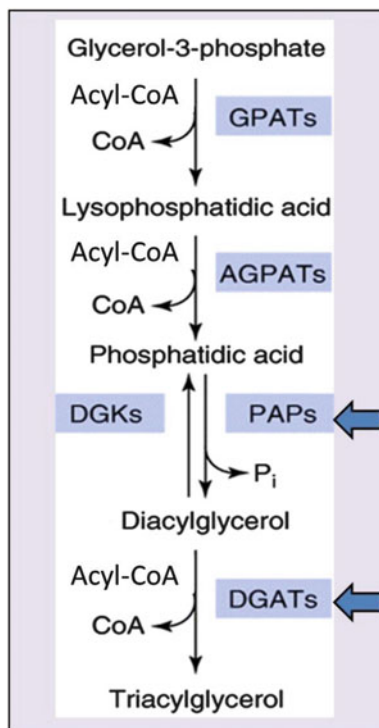


**Fig. 1** Kennedy pathway reactions for the biosynthesis and accumulation of TAG. *GPATs* glycerol-3-phosphate acyltransferases, *AGPATs* acyl-glycerol-3-phosphate acyltransferases, *PAPs* phosphatidic acid phosphatases, *DGKs* diacylglycerol kinases, *DGATs* diacylglycerol acyltransferases

In this context, the present chapter describes two previously reported strategies focused on the Kennedy pathway for improving TAG accumulation in oleaginous *Rhodococcus* strains, including:

1. Overexpression of *ro00075* gene encoding a PAP2 enzyme (see Fig. 1) in *Rhodococcus jostii* RHA1 and *Rhodococcus opacus* PD630 by using the pJAM2 and pTip-QC2 expression vectors
2. Individual overexpression of two *atf* genes (*atf1* and *atf2*) coding for 2 WS/DGAT enzymes (see Fig. 1) in *Rhodococcus opacus* PD630 by using the pJAM2, pPR27*ace*, and pTip-QC2 expression vectors

In addition, the integrative plasmid for *Mycobacterium* (pMV*ace*) is herein used as a genetic tool for introducing an extra single copy of the *atf2* gene under the P<sub>*ace*</sub> promoter into the chromosomal DNA of *Rhodococcus opacus* PD630. Finally, a brief protocol for the semiquantitative analysis of TAG content in recombinant strains is also described.

**Table 3**  
**Oligonucleotides for PCR assays described in this chapter**

Primers	Sequence <sup>a</sup>
ro00075F	5' <u>TGGATCC</u> ATGCCCCACACCTCCATCGCCA 3'
ro00075R	5' <u>GTTCCCTCTAGAGCCTCC</u> ACTCGGT 3'
atf2MHF	5' <u>TGGGGCATATG</u> CCGGTTACCGATT 3'
atf2MHR	5' <u>AAGCTTT</u> CAGAGCAATGCCGCCTCGA 3'
atf1MHF	5' <u>ACGAATCAGGGATCC</u> ATGACCCAGACGGA 3'
atf1MHR	5' <u>GTGCGTGTGTCTAGAGC</u> ACGAGG 3'
aceF	5'TCGCAGCGCCGTCAGTCACCAA 3'
thioF	5'TACATATCGAGGCGGGCTCCCA 3'

<sup>a</sup>Restriction sites used for subcloning purposes are underlined

## 2 Materials

### 2.1 DNA Amplification, Cloning, and Sequencing

1. PCR reaction mix: 13.5  $\mu$ L H<sub>2</sub>O, 5  $\mu$ L 5 $\times$  PCR buffer (50 mM TrisHCl, pH 8.5, MgCl<sub>2</sub> 7.5 mM), 1  $\mu$ L dNTP mix (containing 5 mM of each dNTP), 1  $\mu$ L primer F, 1  $\mu$ L primer R, 1.25  $\mu$ L DMSO, 0.25  $\mu$ L *Taq* polymerase (5 U/  $\mu$ L), and 2  $\mu$ L of DNA.
2. PCR primers: Synthetic oligonucleotides used in the protocols described in this chapter are listed in Table 3 (*see Note 1*). Primers are diluted to 25 pmol/ $\mu$ L from a stock solution of 100 pmol/ $\mu$ L.
3. DNA template: Total DNA of *R. jostii* RHA1 and *R. opacus* PD630 are used for amplification of *ro00075* gene and the two *atf* genes, respectively.
4. Bacteria and TA cloning vector: For cloning purposes, use *E. coli* (JM109 or DH5 $\alpha$  strains) and a TA cloning plasmid and its ligation buffer purchased from any supplier.
5. Blue/white colony selection: Use solid LB media supplemented with ampicillin (100  $\mu$ g/mL), X-Gal (80  $\mu$ g/mL), and IPTG (0.5 mM).
6. Other reagents: Agarose molecular grade and DNA purification kit (from enzymatic reaction and agarose gels).

### 2.2 Subcloning Strategies

1. Bacteria and expression vectors: *E. coli* DH5 $\alpha$  can be used for subcloning purposes. *Rhodococcus* parental strains, expression plasmids, recombinant plasmids, and resultant recombinant strains described in this chapter are listed in Table 4. Vectors

**Table 4**  
**Strains and plasmids described in this chapter**

Strain or plasmid	Description	Source
<b>Strains</b>		
<i>E. coli</i> DH5 $\alpha$	<i>E. coli</i> K-12 F- <i>lac</i> U169 ( $\phi$ 80 <i>lacZ</i> $\Delta$ M15) <i>endA1 recA1 hsdR17 deoR supE44 thi-1-l2 gyrA96 relA1</i> . Use for cloning and subcloning purposes	[56]
JM109	<i>endA1 glnV44 thi-1 relA1 gyrA96 recA1 mcrB<sup>+</sup> <math>\Delta</math>(lac-proAB) e14- [F<sup>+</sup> traD36 proAB<sup>+</sup> lacI<sup>q</sup> lacZ<math>\Delta</math>M15] hsdR17(r<sub>K</sub><sup>-</sup> m<sub>K</sub><sup>+</sup>)</i> . Use for cloning purposes	Promega
<i>Rhodococcus</i>		
<i>R. jostii</i>		
RHA1	Parental strain	[57]
RHA1 pJAM2	RHA1 derivative carrying pJAM2 plasmid, used as control strain; Km <sup>R</sup>	[12]
RHA1 pJAM2/RO00075	RHA1 derivative carrying pJAM2/ <i>ro00075</i> ; Km <sup>R</sup>	[12]
RHA1 pTip-QC2	RHA1 derivative carrying pTip-QC2 plasmid, used as control strain; Cm <sup>R</sup>	[12]
RHA1 pTip-QC2/RO00075	RHA1 derivative carrying pTip-QC2 / <i>ro00075</i> ; Cm <sup>R</sup> , Thio <sup>R</sup>	[12]
<i>R. opacus</i>		
PD630	Parental strain	DSM 44193
PD630 pJAM2	PD630 derivative carrying pJAM2 plasmid, used as control strain; Km <sup>R</sup>	[11]
PD630 pJAM2/RO00075	PD630 derivative carrying pJAM2/ <i>ro00075</i> ; Km <sup>R</sup>	[12]
PD630 pTip-QC2	PD630 derivative carrying pTip-QC2 plasmid, used as control strain; Cm <sup>R</sup>	[12]
PD630 pTipQC2/RO00075	PD630 derivative carrying pTip-QC2 / <i>ro00075</i> ; Cm <sup>R</sup> , Thio <sup>R</sup>	[12]
PD630 pJAM2/ <i>atf1</i>	PD630 derivative carrying pJAM2/ <i>atf1</i> ; Km <sup>R</sup>	[11]
PD630 pPR27 <sub>acc</sub> / <i>atf2</i>	PD630 derivative carrying pPR27 <sub>acc</sub> / <i>atf2</i> ; Gm <sup>R</sup>	[11]
PD630 pMV <sub>acc</sub> / <i>atf2</i>	PD630 derivative carrying integrative plasmid pMV <sub>acc</sub> / <i>atf2</i> ; Km <sup>R</sup>	[11]
<b>Plasmids</b>		
pGEM-T-easy vector	Linear plasmid used for cloning PCR products; Ap <sup>R</sup>	Promega
pJAM2	Shuttle <i>E. coli</i> - <i>Mycobacterium</i> - <i>Rhodococcus</i> with <i>Pace</i> promoter; Km <sup>R</sup>	[32]
pJAM2/ <i>ro00075</i>	pJAM2 derivatives carrying <i>ro00075</i> gene under control of <i>Pace</i> ; Km <sup>R</sup>	[12]
pTip-QC2	Expression vector for <i>Rhodococcus</i> with <i>PtipA</i> promoter, <i>repAB</i> (pRE2895); Cm <sup>R</sup>	[36]

(continued)

**Table 4**  
**(continued)**

Strain or plasmid	Description	Source
pTip-QC2/ <i>ro00075</i>	pTip-QC2 carrying <i>ro0075</i> gene under control of <i>PtipA</i> ; Cm <sup>R</sup>	[12]
pJAM2/ <i>atf1</i>	pJAM2 derivatives carrying <i>atf1</i> gene under control of <i>Pace</i> ; Km <sup>R</sup>	[11]
pPR27	<i>E. coli</i> - <i>Mycobacterium</i> shuttle vector, oriM temps, sacB, XylE; Gm <sup>R</sup>	[39]
pPR27 <sub>acc</sub> / <i>atf2</i>	pPR27 derivatives carrying <i>atf2</i> gene under control of <i>Pace</i> ; Gm <sup>R</sup>	[11]
pTip-QC2/ <i>atf2</i>	pTip-QC2 carrying <i>atf2</i> gene under control of <i>PtipA</i> ; Cm <sup>R</sup>	[11]
pMV <sub>acc</sub> (pMR22)	Integrative plasmid derived from pMV306 and containing a <i>Pace</i> promoter; Km <sup>R</sup>	[45], this chapter
pMV <sub>acc</sub> / <i>atf2</i>	pMV <sub>acc</sub> carrying <i>atf2</i> gene under control of <i>Pace</i> ; Km <sup>R</sup>	[11]

of DNA are prepared by a commercial mini-prep extraction and stored at  $-20^{\circ}\text{C}$ .

2. Restriction endonucleases and other enzymes: *Bam*HI, *Xba*I, *Hind*III, *Nde*I, *Not*I, T4 DNA ligase, and its buffers. All enzymes may be purchased from any supplier.
3. Other reagents: Agarose molecular grade and DNA purification kit (from enzymatic reactions and agarose gels).

### 2.3 Electroporation of *Rhodococcus* Cells

1. Electroporator: Electroporation of *Rhodococcus* cells requires a high-voltage electroporator. Good efficiencies have been obtained with the model 2510 electroporator (Eppendorf-Netheler-Hinz, Hamburg, Germany).
2. Cuvettes of 400  $\mu\text{L}$  with electrode gaps of 2 mm.
3. Cold bidistilled water and ice containers.
4. LB media and LB media supplemented with glycine (0.85% w/v) and sucrose (1% w/v).

### 2.4 Bacterial Cultures

1. For routine growth of *E. coli* and *Rhodococcus* strains, use solid or liquid Luria-Broth (LB) media and incubate them at  $37^{\circ}\text{C}$  and  $28^{\circ}\text{C}$ , respectively. LB medium may be purchased for any supplier or prepared from individual components as:
  - (a) 10 g/L peptone, 5 g/L yeast extract, and 5 g/L NaCl in distilled water

2. To allow TAG accumulation, use a minimal salt medium (MSM) prepared from individual components as:
  - (a) 9 g/L Na<sub>2</sub>HPO<sub>4</sub>· 12 H<sub>2</sub>O, 1.5 g/L KH<sub>2</sub>PO<sub>4</sub>, 0.1 g/L NH<sub>4</sub>Cl, 0.2 g/L MgSO<sub>4</sub>· 7 H<sub>2</sub>O, 20 mg/L CaCl<sub>2</sub>· 2 H<sub>2</sub>O, 1.2 mg/L Fe(III)NH<sub>4</sub>-citrate, and 0.1 mL/L of trace element solution SL6 (10 mg/L ZnSO<sub>4</sub>· 7 H<sub>2</sub>O, 3 mg/L MnCl<sub>2</sub>· 4 H<sub>2</sub>O, 30 mg/L H<sub>3</sub>BO<sub>3</sub>, 20 mg/L CoCl<sub>2</sub>· 6 H<sub>2</sub>O, 1 mg/L CuCl<sub>2</sub>· 2 H<sub>2</sub>O, 2 mg/L NiCl<sub>2</sub>· 6 H<sub>2</sub>O, 3 mg/L Na<sub>2</sub>MoO<sub>4</sub>· 2 H<sub>2</sub>O) in distilled water. Use glucose as sole carbon source at a final concentration of 1% (w/v) in MSM media (*see Note 2*). Use 0.1 g/L of ammonium chloride in MSM0.1 culture media. Do not add ammonium chloride for preparing MSM0 culture media (*see Note 3*).
3. Use agar-agar for solid media at a final concentration of 1.4% (w/v). Autoclave under standard condition and adjust the pH to 7. If necessary, add antibiotics after autoclaving at different final concentrations as follows: 100 µg/mL ampicillin (Ap), 50 µg/mL kanamycin (Km), 5 µg/mL gentamicin (Gm), and 34 µg/mL chloramphenicol (Cm) for both *E. coli* and *Rhodococcus* cell cultures.
4. For overexpression analysis of genes under the acetamidase promoter P<sub>acc</sub> of pJAM2/pPR27<sub>acc</sub>/pMV<sub>acc</sub> vectors, add 0.5% (w/v) of acetamide to cell cultures at time zero. For overexpression analysis of genes under the thioestrepton promoter P<sub>TipA</sub> of pTip-QC2 vector, add 1 µg/mL of thioestrepton to cell cultures at time zero (*see Note 4*).

## 2.5 Lipid Analysis

1. Solvents for lipid extraction: Chloroform and methanol. HPLC grade.
2. Solvents for TLC development: Hexane, diethyl ether, and acetic acid. HPLC grade.
3. TLC plates: Silica gel 60 F254 plates (Merck). Activate at 65°C before use for 30 min.
4. Pure iodine crystals (*see Note 5*).
5. Reference lipids: Use tripalmitin dissolved in chloroform as TAG standard at a final concentration of 1 mg/mL.

---

## 3 Methods

This section describes a protocol for TAG overproduction in oleaginous *Rhodococcus* strains by overexpression of three genes: *ro00075*, *atf1*, and *atf2*. For this, construction of several recombinant molecules using the vectors pJAM2, pTip-QC2, pPR27<sub>acc</sub>, and pMV<sub>acc</sub> is described. Some of these constructions contain a

C-terminal or N-terminal 6×His-tag fusion, and gene products can be detected by Western blotting. The resulted recombinant strains are then subjected to semiquantitative TLC analysis of TAG content.

### 3.1 DNA Amplification, Cloning, and Sequencing

The first step for construction of recombinant molecules is the correct amplification of complete coding sequence of interest. For specific DNA amplification of *ro00075*, *atf1*, and *atf2* genes described in this chapter, perform PCR assays with specific primers listed in Table 4. Use total DNA of *R. jostii* RHA1 and *R. opacus* PD630 as template for amplification of *ro00075* and the two *atf* genes, respectively. In all cases, use the following thermocycler parameters: 5 min at 94°C, 30 cycles of 1 min at 94°C, 30 s at 60°C, 1 min at 72°C, and finally 5 min at 72°C. After checking on 1% agarose gel, clone the PCR products into any TA cloning vector, transform in *E. coli*, and perform screening of colonies by the blue/white color selection and then by colony PCR. Select positive clones and verify the correct amplification by DNA sequencing of purified plasmid.

### 3.2 Subcloning Strategies

#### 3.2.1 Subcloning of *ro00075* Gene in pJAM2 Vector (see Fig. 2)

To achieve overexpression of *ro00075* in *R. jostii* RHA1 and *R. opacus* PD630 strains under an inducible acetamide promoter  $P_{ace}$  (also called  $P_{ami}$ ), proceed as follows:

1. Cut both purified plasmids pJAM2 and pGEM-T-easy/*ro00075* with the enzymes *Bam*HI and *Xba*I. Purify the linearized pJAM2 vector directly from the enzymatic reaction. After running the cut pGEM-T-easy/*ro00075* on a 1% agarose gel, purify the *ro00075* gene of ~700 bp from TBE agarose gel using a DNA purification kit.
2. To a 0.5-mL tube, add the cut pJAM2 vector and the *ro00075* insert at molar ratios ranging from 1:1 to 1:2, 10× ligation buffer, and dH<sub>2</sub>O to 10 μL. Add T4 DNA ligase, mix, and incubate overnight at 8°C.
3. Transform in *E. coli* DH5α and check kanamycin-resistant colonies by colony PCR using the primers aceF/RO00075R (Table 4).

#### 3.2.2 Subcloning of *ro00075* Gene in pTip-QC2 Vector (see Fig. 2)

To achieve overexpression of *ro00075* in *R. jostii* RHA1 and *R. opacus* PD630 strains under an inducible thioestrepton promoter ( $P_{TipA}$ ), proceed as follows:

1. Cut both plasmids pTip-QC2 vector and pJAM2/*ro00075* obtained above with the enzymes *Bam*HI and *Hind*III (see Note 6). Purify the linearized pTip-QC2 vector directly from the enzymatic reaction using a DNA purification kit. After running the cut pJAM2/*ro00075* on a 0.8% agarose gel, purify the fragment of ~2.27 kb carrying the *ro00075* gene from the gel using a DNA purification kit.

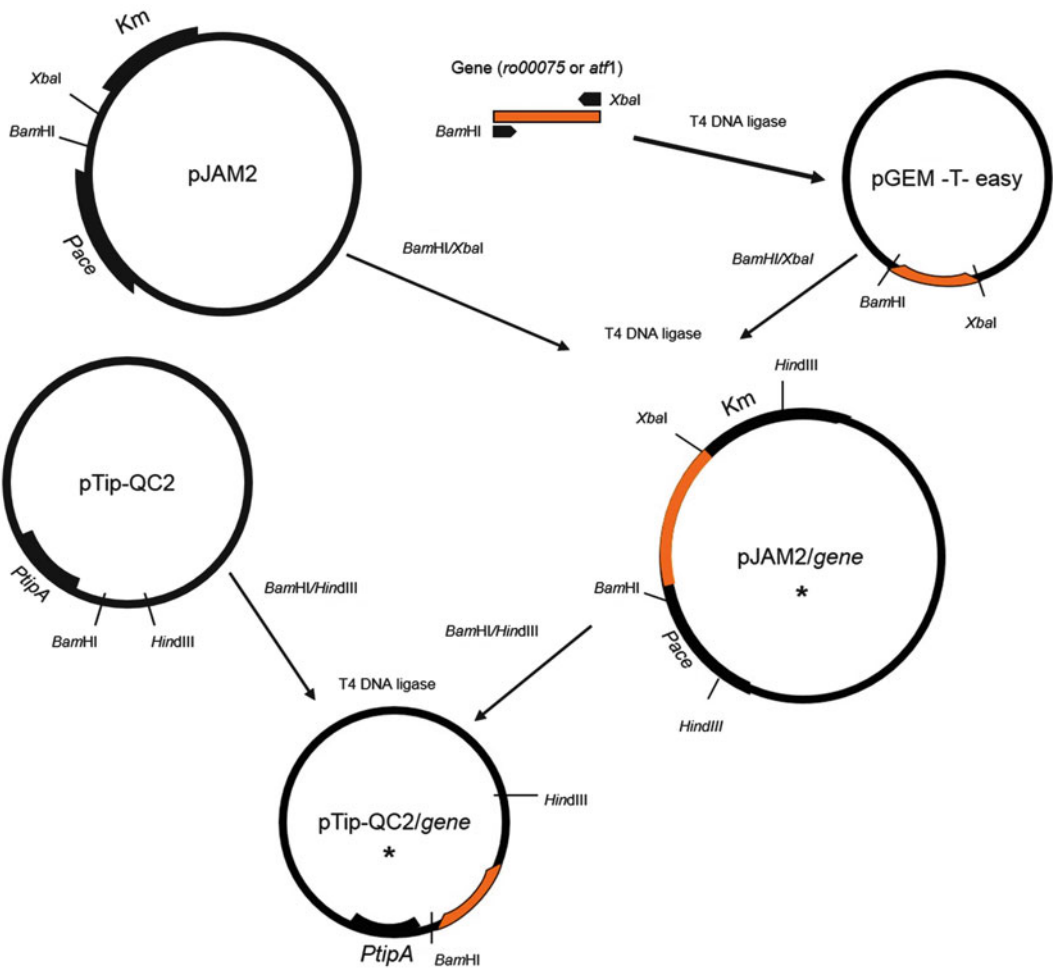


**Fig. 2** Overview of molecular strategies described in this chapter for *ro00075* and *atf1* overexpression in pJAM2 and pTip-QC2 vectors. The transferred molecules to *Rhodococcus* cells are marked with an asterisk. The size of plasmids is not to scale

2. To a 0.5-mL tube, add the cut pTip-QC2 vector and the *ro00075*-carrying fragment at molar ratios ranging from 1:1 to 1:2, 10× ligation buffer, and dH<sub>2</sub>O to 10 μL. Add T4 DNA ligase, mix, and incubate overnight at 8°C.
3. Transform in *E. coli* DH5α and check ampicillin-resistant colonies by colony PCR using the primers thioF/RO00075R (Table 4).

### 3.2.3 Subcloning of *atf1* Gene in pJAM2 Vector (see Fig. 2)

To achieve overexpression of *atf1* in *Rhodococcus opacus* PD630 strain under an inducible acetamide promoter P<sub>acc</sub>, proceed as follows:

1. Cut both purified plasmids pJAM2 and pGEM-T-easy/*atf1* with the enzymes *Bam*HI and *Xba*I. Purify the linearized

pJAM2 vector directly from the enzymatic reaction. After running the cut pGEM-T-easy/*atf1* on a 1% agarose gel, purify the *atf1* gene of ~1,460 bp from TBE agarose gel using a DNA purification kit.

2. To a 0.5-mL tube, add the cut pJAM2 vector and the *atf1* insert at molar ratios ranging from 1:1 to 1:2, 10× ligation buffer, and dH<sub>2</sub>O to 10 μL. Add T4 DNA ligase, mix, and incubate overnight at 8°C.
3. Transform in *E. coli* DH5α and check kanamycin-resistant colonies by colony PCR using the primers aceF/*atf1*MHR (Table 4).

### 3.2.4 Subcloning of *atf2* Gene in the Integrative Plasmid pMV<sub>ace</sub> Vector (see Fig. 3)

To achieve overexpression of *atf2* under an inducible acetamide promoter P<sub>ace</sub> as a single extra copy in *Rhodococcus opacus* PD630 strain by using an integrative plasmid, proceed as follows:

1. Cut both purified plasmids pMV<sub>ace</sub> and pGEM-T-easy/*atf2* with the enzymes *Nde*I and *Hind*III. Purify the linearized pMV<sub>ace</sub> vector directly from the enzymatic reaction. After running the cut pGEM-T-easy/*atf2* on a 1% agarose gel, purify the *atf2* gene of ~1,380 bp from TBE agarose gel using a DNA purification kit.
2. To a 0.5-mL tube, add the cut pMV<sub>ace</sub> vector and the *atf2* insert at molar ratios ranging from 1:1 to 1:2, 10× ligation buffer, and dH<sub>2</sub>O to 10 μL. Add T4 DNA ligase, mix, and incubate overnight at 8°C.
3. Transform in *E. coli* DH5α and check kanamycin-resistant colonies by colony PCR using the primers aceF/*atf2*MHR (Table 4).

### 3.2.5 Subcloning of *atf2* Gene in pPR27<sub>ace</sub> Vector (see Fig. 3)

To achieve overexpression of *atf2* in *Rhodococcus opacus* PD630 strain under an inducible acetamide promoter P<sub>ace</sub> in a replicative plasmid version with a gentamicin resistance (see Note 7), proceed as follows:

1. Cut both purified plasmids pPR27 and pMV<sub>ace</sub>/*atf2* obtained above with the enzymes *Bam*HI and *Not*I. Purify the linearized pPR27 vector directly from the enzymatic reaction using a DNA purification kit. After running the cut pMV<sub>ace</sub>/*atf2* in a 0.8% agarose gel, purify the fragment of ~3.6 kb carrying the *atf2* gene under P<sub>ace</sub> promoter from the agarose gel using a DNA purification kit (see Note 8).
2. To a 0.5-mL tube, add the cut pPR27 vector and the *atf2*-carrying fragment at molar ratios ranging from 1:1 to 1:2, 10× ligation buffer, and dH<sub>2</sub>O to 10 μL. Add T4 DNA ligase, mix, and incubate overnight at 8°C.

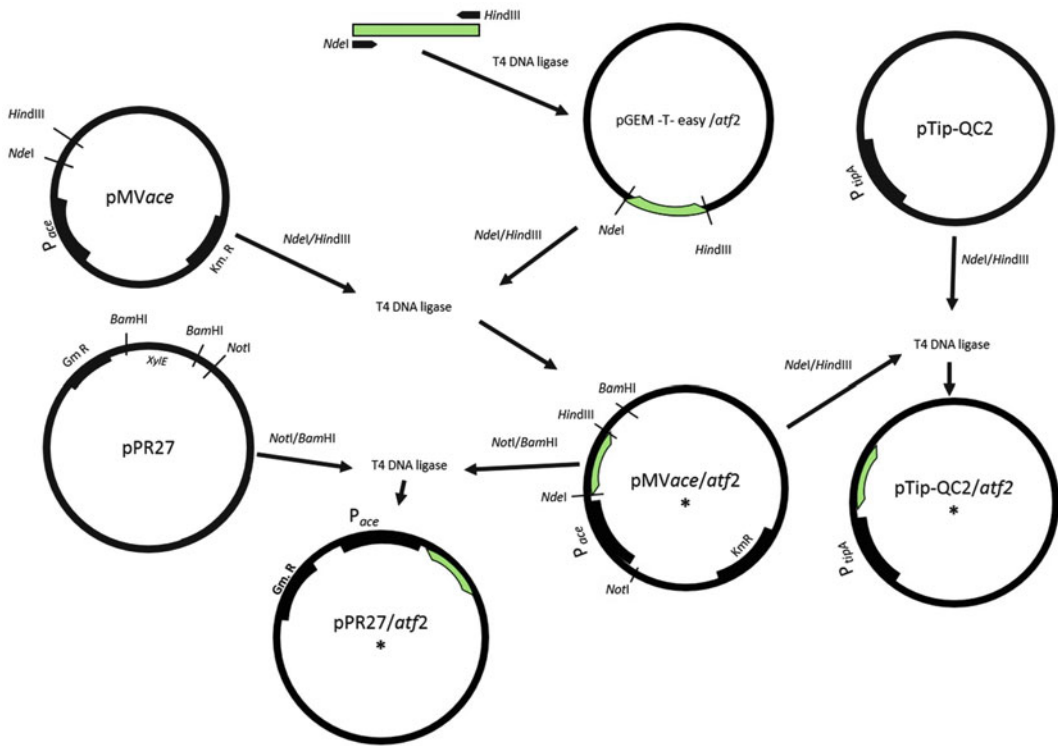


**Fig. 3** Overview of molecular strategies described in this chapter for *attf2* overexpression in pMV<sub>ace</sub>, pPR27<sub>ace</sub>, and pTip-QC2 vectors. The transferred molecules to *Rhodococcus* cells are marked with an asterisk. The size of plasmids is not to scale

3. Transform in *E. coli* DH5 $\alpha$  and check gentamicin-resistant colonies by colony PCR using the primers aceF/attf2MHR (Table 4).

### 3.2.6 Subcloning of *attf2* Gene in pTip-QC2 Vector (See Fig. 3)

To achieve overexpression of *attf2* in *Rhodococcus opacus* PD630 strains under an inducible thioStrepton promoter ( $P_{TiPA}$ ), proceed as follows:

1. Cut both purified plasmids pTip-QC2 and pMV<sub>ace</sub>/attf2 obtained above with the enzymes *NdeI* and *HindIII* (see Note 9). Purify the linearized pTip-QC2 vector directly from the enzymatic reaction using a DNA purification kit. After running the cut pMV<sub>ace</sub>/attf2 in a 0.8% agarose gel, purify the *attf2* fragment of ~1,364 bp from the agarose gel using a DNA purification kit.
2. To a 0.5-mL tube, add the cut pTip-QC2 vector and the *attf2* insert at molar ratios ranging from 1:1 to 1:2, 10 $\times$  ligation buffer, and dH<sub>2</sub>O to 10  $\mu$ L. Add T4 DNA ligase, mix, and incubate overnight at 8 $^{\circ}$ C.
3. Transform in *E. coli* DH5 $\alpha$  and check ampicillin-resistant colonies by colony PCR using the primers thioF/attf2MHR (Table 4).

### 3.3 Electroporation of *Rhodococcus* Cells

Transfer all recombinant plasmids to *R. jostii* RHA1 and *R. opacus* PD630 by electroporation based on the method described by Kalscheuer et al. (1999) [17]:

1. To obtain electrocompetent *Rhodococcus* cells, inoculate 25 mL of LB medium in a 100 mL Erlenmeyer flask supplemented with 0.85% (w/v) glycine and 1% (w/v) sucrose with 1 mL of an overnight LB preculture and grown at 28°C to an optical density of 0.5 at 600 nm.
2. Harvest cells, wash twice with ice-cold bidistilled H<sub>2</sub>O, and concentrate 20-fold in ice-cold bidistilled H<sub>2</sub>O.
3. Immediately before the electroporation, mix 400 µL of competent cells with DNA (0.1–1 µg/mL) and preincubate at 40°C for 5 min. Perform electroporation in cuvettes with gaps of 2 mm and the following settings: 10 kV/cm, 600 Ω, and 25 µF. Accept time constants of 3–5 ms only. Dilute immediately pulsed cells with 600 mL of LB and incubate at 28°C for 4 h (see Note 10) before plating on appropriate selective media. Check plates after 3–4 days.

Additionally, transfer to *R. jostii* RHA1 and *R. opacus* PD630 the correspondent empty plasmids to obtain control cells. Perform colony PCR of at least five individual clones to check the presence of each gene in the recombinant plasmids. For this, use the set primers aceF/RO00075R, aceF/atf1MHR, and aceF/atf1MHR to check *ro00075*, *atf1*, and *atf2* genes under P<sub>ace</sub> and thioF/RO00075R, thioF/atf1MHR, and thioF/atf2MHR to check *ro00075*, *atf1*, and *atf2* genes under P<sub>TipA</sub> promoters, respectively (see Table 4). Select one positive clone of each recombinant strain for further analysis.

### 3.4 Bacterial Cultures

After obtaining recombinant strains, the next step is to analyze the phenotype. The next protocol is focused particularly in the cellular conditions for TAG accumulation. For this, proceed as follows:

1. Pick isolated colonies of both recombinant *Rhodococcus* strains and its respective controls (cells containing the empty vector) from fresh plates and transfer into 20 mL liquid Luria-Broth (LB) medium and cultivate cells aerobically at 28°C and 200 rpm overnight. Use the appropriate antibiotic (see Sect. 2).
2. Inoculate fresh LB media with 2 mL of the overnight precultures and incubate again at 28°C and 200 rpm for 24 h. Harvest cells and wash twice with sterile physiological solution (NaCl 0.85% w/v).
3. Inoculate 1 mL of resuspended cells (DO<sub>600</sub> 4) into 20 mL of MSM0.1 media or resuspend all harvest cells in 25 mL MSM0. Use glucose as sole carbon source at a final concentration of 1% (w/v).

4. Add the appropriate antibiotic and inducers as described in Materials section.
5. Incubate cell cultures at 28°C and 200 rpm for 48 h. Harvest cells and lyophilize or dry to constant weight at 37°C (*see* **Note 11**).

### 3.5 TLC Lipid Analysis

To semiquantitatively analyze the total intracellular lipids in *Rhodococcus* cells, perform the next steps as:

1. Weigh 5 mg of dried cells (*see* **Note 12**) in 1.5 mL tubes and extract lipids with 300  $\mu$ L of mix chloroform/methanol (2:1, v/v) for 90–120 min. Vortex vigorously each for 30 min.
2. Centrifuge the extracts at 13,000 rpm for 5 min. Remove 100  $\mu$ L of chloroformic phase to fresh tubes. Perform TLC analysis by loading 20  $\mu$ L of chloroformic phase on silica gel 60 F254 plates (Merck).
3. Run TLC with hexane/diethyl ether/acetic acid (80:20:1, v/v/v) as mobile phase. Compare spots with a reference substance of TAG (*see* Sect. 2).
4. Visualize different lipid fractions using iodine vapor (*see* an example in Fig. 4).

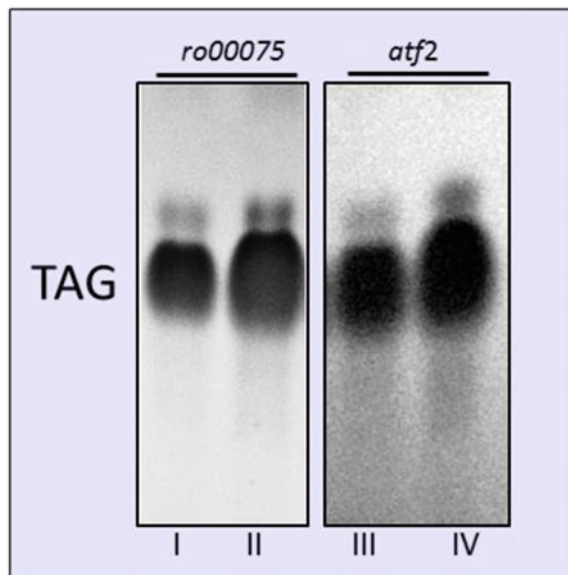


**Fig. 4** Example of a TLC analysis of TAG from whole-cell extracts overexpressing *ro00075* and *atf2* in pTip-QC2 vector. (I and III) PD630 cells with empty pTip-QC2, (II) PD630 cells carrying pTip-QC2/*ro00075*, and (IV) PD630 cells carrying pTip-QC2/*atf2*

Additionally, TAG content can be quantified as total fatty acids from dried *Rhodococcus* cells by GC analysis or a colorimetric method as described in previous works [58, 59].

---

## 4 Notes

1. Alternative restriction sites can be used in primers for subcloning purposes according to the cloning sites in vector systems described in this chapter [32, 36, 39].
2. In this chapter, glucose is proposed as carbon source; however, another carbon source can be used at appropriate final concentration [2, 3].
3. MSM0 medium is used to analyze more accurately TAG biosynthesis, independently of the cellular growth. Under these conditions, cell growth is impaired because the nitrogen source is lacking in the medium; thus, cells utilize the available carbon source principally for TAG biosynthesis and accumulation. We observed that the use of MSM0 medium containing an excess of a carbon source promotes more pronounced differences in TAG concentrations between control and recombinant cells.
4. To our experience, we observed a better recombinant protein production when the inducer is added at the beginning of the cell cultivation without a loss of cellular viability; however, variations in the addition times and final concentrations of inducers can be applied for different genes in the same expression vectors.
5. Because oleaginous *Rhodococcus* cells are able to accumulate large amounts of neutral lipids (mainly TAG and minor amounts of free fatty acids, DAG and MAG), iodine vapors are sufficient for a rapid and sensitive visualization of them. In addition, the sensibility can be increased putting periodine-stained plates under UV light of a transilluminator. Other techniques can be used to visualize lipids on TLC plates as the cupric-phosphoric staining.
6. Please note that *ro00075* gene (~700 bp) can be also directly amplified and subcloned into pTip-QC2 vector using the appropriate restriction enzymes such as *NdeI/HindIII* and *BamHI/HindIII*, among others.
7. Please note that *atf2* gene (~1,380 bp) can be directly amplified and subcloned into pJAM2 vector (which is also a replicative plasmid containing the  $P_{ace}$  promoter, but with a kanamycin resistance) using the restriction enzymes *BamHI/XbaI*.
8. At this point, two fragments are visualized in agarose gel: a 3.2 kb and a 3.6 kb fragment. Because of the similar size of both fragments, we recommend using a low-concentration agarose gel to separate them. Purify only the 3.6 kb fragment.

9. Please note that *atf2* gene (~1,380 bp) can be also subcloned into pTip-QC2 vector with *NdeI*/*HindIII* from pGEM-T-easy/*atf2* directly. Alternatively, other restriction enzymes can be used.
10. Overnight incubation can also be performed with good results.
11. Wet biomass can be also used for a rapid analysis of neutral lipids. For this, normalize cell pellets by OD<sub>600</sub> measurements of cellular cultures by triplicate.
12. The chosen amount of dry biomass depends on the expected levels of TAG. For oleaginous strains, 5 mg is sufficient for TLC assays as well as the quantitative analyses. For non-oleaginous strains or assays under non-accumulation conditions, at least 10 mg of dry biomass is required.

## References

1. Alvarez HM, Steinbüchel A (2002) Triacylglycerols in prokaryotic microorganisms. *Appl Microbiol Biotechnol* 60:367–376
2. Alvarez HM, Mayer F, Fabritius D, Steinbüchel A (1996) Formation of intracytoplasmic lipid inclusion by *Rhodococcus opacus* PD630. *Arch Microbiol* 165:377–386
3. Alvarez HM, Kalscheuer R, Steinbüchel A (1997) Accumulation of storage lipids in species of *Rhodococcus* and *Nocardia* and effect of inhibitors and polyethylene glycol. *Fett-Lipid* 99:239–246
4. Barksdale L, Kim KS (1977) *Mycobacterium*. *Bacteriol Rev* 41:217–372
5. Daniel J, Deb C, Dubey VS, Sirakova TD, Abomoelak B, Morbidoni HR, Kolattukudy PE (2004) Induction of a novel class of diacylglycerol acyltransferases and triacylglycerol accumulation in *Mycobacterium tuberculosis* as it goes into a dormancy-like state in culture. *J Bacteriol* 186:5017–5030
6. Olukoshi ER, Packter NM (1994) Importance of stored triacylglycerols in *Streptomyces*: possible carbon source for antibiotics. *Microbiology* 140:931–943
7. Hernández MA, Mohn WW, Martínez E, Rost E, Alvarez AF, Alvarez HM (2008) Biosynthesis of storage compounds by *Rhodococcus jostii* RHA1 and global identification of genes involved in their metabolism. *BMC Genomics* 12:600
8. Alvarez HM (2010) Biotechnological production and significance of triacylglycerols and wax esters. In: Kenneth NT (ed) *Microbiology of hydrocarbons, oils, lipids, and derived compounds*. Springer, Heidelberg, pp 2995–3002
9. Holder JW, Ulrich JC, DeBono AC, Godfrey PA, Desjardins CA, Zucker J, Zeng Q, Leach ALB, Ghiviriga I, Dancel C, Abeel T, Gevers D, Kodira CD, Desany B, Affourtit JP, Birren BW, Sinskey AJ (2011) Comparative and functional genomics of *Rhodococcus opacus* PD630 for biofuels development. *PLoS Genet* 7(9), e1002219. doi:10.1371/journal.pgen.1002219
10. Alvarez AF, Alvarez HM, Kalscheuer R, Wältermann M, Steinbüchel A (2008) Cloning and characterization of a gene involved in triacylglycerol biosynthesis and identification of additional homologous genes in the oleaginous bacterium *Rhodococcus opacus* PD630. *Microbiology* 154:2327–2335
11. Hernández MA, Arabolaza A, Rodríguez E, Gramajo H, Alvarez HM (2013) The *atf2* gene is involved in triacylglycerol biosynthesis and accumulation in the oleaginous *Rhodococcus opacus* PD630. *Appl Microbiol Biotechnol* 97:2119–2130
12. Hernández MA, Comba S, Arabolaza A, Gramajo H, Alvarez HM (2014) Overexpression of a phosphatidic acid phosphatase type 2 leads to an increase in triacylglycerol production in oleaginous *Rhodococcus* strains. *Appl Microbiol Biotechnol*. doi:10.1007/s00253-014-6002-2
13. Villalba MS, Alvarez HM (2014) Identification of a novel ATP-binding cassette transporter involved in long-chain fatty acid import and its role in triacylglycerol accumulation in *Rhodococcus jostii* RHA1. *Microbiology* 160:1523–1532
14. MacEachran DP, Prophete ME, Sinskey AJ (2010) The *Rhodococcus opacus* PD630 heparin-binding hemagglutinin homolog TadA mediates lipid body formation. *Appl Environ Microbiol* 76(21):7217–7225

15. Ding Y, Yang L, Zhang S, Wang Y, Du Y, Pu J, Peng G, Chen Y, Zhang H, Yu J, Hang H, Wu P, Yang F, Yang H, Steinbüchel A, Liu P (2012) Identification of the major functional proteins of prokaryotic lipid droplets. *J Lipid Res* 53(3):399–411
16. MacEachran DP, Sinskey AJ (2013) The *Rhodococcus opacus* TadD protein mediates triacylglycerol metabolism by regulating intracellular NAD(P)H pools. *Microb Cell Fact* 12:104
17. Kalscheuer R, Arenskötter M, Steinbüchel A (1999) Establishment of a gene transfer system for *Rhodococcus opacus* PD630 based on electroporation and its application for recombinant biosynthesis of poly(3-hydroxyalkanoic acids). *Appl Microbiol Biotechnol* 52:508–515
18. Arenskoetter M, Baumeister D, Kalscheuer R, Steinbuechel A (2003) Identification and application of plasmids suitable for transfer of foreign DNA to members of the genus *Gordonia*. *Appl Environ Microbiol* 69:4971–4974
19. Matsui T, Saeki H, Shinzato N, Matsuda H (2006) Characterization of *Rhodococcus-E. coli* shuttle vector pNC9501 constructed from the cryptic plasmid of a propene-degrading bacterium. *Curr microbiol* 52:445–448
20. Kostichka K, Tao L, Bramucci M, Tomb JF, Nagarajan V, Cheng Q (2003) A small cryptic plasmid from *Rhodococcus erythropolis*: characterization and utility for gene expression. *Appl Microbiol Biotechnol* 62(1):61–68
21. De Mot R, Nagy I, De Schrijver A, Pattanapitpaisal P, Schoofs G, Vanderleyden J (1997) Structural analysis of the 6 kb cryptic plasmid pFAJ2600 from *Rhodococcus erythropolis* NI86/21 and construction of *Escherichia coli*-*Rhodococcus* shuttle vectors. *Microbiology* 143:3137–3147
22. Singer ME, Finnerty WR (1988) Construction of an *Escherichia coli*-*Rhodococcus* shuttle vector and plasmid transformation in *Rhodococcus* spp. *J Bacteriol* 170:638–645
23. Shao Z, Dick WA, Behki RM (1995) An improved *Escherichia coli*-*Rhodococcus* shuttle vector and plasmid transformation in *Rhodococcus* spp. using electroporation. *Lett Appl Microbiol* 21:261–266
24. Dabbs ER, Gowan B, Anderson SJ (1990) Nocardioform arsenic resistance plasmid and construction of *Rhodococcus* cloning vectors. *Plasmid* 23:242–247
25. Dabbs ER (1998) Cloning of genes that have environmental and clinical importance from rhodococci and related bacteria. *Antonie van Leeuwenhoek* 74:155–168
26. Zheng H, Tkachuk-Saad O, Prescott JF (1997) Development of a *Rhodococcus equi*-*Escherichia coli* plasmid shuttle vector. *Plasmid* 38(3):180–187
27. Lessard PA, O'Brien XM, Currie DH, Sinskey AJ (2004) pB264, a small, mobilizable, temperature sensitive plasmid from *Rhodococcus*. *BMC Microbiol* 4:15
28. Veselý M, Pátek M, Nesvera J, Cejková A, Masák J, Jirků V (2003) Host-vector system for phenol-degrading *Rhodococcus erythropolis* based on *Corynebacterium* plasmids. *Appl Microbiol Biotechnol* 61:523–527
29. Rhee J, Cho J, Lee S, Park O (2006) *Rhodococcus-E. coli* vector. PCT WO2006/088307 A1 August 2006
30. Desomer J, Dhaese P, Montagu MV (1990) Transformation of *Rhodococcus fascians* by high-voltage electroporation and development of *R. fascians* cloning vectors. *Appl Environ Microbiol* 56(9):2818–2825
31. Masai E, Yamada A, Healy JM, Hatta T, Kimbara K, Fukuda M, Yano K (1995) Characterization of biphenyl catabolic genes of gram-positive polychlorinated biphenyl degrader *Rhodococcus* sp. strain RHA1. *Appl Environ Microbiol* 61:2079–2085
32. Van der Geize R, Hessels GI, Van Gerwen R, Van der Meijden P, Dijkhuizen L (2002) Molecular and functional characterization of kshA and kshB, encoding two components of 3-ketosteroid 9  $\alpha$ -hydroxylase, a class IA monooxygenase, in *Rhodococcus erythropolis* strain SQ1. *Mol Microbiol* 45:1007–1018
33. Yang JC, Lessard PA, Sinskey AJ (2007) Characterization of the mobilization determinants of pAN12, a small replicon from *Rhodococcus erythropolis* AN12. *Plasmid* 57:71–81
34. Kurosawa K, Wewetzer SJ, Sinskey AJ (2013) Engineering xylose metabolism in triacylglycerol producing *Rhodococcus opacus* for lignocellulosic fuel production. *Biotechnol Biofuels* 6:134
35. Triccas JA, Parish T, Britton WJ, Giquel B (1998) An inducible expression system permitting the efficient purification of a recombinant antigen from *Mycobacterium smegmatis*. *FEMS Microbiol Lett* 167:151–156
36. Hänisch J, Wältermann M, Robenek H, Steinbüchel A (2006) The *Ralstonia eutropha* H16 phasin PhaP1 is targeted to intracellular triacylglycerol inclusions in *Rhodococcus opacus* PD630 and *Mycobacterium smegmatis* mc2155, and provides an anchor to target other proteins. *Microbiology* 152:3271–3280

37. Jackson M, Brigitte G (2003) Method of screening anti-mycobacterial molecules. US Patent 6,573,064 B1 Jun 2003
38. Nakashima N, Tamura T (2004) A novel system for expressing recombinant proteins over a wide temperature range from 4 to 35°C. *Bio-technol Bioeng* 86:136–148
39. Nakashima N, Tamura T (2004) Isolation and characterization of a rolling-circle-type plasmid from *Rhodococcus erythropolis* and application of the plasmid to multiple-recombinant-protein expression. *Appl Environ Microbiol* 70:5557–5568
40. Mitani Y, Nakashima N, Sallam KI, Toriyabe T, Kondo K, Tamura T (2006) Advances in the development of genetic tools for the genus *Rhodococcus*. *Actinomycetologica* 20:55–61
41. Pelicic V, Jackson M, Reyrat JM, Jacobs WR Jr, Gicquel B, Guilhot C (1997) Efficient allelic exchange and transposon mutagenesis in *Mycobacterium tuberculosis*. *Proc Natl Acad Sci USA* 94:10955–10960
42. Margarit R (2001) Means and methods for the expression of homologous proteins in strains of *Rhodococcus*. European patent application EP1 127943 A2
43. Stover CK, De la Cruz VF, Fuerst TR, Burlein JE, Benson LA, Bennett LT, Bansal GP, Young JF, Lee MH, Hatfull GF, Snapper SB, Barletta RG, Jacobs WR Jr, Bloom BR (1991) New use of BCG for recombinant vaccines. *Nature* 351:456–460
44. Kong D, Kunimoto D (1995) Secretion of Human Interleukin 2 by Recombinant *Mycobacterium bovis* BCG. *Infect Immun* 63 (3):799–803
45. Salzman V, Mondino S, Sala C, Cole ST, Gago G, Gramajo H (2010) Transcriptional regulation of lipid homeostasis in mycobacteria. *Mol Microbiol* 78(1):64–77
46. Hong Y, Hondalus MK (2008) Site-specific integration of *Streptomyces*ΦC31 integrase-based vectors in the chromosome of *Rhodococcus equi*. *FEMS Microbiol Lett* 287:63–68
47. Dotson EM, Plikaytis B, Shinnick TM, Durvasula RV, Beard CB (2003) Transformation of *Rhodococcus rhodnii*, a symbiont of the Chagas disease vector *Rhodnius prolixus*, with integrative elements of the L1 mycobacteriophage. *Infect Genet Evol* 3(2):103–109
48. Voeykova T, Emelyanova L, Tabakov V, Mkrumyan N (1998) Transfer of plasmid pTO1 from *Escherichia coli* to various representatives of the order Actinomycetales by intergeneric conjugation. *FEMS Microbiol Lett* 162:47–52
49. Voeykova T, Tabakov V, Ryabchenko L, Mkrumyan N, Yanenko A (1994) Conjugative transfer of plasmid pTO1 from *Escherichia coli* to *Rhodococcus* spp. *FEMS Microbiol Lett* 16:555–560
50. Sallam KI, Tamura N, Tamura T (2007) A multipurpose transposon-based vector system mediates protein expression in *Rhodococcus erythropolis*. *Gene* 386:173–182
51. Sallam KI, Tamura N, Imoto N, Tamura T (2010) New vector system for random, single-step integration of multiple copies of DNA into the *Rhodococcus* genome. *Appl Environ Microbiol* 2531–2539
52. Zhang YM, Rock CO (2008) Membrane lipid homeostasis in bacteria. *Nat Rev Microbiol* 6:222–233
53. Parsons JB, Rock CO (2013) Bacterial lipids: metabolism and membrane homeostasis. *Prog Lipid Res* 52(3):249–276
54. Comba S, Menendez-Bravo S, Arabolaza A, Gramajo H (2013) Identification and physiological characterization of phosphatidic acid phosphatase enzymes involved in triacylglycerol biosynthesis in *Streptomyces coelicolor*. *Microb Cell Fact* 12:9
55. Arabolaza A, Rodriguez E, Altabe S, Alvarez H, Gramajo H (2008) Multiple pathways for triacylglycerol biosynthesis in *Streptomyces coelicolor*. *Appl Environ Microbiol* 74:2573–2582
56. Hanahan D (1983) Studies on transformation of *Escherichia coli* with plasmids. *J Mol Biol* 166:557–580
57. Seto M, Kimbara K, Shimura M, Hatta T, Fukuda M, Yano K (1995) A novel transformation of polychlorinated biphenyls by *Rhodococcus* sp. strain RHA1. *Appl Environ Microbiol* 61(9):3353–3358
58. Duncombe WG (1963) The colorimetric micro-determination of long chain fatty acids. *Biochem J* 88(1):7–10
59. Wawrik B, Harriman BH (2010) Rapid colorimetric quantification of lipid from algal cultures. *J Microbiol Methods* 80(3): 262–266

# Production of Biofuel-Related Isoprenoids Derived from *Botryococcus braunii* Algae

William A. Muzika, Nymul E. Khan, Lauren M. Jackson,  
Nicholas Winograd, and Wayne R. Curtis

## Abstract

The colony algae *Botryococcus braunii* produces large amounts of C<sub>30+</sub> triterpene hydrocarbons. Recent discovery of the associated biosynthetic genes has facilitated the metabolic engineering of these triterpene hydrocarbons in alternative hosts – where squalene has served as an analytical standard and a closely associated model hydrocarbon biosynthetic pathway. An extraction and analysis method is provided for both the native and heterologous systems. In the case of the native algae, the hydrocarbons are tightly associated with a complex wall matrix. In addition to quantification of extracted triterpenes by GC-FID, secondary ion mass spectrometry (SIMS) has also provided an assessment from “in vivo” samples at room temperature. For heterologous expression of the triterpene pathway in alternative hosts, the hydrocarbons are found both intracellularly and extracellularly. The highly hydrophobic nature of these triterpenes provides for relatively straightforward recovery by extraction into an organic phase. The methylation of the *Botryococcus braunii* race B hydrocarbons (which enhances its fuel precursor value) is readily resolved by GC-FID methods for routine analysis.

**Keywords:** Botryococcene, Extraction, Heterologous expression, Hydrocarbon, Triterpene

---

## 1 Introduction

*Botryococcus* is a prehistoric alga that produces hydrocarbons which surround the colony as a dominant component of the extracellular matrix [1]. In contrast to lipids for biodiesel, which accumulate as an energy reserve, *B. braunii* hydrocarbons enable floatation of the algae to enhance light access. Therefore, the genes encoding for HC production are expressed to result in a level of 25% or more of the biomass weight that is independent of the algae rate of growth [2]. *Botryococcus* has been studied for decades because the hydrocarbon has been recognized as an ideal “drop-in” feedstock for catalytic cracking and reforming [3]. A particularly unique characteristic of the triterpene botryococcene and its methylated derivatives is that they are highly persistent in the aerobic extracellular

environment and are chemically identifiable as a component of oil shales [4].

Because the oil accumulates to be a significant fraction of the algae weight, there are frequent reports of hydrocarbon production based on gravimetric mass change upon organic extraction. Not surprisingly, other hydrophobic cellular components co-extract with the triterpene hydrocarbons. On the other hand, extensive sample preparation to remove contaminants before precise analytical measurements results in loss of triterpene material. These two approaches represent over- and under-estimations of biomass hydrocarbon content. We recently made an effort to distinguish these differences by clarifying units as mg oil-EG (extracted gravimetric oil) and mg oil-AH (analytically determined hydrocarbon) to provide less ambiguous comparisons [2].

A recent development which increases the breadth of application for analytics is the identification of the hydrocarbon biosynthetic enzymes. Most notably, the generation of a chimeric enzyme to catalyze the conversion of the common isoprene precursor farnesyl pyrophosphate (FPP) to botryococcene in a single step [5]. This provides a means to genetically engineer this pathway into alternative hosts with a subsequent need for analysis to evaluate productivity. C<sub>15</sub> and C<sub>30</sub> production has been reported in the heterologous systems of bacteria [6] and plants [7] with botryococcene being expressed in yeast [8] and *Rhodobacter* [9], and expression in *Ralstonia eutropha* is also noted in a recent thesis from our lab [10]. This focus on botryococcenes as a biofuel precursor will invariably result in much more research to achieve heterologous expression. As an example, we have recently demonstrated a consortium bioprocessing approach to ethanol production using a yeast in combination with a biomass degrading *Clostridium* [11], and our lab is currently implementing the oxygen-mediated symbiotic consortium process using yeast which is engineered for hydrocarbon production.

It is interesting to note that the productivity of the native algae is quite high by comparison to typical carbon fluxes in the terpenoid pathway [2] and is “on par,” or significantly greater than production achieved thus far for heterologous hosts – even those growing heterotrophically [12]. This illustrates that there is much to learn about how these high hydrocarbon metabolic fluxes are achieved.

---

## 2 Materials

### 2.1 Native Algae Botryococcus Hydrocarbons

Cultures of *Botryococcus* are available from nearly every algae culture collection, and we have tabulated references to more than 150 published strains ([www.botryococcus.org](http://www.botryococcus.org)).

### 2.1.1 *Botryococcus* Hydrocarbons

Confusion still exists in these collections as there are very different strains of *Botryococcus* with substantially different hydrocarbon profiles and even different metabolic pathways leading to the production of the hydrocarbons. *B. braunii* Race A produces C<sub>25</sub>–C<sub>31</sub> *n*-alkadienes. Race B (the focus of the majority of our work) produces C<sub>30</sub>–C<sub>34</sub>-methylated triterpenes, and minimally studied Race L produces a C<sub>40</sub> lycopadiene [13]. Hydrocarbon analysis has been suggested as a means of definition of speciation rather than 18S rRNA [14].

### 2.1.2 *Botryococcus* Growth Media

Chu-13 media [15], or minor modifications thereof [16], are commonly utilized for the growth of *Botryococcus*. We utilize a WFAM media designed for better pH control in the absence of CO<sub>2</sub> buffering; however, this introduces considerations for nitrogen feeding strategy [17]. These media are inorganic salt formulations and are therefore not prone to degradation; nonetheless, we prepare fresh liquid media for periods of 3–4 months. The handling of Ca<sup>2+</sup> and Mg<sup>2+</sup> in media can require special consideration as these promote precipitate formation which is particularly problematic if efforts include more concentrated media to achieve higher algae cell concentration growth (*see Note 1*).

## 2.2 *Metabolic* *Pathway Engineered* *Triterpenes*

Terpenoid hydrocarbons have been extensively studied as possible next-generation biofuels [18]. This involves manipulation of either the predominantly prokaryotic methylerythritol (MEP) or the predominantly eukaryotic mevalonate (MVA) pathways. Our laboratory has worked with constructs generated in collaboration with Dr. Joe Chappell (U. Kentucky) as part of a DOE-sponsored ARPA-e project. Vector construction is dependent on the host, and details are available in a wide range of papers examining the basic flux of the isoprene pathway [19, 20]. In our work with *Rhodobacter* and *Ralstonia*, broad host range plasmids such as pBBR and pIND are typically used (*see Note 2*). Transformation of the isoprene metabolic pathways into alternative platforms can be challenging, and we have recently reviewed aspects of transformation methods in a recent assessment of the status of chemolithoautotrophic metabolic engineering [12]. The key aspect of producing botryococcene is to express the botryococcene synthase chimeric gene in the presence of the C<sub>15</sub> precursor farnesyl pyrophosphate (FPP) which is derived from isopentenyl diphosphate (IPP) and its isomer dimethylallyl diphosphate (DMAP) [21]. Those interested in the details of metabolic engineering can find those details in the associated references.

The method described below for GC-FID analysis was used to measure the intracellular and extracellular botryococcene triterpene level during autotrophic bioreactor runs of transgenic *Rhodobacter capsulatus* growing on gas mixture of H<sub>2</sub>, CO<sub>2</sub>, and O<sub>2</sub> [9]. Surprisingly, a significant fraction of the botryococcene was found

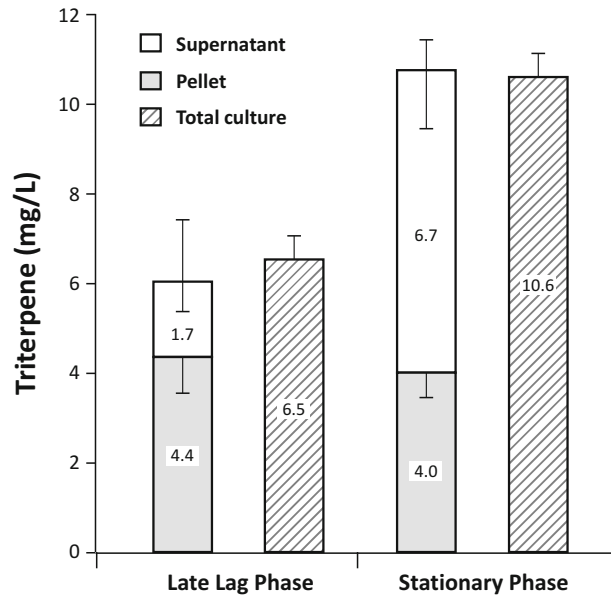


**Fig. 1** Analysis of hydrocarbon production by *Rhodobacter capsulatus* genetically engineered with botryococcene synthase and enhanced flux through the isoprene pathway. Cultures are grown autotrophically on CO<sub>2</sub>, H<sub>2</sub>, and O<sub>2</sub> during late lag and stationary phase. Error bars represent analysis from independent batch cultures

outside the cells in Fig. 1 – more than half at stationary phase [10]. The mechanism by which this highly hydrophobic lipid exits cells is not clear, particularly for the high fluxes of hydrocarbon observed in the extracellular matrix of the native *Botryococcus braunii* algae.

### 3 Methods

#### 3.1 Growth of Algae and Metabolically Engineered Hosts

##### 3.1.1 Growth of Algae

*Botryococcus braunii* algae can be grown in a range of lighting, CO<sub>2</sub>, and temperature levels (*see Note 3*). Nominal conditions of 25 °C, lighting PAR = 100 μE/m<sup>2</sup>/s, and 2% CO<sub>2</sub> are reasonable with very large natural variations: 20–30°C, darkness to full sun (PAR = 2,000 μE/m<sup>2</sup>/s). While CO<sub>2</sub> does not vary greatly in nature, the role of CO<sub>2</sub> concentrations can relate to buffering rather than the simplistic interpretation of CO<sub>2</sub> availability (*see Note 3*).

##### 3.1.2 Growth of Bacteria

*E. coli* harboring plasmids for triterpene production follows standard growth methods. We recently demonstrated that vastly different trophic modes of growth of *Rhodobacter* (aerobic heterotrophic, anaerobic photoheterotrophic, and chemolithoautotrophic) all yielded surprisingly similar levels of triterpene hydrocarbon [9]. Recent unpublished work using *Ralstonia eutropha* expressing these pathways yielded similar levels of expression

which was surprisingly unaffected by utilizing wild-type or PHB knockout strains (where the knockout is often presumed as the approach to increase heterologous flux by eliminating this dominant storage biopolymer flux).

### 3.2 Extraction of Hydrocarbon

In the native algae host, hydrocarbon can be gently extracted from the extracellular matrix with minimal reduction in cell growth rates [22]; however, a careful analysis of this data can reveal that there is not a net increase in cellular productivity. We have used hexane rinses to establish axenic lines of *Botryococcus* [23] but focus here on a disruptive whole culture extraction procedure. This can be applied to both native and heterologous triterpene production and on culture fractions to assess location of hydrocarbon within the culture. The hydrophobic nature of isoprenes makes them amenable to integrated extraction which involves extraction during bioreactor operation (*see Note 4*).

*Extraction materials* are acetone, *n*-hexane, hexanes, nitrogen gas, silica gel, silane-treated glass wool, glass pasture pipettes, 1.5 mL glass GC vial, 2 mL glass HPLC vial, and 2 mL HPLC vial screw caps with PTFE septum (plastic can introduce plasticizers that adversely affect chromatogram; *see Note 5*).

#### 3.2.1 Disrupt Cells with Acetone

Place 0.5 mL of culture and 0.5 mL of acetone in a 2 mL glass HPLC vial and vortex for 30 s. Let it sit for 5–10 min to allow cells to be fully permeabilized.

#### 3.2.2 Extract Hydrocarbons into a Hexane Phase

Add an additional 0.5 mL of hexane and vortex vigorously for 1 min to partition hydrocarbons into the organic phase. Let it sit for 5–10 min.

#### 3.2.3 Isolate Hexane Layer for Analysis of the Hydrocarbons

Centrifuge the extraction mixture at moderate speed (>2,000 RCF) for 10 min. Carefully remove the hexane phase and place it in a new, clean vial. Take care not to touch the phase interface.

#### 3.2.4 Purification of Hydrocarbons by Removal of Oxidized Species

The hexane phase can be poured over a column of silica gel. This is readily constructed from ~0.4 g of silica placed within 5 3/4" Pasteur pipette and pre-wetted with hexane before use. Triterpene is flushed from the column with three column volume washes and nitrogen to push the interstitial hexane into a 1.5 mL vial and dried under N<sub>2</sub> to avoid further oxidation. This purification step can introduce reduced yield and reproducibility for analysis (*see Note 6*).

- Add a pinch of silane-treated glass wool to a Pasteur pipette and stuff it into the taper of the pipette.
- Add 0.4 g of 230–240 mesh silica gel.
- Wet the column with *n*-hexane until the first drop exits the column.

- Add an additional 1 mL of hexane and purge with nitrogen; do not allow the column to dry.
- Place a new collection vial below the column and add the hexane layer to the top of the column.
- Purge the column with nitrogen.
- Wash the column twice with 1 mL of hexane. Collect this wash in the same vial.
- Evaporate the collected hexane with a gentle stream of nitrogen.
- Once dried down, resuspend the eluted oil in 500  $\mu\text{L}$  of isooctane.
- Transfer the extract into a 2 mL sampling vial with a PTFE lined lid.

### 3.2.5 Hydrocarbon Analysis by GC-FID

A 1  $\mu\text{L}$  aliquot of the organic phase of the extraction mixture was measured by GC-FID for analysis. The injection port is equipped with an inlet liner having silica wool (deactivated) to trap the nonvolatile components. GC-FID analysis was conducted on an Agilent 7820A GC using a Restek, Rxi-5sil MS fused silica capillary column (30 m  $\times$  0.25 mm  $\times$  0.25  $\mu\text{m}$  film thickness). Squalene standard was analyzed in concentrations ranging from 1 ng to 100 ng to generate standard curves. 1  $\mu\text{L}$  containing about 25 ng triterpene oil is injected into the GC. The initial oven temperature was set to 100°C, ramped to 250°C at 15°C/min, and then ramped to 300°C at 5°C/min. Reported variations are given in the table of **Note 7**.

The chromatogram of Fig. 2 demonstrates resolution of the methylated forms of botryococcene that occur in the B-race of *Botryococcus braunii* which occurs at locations C-3, 7, 16, and 30 through the actions of methyltransferases [8]. Many different permutations of columns and operational conditions have been used to achieve run times less than 10 min, which may result in reduced resolution of methylated forms; however, loss of resolution may not be a major concern for measurements of total triterpene production or in the case of genetically engineered hosts where only one form is present (e.g., Fig. 1). Standards for GC analysis to resolve different methylated forms have typically been isolated by HPLC with numerous references in the literature with varying degrees of separation [8, 24, 25]. Mass spectra and additional spectroscopy have been utilized to further examine details of methylation in both native and heterologous hosts [25, 26].

### 3.2.6 Hydrocarbon Analysis by Secondary Ion Mass Spectroscopy (SIMS)

SIMS provides a means to measure hydrocarbons within biomass without requiring an extraction by vaporizing the sample using bombardment with buckminsterfullerene (buckyball) ions [27]. A 5 mL aliquot of algal suspension was deposited onto an 11  $\mu\text{m}$

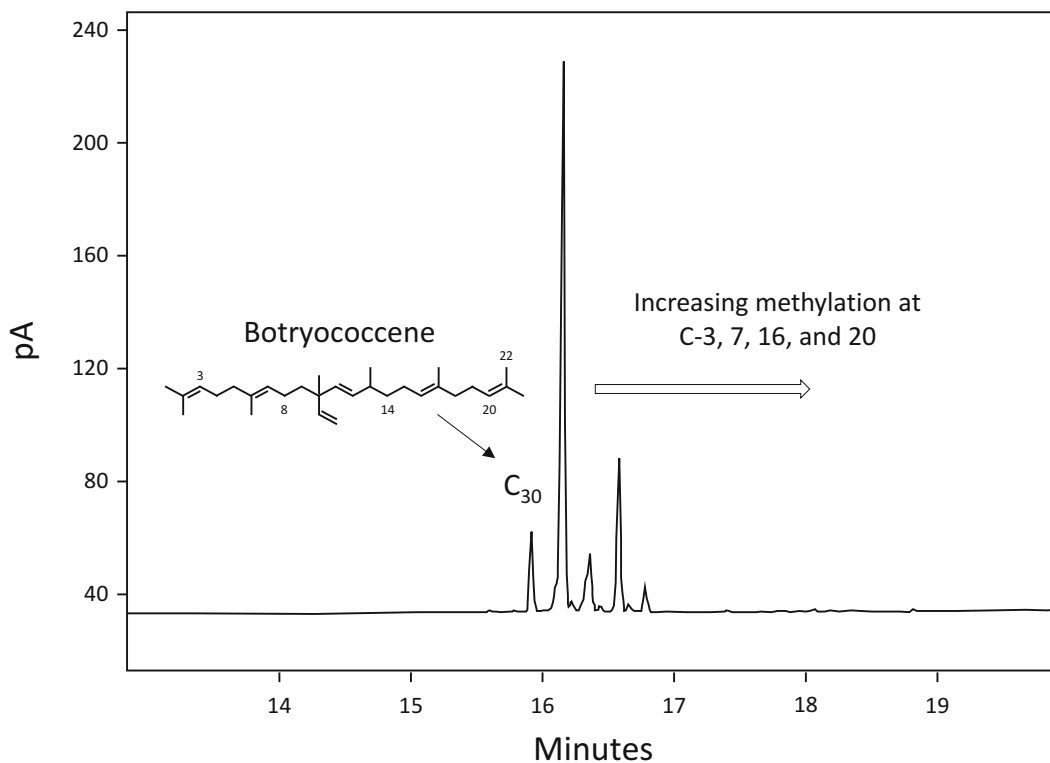


**Fig. 2** Chromatogram of triterpene hydrocarbons extracted from *Botryococcus braunii* B algae cultures. Botryococcene elutes at 15.92 min for the conditions and column described in this work

nylon filter mesh (Millipore) held at a vacuum of approximately 1 torr. The algae were gently washed three times with 150 mM ammonium formate (Alfa Aesar, 97%) solution to remove excess media materials. The vacuum was turned off and 0.5 mL of deionized water was immediately deposited onto the algae on the filter and mixed gently. A silicon shard (Ted Pella, Inc.) was cleaned by sonication 3x with methanol and water solutions, respectively. 10  $\mu$ L of the algae/water was deposited on the shard and dried in a desiccator for 10 min before introduction into the mass spectrometer for analysis.

The SIMS analysis was done on the *J105 Chemical Imager* at room temperature. A 0.5 pA 40 keV  $C_{60}^+$  primary ion current with a 75% duty cycle on a  $100 \times 100 \mu\text{m}^2$  area at  $32 \times 32$  pixels<sup>2</sup> was used to depth profile through the *B. braunii* cells at a total ion dose of  $2.35 \times 10^{13} C_{60}^+/\text{cm}^2$ . Each SIMS image was collected over a  $100 \times 100 \mu\text{m}^2$  field of view at  $256 \times 256$  pixels.

The surface of the *Botryococcus braunii* race A is observed to be rich in wax esters as noted in the top panel of Fig. 3. This invariably gives *Botryococcus* tremendous resistance to desiccation [28], similar to the role in of these hydrocarbons in human skin.

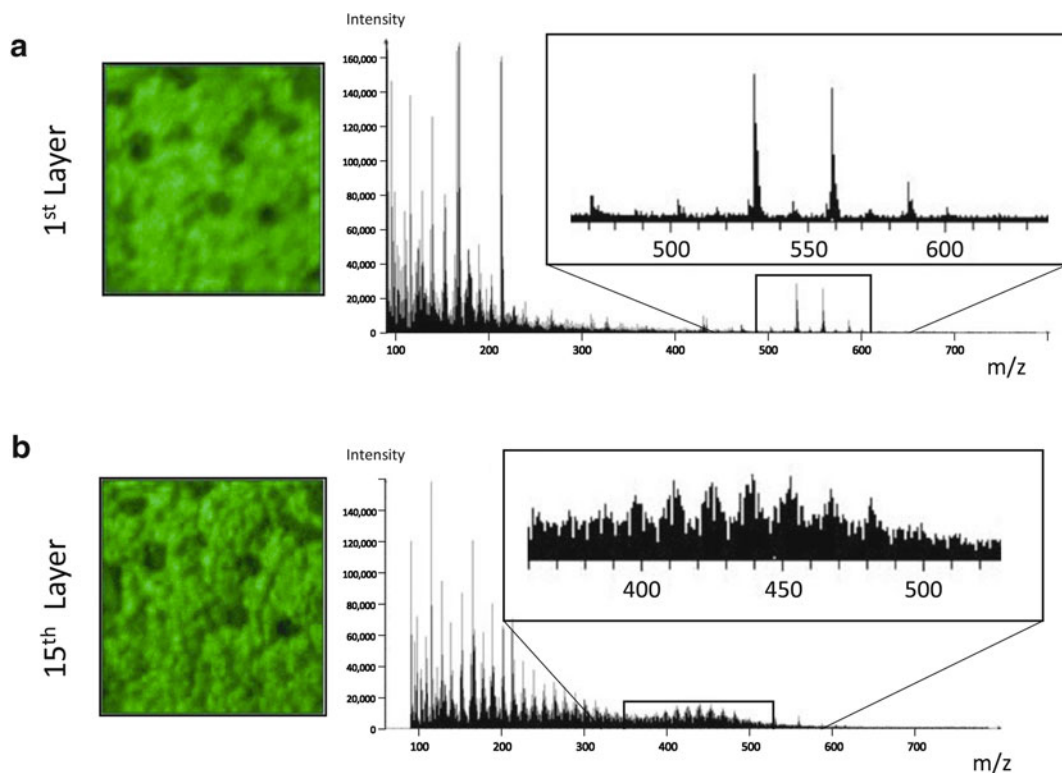


**Fig. 3** Chemical images and mass spectra of *Botryococcus braunii* race A using secondary ion mass spectrometry. Depth profiling is achieved by etching away the sample using  $C_{60}$  ion bombardment with the chemical images being reconstructed from the mass spectra of the secondary ions that are dislodged from the surface due to ion impact: (a) Image of wax monoester region, (b) hydrocarbon region. Although race A produces alkadiene hydrocarbons, the procedure is equally applicable for isoprene hydrocarbons of *B. braunii* race B which will be described elsewhere

The triterpene hydrocarbons are found deeper within the colonies of cells and characterized by small lipid bodies, consistent with ultrastructural microscopic studies of these colony algae [29].

## 4 Notes

1. We routinely prepare autoclave sterilized magnesium and calcium solutions separately and add these inorganics immediately before algae inoculation to minimize issues of precipitation: 1 mL/L media of 0.51 mM  $MgCl_2$ , 0.49 mM  $MgSO_4$ ; 0.88 mL/L media of 0.9 mM  $CaCl_2$ . Iron is added in chelated form with EDTA, where historically  $Na_2$ -EDTA and  $FeSO_4$  were prepared as a separate stock; it is now more typical to use the FeNa-EDTA even though the hydration state can be variable. Care should be made to avoid variation in hydration state during storage and different chemical lots.

2. While pIND has been shown to be stable in *Rhodobacter sphaeroides* [30], in our hands, it was highly unstable in the closely related species (*R. capsulatus*) which is of particular interest due to robust chemolithoautotrophic growth. This emphasizes the potential difficulty of extending methods across platform organisms that are less well characterized.
3. *Botryococcus* is often viewed as being a relatively difficult alga to grow. Where some have had trouble growing under high light (Chappell, personal communication), we have found that it can be slowly adapted to light levels > 300 PAR ( $\mu\text{E}/\text{m}^2/\text{s}$ ). Growth on elevated  $\text{CO}_2$  seems to be particularly important and may well be due to overcoming diffusional transport limitations of  $\text{CO}_2/\text{O}_2$  and associated effects on photorespiration [31].  $\text{CO}_2$  dissolves into water to produce carbonic acid and associated equilibrium with carbonate species:



This can result in buffering pH when used in conjunction with carbonate media components (as with mammalian cell culture) or more typically in algae to offset the effects of media basification during assimilation of nitrate [17, 32].

4. The integrated extraction of biologically produced products during production has long been recognized to have advantages in protecting the product of interest or facilitating greater production rates by reducing “feedback inhibition” [33]. Based on our prior work with sesquiterpene extraction and recovery, the use of hydrophobic resins such as XAD-16 might be an ideal way to “trap” and enhance extracellular production [34].
5. Glass vials must be used for all steps of the extraction. The hydrocarbon extractants will dissolve components of the plastic vials, leading to excess baseline noise when the sample is run through the GC.
6. Although we report the silica gel purification step in our most recent work [9], we have subsequently found that the silica gel treatment decreases reproducibility in measurements, and we have subsequently opted for routine analysis to avoid this step and alternatively make more frequent changes to the GC septa and column regeneration by baking to accommodate for the slightly increased rate of fouling. We have also found that the use of resuspension in isooctane instead of hexane provides a less volatile extract and, therefore, has reduced issues of evaporative concentration of the extracted samples. The culture acetone–isooctane mixture is then centrifuged for 5 min at >2000 rcf. Cell debris pellets at the bottom and liquid phases

separate into acetone–water (bottom) and the predominantly isooctane (top) layers.

7. Many permutations of GC columns and conditions have been used for *Botryococcus braunii* hydrocarbon analysis, even in our own lab, with collaborators and in the literature. The table below provides a sample of variations with associated references from which one can find more details.

Chromatograph	Column details	References
Agilent 7820A	Restek, Rxi-5Sil MS fused silica (30 m × 0.25 mm × 0.25 μm film) 1,4-bis(dimethylsiloxy)phenylene dimethyl polysiloxane	Here
Shimadzu GC-2014	J & W Science, DB-1 (60 m × 0.25 mm × 0.25 μm film), dimethylpolysiloxane	[25]
Varian CP-3800	Supelco, SLB-5MS fused silica, (30 m × 0.25 mm × 0.25 μm film), cross-linked silphenylene	[8]
HP 5890	Restek, Rtx-5 ms fused silica (30 m × 0.25 mm × 0.25 μm film), diphenyl dimethyl polysiloxane	[2]
-na-	Macherey-Nagel fused silica, OPTIMA 5, SE 52 (25 m × 0.31 mm × 0.19 μm film), 5% diphenyl – 95% dimethylpolysiloxane	[35]

## Acknowledgments

We acknowledge the generous efforts of Dr. Joe Chappell throughout our development of algae and heterologous production of triterpenes, including “in-house/hands-on” training on initial extraction and GC analytical methods. Amalie Tuerk and Justin Yoo are acknowledged for their extensive efforts in the culturing of *Botryococcus braunii* strains and various growth and hydrocarbon production studies. This collaborative work with W. R. C. was supported by US Department of Energy. Grant Number: ARPA-e Electrofuels, DE-AR0000092, and the National Science Foundation Collaborative Grant No. CBET-0828648 titled “Development of a Sustainable Production Platform for Renewable Petroleum Based Oils in Algae.” Any opinions, findings, and conclusions or recommendations expressed in this material are those of the authors and do not necessarily reflect the views of the National Science Foundation.

## References

1. Wolf FR, Nonomura AM, Bassham JA (1985) Growth and branched hydrocarbon in a strain of *Botryococcus braunii* (Chlorophyta). *J Phycol* 21:388–396
2. Khatri W, Hendrix R, Niehaus T, Chappell J, Curtis WR (2014) Hydrocarbon production in high density *Botryococcus braunii* race B continuous culture. *Biotechnol Bioeng* 111:493–503
3. Hillen LW, Pollard G, Wake LV, White N (1982) Hydrocracking of the oils of *Botryococcus braunii* to transport fuels. *Biotechnol Bioeng* 24:193–205
4. Glikson M, Lindsay K, Saxby J (1989) *Botryococcus*—A planktonic green alga, the source of petroleum through the ages: transmission electron microscopical studies of oil shales and petroleum source rocks. *Org Geochem* 14:595–608
5. Niehaus TD, Okada S, Devarenne TP, Watt DS, Sviripa V, Chappell J (2011) Identification of unique mechanisms for triterpene biosynthesis in *Botryococcus braunii*. *Proc Natl Acad Sci U S A* 108:12260–12265
6. Kirby J, Romanini DW, Paradise EM, Keasling JD (2008) Engineering triterpene production in *Saccharomyces cerevisiae*-beta-amyrin synthase from *Artemisia annua*. *FEBS J* 275:1852–1859
7. Wu S, Jiang Z, Kempinski C, Eric Nybo S, Husodo S, Williams R, Chappell J (2012) Engineering triterpene metabolism in tobacco. *Planta* 236:867–877
8. Niehaus TD, Kinison S, Okada S, Yeo Y, Bell SA, Cui P, Devarenne TP, Chappell J (2012) Functional identification of triterpene methyltransferases from *Botryococcus braunii* race B. *J Biol Chem* 287:8163–8173
9. Khan NE, Nybo SE, Chappell J, Curtis WR (2015) Triterpene hydrocarbon production engineered into a metabolically versatile host – *Rhodobacter capsulatus*. *Biotechnol Bioeng* 112:1523–1532
10. Khan N (2015) Development of biological platform for the autotrophic production of biofuels. The Pennsylvania State University, State College
11. Zuroff TR, Barri Xiques S, Curtis WR (2013) Consortia-mediated bioprocessing of cellulose to ethanol with a symbiotic *Clostridium phytofermentans*/yeast co-culture. *Biotechnol Biofuels* 6:59
12. Nybo SE, Khan N, Woolston BM, Curtis WR (2015) Metabolic engineering in chemolithoautotrophic hosts for the production of fuels and chemicals. *Metab Eng* 30:105–120
13. Eroglu E, Okada S, Melis A (2011) Hydrocarbon productivities in different *Botryococcus* strains: comparative methods in product quantification. *J Appl Phycol* 23:763–775
14. Kawachi M, Tanoi T, Demura M, Kaya K, Watanabe MM (2012) Relationship between hydrocarbons and molecular phylogeny of *Botryococcus braunii*. *Algal Res* 1:114–119
15. Largeau C, Casadevall E, Berkaloﬀ C, Indexbotryococcus KW (1980) Sites of accumulation and composition of hydrocarbons in *Botryococcus braunii*. *Phytochemistry* 19:1043–1051
16. Grung M, Metzger P, Liaaen-Jensen S (1989) Primary and secondary carotenoids in two races of the green alga *Botryococcus braunii*. *Biochem Syst Ecol* 17:263–269
17. Scherholz ML (2012) Achieving pH control through stoichiometrically balanced media in algae photobioreactors. The Pennsylvania State University, State College
18. Maury J, Asadollahi MA, Formenti LR, Schalk M, Nielsen J (2013) Metabolic engineering of isoprenoid production: reconstruction of multistep heterologous pathways in tractable hosts. In: Bach TJ, Rohmer M (eds) *Isoprenoid synthesis in plants and microorganisms: new concepts and experimental approaches*. Springer, New York, pp 73–89
19. Yang J, Xian M, Su S, Zhao G, Nie Q, Jiang X, Zheng Y, Liu W (2012) Enhancing production of bio-isoprene using hybrid MVA pathway and isoprene synthase in *E. coli*. *PLoS One* 7, e33509
20. Chandran SS, Kealey JT, Reeves CD (2011) Microbial production of isoprenoids. *Process Biochem* 46:1703–1710
21. Okada S, Devarenne T, Murakami M, Abe H, Chappell J (2004) Characterization of botryococcene synthase enzyme activity, a squalene synthase-like activity from the green microalga *Botryococcus braunii*, Race B. *Arch Biochem Biophys* 422:110–118
22. Choi SP, Bahn SH, Sim SJ (2013) Improvement of hydrocarbon recovery by spouting solvent into culture of *Botryococcus braunii*. *Bioprocess Biosyst Eng* 36:1977–1985
23. Yoo J (2013) Establishment and maintenance of axenic *Botryococcus braunii* race B algae culture. The Pennsylvania State University, State College
24. Wolf FR, Nemethy EK, Blanding JH, Bassham JA (1985) Biosynthesis of unusual acyclic isoprenoids in the alga *Botryococcus braunii*. *Phytochemistry* 24:733–737
25. Weiss TL, Chun HJ, Okada S, Vitha S, Holzenburg A, Laane J, Devarenne TP (2010) Raman

- spectroscopy analysis of botryococcene hydrocarbons from the green microalga *Botryococcus braunii*. *J Biol Chem* 285:32458–32466
26. Metzger P, Casadevall E, Pouet M, Pouet Y (1985) Structures of some botryococcenes: branched hydrocarbons from the b-race of the green alga *Botryococcus braunii*. *Phytochemistry* 24:2995–3002
  27. Jackson L (2014) New analytical approaches to understand biological systems with Secondary Ion Mass Spectrometry (SIMS). The Pennsylvania State University, State College
  28. Demura M, Ioki M, Kawachi M, Nakajima N, Watanabe MM (2014) Desiccation tolerance of *Botryococcus braunii* (Trebouxiophyceae, Chlorophyta) and extreme temperature tolerance of dehydrated cells. *J Appl Phycol* 26:49–53
  29. Weiss TL, Roth R, Goodson C, Vitha S, Black I, Azadi P, Rusch J, Holzenburg A, Devarenne TP, Goodenough U (2012) Colony organization in the green alga *Botryococcus braunii* (Race B) is specified by a complex extracellular matrix. *Eukaryot Cell* 11:1424–1440
  30. Ind AC, Porter SL, Brown MT, Byles ED, de Beyer JA, Godfrey SA, Armitage JP (2009) Inducible-expression plasmid for *Rhodobacter sphaeroides* and *Paracoccus denitrificans*. *Appl Environ Microbiol* 75:6613–6615
  31. Eckardt NA (2005) Photorespiration revisited. *Plant Cell* 17(August):2139–2141
  32. Wang J, Curtis WR (2015) Proton stoichiometric imbalance during algae photosynthetic growth on various nitrogen sources: towards metabolic pH control. *J Appl Phycol*, pp 1–10. doi: [10.1007/s10811-015-0551-3](https://doi.org/10.1007/s10811-015-0551-3)
  33. Daugulis AJ (1994) Integrated fermentation and recovery processes. *Curr Opin Biotechnol* 5:192–195
  34. Corry JP, Reed WL, Curtis WR (1993) Enhanced recovery of solavetivone from Agrobacterium transformed root cultures of *Hyoscyamus muticus* using integrated product extraction. *Biotechnol Bioeng* 42:503–508
  35. Metzger P, Berkaloff C, Casadevall E, Coute A (1985) Alkadiene-and botryococcene-producing races of wild strains of *Botryococcus braunii*. *Phytochemistry* 24:2305–2312

# Protocols for Monitoring Growth and Lipid Accumulation in Oleaginous Yeasts

Jean-Marc Nicaud, Anne-Marie Crutz-Le Coq, Tristan Rossignol, and Nicolas Morin

## Abstract

Oleaginous yeasts can synthesize and store lipids up to 20% of their dry weight and have emerged as resources of choice for biotechnological applications, such as bio-lipid production. The number of species and mutant libraries consequently available for screening is exponentially growing. Cultivation strategies and growth media for bio-lipid production need to be optimized to accelerate screening and identification of production strains. In this chapter we describe methods for high-throughput cell growth in 96 microtiter plates in various media including opaque broth by using a fluorescent reporter, carbon/nitrogen ratio determination for optimal lipid accumulation, and in vivo real-time detection of lipid accumulation using a neutral lipid fluorescent dye. We provide examples using two well-established oleaginous yeasts, *Yarrowia lipolytica* and *Rhodospiridium toruloides*. These methods can be extended to other oleaginous yeast species for high-throughput screening of bio-lipid accumulation.

**Keywords:** Lipid accumulation, Oleaginous yeast, *Rhodospiridium*, Single cell oil, *Yarrowia*

---

## 1 Introduction

Oleaginous yeasts are naturally able to synthesize and accumulate lipids above 20% of their dry weight. Among the large number of known yeasts, few are referred as such so far. They were found both in the *Basidiomycota* and *Ascomycota* phyla, mainly in the genera *Cryptococcus*, *Lipomyces*, *Rhodospiridium*, *Rhodotorula*, *Trichosporon*, and *Yarrowia* [1–3]. Within these genera, few species can accumulate lipids to a high proportion exceeding 65% of biomass, i.e., *Rhodotorula glutinis*, *Trichosporon pullulans*, *Cryptococcus albidus*, and *Rhodospiridium toruloides*. Like most other oleaginous species, *Yarrowia lipolytica* accumulates lipids at a slightly lower level, yet still around ca. 40% of its dry weight [1]. It has however reached a status of model organism [4], especially for lipid metabolism. Thus far, the prominent advantage of *Y. lipolytica* for both basic research and biotechnology resides in its fully sequenced and

manually annotated genome [5], combined with efficient genetic tools developed over decades [6–8]. A metabolic model for this oleaginous yeast has been published by two different groups [9, 10].

Despite being critical for biotechnological applications, genetic information on other species remains scarce. Only few oleaginous yeast species have been sequenced over the last few years, including strains of the *Rhodospiridium*, *Rhodotorula*, or *Lipomyces* genera. *Rhodospiridium torulooides*, accumulating high level of lipids and able to assimilate economically attractive C5 sugars, has been the subject of fruitful research efforts leading to the recent publication of the complete genome sequence of two strains [11, 12] supplemented for one of them with transcriptomic and proteomic data [12]. In parallel, appropriate genetic tools for related species are emerging [13] but proved to be difficult to optimize [14].

Due to the great industrial interest in discovering and adapting oleaginous microorganisms for specific applications, it is likely that new oleaginous yeast species and many other physiological, genetic, and omic studies will be continuously published.

Yeasts greatly differ in their ability to metabolize various substrates for growth and lipid storage. For example, sugars derived from diverse raw materials such as xylose or arabinose may be interesting to test as carbon sources. Conditions of lipid accumulation also need to be investigated. Lipid storage is triggered by a nutrient limitation other than carbon, usually nitrogen. The C/N ratio has a strong impact on the optimal routing of carbon toward lipid synthesis instead of being directed to other metabolites such as citric acid in the case of *Y. lipolytica* [1]. This ratio must therefore be well defined to set up proper culture conditions for lipid accumulation.

In yeasts, lipids are mainly stored as triacylglycerols in specific structures called lipid bodies. The nature of esterifying fatty acids was observed to follow a distribution varying for each species in chain length (usually between C16 and C24) and degree of unsaturation [3]. As a result, not only lipid accumulation levels but also lipid profiles may differ from species to species.

When selecting a strain for a bioconversion process, all these parameters need to be taken into account, depending on the molecule to be produced and the carbon sources available.

Such studies are used to be carried out in several experiments using batch cultures in “traditional” or baffled Erlenmeyer flasks and multiple sampling. A high-throughput cell growth system coupled to a detection system represents a valuable alternative. This is particularly helpful for setting up growth and lipid production conditions or to screen libraries of strains or mutants for their capacity to grow and accumulate lipids on various substrates.

The use of standard microtiter plates is very attractive due to the compatibility with standard commercial microtiter plate readers

and robots. It has the advantages of being automatable, fast, standard, and of using small volumes (i.e., less than 200  $\mu\text{L}$ ), which can be a strong advantage when testing expensive compounds as substrate or inhibitors, for example. Such a system allows to perform multiple cultures in parallel and to replicate them easily to generate robust data.

Moreover, high-throughput methods using a microtiter plate reader provide the advantage of monitoring various parameters almost continuously, in real time, by rapid scanning with short time interval without human intervention (e.g., stopping culture, sampling). This is particularly suited for identifying changes in the growth rate  $\mu$ , as it can be precisely estimated all along the experiment. The precision level of the  $\mu$  calculation can even be adjusted over time, using a user-defined sliding window, which would otherwise be difficult to perform using standard cultivation methods.

In this chapter, we describe a general protocol for growing oleaginous yeasts in microtiter plates. We also propose two methods for evaluating growth aspects more related to the oleaginous character of these yeasts, that is, assimilation of hydrophobic compounds (e.g., fatty acids sometimes used as substrates for bioconversion into more valuable lipids) and determination of the C/N ratio of the broth optimized for lipid accumulation. We finally propose a method to monitor real-time lipid accumulation. All these methods use microtiter plates. As for any culture method, scaling up to flask and/or fermentor will need optimization and adaptation. The choice of the plate reader and of microtiter plate shape could be important parameters. One of the distinctive features of oleaginous yeasts, i.e., identifying the fatty acid profile, could not be accommodated in this miniaturized system and has still to rely on sampling, extraction, and analysis with gas chromatography, for example.

This chapter will include four methods that we have applied to at least one of the yeasts *Y. lipolytica* and *R. toruloides*:

1. Growth in microtiter plates. This is the general protocol for obtaining and analyzing growth in microtiter plates.
2. Growth kinetics on hydrophobic substrates using a fluorescent reporter. Broths opaque to light, such as those containing lipid emulsions, do not enable to follow growth directly by the optical density. Alternative reporter systems must be implemented in order to monitor growth in such media. Here we use a red fluorescent protein.
3. Definition of C/N ratio for optimum lipid accumulation in microtiter plates. This section will describe how to vary the amount of nitrogen source in the medium and to check the effect on lipid accumulation.

4. Real-time detection of lipid accumulation by fluorescent methods. In this section we describe the concurrent use of the green dye BODIPY largely used to detect neutral lipids and a quencher.

---

## 2 Materials

General materials for growth in microtiter plates are listed in sub-heading 2.1. Additional reagents and/or equipments required for specific applications are described in the relevant subheadings.

### 2.1 Growth in Microtiter Plates

1. Media compounds can be purchased from any common growth media supplier.  
YNB: Yeast nitrogen base without amino acids and ammonium sulfate 1.7 g, NH<sub>4</sub>Cl 5 g, phosphate buffer KH<sub>2</sub>PO<sub>4</sub>-Na<sub>2</sub>HPO<sub>4</sub> pH 6,8 (50 mM final) per liter. Carbon source (e.g., glucose, glycerol, oleic acid) is added accordingly to the desired final concentration (e.g., 0.1–3%).  
YPD: Bacto yeast extract 10 g, Bacto peptone 20 g, glucose 20 g per liter.
2. Strains: the strains used as examples in this chapter are *Yarrowia lipolytica* wild-type strain W29 (CBS 7504, CLIB 89) or derivatives and *Rhodospiridium toruloides* wild-type strain CECT 1137.
3. Microtiter plates: 96-well polystyrene culture plate Greiner Bio-One sterile flat bottom with lid (*see Note 1*).
4. Multichannel pipettes from any suppliers, electronic, are recommended.
5. Microtiter plate reader: we routinely use two apparatus from BioTek instruments (<http://www.biotek.com>), Synergy 2 and Synergy MX, both adapted for OD and fluorescence. The first one is equipped with filters (i.e., fixed wavelength and band-pass), while the second one is provided with a double monochromator system allowing a fine tuning of both wavelength and bandpass (i.e., 1 nm increment). Both models are equipped with agitation and temperature controls. Other microtiter plate readers with equivalent specificities can be used. Measurements for each wavelength are generally performed every 20 min during cultivation (*see Note 2* for graphical representation).

### 2.2 Growth Kinetics on Hydrophobic Substrates Using a Fluorescent Reporter

1. Delivery vectors for intracellular expression of fluorescent protein, to be constructed for your application. *See Note 3* for *Y. lipolytica*.
2. Oleic acid. We usually do not use high purity grade. Oleic acid from Sigma (ref: 27728) is a solution at 70%.
3. Sonicator.

**Table 1**

**Composition for 100 mL YNB medium with a C/N ratio varying from 1 to 120. Glucose is used as a fixed carbon source (final concentration 3%, ca. 12 g/L of C). The C/N ratio is adapted by reducing the amount of NH<sub>4</sub>Cl (stock solution 25%, ca. 65.4 g/L of N)**

Stock solutions	Volume (mL) required for a C/N of						
	1	10	20	30	60	90	120
YNB 50 g/L	3.4	3.4	3.4	3.4	3.4	3.4	3.4
Glucose 500 g/L	6	6	6	6	6	6	6
NH <sub>4</sub> Cl 250 g/L	18	1.8	0.9	0.6	0.3	0.2	0.15
KH <sub>2</sub> PO <sub>4</sub> Na <sub>2</sub> HPO <sub>4</sub> 0.5 M	10	10	10	10	10	10	10
H <sub>2</sub> O	<i>qs</i> 100 mL						

### 2.3 Definition of C/N Ratio for Optimum Lipid Accumulation in Microtiter Plates

1. For lipid production, YNB medium described in 2.1 can be adapted with various C/N ratios. The C/N ratio (or carbon-to-nitrogen ratio) is a ratio of the mass of carbon to the mass of nitrogen. In our experiments, we generally fix the carbon source in the medium and reduce the amount of nitrogen in order to increase the C/N ratio. We use glucose as a carbon source, with a final concentration of 30 g/L (ca. 166 mM). Under these conditions, the concentration of C within every medium is fixed at ca. 12 g/L (ca. 1 M). Nitrogen is supplied by the NH<sub>4</sub>Cl stock solution (250 g/L, ca. 4.67 M), which contains ca. 65.4 g/L of nitrogen (ca. 4.67 M). Knowing these concentrations, the volume of NH<sub>4</sub>Cl added to the medium is adapted to define the C/N ratio (*see* Table 1).
2. Stock solution of BODIPY D-3922 4,4-difluoro-1,3,5,7,8-pentamethyl-4-bora-3a,4a-diaza-s-indacene (BODIPY<sup>®</sup> 493/503) from Life Technologies (<http://www.lifetechnologies.com>) at 1 mg/mL (3.8 mM) in DMSO, referred here as BODIPY. Store at -20°C and protect from light.
3. Microscope equipped with a YFP filter. We use a Zeiss Imager M2 microscope equipped with filter set 46 and with an HXP 120 C lamp (<http://www.zeiss.com>).

### 2.4 Real-Time Detection of Lipid Accumulation by Fluorescent Methods

1. Medium: YNB C/N 30 (*see* subheading 2.3).
2. Potassium iodide stock solution at 4 M (Sigma ref: 60400). When resuspended in water, store at -20°C and protect from light.
3. BODIPY 493/503 at 1 mg/mL (*see* subheading 2.3).

### 2.5 Software and Analytical Tools

1. Microtiter plate reader software, e.g., Gen5 2.0 from BioTek (<http://www.biotek.com>).
2. R statistical software for data analysis and visualization [15].

### 3 Methods

Different methods to evaluate growth of *Y. lipolytica* and *R. toruloides* and their capacity of lipid accumulation are described below. Each method could be easily adapted to a wide variety of yeasts and/or substrates.

#### 3.1 Growth in Microtiter Plates

When measuring OD in a microtiter plate, one should always keep in mind the fact that the optical path length is usually shorter than the 1 cm standard. A correction factor can however be applied to the data after measurement (*see Note 4*).

1. Prepare your experimental design (i.e., location of samples/blanks, number of replicates), taking into account that outer wells should be avoided for your samples when running long-term experiments (*see Note 5*). Include technical replicates whenever possible. When testing for carbon source utilization (*see Note 6*), make sure to include a “no growth” standard (i.e., minimal medium without the carbon source under investigation, inoculated with the yeast).
2. Using the microtiter plate reader software, set up a protocol for running your experiment. A typical protocol for growth monitoring should at least include the following parameters: (i) agitation (e.g., continuous and vigorous; *see Note 7*), (ii) wavelength for OD measurement (e.g., 600 nm), (iii) periodicity of measurement (e.g., 20 min), (iv) duration of cultivation (e.g., 12–72 h), and (v) temperature. Additional information (e.g., description of the experimental design, sample coordinates) can also be included at this step, but are not mandatory.
3. Grow a preculture, according to the growth characteristics of your yeast/strain. Typically, grow cells for 24 h in a test tube by picking a fresh colony in 4 mL YPD medium and incubating at 28°C with agitation (e.g., 160 rpm).
4. Before inoculating the microtiter plate, control growth of your preculture by measuring OD at 600 nm. A typical *Yarrowia* or *Rhodosporidium* preculture should have reached an OD<sub>600</sub> of ca. 10–16 with 1 cm light path cuvette and spectrophotometer (Novaspec II, LKB).
5. Centrifuge 0.2 mL of cell suspension, eliminate supernatant carefully, and resuspend cells in the appropriate volume of YNB medium to reach a cell concentration of OD<sub>600</sub> = 4. For high-throughput studies, an alternative method for growing multiple precultures in a microtiter plate is detailed in **Note 8**.
6. Fill each well with the appropriate medium according to your planned scheme. It is advisable to test filling volumes for sample wells from 0.1 to 0.2 mL in preliminary experiments. For *Yarrowia* and *Rhodosporidium*, we routinely use 100 µL.

7. Inoculate the samples to obtain an initial OD<sub>600</sub> of ca. 0.2 (i.e., 5 μL of standardized cell suspension at OD<sub>600</sub> ~ 4 in each 100 μL-filled sample well).
8. Once the plate is ready, place it immediately into the reader and run your protocol for the planned time course.
9. After the run, data can be extracted as a spreadsheet and imported in conventional statistical software for analysis. Whenever necessary, preprocessing methods can be applied at this stage, such as background correction and optical path correction (*see* **Notes 9** and **4**).
10. Besides traditional growth curves, an interesting way to look at the data is to calculate the evolution of the growth rate  $\mu$  during the experiment, using a sliding window. Growth rate between sampling points  $i$  and  $j$  can be assessed using the equation:

$$\mu_{ij} = (\text{LN}(x_j) - \text{LN}(x_i)) / (t_j - t_i) \quad (\text{v})$$

where  $x_j$  and  $x_i$  are the OD values measured at time  $t_j$  and  $t_i$ , respectively. Monitoring of the growth rate can be helpful to understand the behavior of a sample or a strain during the different stages of the cultivation, especially when comparing carbon source utilization (*see* Fig. 1).

### **3.2 Growth Kinetics on Hydrophobic Substrates Using a Fluorescent Reporter**

In opaque media such as emulsion of oleic acid, optical density cannot be measured accurately. In such conditions, constitutive expression of a fluorescent protein provides an alternative for monitoring the growth.

Red fluorescent proteins (RFP) have maxima of fluorescence emission above 560 nm. They represent a valuable alternative or a complement to the widely used green fluorescent proteins (GFP), to which they are structurally related (for review see [16]). Due to longer wavelength excitation, *in vivo* use of RFP benefits from a lower autofluorescence background and a reduced cellular phototoxicity. drFP583, better known as DsRed, was the first available RFP, isolated from a coral *Discosoma* species in 1999 [17]. No known cofactors or external conditions other than oxidation are required for chromophore maturation. The process relies on molecular oxygen, but only rigorous anoxia prevents fluorescence [18]. DsRed is insensitive to pH from 5 to 12, is relatively resistant to photobleaching, and is stable [17, 19]. In its original form, DsRed had several shortcomings, including the severe drawback of very slow maturation ( $t_{1/2} \sim 24$  h). Many improved versions or proteins from different sources have however been obtained by different teams [18]. We use RedStar2, a combination of two variants of DsRed (i.e., RedStar [20] and T4 DsRed), cumulating optimized codon usage for yeast, brightness, fast maturation, and solubility [21]. In our experiments, RedStar2 gave robust fluorescence and allowed to easily compare growth of different strains of

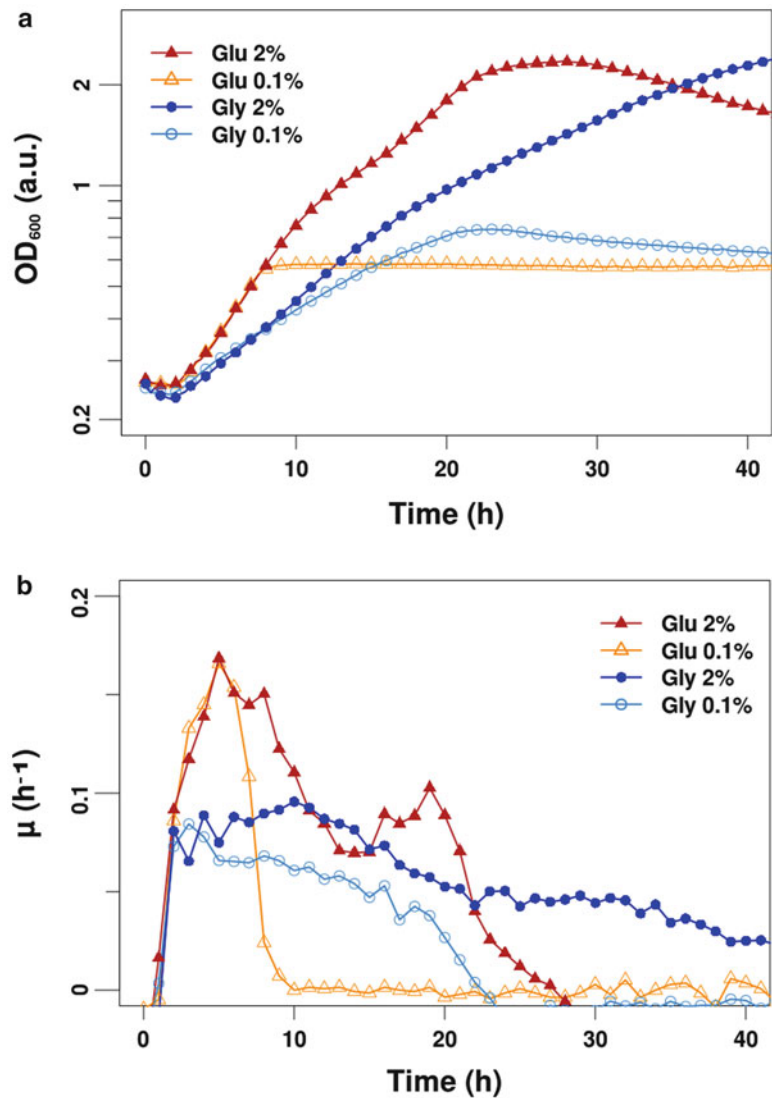


**Fig. 1** Growth kinetics of *R. toruloides* on glucose and glycerol at various concentrations (0.1 and 2%). (a) Optical density and (b) growth rate  $\mu$  ( $\text{h}^{-1}$ ).  $\mu$  was calculated using a sliding window of 1 h. Calculating  $\mu$  with sliding windows allows to detect easily a two-phase growth in the 2% glucose medium. Data were acquired using a Synergy MX microplate reader

*Yarrowia lipolytica* on non-translucent media which usually prevent direct read of OD or scatter light (*see* **Note 10**). However, one has to consider the fact that emulsions of hydrophobic substrates, such as oleic acid, may give a high background signal that changes over time. This is especially true for concentrations above 0.4% that may hamper correct detection of slow-growing strains. We thus encourage preliminary experiments to validate the conditions of growth in

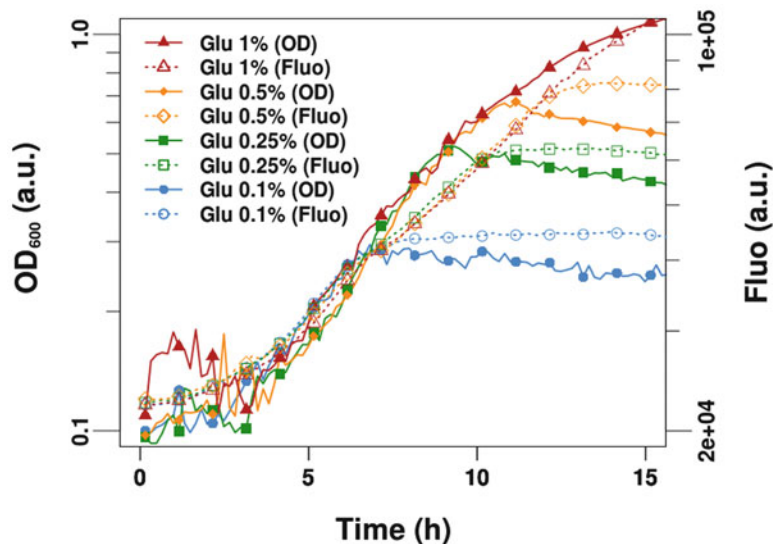


**Fig. 2** Assessment of RedStar2 fluorescence, as a growth indicator for *Y. lipolytica*. A *Y. lipolytica* WT strain, constitutively expressing the RFP, was grown in YNB medium supplemented with glucose at different concentrations. For each condition, the kinetics obtained through the traditional measurement of  $OD_{600}$  and the fluorescence intensity both produced a similar growth curve. Data were acquired using a Synergy 2 microplate reader

the plate reader and the measurement of the fluorescence signal with appropriate controls.

1. Construct strains “labeled” with the fluorescent protein using appropriate genetic tools for your organism. The RFP gene should be expressed from a strong and constitutive promoter. See **Note 3** for a summarized description of the procedure we follow for *Y. lipolytica*.
2. Check transformants for proper growth, correct expression, and possible multiple integration of the RFP cassette. This is readily performed by comparing the fluorescence level of several transformants during a preliminary experiment in which growth in glucose allows measurement of both  $OD_{600}$  and fluorescence intensity. Figure 2 shows characteristic growth curves obtained with a RFP-producing strain of *Y. lipolytica* by OD or fluorescence measurement, varying the sugar concentration.
3. Prepare an emulsion of fatty acid at 20%. Mix the solution of oleic acid with water and 0.5% (v/v) Tween 40 (see **Note 11**). Sonicate for three cycles of 1 min, interrupted by 1 min incubation on ice. Use this stock solution to prepare the YNB medium supplemented with oleic acid at the desired concentration (usually in the range of 0.1–1%).

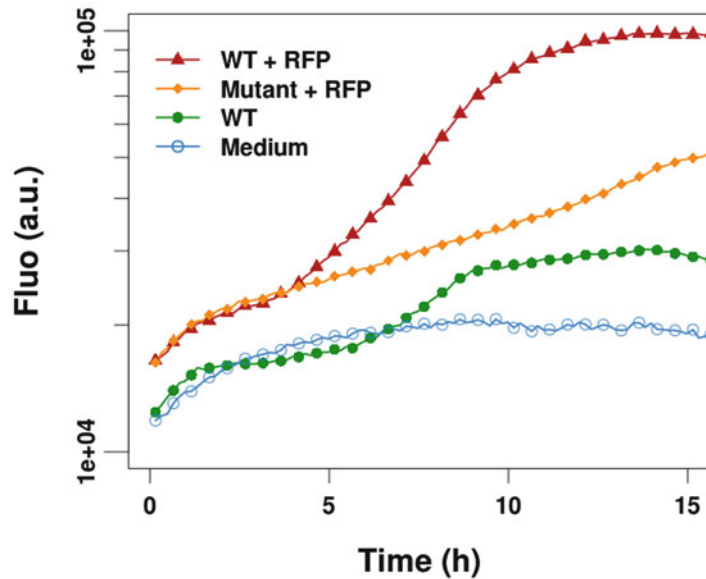


**Fig. 3** Comparative growth of two strains of *Y. lipolytica* showing different ability to use oleic acid as a carbon source. WT strain efficiently uses oleic acid via peroxisomal  $\beta$ -oxidation and therefore grows rapidly. Mutant strain is affected in several *POX* genes, decreasing the efficiency of the  $\beta$ -oxidation pathway. Growth of both strains is followed through the expression and fluorescence of the red fluorescent protein RedStar2. The inherent autofluorescence of *Y. lipolytica* during growth is measured by the WT strain not expressing the RFP. Data were acquired using a Synergy 2 microplate reader

4. Prepare your experiment as described in subheading 3.1. The preculture can be grown in YPD medium.
5. In the microtiter plate reader, add a step for fluorescence measurement, including excitation and emission wavelengths (e.g., for RedStar2 monitoring using the BioTek Synergy MX, we routinely use 545 nm for the excitation wavelength and 585 nm for the emission). To further optimize signal detection, set bandpass relatively wide for emission (e.g., 13.5) and narrower for excitation (e.g., 9), if the apparatus allows it. See **Note 12** for a complement on setting up filter-based apparatus.
6. Inoculate the microtiter plate and start culture, as described in steps 4 to 8 of subheading 3.1.
7. Display curves of fluorescence versus time for each sample, so that you can compare growth of different strains as in Fig. 3. Subtracting the background signal of the medium may not be recommended, as this will amplify the variability of the signal, due to the different evolution of the medium being a substrate for a growing strain or not.

### **3.3 Definition of C/N Ratio for Optimum Lipid Accumulation in Microtiter Plates**

As described in the literature, lipid accumulation in oleaginous yeasts can be triggered by a nutrient limitation, usually nitrogen. The mass ratio of carbon versus nitrogen molecules in the medium has been shown to play a critical role on the optimal routing of carbon fluxes toward lipid synthesis, instead of other metabolism (e.g., citric acid synthesis in *Y. lipolytica*) [1].

By parallelizing multiple growth conditions on a single microtiter plate, one can easily set up an experimental design to identify the best C/N ratio(s) for lipid accumulation.

1. Prepare your experimental design and protocol according to steps 1 and 2 of subheading 3.1. Include replicates using various YNB C/N media, prepared as described in subheading 2.3 (see Note 13).
2. Grow a preculture as described in step 3 of subheading 3.1.
3. Proceed with inoculation and cultivation, as described in steps 4 to 8 of subheading 3.1.
4. Harvest samples in late exponential phase to assess their lipid content. Do not wait until stationary phase, as cells will start to assimilate their own lipid stocks to compensate with the lack of carbon source in the medium.
5. For 100  $\mu$ L sample, add 1  $\mu$ L of a 0.1 $\times$  BODIPY stock solution.
6. Evaluate the lipid content using fluorescence microscopy with a YFP filter. Imaging parameters (e.g., excitation intensity, exposure time) must be set up on a sample showing an intermediate accumulation level (e.g., C/N 30) and applied to all samples. Combining fluorescence with illumination techniques such as differential interference contrast (i.e., DIC, Nomarski) can be useful to distinguish the lipid bodies (see Fig. 4). Alternatives to fluorescence microscopy are discussed in Note 14.

### **3.4 Real-Time Detection of Lipid Accumulation by Fluorescent Methods**

Another advantage of growing oleaginous yeast in microtiter plates is the possibility to follow lipid accumulation during the growth by measuring the time course of the fluorescence intensity of a dye specific for neutral lipids. Here we use the BODIPY 493/503 as a specific dye for lipid bodies (Nile red can be used as an alternative). Adding BODIPY directly to the medium during growth generates fluorescent background not specific to the staining of lipid bodies. Background fluorescence can however easily be avoided by using a quencher such as potassium iodide (KI). Being excluded from cells, KI will solely quench BODIPY fluorescence in the medium, thus making fluorescent detection specific to intracellular lipids [22]. The protocol can be used to identify strains with lipid accumulation defect/improvement and to follow kinetics of accumulation.

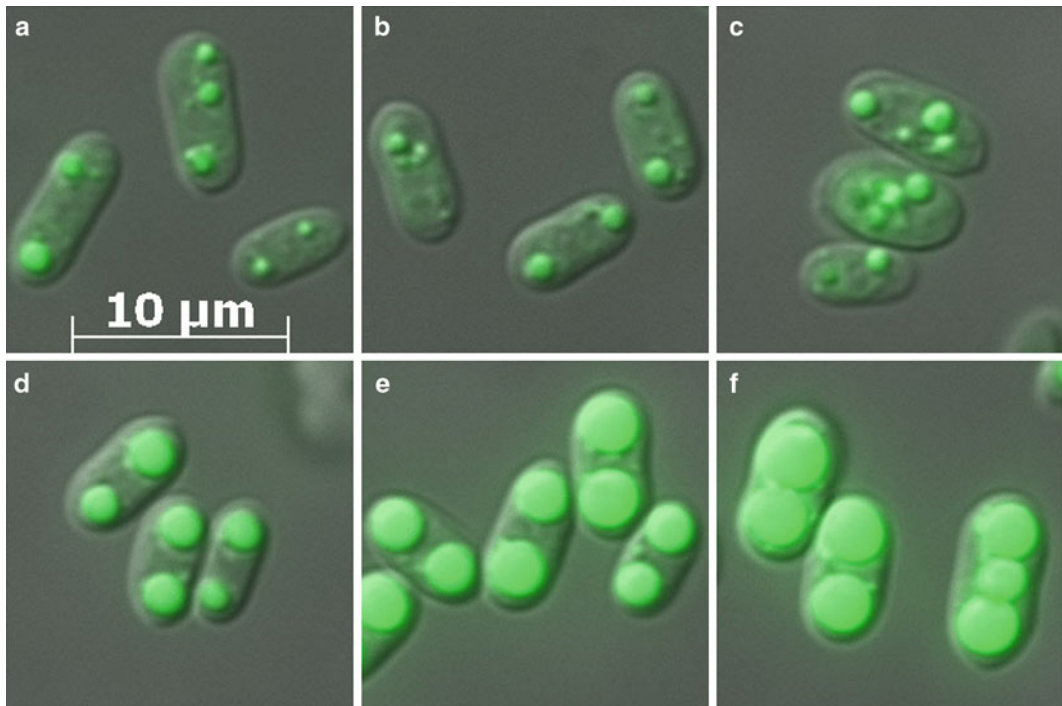


**Fig. 4** Cells of *Rhodosporidium toruloides* CECT1137, grown on media with C/N ratio of (a) 10, (b) 20, (c) 30, (d) 60, (e) 90, (f) 120. Lipids are stained with BODIPY. Pictures were taken by microscopy, using a YFP fluorescence filter and a Nomarski illumination

1. Grow precultures, as described in step 3 of subheading 3.1.
2. Prepare YNB medium with a C/N of 30, as described in subheading 2.3, or with the appropriate C/N according to the species tested. Complement the medium with KI (see Note 15) at a final concentration of 0.4 M and BODIPY at a final concentration of 3.8  $\mu\text{M}$  (1  $\mu\text{g}/\text{mL}$ ).
3. Inoculate the microtiter plate and start culture, as described in steps 4 to 8 of subheading 3.1. Monitor the cultivation every 20 min at 600 nm for absorbance and for fluorescence at 480/501 nm for excitation and emission, respectively, with a band-pass of 9 and a gain setup at 80. Gain must be set up for each medium/species/equipment to stay in the range of detection (without saturation of the signal) at the maximum accumulation stage (see Note 16).
4. Display graphically the growth kinetics (i.e., relative  $\text{OD}_{600}$ ) and fluorescence (i.e., relative fluorescence unit) to visualize growth and lipid accumulation (Fig. 5). If growth (i.e., biomass) in the different wells is not comparable (e.g., growth differences between strains/conditions), it is necessary to calculate the fluorescence/ $\text{OD}$  ratio in order to normalize fluorescent data.

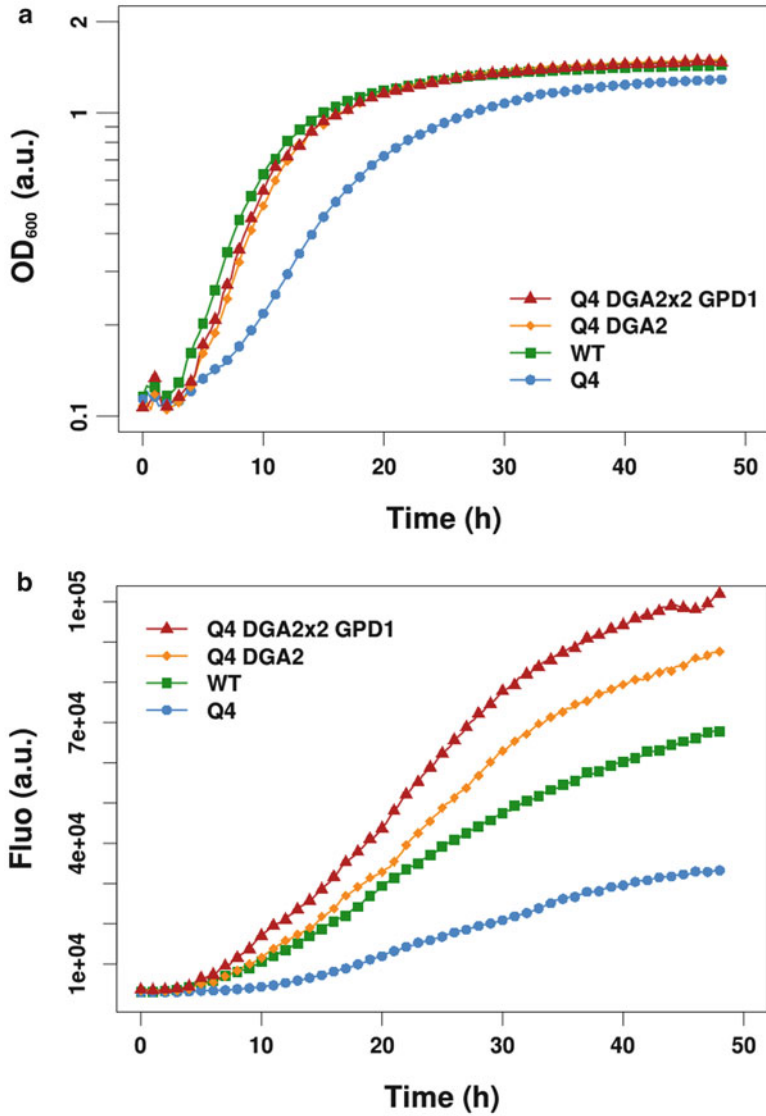


**Fig. 5** Four *Y. lipolytica* strains with various levels of lipid accumulation, from very low accumulation (Q4), wild-type accumulation, high accumulation (Q4-DGA2), and very high accumulation (Q4-DGA2 $\times$ 2, GPD1). See **Note 17** for description of the strains. Cultivation was performed in YNB glucose 0.5% with C/N = 30. **(a)** Relative OD<sub>600</sub> kinetics of the four strains tested. **(b)** Relative fluorescence kinetics of the four strains tested corresponding to lipid accumulation kinetics. Data were acquired using a Synergy MX microplate reader

## 4 Notes

1. For fluorescent detection, we did not find necessary to use black plates (with clear bottom for OD<sub>600</sub> measurement) as interference in fluorescence signals between wells is not significant in our hand. However, this must be checked for each species/conditions/apparatus.
2. Depending on the experimental setup (e.g., duration of cultivation, frequency of measurement), a microtiter plate reader can produce a large amount of data. To enhance clarity and readability, it might prove useful not to plot every spot when drawing a growth curve. As an example, the growth curves illustrating subheadings 3.1, 3.2, and 3.4 have been generated using a combined method: for each figure, the complete dataset was used to draw the line of each curve, while only a subset of the same data was used to draw the spots (e.g., 1 out of 3 spots).
3. Chromosomal integration of the gene coding for RedStar2 is easily done in *Yarrowia* for which efficient transformation and numerous genetic tools exist. In this case, we used random integration [7] of cassettes in which the RedStar2 gene is placed under the pTEF1 promoter associated with a choice of three selective markers. These cassettes are cut from vectors JMP1394 (carrying the *LEU2* prototrophic marker), JMP1491 (carrying the *URA3* prototrophic marker), or JMP1492 (conferring resistance to hygromycin), available upon request.
4. When using a microtiter plate instrument, OD measurement is taken vertically. Consequently, the optical path length (i.e., the distance light travels through the sample) varies depending on the volume of cultivation and the shape of the well (i.e., dimensions of the wells may differ, depending on the brand of the microtiter plate). A correction factor can be applied to the data after measurement, based on Beer-Lambert's law of light absorption (i.e., absorbance is proportional to the distance that light travels through the sample). This factor can be calculated mathematically: if the shape (e.g., cylindrical, cubic) and dimensions of the well are known, one can directly calculate the path length depending on the volume of the sample. Alternatively, the path length can be calculated experimentally by using the absorbance properties of water at 900 and 977 nm wavelengths. At room temperature, in a 1 cm cuvette, the difference between OD<sub>977</sub> and OD<sub>900</sub> of a water sample is ca. 0.18. By measuring in a microtiter plate the absorbance of a water sample at 900 and 977 nm, one can calculate the path length (in cm) of a sample using the equation:  $(OD_{977} - OD_{900})_{\text{water sample}}/0.18 = \text{path length}$ .

5. When preparing an experimental design (i.e., location of samples/blanks, on the plate, number of replicates), one should take into account evaporation. For long-term experiments (i.e., 24 h and more), we strongly recommend not to use the wells located on the outer lines/columns of the microtiter plate. Instead, we fill these outer wells with 200  $\mu$ L water (or blank medium) to act as a buffer against evaporation of the inner wells. By doing so, we limit the number of wells available for sample to 60 in a 96-well plate, but we improve the consistency of the measurement over long period.
6. Sample dilution before OD measurement is not possible. Nevertheless, OD linearity is generally certified by the manufacturers, with less than 1% error for OD values ranging from 0 to ca. 3 units. Consequently, it is recommended not to add an excess of carbon source in order to limit biomass.
7. Shaking is an important parameter affecting both aeration and cell sedimentation (e.g., *Y. lipolytica* has a tendency to sediment easily). Limitation of oxygen transfer rate could be a particular problem for strictly aerobic microorganism. Usually, lower volume and intense shaking increase oxygen rate transfer within cell suspensions.
8. When inoculating numerous different strains on the same plate (e.g., screening of various clones/species in the same medium), one can perform the preculture in 96-well microtiter plate instead of individual test tubes. This allows rapid inoculation of the experimental plate by using multichannel pipette. To avoid fastidious per well inoculum standardization, we recommend to grow the precultures for at least 36 h, so that all the strains reach stationary phase and a similar OD. This proved to reduce variability between inoculated wells. Preculture time has to be adapted according to the yeasts and/or strains used.
9. When preparing an experimental design, one can use nonsample wells to measure the background absorption of a blank medium. When processing the data, background can then be subtracted from the signal, but is not mandatory. When subtracting background, we recommend to use a mean background value calculated over the experiment, rather than subtracting a background measured point by point. The latter approach might induce more noise than correction in the processed data.
10. According to [23], dense/turbid suspensions can interfere with excitation light and emission signal. While this may potentially lead to lower absolute fluorescence measurements for cultures in stationary phase, it does not affect the reliability of comparative analyses.

11. Alternative emulsifying agents may be used (e.g., Tween 80), although Tween 40 happened to be the most efficient for creating a stable emulsion in our experience. You can store the emulsion at room temperature for 1 week.
12. For BioTek Synergy 2, wavelength and bandpass are determined by the chosen filters, 530/25 for emission and 620/40 for excitation.
13. C/N media can be prepared by either fixing the concentration of the carbon and/or the nitrogen source. To induce lipid storage, it is however recommended to fix the carbon source and to modify the nitrogen concentration, rather than the opposite, as described in subheading 2.3. Reducing nitrogen concentration to increase C/N ratio will be a better mimic of a nitrogen limitation.
14. Fluorescent microscopy, as described in subheading 3.3, is an efficient and relatively cheap method to compare the lipid content of cells grown using different C/N ratio, qualitatively. Flow cytometry could be an interesting alternative. It combines the advantages of working with limited sample amount, measuring data at a single cell scale, and extrapolating information at the population scale. Furthermore, it combines the qualitative aspect of microscopy, with a quantitative measure of fluorescence. Alternatively, one can also combine the methods described in subheadings 2.3 and 2.4, for continuous monitoring of lipid accumulation under various C/N conditions.
15. Quenching of external BODIPY fluorescence by KI is not suited for oleic acid-containing broth, at least for *Y. lipolytica*, for which no growth was observed under these conditions.
16. For proper measurement of BODIPY in microtiter plate reader, we recommend to test several gains in conditions where accumulation reaches its maximum in order to define the maximum level of fluorescence to be detected. Set up the gain to be under the saturating level of the detection system of the apparatus.
17. The *Y. lipolytica* strain Q4 is deleted for all the acyltransferases and therefore is not able to store lipids in lipid bodies [24]. The Q4-*DGA2* strain corresponds to the Q4 strain overexpressing the acyltransferase gene *DGA2*, which increases storage capacity [24]. The Q4-*DGA2*×2 *GPD1* strain (unpublished data) overexpresses two copies of *DGA2* and 1 copy of the glycerol-3-phosphate dehydrogenase gene *GPD1* which increases lipid accumulation [25]. All strains have been transformed to be prototroph.

## References

1. Beopoulos A, Cescut J, Haddouche R, Uribealra JL, Molina-Jouve C, Nicaud JM (2009) *Yarrowia lipolytica* as a model for bio-oil production. *Prog Lipid Res* 48:375–387
2. Ratledge C, Wynn JP (2002) The biochemistry and molecular biology of lipid accumulation in oleaginous microorganisms. *Adv Appl Microbiol* 51:1–51
3. Thevenieau F, Nicaud JM (2013) Microorganisms as sources of oils. *OCL* 60:D603
4. Nicaud JM (2012) *Yarrowia lipolytica*. *Yeast* 29:409–418
5. Dujon B, Sherman D, Fischer G et al (2004) Genome evolution in yeasts. *Nature* 430:35–44
6. Le Dall MT, Nicaud JM, Gaillardin C (1994) Multiple-copy integration in the yeast *Yarrowia lipolytica*. *Curr Genet* 26:38–44
7. Pignede G, Wang HJ, Fudalej F, Seman M, Gaillardin C, Nicaud JM (2000) Autocloning and amplification of *LIP2* in *Yarrowia lipolytica*. *Appl Environ Microbiol* 66:3283–3289
8. Fickers P, Le Dall MT, Gaillardin C, Thonart P, Nicaud JM (2003) New disruption cassettes for rapid gene disruption and marker rescue in the yeast *Yarrowia lipolytica*. *J Microbiol Methods* 55:727–737
9. Loira N, Dulermo T, Nicaud JM, Sherman DJ (2012) A genome-scale metabolic model of the lipid-accumulating yeast *Yarrowia lipolytica*. *BMC Syst Biol* 6:35
10. Pan P, Hua Q (2012) Reconstruction and in silico analysis of metabolic network for an oleaginous yeast, *Yarrowia lipolytica*. *PLoS One* 7:e51535
11. Kumar S, Kushwaha H, Bachhawat AK, Raghava GP, Ganesan K (2012) Genome sequence of the oleaginous red yeast *Rhodospiridium toruloides* MTCC 457. *Eukaryot Cell* 11:1083–1084
12. Zhu Z, Zhang S, Liu H et al (2012) A multi-omic map of the lipid-producing yeast *Rhodospiridium toruloides*. *Nat Commun* 3:1112
13. Lin X, Wang Y, Zhang S et al (2014) Functional integration of multiple genes into the genome of the oleaginous yeast *Rhodospiridium toruloides*. *FEMS Yeast Res*. doi:10.1111/1567-1364.12140
14. Abbott EP, Ianiri G, Castoria R, Idnurm A (2013) Overcoming recalcitrant transformation and gene manipulation in *Pucciniomycotina* yeasts. *Appl Microbiol Biotechnol* 97:283–295
15. R-Core-Team (2014) R: a language and environment for statistical computing. R Foundation for Statistical Computing, Vienna, Austria
16. Piatkevich KD, Efremenko EN, Verkhusha VV, Varfolomeev DD (2010) Red fluorescent proteins and their properties. *Russ Chem Rev* 79:243–258
17. Matz MV, Fradkov AF, Labas YA et al (1999) Fluorescent proteins from nonbioluminescent Anthozoa species. *Nat Biotechnol* 17:969–973
18. Shaner NC, Steinbach PA, Tsien RY (2005) A guide to choosing fluorescent proteins. *Nat Methods* 2:905–909
19. Baird GS, Zacharias DA, Tsien RY (2000) Biochemistry, mutagenesis, and oligomerization of DsRed, a red fluorescent protein from coral. *Proc Natl Acad Sci U S A* 97:11984–11989
20. Knop M, Barr F, Riedel CG, Heckel T, Reichel C (2002) Improved version of the red fluorescent protein (drFP583/DsRed/RFP). *Biotechniques* 33:592, 594, 596–598 passim
21. Janke C, Magiera MM, Rathfelder N et al (2004) A versatile toolbox for PCR-based tagging of yeast genes: new fluorescent proteins, more markers and promoter substitution cassettes. *Yeast* 21:947–962
22. Bozaquel-Morais BL, Madeira JB, Maya-Monteiro CM, Masuda CA, Montero-Lomeli M (2010) A new fluorescence-based method identifies protein phosphatases regulating lipid droplet metabolism. *PLoS One* 5:e13692
23. Lakowicz JR (2006) Principles of fluorescence spectroscopy, 3rd edn. Springer, New York
24. Beopoulos A, Haddouche R, Kabran P, Dulermo T, Chardot T, Nicaud JM (2012) Identification and characterization of *DGA2*, an acyltransferase of the DGAT1 acyl-CoA: diacylglycerol acyltransferase family in the oleaginous yeast *Yarrowia lipolytica*. New insights into the storage lipid metabolism of oleaginous yeasts. *Appl Microbiol Biotechnol* 93:1523–1537
25. Dulermo T, Nicaud JM (2011) Involvement of the G3P shuttle and beta-oxidation pathway in the control of TAG synthesis and lipid accumulation in *Yarrowia lipolytica*. *Metab Eng* 13:482–491

# Protocol for Start-Up and Operation of CSTR Biogas Processes

A. Schnürer, I. Bohn, and J. Moestedt

## Abstract

There is currently a lack of consensus on how biogas processes should be started and run in order to obtain stable, efficient operation. Agreement on start-up and operating parameters would increase the quality of research, allow better comparison of scientific results and increase the applicability of new findings in a general perspective. It would also help full-scale operators avoid common costly mistakes during start-up and operation of biogas processes. The biogas protocol presented in this paper describes appropriate approaches for characterisation of substrate, determination of methane potential, formulation of a suitable substrate, start-up of reactors and monitoring and operation of the biogas process in CSTR reactors.

**Keywords:** Biogas, BMP, CSTR, Monitoring, Operation, Start-up, Substrate composition

---

## 1 Introduction

Anaerobic digestion (AD) is a biological treatment method for reducing and stabilising various types of organic matter in the absence of oxygen, while at the same time producing biogas. In the past this technology has mainly been applied in waste treatment and management, but recently the focus has shifted to energy generation and nutrient recovery, including not only organic wastes but also dedicated energy crops in some countries [1, 2]. Biogas is a versatile renewable energy source that can be used for replacement of fossil fuels in power and heat production and can also be converted to vehicle fuel [3]. Methane-rich biogas can also replace natural gas as a feedstock for production of other biochemicals [3, 4]. Moreover, during the process nutrients are retained, making the digestion residue suitable as an organic fertiliser that can replace fossil energy-requiring mineral fertilisers [5, 6]. Materials used for biogas production include sewage and industrial organic wastewater, waste from the food and animal feed industries, source-sorted municipal solid waste, livestock and poultry manure and stillage from ethanol production [3, 7, 8]. Typical crops for biogas include,

for example, maize and grass silage [2, 3, 9]. The AD technology can be implemented on either small or large scale, making it interesting when designing flexible and sustainable energy solutions for industrial applications and also for farms and even single households, as typically seen in developing countries [10, 11]. In a number of studies, production of biogas has been shown to offer significant advantages over other forms of bioenergy production and it has been rated one of the most energy-efficient and environmentally beneficial technologies for bioenergy production [11, 12].

Anaerobic digestion of organic material to biogas is a complex microbiological process requiring the combined activity of several groups of microorganisms with different metabolic capacities and growth requirements [13]. The degradation process can be divided into four main steps; hydrolysis, acidogenesis, acetogenesis and methanogenesis. In the latter steps many organisms operate in intricate and sometimes obligate relationships, e.g. syntrophy, in which neither organism can thrive without the other and together they exhibit metabolic activities that they could not accomplish on their own [14]. To obtain a stable and efficient biogas process, all these conversion steps and microorganisms must work in a synchronised manner and it is important to fulfil the requirements of all microorganisms involved. In order to achieve a stable, efficient process, the material added to the degradation process must have a good balance of both macro- and micronutrients [13]. Some materials work well as a single substrate, while others can only be used during co-digestion with other substrates that result in favourable nutrient and water content and dilution of potential inhibitors [7]. To ensure sufficient microbial activity, some materials and mixtures of materials may also have to be complemented with process additives such as iron, trace metals or buffering chemicals [15–17, 136]. In addition to the nutrient composition, operating parameters such as pre-treatment method, load of input material, duration of degradation, process temperature and stirring are of critical importance and have to be set properly to ensure high activity and gas yields with minimised risk of inhibition or washout of critical functions and microorganisms [18–21]. In conclusion, many different aspects need to be taken into consideration to reach optimal degradation and gas production. In addition, consideration must be given to achieving good digestate quality not only regarding nutrient content, but also regarding the content of chemical inhibitors or biological contaminants such as different pathogens [5, 22, 23]. It should be borne in mind that many operating and biological parameters are interlinked, sometimes with counteracting effects.

Prior to start-up of a full-scale process or as a tool to optimise and evaluate a specific biogas process or substrate, evaluation at laboratory scale may be advisable. By performing such studies, different factors can be evaluated alone or in combination under controlled conditions, without risking loss of stability and/or loss

of gas production in the full-scale process. It has been shown that such laboratory experiments result in similar gas yields and process performance as full-scale processes [24–27]. However, large-scale processes typically exhibit a variability regarding substrate composition and operating parameters that is difficult to replicate in a laboratory-scale scenario. Moreover, some parameters of a technical and logistics character are difficult to evaluate at laboratory scale. Thus in order to fully evaluate and comprehend all parameters of importance for starting up and operating an AD process, results from both small-scale and large-scale studies need to be considered [28]. Furthermore, in order to obtain reliable results for practical full-scale applications, the set-up of laboratory-scale experiments in terms of start-up and operation, preparation of substrate, application of process additives, etc., and monitoring and evaluation of the biogas process is critical. This protocol provides guidance on setting up, operating and monitoring biogas processes in a uniform manner.

---

## 2 Materials

For start-up and operation of laboratory-scale biogas processes, materials and equipment are needed for the process itself and for the preparation of substrates, monitoring and evaluation of the process. Many different set-ups are possible and can be used as long as some basic principles are observed, such as airtight container, efficient stirring, temperature regulation and appropriate dimensioning. The concept can be rather simple and low cost, requiring operation mainly by manual mode, or more advanced and highly automated. Thus this protocol does not suggest any particular equipment, but merely refers to different studies where such information is available. The equipment and materials needed for different analytical methods are given in the protocol when mentioned. The most frequently used design is the continuously stirred tank reactor (CSTR), which compared with many other configurations is rather simple to construct and operate [24, 29]. A schematic diagram of a CSTR reactor is presented in Fig. 1. The reactor has a stirrer and an inlet/outlet for substrate/digestate. Depending on the character of the material, the influent stream can either be pumped continuously or fed manually in semi-continuous mode. The inlet tube is typically placed under the surface of the liquid to minimise oxygen entry during feeding. In full-scale plants the material is inserted directly to the reactor or indirectly via a circulation circuit. Material is usually taken out through a separate outlet, typically placed in line with the liquid level, allowing excess material to flow over or alternatively actively pumped out. In lab-scale mode material can also be taken out from the reactor through the inlet tube (by use of a vacuum

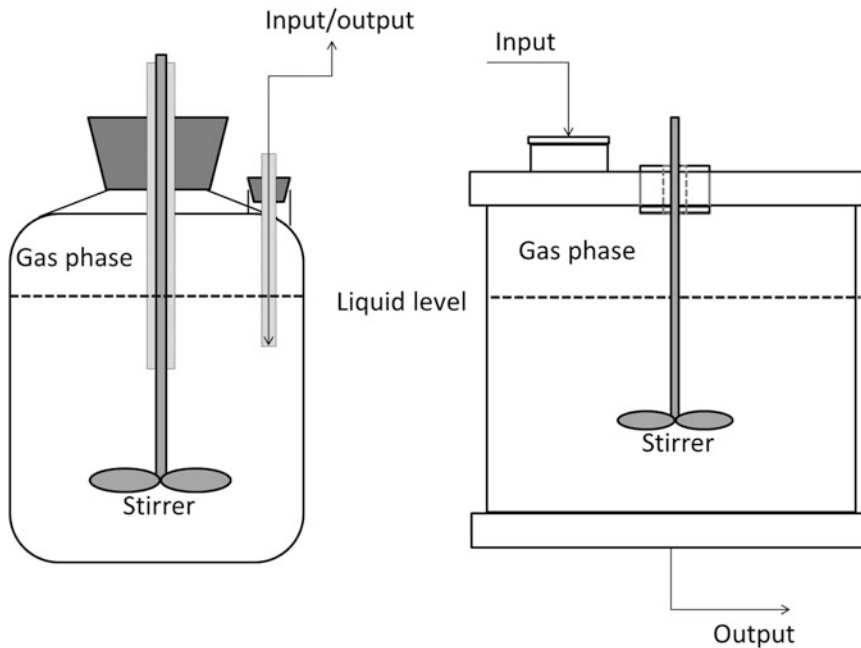


**Fig. 1** Schematic diagram of continuously stirred tank reactors for laboratory or full-scale application. *Left:* A simpler design of reactor typically operated in manual mode. *Right:* A more advanced reactor typically designed to allow automatic adjustment to the desired volume, completely air-free operation and sometimes continuous pumping of substrate

pump). The gas is taken out from headspace at the top and passes through a gas volume counter. The gas can also be measured through water displacement or by collection to a gas bag for later volume measurement.

### 3 Methods

This section provides information concerning the start-up and operation of a continuous anaerobic digestion process for laboratory-scale or large-scale application. The type of process described is a one-stage CSTR, the digestion system most commonly used in full-scale biogas plants in Europe [3], but many of the factors listed in the protocol are also applicable to other type of processes. The protocol focuses on parameters important for the functioning and stability of the biological biogas process and can be used as guidelines for large-scale operation and/or for evaluation/operation of processes in laboratory reactors used in research.

#### 3.1 Chemical Characterisation of the Organic Substrate

The chemical composition of the substrate has a strong impact on the process and needs to be considered when determining the individual proportion of different materials to be used in a substrate mixture and the need for process additives, and when setting

operating conditions. Optimally, the substrate should have a composition that meets the nutrition requirements of the microorganisms involved and also results in high biogas and methane yield and a high quality digestate in terms of high nutrient composition and low levels of contaminants. Different analyses can be used to determine the composition of the substrate, depending on the purpose (industrial plant or research process) and available equipment. Below are some suggestions of relevant analyses and procedures.

1. Sampling for chemical analysis should be performed to ensure that a representative sample of the substrate can be taken (*see Note 1*). Thus it is important that the sample is well mixed and that the sample size is adjusted to ensure that a representative sample can be obtained. Each sample should also be analysed at least in triplicate.
2. Determination of the dry matter, organic content and ash. This analysis can be performed by different methods (*see Note 2*), but one common procedure is to analyse the content of total solids (TS) and volatile solids (VS) by initial drying at 105°C for 20 h, followed by incineration at 550°C for 3 h (APHA, 1998). The material left after drying and burning represents the TS and ash content, respectively. The weight loss after the initial drying and incineration corresponds to the water and VS content, respectively (*see Note 2*).
3. Analysis of total ammonium-nitrogen and total organic nitrogen (*see Note 3*). Here, the Kjeldahl method is standard. The procedure for total organic nitrogen (Kjeldahl-nitrogen) consists of three basic steps: (1) digestion of the sample in sulphuric acid with a catalyst, which results in conversion of nitrogen to ammonia; (2) distillation of the ammonia in boric acid and (3) quantification of the ammonium by titration with hydrochloric acid (Kjeltec application subnote 3502). For ammonium-nitrogen (NH<sub>4</sub><sup>+</sup>-N), determination steps 2 and 3 of the Kjeldahl procedure are applied.
4. pH analysis. Some substrate streams can have low/high pH. Low alkalinity can potentially affect the process negatively (*see Note 4*).
5. Volatile fatty acid (VFA) analysis. For easily degradable material, fatty acid production can be induced during transportation/storage by activation of hydrolysis and fermentation. If levels are high, there are potential risks of underestimating the TS and VS content and of acidification of the process. Methods of analysis are described in the section on monitoring (*see Notes 2 and 5 and Subheading 3.5*).
6. Analysis of phosphate and phosphorus is of interest regarding fertiliser quality, but also as too low levels can cause deficiency and hence process instability. Phosphate phosphorus (PO<sub>4</sub>-P)

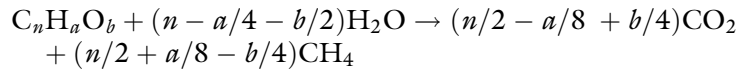
can be spectrophotometrically determined after acidification with sulphuric acid ( $\text{H}_2\text{SO}_4$ ) and reaction with antimony potassium tartates, ammonium molybdate and ascorbic acid (ISO 15923-1:2013). For total phosphorus (P-tot), extraction is performed at 30 min and  $120^\circ\text{C}$  with potassium peroxide monosulphate according to SS-EN ISO 6878:2005 and then according to the method for phosphate phosphorus.

7. Metal analysis is performed in order to determine the levels of heavy metals for fertiliser quality and trace elements (*see Note 6*). Metals are typically extracted from sludge using concentrated nitric acid ( $\text{HNO}_3$ ) and heating for 15 min at  $150^\circ\text{C}$ . The extracted samples can be analysed with ICP-AES (ISO 11885:2009 edition 2).
8. Determination of component and element composition (*see Note 7*). In order to compose a suitable substrate mixture, regarding both gas production and estimation of biogas potential and biogas production rate, it can be of interest to know the content of protein, lipids, carbohydrates and lignin (*see Subheading 3.2*). The analysis can be performed as, e.g. for animal feeds [30]. Alternatively, an elemental composition analysis to determine the composition of C, H, O and N can be of value [31].
9. The sulphur and sulphate content in the substrate mixture is important due to the effect on gas quality, e.g. hydrogen sulphide ( $\text{H}_2\text{S}$ ), gas yield and the performance of the microbial degradation process (*see Note 8*). Analysis of sulphur can be performed with ICP-AES after acidification and heating to  $120^\circ\text{C}$  for 2 h [32]. Sulphate can be measured indirectly using simple cuvette tests measuring turbidity or spectrometric analyses according to, e.g., ISO 22743.

### **3.2 Determination of Biogas Potential**

Determination of the methane potential is of great importance not only for economic calculations during planning and operation of industrial biogas plants, but also for evaluation of process performance, i.e. comparison of expected yield and that obtained in practice (*see Subheading 3.5*). The chemical composition of the material used as substrate affects the biogas yield and the methane content of the gas [30, 33]. Moreover, the composition influences the biodegradability and degradation kinetics [34, 35]. Different methods can be used to estimate the biogas potential and biogas production rate in a material of interest for biogas production, either by using the chemical composition for theoretical calculations (1 and 2 below) or by using a practical method (3 below). The theoretical calculations usually give an overestimate of the methane potential as they do not consider that some carbon compounds are recalcitrant to degradation and that part of the material is used for formation of new biomass.

1. Calculation with the Buswell formula: This formula can be used for calculating the theoretical methane production of a specific material if the composition regarding C, H, O and N is known [36];



2. Calculation based on the component composition. By assuming the elemental composition  $(C_6H_{12}O_5)_n$ ,  $C_{57}H_{104}O_6$  and  $C_5H_7N_2O_2$  for carbohydrates, lipids and proteins, respectively, and applying the Buswell formula, the methane potential of these materials is estimated to be 0.415, 1.014 and 0.496  $CH_4$   $m^3/kg$  VS, respectively [37].
3. Biochemical methane potential (BMP) test. In this test, an inoculum containing a variety of anaerobic microorganisms is incubated with the substrate in a suitable medium and temperature. The biogas and methane production is determined over time and an accumulated methane curve is constructed, giving the methane potential. There are many parameters with an impact on the outcome of a BMP, including the character of the material and the set-up of the experiment, as reviewed in Raposo, De la Rubia, Fernández-Cegrí and Borja [33]. A typical set-up of a BMP-test is as follows:
  - (a) Selection of an appropriate inoculum (*see Note 9*).
  - (b) Pre-incubation of the inoculum for about 2–7 days at the temperature of interest to decrease the amount of gas arising from endogenous materials present in the inoculum (*see Note 9*).
  - (c) Mixing of inoculum and substrate in anaerobic bottles, preferably in triplicate, to a substrate:inoculum ratio of between 1:2 and 1:4, based on VS content (*see Note 10*). A suitable load of substrate in the test is 3 g VS/L, thus resulting in an inoculum corresponding to 6–12 g VS/L. The mixing should be performed under flushing with  $N_2/CO_2$  (80:20) to ensure anaerobic conditions.
  - (d) Dilution of the substrate/inoculum mixture with a suitable medium to reach the same volume in all test bottles. This medium can either be tap water or a buffer, depending on the alkalinity of the mixture and the character of the inoculum and substrate. It is important to ensure that the final pH is around 7–8 (*see Note 11*).
  - (e) Preparation of triplicate controls without substrate, so that gas production from the endogenous material present in the inoculum alone can be accounted for.

- (f) Preparation of triplicate control bottles using a compound with known methane potential as a substrate (*see Note 12*).
- (g) Incubation of the experimental bottles under shaking at the desired temperature (*see Note 11*).
- (h) Sampling of the bottles for analysis of gas production over time considering both volume produced and methane content of the gas (*see Note 13*). The incubation period is typically around 20–40 days and the gas analysis can be performed either in automatic mode, continuously monitoring both gas volume and methane content [38], or by manual sampling (*see Note 13*).
- (i) Construction of an accumulated methane production curve. The methane potential is reached when the production rate levels off to a plateau. The value obtained after deducting the gas production from the endogenous material in the inoculum represents the methane potential. The volumetric methane value should be normalised according to standard temperature (273.15 K) and pressure (1 bar), which can be done using the ideal gas law, and expressed as Nml CH<sub>4</sub>/g VS [38].

### 3.3 Composing a Suitable Substrate

Many different types of organic material can potentially be used for biogas production and the material selected should have a composition that meets the nutrient requirements of the microorganisms. However, as already mentioned, the substrate should optimally also result in high biogas and methane yield, as well as a digestate of good quality regarding high nutrient composition and low levels of contaminants. Sometimes these different requirements are difficult to meet, for example, some materials with high methane potential typically also cause problems in the biogas process due to formation of inhibitory components such as long chain fatty acids from fat or ammonia and sulphides from proteins [20]. In addition, some materials, such as plant-based materials, are restricted by low content of trace metals or low buffering capacity, [39]. Moreover, in large-scale applications the choice of material may be restricted to availability in the vicinity of the biogas plant. To overcome the drawbacks of a single material, simultaneous co-digestion using two or more substrates in a mixture is a feasible option to monodigestion [7, 40, 41]. For full-scale applications it is also important to consider additional parameters such as availability, cost, legislation/regulations and need for pre-treatments (*see Note 14*). Some selected typical materials and some parameters of importance with regard to biogas production are as follows:

1. Protein-rich materials, for example, slaughterhouse waste, food waste, fish waste, swine and chicken manure and stillage, typically give good biogas yield but have a low C/N ratio, and thus

may result in ammonia inhibition [42–46] (*see* **Notes 3, 8 and 15**). In addition, these materials result in high levels of hydrogen sulphide (*see* **Note 23**), influencing gas quality and the overall process [20, 47].

2. Materials rich in lipids, such as fat, oils, fish waste, slaughterhouse waste and sometimes food wastes have high biogas potential, but can cause process inhibition and foaming due to release of long chain fatty acids [43, 44, 48] (*see* **Note 5**).
3. Materials with a high degree of lignocellulose, such as straw and crop residues, give somewhat restricted biogas production and result in low biogas potential and slow degradation [49]. Some plant-based materials in this category also contain low levels of trace metals and alkalinity [19, 50].
4. Materials with a high level of easily accessible carbon, such as fruit residues, potato and sugar beets, undergo rapid initial conversion rate and can cause acidification in the process if added in high amounts [51].

### **3.4 Start-Up and Operation of the Reactor**

Laboratory-scale operation of a biogas process provides the opportunity for setting up experiments for evaluation of substrates and operating parameters under more controlled conditions than those in large-scale plants. However, each process is unique and can develop somewhat differently. A factor to consider during set-up is that two parallel, identically operated processes can still differ in terms of performance and microbiology [52]. On the other hand, there are examples in the literature of parallel reactors maintaining exactly the same performance over a long time [53, 54]. Another parameter to take into consideration is the evaluation period. A minimum operating period is three retention times after reaching the target operating parameters. This is the theoretical time needed to reach complete washout of non-active microorganisms and to reach steady state of the chemical composition. However, the time needed to reach a stable microbial community can be longer than three retention times [55]. Consequently, to secure good and reliable results, it might be appropriate to initiate more than one reactor and also to operate the process over a longer period than three retention times. If changes in process parameters are being evaluated, it is also recommended to have a control reactor not subjected to these changes, thus ensuring that the results obtained from the changes can be distinguished from changes caused just by time [53, 54].

1. Select a suitable inoculum. As with the BMP test, it is recommended to use inoculum taken from a well-functioning biogas process preferably using a similar substrate and operating parameters as planned for the new process (*see* **Note 16**).
2. Inoculate the reactor with a desired volume (typically about 70% of the total reactor volume) of the selected inoculum.

Optimally, the inoculum volume should be added on one occasion, but if there is not enough inoculum available add as much as possible and start feeding to reach the full volume (*see Note 17*)

3. Set the operating temperature and stirring frequency. Biogas production can proceed at different temperatures, but in industrial production is typically set to mesophilic (35–42°C) or thermophilic (46–60°C). Biogas production can also proceed at psychrophilic temperature (15–25°C) [56]. The temperature and stirring mode chosen depend on the type of process, substrate and other operating parameters (*see Notes 18 and 19*).
4. Set feeding amount. To ensure stable operation, the organic loading rate (OLR), defined as the amount of organic material added per reactor volume (active) and day, should be gradually increased. The organic content is typically defined as volatile solids (VS) or chemical oxygen demand (COD). The optimal initial and final load and the increase rate of OLR depend on several factors (*see Note 20*). If the process is operating with the same substrate or a substrate similar to that treated by the processes from which the inoculum was taken, the OLR can immediately be set as similar to that in the original process. Otherwise, a guideline is to start feeding with an initial load of around 0.5–1 g VS/L/day and to increase the load by 0.5 g VS/L/day every week until full load is reached (*see Note 20*). To ensure that the increase in OLR is not too high, monitoring is recommended (*see Subheading 3.5*).
5. Decide the feeding frequency. Feeding frequency in full-scale applications varies depending on the character of the substrate and can either be continuous or semi-continuous, the latter with a feeding frequency of approximately 1–10 times per day (*see Note 21*).
6. Set the hydraulic retention time (HRT). This time should be sufficiently long to allow efficient degradation of the input material at a minimum volume (*see Note 22*). The HRT should typically be set to 15–40 days, but can also be shorter or longer depending on substrate availability and operating parameters such as temperature and OLR [19] (*see Notes 18 and 20*).

### **3.5 Monitoring/ Evaluation**

It is important to carefully monitor the biogas process, as many different parameters can result in instability and failure of the process [49]. Monitoring makes it possible to detect problems in a timely manner and rectify them before things have gone so far that the process deteriorates. Some microorganisms, such as methane producers, are extremely sensitive and may stop growing and/or are washed out of the process if they do not thrive. For example, the process temperature must be closely monitored because

**Table 1**  
**Suggested frequency of off-line measurements for monitoring purposes**

Analysis	Times per week	Comment
Gas volume	Continuously/every day	Informative measure on process performance
Methane/carbon dioxide content	Continuously/every day	Informative measure on process performance
Hydrogen sulphide	Continuously/every day	To ensure good gas quality
pH	1–2	Needed for calculation of ammonia concentration
VFA	1–2	Analytical results must be obtained during 1–2 days to allow operating parameters, such as OLR, to be adjusted if VFA accumulate
NH <sub>4</sub> <sup>+</sup> -N	1	Does not change rapidly
VS	1	Used to calculate the degree of degradation
Temperature	Continuously	Rapid changes can cause instability
Alkalinity	1	Alkalinity changes prior to pH and can indicate risk for acidification

anaerobic microorganisms are very sensitive to temperature fluctuations. Alkalinity and pH, the concentration of fatty acids and ammonium and the carbon dioxide and methane content of the gas are other important parameters that should be followed throughout the process. A more detailed description of important parameters to analyse in regular monitoring and surveillance is given below and summarized in Table 1. A review can also be found in the recent report by Drogg [49].

1. pH. The growth rate of different organisms active in the biomechanisation process is affected by pH and different microbial groups have different pH optima. A neutral pH is favourable for biogas production, since most methanogens grow at the pH range 6.7–8.0 (*see Note 4*).
2. Gas amount and gas composition. The amount and composition of the gas reflect the composition of the ingoing material (*see Subheading 3.3*) and also the process performance, and are thus a valuable tool for monitoring. The gas volume can be measured in different ways, such as measuring the flow, by water displacement or by collecting the gas in a bag for later volume determination [27, 57, 58]. The gas composition may be measured on-line (common for full scale) or off-line. For laboratory-scale applications, off-line measurements by gas chromatography (GC) are common [59], but it is also possible to use on-line sensors to determine the methane concentration [24, 60]. It is relevant to analyse the major components

methane and carbon dioxide, but also the level of hydrogen sulphide (*see Note 23*).

3. Alkalinity. Biogas processes typically operate at neutral pH or slightly above neutral (pH 7.0–8.5). Maintaining neutral and stable pH values is critical for the functioning of the microbial process and requires relatively high and constant alkalinity. Combined with VFA and pH analysis, alkalinity gives a good measure of process endurance and the risk of instability. One common method to measure alkalinity is by titration [49]. For this, a reactor sample is centrifuged and the supernatant is titrated to pH 5.75 for partial alkalinity (PA) and to pH 4.3 for total alkalinity (TA) [75] (*see Note 4*).
4. Degradation intermediates. Degradation intermediates such as VFA typically accumulate when there is an imbalance in the different microbial degradation steps. This imbalance can be caused by a number of different factors, such as overloading, temperature fluctuations and toxicity. VFA analysis is one of the most common parameters used for monitoring biogas processes and numerous studies have shown that VFA content correlates well with process performance [61–63]. VFA can be analysed as total concentration of carboxylic acids, or as concentration of each of the individual acids (*see Note 5*). Typical methods used include GC [64] and high pressure liquid chromatography (HPLC) or titration [62, 65], or on-line measurement techniques [63].
5. Temperature. Biogas production can proceed at a wide range of temperatures (*see Subheading 3.4*), but to avoid process instability the temperature should not vary too much from that selected for a specific process (*see Note 18*).
6. Ammonium-nitrogen, i.e. the sum of ammonium and ammonia. Ammonium is released during the degradation of proteinaceous materials and exists in equilibrium with ammonia. High levels are often associated with reactor instability, indicated by reduced methane production rate and high effluent concentration of VFA [20, 42]. The concentration that results in inhibition varies from one process to the next and depends on the prevailing operating conditions. Ammonia is considered to be the inhibitory component and a range of values (53–1,100 mg/L) have been reported to result in instability [42] (*see Note 15*). Methods of analysis are described in Subheading 3.1.
7. Specific methane yield and degree of degradation. The volume of gas produced and the methane concentration in the gas give the methane production from the reactor. Together with the amount of VS fed to the reactor, this allows the specific methane yield to be calculated as  $\text{m}^3\text{CH}_4$  per kg VS fed to the reactor. The methane yield obtained can be compared against

the measured biogas potential of the substrate (*see* Subheading 3.2). Yield corresponding to 70–90% of that determined by the BMP test can be expected, but the results also depend on the time allowed for degradation, i.e. the hydraulic retention time. Specific methane yield is calculated as:

$$\text{m}^3\text{CH}_4 \text{ kgVS}^{-1} = \frac{V_g \times \% \text{CH}_4}{Q_s \times \text{VS}_{\text{in}} \times \text{TS}_{\text{in}}}$$

where  $Q_s$  is flow into the reactor/day,  $\text{VS}_{\text{in}}$  is VS content in incoming substrate,  $\text{TS}_{\text{in}}$  is TS content in incoming substrate and  $V_g$  is volume gas produced/day.

8. Degree of degradation or VS reduction. This is a measure of the proportion of organic matter fed to the reactor that has been digested, i.e. converted into biogas. A high degree of VS reduction suggests a higher degree of degradation and hence a more efficient biogas process (*see* Note 24).

VS reduction is calculated as:

$$\text{VS}_{\text{red}} = \frac{Q_s \times \text{VS}_{\text{in}} - Q_r \times \text{VS}_r}{Q_s \times \text{VS}_{\text{in}}}$$

where  $Q_s$  is flow into the reactor,  $Q_r$  is flow out of the reactor and  $\text{VS}_r$  is VS content in effluent.

### 3.6 Implementation of Monitoring Results

As listed above, many different parameters can affect the efficiency of a biogas process, as well as its stability and risk of failure. Thus it is difficult to give direct advice on measures to be taken when the process is going towards values outside the stability limits and/or has low efficiency regarding gas production and degree of degradation. However, using the protocol given above and considering Notes 1–24, a good understanding of the process and its limitations and possibilities, as well as reasons for instability or failure, can be achieved. With this knowledge it is also possible to take actions to manage the process towards high efficiency and stability.

---

## 4 Notes

1. During characterisation of a specific material, it is important to bear in mind that the composition may vary from batch to batch and thus multiple random sampling must be performed over time to ensure that reliable data are obtained. Repeated analysis over time gives information not only on the time-specific composition, but also on the variability of the material, which can be taken into consideration later when composing feedstock mixtures. One way to minimise errors caused by sample heterogeneity is to pool subsamples from different

batches and grind the bulk sample prior to sampling, as suggested by Hansen et al. [66]. Taking out rather large samples (>1 L) can also decrease errors. Sample storage is another critical parameter, as it can sometimes change the composition of the material. To avoid biological decomposition before analysis, freezing at  $-20^{\circ}\text{C}$  is recommended if the sample cannot be analysed directly after sampling.

2. The content of water, mineral and organic material is important when setting operating parameters such as OLR and HRT (*see* Subheading 3.4). In addition, this is a critical parameter for judging the capacity for efficient pumping and stirring and also for evaluating the biogas potential (*see* Subheading 3.2). A common TS value for the ingoing substrate of a CSTR process is around 2–15%. Analysis of TS and VS by drying and incineration is a simple and low-cost analysis. In addition, TS content is sometimes analysed on-line in full-scale biogas plants and used as an estimate of the load to the reactor. During analysis of VS/TS content, it is important to take into consideration possible loss of volatile organic matter during the drying process [33, 67]. This loss needs to be estimated for correct determination of the organic load (*see* Note 20), as well as for calculation of specific methane yield (*see* Subheading 3.5, item 7). The organic matter content can also be determined by other methods, such as Chemical Oxygen Demand (COD, APHA 1997). COD is a general measure of the amount of soluble organic compounds present in the sample that could give rise to methane and is often used as a standardised method for more dilute samples, such as wastewater and sludge. COD analysis is somewhat more complicated for samples with high TS content, although by homogenisation and dilution good results can also be obtained with solid samples [33, 68]. For analysis of dry matter and water content, a recent publication also suggests Karl Fisher titration as a method giving high accuracy and as being particularly suitable for pre-treated lignocellulosic material, where oven drying typically underestimates the dry matter content due to loss of volatiles [69].
3. Analysis of total nitrogen and total ammonium-nitrogen is of relevance for composing a suitable feedstock mixture and also during evaluation of the process, e.g. calculation of degree of mineralisation (*see* Note 24). Organically bound nitrogen will during the degradation process be released as ammonium and ammonia (*see* Note 15).  $\text{pK}_a$  (9.25) for  $\text{NH}_4/\text{NH}_3^+$  is higher than a typical pH (<8) for an anaerobic digestion process and thus this release will contribute with an increase in the buffer capacity (e.g. alkalinity, *see* Note 4) further on increasing also the level of dissolved bicarbonate ( $\text{HCO}_3^-$ ) [70]. In this sense high nitrogen in the feedstock can be beneficial for the process.

However, as described below as well as in **Note 15** it can also have negative effects. For the feedstock, the C/N ratio (total organic carbon and nitrogen) is of great importance. For optimal degradation in an AD process, this ratio has been suggested to be set between 15 and 25 [19, 71], but biogas production at C/N ratios outside this range has also been reported [53]. If the ratio is too low, the process risks suffering from ammonia inhibition, while if it is too high the bacteria might experience nitrogen limitation [19, 71]. Another factor to consider in this regard is the carbon source. A high C/N ratio poses a greater risk of process problems arising if the majority of the carbon is easily accessible, e.g. that in starch. In that case the carbon is quickly degraded and there is a risk of acidification. On the other hand, excessively high levels of nitrogen typically result in high levels of ammonia, which is specifically inhibitory for the methanogens, also typically resulting in process instability [42]. The C/N ratio can be adjusted by co-digesting materials that are complementary in this regard [7]. Studies have also shown that adjustment of the C/N ratio by addition of glucose or urea has positive effects on the methane potential [19].

4. pH is an important parameter influencing methane production efficiency [72]. The optimal range of pH for methane production is 6.5–7.5, but the range varies with different substrates and operating parameters [73, 74]. With an acid substrate or an easily degradable substrate resulting in rapid acid production, a pH change can occur in the reactor. The degree of such a pH change depends on the available alkalinity in the reactor, which also regulates how fast the pH is restored to optimal levels. Alkalinity is a measure of the buffer capacity, i.e. the ability of a solution to neutralise acids, and can be expressed in different ways. The total alkalinity (TA) gives a measure of the combined effect of several different buffering systems [76]. The partial alkalinity (PA) represents the buffering capacity of the carbonate system, and includes in addition the ammonium–ammonia system. The intermediate alkalinity (IA) is the difference between TA and PA and includes mainly the buffering capacity of the VFA [75, 76]. The stability of the process can be evaluated by calculating the IA/PA ratio where a ratio of 0.3 or less indicates a stable process [75, 77]. A value between 0.3 and 0.8 indicates, on the other hand, a risk of instability and a value above 0.8 suggests instability [49]. The VFA to alkalinity ratio is also known as the FOS/TAC ratio and is commonly analysed at full-scale biogas plants by the use of an automatic titration equipment [49]. If necessary, alkalinity and pH can be adjusted in the biogas process by adding various stabilising agents such as carbonates and bicarbonates combined with sodium or

potassium, calcium carbonate (lime) and HCl [78, 79]. Sodium carbonate, sodium bicarbonate, potassium carbonate and potassium bicarbonate are common stabilising agents for large-scale applications as they are easy to apply and difficult to overdose. Other alkaline substances, such as lime, ammonia, lye and urea, can be used but are more easily overdosed and may not always contribute to increased alkalinity in the process. In addition, urea and ammonia can have toxic effects on microorganisms (*see* **Notes 3** and **15**). The exact amount of buffering substance that must be added to alter the alkalinity may vary between different biogas processes and is dependent on several factors, such as the bicarbonate content, temperature, pH, fatty acid concentration and ammonia content [80]. Therefore, it can be difficult to calculate exactly what should be added to adjust the alkalinity. It is best to add small doses repeatedly and test between additions to see how the process is responding. Examples of how various stabilisers may be added in order to increase alkalinity are provided in Capri and Marais [80].

5. Accumulation of VFA and other degradation intermediates, such as long chain fatty acids (LCFA), is highly undesirable as it is a sign of an inefficient process and also represents a significant loss of biogas. These compounds represent intermediates from the acidogenesis and acetogenesis steps and typically the degradation proceeds through syntrophic reactions involving acid degraders and methanogens [14, 81]. Accumulation is believed to be a consequence of lower activity of methanogens compared with acid producers and to be caused either by organic overloading or inhibition of the methanogenic microbial communities. Alternatively, accumulation can be a consequence of direct inhibition of the acid-degrading community. The feedstock itself can also have high levels of acids, often due to initiation of the degradation process during transportation and storage. Irrespective of the origin, VFA and LCFA can cause a drop in pH, foaming and, at high levels, toxicity to the microbial community [7, 20, 48]. Acclimatisation to inhibitory levels of LCFA has, however, been shown possible by subsequent exposure of the process followed by periods of recovery [82, 83]. An alternative strategy to access the high biogas potential in lipid rich waste is to use a step-wise start-up strategy in order to allow development of a specialised microbial community [84]. For monitoring, the propionate:acetate ratio is reported to be a useful early indicator of imminent process failure [85], with an increasing ratio suggesting a higher risk. With increasing VFA concentration there is also a significant risk of a pH drop, particularly in processes with low buffering capacity (*see* **Note 4**).

6. Trace metals are essential for enzymatic activity and for optimal degradation efficiency it is important that the substrate contains sufficient amounts. Trace element deficiency is suggested to be a limiting factor for achieving high biogas production, especially at high OLR, and addition of trace elements has been shown to circumvent accumulation of degradation intermediates and lower the risk of process instabilities due to, e.g. ammonia inhibition [39, 86, 137]. Addition of trace metals has given positive results with various types of substrate, such as food waste [16, 43], crop material [87] and stillage [88]. Cobalt, nickel, molybdenum and selenium are suggested to be critical to process performance, but other metals can also be important [89]. To overcome nutrient deficiency, a broad spectrum of commercial supplementation products is available on the market. It is important to bear in mind that the exact levels needed for stable and efficient degradation are not completely clear and also that some forms of trace metals have low bioavailability and are thus difficult for microorganisms to access [90]. The elements may be kept soluble by chelation (combination with another molecule), but may bind strongly with the chelating agent forming complexes that again render them unavailable [17]. On analysing metals, the bioavailable nutrients represent only a fraction of the total amount measured in the material [91]. Moreover, addition of trace metals also carries the risk of overdosing with heavy metals and causing toxicity to the microbial consortium involved in anaerobic digestion [92]. Elevated heavy metal concentrations may also limit the subsequent use of digestate as fertiliser and can cause environmental pollution [93]. With materials resulting in sulphide formation, such as protein-rich materials, metals can also be precipitated in the form of metal sulphides. Inclusion of iron chloride in addition to trace metals has been shown to give positive effects in such cases, primarily due to removal of sulphide by the iron to levels <50 ppm in the gas phase, allowing higher bioavailability of trace elements [15, 88, 94, 136].
7. Component and element analysis can be of interest for several reasons, but is typically not performed in full-scale applications but rather for research purposes. Information on the composition can be used not only for theoretical calculation of the methane potential (*see* Subheading 3.3) but also to judge the biodegradability of a specific material and limitations or risks of complications as regards substrate specific features. Different materials have different characteristics not only regarding methane potential, but also concerning biodegradability and risks for process failure or problems (*see* Subheading 3.3). As

mentioned, co-digestion if applicable can be one way to overcome issues related to specific materials [7, 40].

8. Anaerobic degradation of proteins typically results in the release of both ammonia (*see Note 3*) and sulphides, the latter originating from the amino acids cysteine and methionine. Reduction of sulphate by sulphate-reducing bacteria represents another source of sulphides. High levels of sulphate are commonly detected in industrial waste streams, typically from distilleries or the pulp and paper industry. Sulphate-reducing bacteria effectively consume substrates otherwise destined for methane, hence presence of sulphate can result in lower gas yields [95]. Sulphides are undesired in methanogenic processes due to reduced bioavailability of trace metals caused by precipitation (*see Note 6*), direct toxic effects [96] and contamination of the biogas, causing bad odour, negative health effects and corrosive effects on pipes and gas engines. Sulphides can be reduced by iron addition (*see Note 6*).
9. There are many parameters with an impact on the outcome of a BMP test, as reviewed by Raposo, De la Rubia, Fernández-Cegrí and Borja [33], but one of the most important is the activity of the inoculum. The inoculum should best be taken from a well-functioning biogas process preferably operating on a mixed substrate to ensure high functional diversity of the microbial community and operating at the temperature of interest for the test. Alternatively, inoculum from different plants operating with different feedstocks can be mixed. If a substrate is to be evaluated for an existing biogas plant, the inoculum should be taken from this specific plant. The inoculum should be used fresh and not stored for a long time. Pre-incubation of the inoculum for a maximum of around 1 week gives an optimum decrease in background gas production. Longer pre-incubation times risk decreasing the microbial activity, but may still be possible depending on the inoculum.
10. The ratio between inoculum and substrate has been shown to be of high importance, as it is critical that the inoculum contains a sufficient amount of microbial cells with high activity to reach maximum rate and methane potential in the test [97]. The optimal ratio differs between different studies and to devise an optimised test for a specific inoculum it is recommended that different ratios be evaluated. One common and easy method for estimating the biomass concentration in the sample is to analyse the content of volatile suspended solids (VSS) or total VS content. Note, however, that this analysis does not distinguish between microbial biomass and other particulate organic matter, such as lignocellulosic residues, resulting in uncertainties. Another consideration when setting up the experiment is that using too high an amount of inoculum might result in high background production of

biogas and lag periods caused by potential toxicants present in the inoculum.

11. The environmental conditions in the test vials are vital for the test outcome and the dilution medium is one parameter of particular importance. For biodegradation to proceed, all nutrients required by the microorganisms, including trace metals, need to be available. In addition, the environmental conditions regarding pH and temperature need to be in a range allowing microbial growth. Moreover, stirring and the flushing gas used are influential parameters. The optimal pH for the test is around 7–8, set according to levels optimal for methanogenic activity. Regarding temperature, this parameter strongly regulates the growth rate and sometimes also the efficiency of the degradation. Anaerobic digestion typically proceeds in the mesophilic, thermophilic or sometimes psychrophilic temperature range (*see* Subheading 3.4). In the BMP test, using the same temperature as the biogas plant from which the inoculum is taken is recommended. Flushing to avoid introduction of oxygen in the test can be performed with different gases, but a recent publication showed that N<sub>2</sub>/CO<sub>2</sub> is preferable to N<sub>2</sub> alone [98]. Mixing increases the contact between substrate and microorganisms and thus stirring, manually or automatically, typically increases the degradation rate (*see* Note 19). If the inoculum/substrate mixture lacks important trace metals and/or other nutrients, those can be supplied using a mineral growth medium as a dilution agent. In a test system with low initial pH or low alkalinity, a buffer is recommended as the dilution medium. Using a buffer decreases the risk of a pH decrease during the course of the experiment due to the formation of degradation intermediates (VFA). However, sufficient amounts of nutrient and buffering capacity may already be supplied by the inoculum, in which case tap water can be used as a dilution medium.
12. It is recommended that the activity of the inoculum be evaluated by preparing experimental bottles using a compound with known methane potential as a substrate. Different chemicals can be used depending on the activity of interest to measure, but it is best to use a component that needs all the microbial degradation steps to be converted into biogas, i.e. hydrolysis, acidogenesis, acetogenesis and methanogenesis. Cellulose is one such commonly used compound, with a theoretical methane yield of 415 Nml/g.
13. In a BMP test it is important to have a procedure considering the actual volume of the gas produced and to analyse the methane content of the gas. This can be done in different ways. The gas can, for example, constantly be released and the carbon dioxide produced removed by letting the outflow gas

pass through an alkali solution and finally a flow measurement device [49]. The gas produced can also be collected in a gas-tight bag followed by analysis of gas volume and composition. Alternatively a pressure is allowed to build up and a fixed volume of gas can either be sampled with the same actual pressure as in the bottles, e.g. using a syringe with a pressure lock [66] or by sampling at atmospheric pressure combined with measuring the pressure in the bottles [59]. The gas samples can then be analysed by gas chromatography. The sampling interval depends on the type of material tested, but is typically every day/every other day in the first week of incubation, after which the time between sampling occasions can be expanded.

14. The selection of appropriate substrates for full-scale application depends on several complex factors, such as the availability and logistic feasibility of particular materials [99]. Regulations and legislation regarding the use and quality of digestate (heavy metals, contamination with, e.g. plastics, potential pathogens/need for substrate sanitisation, etc.) are other factors that need to be considered. The need for dilution of the substrate, which also affects the amount of digestate to allocate, might also be a limiting factor. In addition, different substrates require different mechanical pre-treatments [100–102]. Finally, requirements on gas quality may also affect selection of substrates, for example, avoidance of sulphate-containing materials, which lead to sulphide production, or determine the need for iron addition to the process to reduce sulphide production (*see* **Notes 6** and **8**).
15. Ammonium is released during degradation of proteins but can also be present in the feedstock from the beginning, e.g. in manure. The level of ammonium-nitrogen in the process depends on the substrate composition and on the degree of mineralisation of the process, i.e. the proportion of organic material converted to methane. A smaller proportion of the organic nitrogen in the substrate is mineralised to ammonium-nitrogen at a low compared with a higher degree of decomposition, which in turn is dependent on sludge retention time, temperature and the microbial community [24]. A high content of ammonium provides the process with alkalinity and increases the value of the digestate as a fertilising agent, but unfortunately it also causes inhibition of the process, specifically of the methanogenic community [42]. Temperature and pH indirectly affect the level of inhibition, since these parameters shift the equilibrium of ammonium ( $\text{NH}_4^+$ ) and ammonia ( $\text{NH}_3$ ) towards the latter, which has been shown to be the actual cause of the inhibition [42, 103, 104]. Inhibition has been reported to occur at varying concentrations ranging from 53 to 1,450 mg  $\text{NH}_3/\text{L}$  [42, 105]. This wide span is probably

the result of differences in substrate composition, reactor design and operating parameters, such as HRT and temperature, as reviewed in Moestedt [95]. In addition, adaptation to high ammonia levels has long been emphasised in the literature [105–108]. Allowing the microbial community to acclimatise to the prevailing conditions can allow efficient biogas production at ammonia levels up to around 1,000 mg/L [95]. Adaptation to high ammonia levels has been shown to be correlated with a shift in the methane-producing pathway, with significant contributions by syntrophic acetate oxidation (SAO) to methane formation [57, 109].

Free ammonia is calculated as:

$$\text{NH}_3 = \text{NH}_4 \left( 1 + \frac{10^{-\text{pH}}}{10^{-(0.09018 + \frac{2729.92}{T})}} \right)$$

where  $\text{NH}_4$  is the total ammonia nitrogen and  $T$  is temperature expressed in Kelvin.

16. Some materials and/or conditions typically need long periods of microbial adaptation and thus by selecting an inoculum already adapted to the material/conditions, the start-up can be faster and initial instability periods can be avoided. Moreover, for an optimal process it is desirable to have an inoculum with high microbial diversity, which is considered to be correlated with high functional redundancy, i.e. a high number of species performing similar functions so that failure of one species can be compensated for by another, with little impact on essential processes [110]. The importance of inoculum selection has been illustrated for different processes, such as biogas production at elevated total ammonium-nitrogen (TAN) levels [111] and for biogas production from straw and paragrass [112, 113]. However, while the initial microbial composition affects the start-up and initial phase of reactor operation, its long-term importance is still unclear.
17. For start-up of a full-scale reactor from which the digestate leaves the tank by overflow, the reactor may have to be filled with more than 70% of the total volume in order to supply the water-lock and the gas may have to be collected before initiation of feeding. If heat is supplied with the substrate and internal heating is not yet in operation, the associated difference in temperature might also need to be considered when determining the feeding rate.
18. Temperature, together with substrate, is the most strongly determining parameter for stability and process performance. Temperature impacts strongly on community structure and diversity, as well as on the degradation pathways and rates [17, 19, 43, 114]. When optimising an AD system for net

energy production, the additional energy required to raise and maintain feedstock and digester contents at this temperature must also be taken into account [35]. In general, anaerobic digestion at thermophilic temperatures gives higher methane production rates and methane yield, but this is not always the case [53, 115–117]. Moreover, thermophilic digestion results in comparatively higher reduction of pathogens [22, 118], so it can be used as the sole sanitisation method [26], and gives lower viscosity, resulting in less energy consumption for stirring [119]. Disadvantages with higher temperatures include lower microbial diversity [109, 116, 120], with an accompanying risk of a less stable process and less efficient degradation of certain chemical compounds, such as phenols [3, 120]. Moreover, a higher process temperature needs a higher energy input in the form of heating. Processes operating at mesophilic temperature are generally considered to be more stable and less sensitive to inhibitory components such as ammonia. Furthermore, the effects of LCFA are less pronounced at mesophilic temperature [115]. The microbial community, specifically the methanogens, is sensitive to temperature variations and experience from large-scale operation shows that temperature fluctuations should not exceed  $\pm 2\text{--}3^\circ\text{C}$  for best results and to avoid instability [49]. However, biogas production is possible at a wide range of temperatures, even in the range between mesophilic and thermophilic temperatures, and it is also possible to shift from mesophilic to thermophilic temperature and vice versa [24, 53, 121, 122]. To allow the microbial community to develop in line with a change in temperature a slow increase/decrease is recommended, with a guideline of  $1^\circ\text{C}$  change per day. However, there are examples in the literature of a higher rate of temperature increase being successful [122, 123].

19. The reactor can either be mixed continuously, using an intermittent mixing mode, or not mixed at all. Mixing mode and mixing intensity have been shown to have direct effects on biogas yield [124]. Mixing ensures even distribution of the substrate, which is particularly important with feedstocks forming floating layers, e.g. straw, and good nutrient supply to the microorganisms active in the biogas process. However, if too harsh, mixing can also disrupt microbial aggregates resulting in less efficient degradation. Mixing is also essential to secure uniform temperature distribution in the reactor.
20. Parameters affecting the optimal initial OLR and rate of load increase include: (1) inoculum origin, i.e. whether the microbial community is already adapted to the conditions applied regarding process operating parameters and substrate composition. With similar conditions as in the original process, the start-up can be rather fast [24, 26]; (2) the time between

collection of inoculum and start-up of the process. If the inoculum has been transported under non-strictly anaerobic conditions and/or stored for some time it is recommended that feeding be initiated slowly; and (3) temperature of the inoculum. If the inoculum temperature is lower than that of the original process and/or will be changed in the new process compared with the original process, it is important to allow time for acclimatisation of the microbial community at the correct temperature and to increase the OLR slowly while carefully monitoring the process (*see Note 18*). OLR values commonly range between 2 and 6 g VS/L day, but lower/higher values have been reported [19, 125]. Note that an increase in OLR is typically followed by a decrease in HRT, giving less time for degradation.

Organic loading rate is calculated as:

$$\text{OLR} = \frac{Q_s \times \text{VS}_{\text{in}} \times \text{TS}_{\text{in}}}{V_R}$$

where  $Q_s$  is flow into the reactor/day,  $\text{VS}_{\text{in}}$  is VS content in incoming substrate,  $\text{TS}_{\text{in}}$  is TS content in incoming substrate and  $V_R$  is reactor volume.

21. The feeding frequency is often set based on practical considerations, i.e. how often the operator can feed the system, but also depends on the character of the feeding material. Materials with low TS content are typically pumped into the reactor and allow more continuous feeding than, e.g. solid materials, which sometimes need to be put into the reactor in batches, e.g. semi-continuous feeding. The feeding approach affects the degradation kinetics, formation of intermediates and biogas production, but usually does not affect the final biogas yield [126]. Dynamic feeding has lately been suggested as an approach to allow flexible electricity supply from biogas [126]. The feeding regime has also been shown to affect the activity and structure of the microbial community and its functional stability [127, 128].
22. The retention time should be sufficiently long to ensure good degradation of a specific material under specific operating parameters. Substrates rich in sugar and starch are typically easily broken down and require shorter retention times. For the degradation of these materials no hydrolysis is necessary and the degradation starts directly at the second degradation step, fermentation. However, much longer times are required for microbial degradation of fibre- and cellulose-rich plant matter. For such materials, it is often the hydrolysis step, and not methanogenesis, that limits the rate of decomposition. A typical sign of too low HRT is either accumulation of degradation intermediates or a low degree of degradation (*see Subheading 3.5*). Hydraulic retention time is calculated as:

$$\text{HRT} = \frac{V_R}{Q_s}$$

where  $Q_s$  is flow into the reactor/day and  $V_R$  is reactor volume.

23. The composition of the gas is highly interesting for a production plant aiming to produce an energy-rich gas of high quality, i.e. high level of methane and low level of hydrogen sulphide [129]. Using carbohydrate feedstocks results in lower levels of methane and hydrogen sulphide and higher levels of carbon dioxide compared with proteinaceous materials. An increase in the  $\text{CO}_2$  concentration of the biogas produced may thus be a result of a change in feedstock. However, a change in gas composition may also be a sign of process instability [130]. In a laboratory-scale reactor operating with a homogeneous substrate, analysis of the carbon dioxide level can be an early warning of instability. In such cases, daily analysis of the carbon dioxide level by, e.g. a simple saccharometer can allow detection of instability from 1 day to another, shown as an increase in the level of a few per cent. In production plants, the input material typically varies over time and thus also the gas composition. In order to detect a deviation from the 'normal' variation, it is thus important to consider the gas composition and carbon dioxide content over a longer period and look for increasing/decreasing trends. In the case of an increase in carbon dioxide caused by instability, measures should be taken to counteract a further increase and to recover the process. The measures that should be taken depend on the substrate and operating parameters used, but typically a decrease in OLR is required. Analysis of  $\text{H}_2\text{S}$  is important for evaluating the gas quality, specifically in full-scale plants as the concentration in the gas should be kept low for further use of the gas in combustion engines and boilers of upgrading plants [129]. The level should optimally be below 50 ppm. Moreover, analysis of hydrogen sulphide is also of interest, as it forms complexes with metals, which can decrease the bioavailability of trace elements essential for microbial activity (see **Notes 6 and 8**) [20, 131]. The level of  $\text{H}_2\text{S}$  can be lowered in different ways. One common strategy is to add iron to the process, binding the sulphide ions. Iron can be added directly to the reactor liquid in different forms in order to precipitate the sulphides and hence also reduce the undesired precipitation of trace elements [129, 132]. Sulphides can also be reduced in biogas by aeration of headspace, resulting in oxidation of reduced sulphides to elemental sulphur, or by biological oxidation of sulphides by, e.g. *Thiobacillus* species in a separate gas-upgrading unit [133, 134]. However, these downstream processes do not affect the precipitation of trace elements or microbial sulphide toxicity.

24. Reducing VS content is a measure with a long response time, so lower degradation rate of the ingoing material cannot be detected until a considerable fraction of the reactor fluid has been replaced. Furthermore, part of the VS represents non-degradable material and thus a small reduction does not always result in inefficient degradation. Materials typically resulting in a low degree of degradation are fibre-rich materials such as manure and straw, which typically has 30–70% VS reduction [53, 135]. Other more easily degradable materials can give a degree of degradation as high as 80–90% [25, 26]. An alternative way of evaluating the degree of degradation is to analyse the mineralisation of total nitrogen to ammonium-nitrogen [24].

## References

1. Hamawand I (2015) Anaerobic digestion process and bio-energy in meat industry: a review and a potential. *Renew Sust Energ Rev* 44:37–51
2. Murphy J, Braun R, Weiland P, Wellinger A (2011) Biogas from crop digestion. IEA Bioenergy Task 37
3. Weiland P (2010) Biogas production: current state and perspectives. *Appl Microbiol Biotechnol* 85:849–860
4. Vanholme B, Desmet T, Ronsse F, Rabaey K, Van Breusegem F, De Mey M, Soetaert W, Boerjan W (2013) Towards a carbon-negative sustainable bio-based economy. *Front Plant Sci* 4:1–17
5. Albuquerque JA, de la Fuente C, Ferrer-Costa A, Carrasco L, Cegarra J, Abad M, Bernal MP (2012) Assessment of the fertiliser potential of digestates from farm and agroindustrial residues. *Biomass Bioenergy* 40:181–189
6. Nkoa R (2014) A comparison of microbial characteristics between the thermophilic and mesophilic anaerobic digesters exposed to elevated food waste loadings. *Agron Sustain Dev* 34:473–492
7. Mata-Alvarez J, Dosta J, Romero-Güiza MS, Fonoll X, Peces M, Astals S (2014) A critical review on anaerobic co-digestion achievements between 2010 and 2013. *Renew Sust Energ Rev* 36:412–427
8. Appels L, Baeyens J, Degréve J, Dewil R (2008) Principles and potential of the anaerobic digestion of waste-activated sludge. *Prog Energy Combust Sci* 34:755–781
9. Amon T, Amon B, Kryvoruchko V, Machmüller A, Hopfner-Sixt K, Bodiroza V, Hrbek R, Friedel J, Pötsch E, Wagentristl H et al (2007) Methane production through anaerobic digestion of various energy crops grown in sustainable crop rotations. *Bioresour Technol* 98:3204–3212
10. Rajendran K, Aslanzadeh S, Taherzadeh MJ (2015) Household biogas digesters—a review. *Energies* 5:2911–2942
11. Lozanovski A, Lindner JP, Bos U (2014) Environmental evaluation and comparison of selected industrial scale biomethane production facilities across Europe. *LCA Waste Manage Syst* 19:1823–1832
12. Borjesson P, Tufvesson LM (2011) Agricultural crop-based biofuels - resource efficiency and environmental performance including direct land use changes. *J Clean Prod* 19:108–120
13. Angelidaki I, Karakashev D, Batstone DJ, Plugge CM, Stams AJM (2011) Biomethanation and its potential. In: Rosenzweig AC, Ragsdale SW (eds) *Methods in enzymology: methods in methane metabolism*, vol 494. Elsevier Academic Press, San Diego, pp 327–351
14. Worm P, Müller N, Plugge CM, Stams AJM, Schink B (2010) Syntrophy in methanogenic degradation. In: Hackstein JHP (ed) *(Endo) symbiotic methanogenic archaea*, vol 19. Springer, Berlin/Heidelberg, pp 149–173
15. Nordell E, Nilsson B, Nilsson Paledal S, Karlismi K, Moestedt J (2015) Co-digestion of manure and industrial waste - the effects of trace element addition. *Waste Manage (In Press)*
16. Moestedt J, Nordell E, Shakeri Yekta S, Lundgren J, Marti M, Sundberg C, Ejlertsson J, Svensson BH, Björn A (2015) Effects of trace elements addition on process stability during anaerobic co-digestion of OFMSW and slaughterhouse waste. *Waste Manage (In Press)*

17. Banks CJ, Zhang Y, Jiang Y, Heaven S (2012) Trace element requirements for stable food waste digestion at elevated ammonia concentrations. *Bioresour Technol* 104:127–135
18. Ward AJ, Hobbs PJ, Holliman PJ, Jones DL (2008) Optimisation of the anaerobic digestion of agricultural resources. *Bioresour Technol* 99:7928–7940
19. Mao C, Feng Y, Wang X, Ren G (2015) Review on research achievements of biogas from anaerobic digestion. *Renew Sust Energ Rev* 45:540–555
20. Chen JL, Ortiz R, Steele TWJ, Stuckey DC (2014) Toxicants inhibiting anaerobic digestion: a review. *Biotechnol Adv* 32:1523–1534
21. Divya D, Gopinath LR, Christy M (2015) A review on current aspects and diverse prospects for enhancing biogas production in sustainable means. *Renew Sust Energ Rev* 42:690–699
22. Sahlström L (2003) A review of survival of pathogenic bacteria in organic waste used in biogas plants. *Bioresour Technol* 87:161–166
23. Risberg K (2015) Quality and function of anaerobic digestion residues. Swedish University of Agricultural Sciences, Uppsala
24. Moestedt J, Nordell E, Schnürer A (2014) Comparison of operating strategies for increased biogas production from thin stillage. *J Biotechnol* 175:22–30
25. Moestedt J, Nordell E, Hallin S, Schnürer A (2016) Two stage anaerobic digestion for reduced hydrogen sulphide production. *J Chem Technol Biotechnol* 91(4):1055–1062
26. Grim J, Malmros P, Schnürer A, Nordberg Å (2015) Comparison of pasteurization and integrated thermophilic sanitation at a full-scale biogas plant – heat demand and biogas production. *Energy* 79:419–427
27. McLeod JD, Othman MZ, Beale DJ, Joshi D (2015) The use of laboratory scale reactors to predict sensitivity to changes in operating conditions for full-scale anaerobic digestion treating municipal sewage sludge. *Bioresour Technol* 189:384–390
28. Ruffino B, Fiore S, Roati C, Campo G, Novarino D, Zanetti M (2015) Scale effect of anaerobic digestion tests in fed-batch and semi-continuous mode for the technical and economic feasibility of a full scale digester. *Bioresour Technol* 182:302–313
29. Usack JG, Spirito CM, Angenent LT (2012) Continuously-stirred anaerobic digesters to convert organic wastes into biogas: system setup and basic operation. *J Vis Exp* 65, e3978
30. Dandikas V, Heuwinkel H, Lichti F, Drewes JE, Koch K (2014) Correlation between biogas yield and chemical composition of energy crops. *Bioresour Technol* 174:316–320
31. Cabbai V, Ballico M, Aneggi E, Goi D (2013) Bmp tests of source selected ofmsw to evaluate anaerobic codigestion with sewage sludge. *Waste Manag* 33:1626–1632
32. Moestedt J, Nilsson Pålédal S, Schnürer A (2013) The effect of substrate and operational parameters on the abundance of sulphate-reducing bacteria in industrial anaerobic biogas digesters. *Bioresour Technol* 132:327–332
33. Raposo F, De la Rubia MA, Fernández-Cegrí V, Borja R (2012) Anaerobic digestion of solid organic substrates in batch mode: an overview relating to methane yields and experimental procedures. *Renew Sust Energ Rev* 16:861–877
34. Li Y, Zhang R, Liu G, Chen C, He Y, Liu X (2013) Comparison of methane production potential, biodegradability, and kinetics of different organic substrates. *Bioresour Technol* 149:565–569
35. Banks CJ, Heaven S (2013) Optimisation of biogas yields from anaerobic digestion by feedstock type. In: Wellinge A, Murphy J, Baxter D (eds). *The Biogas hand book: Science an, production and applications*. Woodhead publishing series in energy (Cambridge, UK). Issue 52, pp 131–165
36. Buswell AM, Mueller HF (1952) Mechanism of methane fermentation. *Ind Eng Chem* 44:550–552
37. Sanders W, Angelidaki I (2004) Workshop on harmonization of anaerobic biodegradation, activity and inhibition assays. *Rev Environ Sci Biotechnol* 3:91–158
38. Strömberg S, Nistor M, Liu J (2014) Towards elimination systematic errors caused by the experimental conditions in biochemical methane potential (bmp) tests. *Waste Manag* 34:1939–1948
39. Demirel B, Scherer P (2011) Trace element requirements of agricultural biogas digesters during biological conversion of renewable biomass to methane. *Biomass Bioenergy* 35:992–998
40. Astals S, Nolla-Ardèvol V, Mata-Alvarez J (2012) Anaerobic co-digestion of pig manure and crude glycerol at mesophilic conditions: biogas and digestate. *Bioresour Technol* 110:63–70
41. Braun R, Wellinger A (2003) Potential of codigestion. IEA Bioenergy Task 37, Technical brochure

42. Rajagopal R, Massé DI, Sing G (2013) A critical review on inhibition of anaerobic digestion process by excess ammonia. *Bioresour Technol* 143:632–641
43. Zhang C, Su H, Baeyens J, Tan T (2014) Reviewing the anaerobic digestion of food waste for biogas production. *Renew Sust Energ Rev* 38:383–392
44. Hejnfelt AAI (2009) Anaerobic digestion of slaughterhouse by-products. *Biomass Bioenergy* 33:1046–1054
45. Solli L, Bergersen O, Sørheim R, Briseid T (2014) Effects of a gradually increased load of fish waste silage in co-digestion with cow manure on methane production. *Waste Manag* 34:1553–1559
46. Nie H, Jacobi HF, Strach K, Xu C, Zhou H, Liebetrau J (2015) Mono-fermentation of chicken manure: ammonia inhibition and recirculation of the digestate. *Bioresour Technol* 178:238–246
47. Jansen S, Gonzalez-Gil G, van Leeuwen HP (2007) The impact of Co and Ni speciation on methanogenesis in sulfidic media - biouptake versus metal dissolution. *Enzym Microb Technol* 40:823–830
48. Rasit N, Idris A, Harun R, Ghani WAWAK (2015) Effects of lipid inhibition on biogas production of anaerobic digestion from oily effluents and sludges: an overview. *Renew Sust Energ Rev* 45:351–358
49. Drog B (2013) Process monitoring in biogas plants. IEA Bioenergy Task 37, Technical Brochure
50. Sawatdeenarunat C, Surendra KC, Takara D, Oechsner H, Khanal SK (2015) Anaerobic digestion of lignocellulosic biomass: challenges and opportunities. *Bioresour Technol* 178:178–186
51. Bouallagui H, Touhami Y, Ben Cheikh R, Hamdi M (2005) Bioreactor performance in anaerobic digestion of fruit and vegetable wastes. *Process Biochem* 40:989–995
52. Hagen LH, Vivekanand V, Linjordet R, Pope PB, Eijsink VH, Horn SJ (2014) Microbial community structure and dynamics during co-digestion of whey permeate and cow manure in continuous stirred tank reactor systems. *Bioresour Technol* 171:350–359
53. Risberg K, Sun L, Levén L, Horn SJ, Schnürer A (2013) Biogas production from wheat straw and manure – impact of pretreatment and process operating parameters. *Bioresour Technol* 149:232–237
54. Sun L, Pope PB, Eijsink VH, Schnürer A (2015) Characterization of microbial community structure during continuous anaerobic digestion of straw and cow manure. *Microb Biotechnol* 8:815
55. Vanwonterghem I, Jensen PD, Dennis PG, Hugenholtz P, Rabaey K, Tyson GW (2014) Deterministic processes guide long-term synchronised population dynamics in replicate anaerobic digesters. *ISME J* 8:2015–2028
56. Dhaked RK, Singh P, Singh L (2010) Biomechanation under psychrophilic conditions. *Waste Manag* 30:2490–2496
57. Westerholm M, Levén L, Schnürer A (2012) Bioaugmentation of syntrophic acetate-oxidising culture in biogas reactors exposed to increasing levels of ammonia. *Appl Environ Microbiol* 78:7619–7625
58. Estevez MM, Sapci Z, Linjordet R, Schnürer A, Morken J (2014) Semi-continuous anaerobic co-digestion of cow manure and steam-exploded salix with recirculation of liquid digestate. *J Environ Manag* 136:9–15
59. Westerholm M, Hansson M, Schnürer A (2012) Improved biogas production from whole stillage by co-digestion with cattle manure. *Bioresour Technol* 114:314–319
60. Moestedt J, Malmberg J, Nordell E (2015) Determination of methane and carbon dioxide formation rate constants for semi-continuously fed anaerobic digesters. *Energies* 8:645–655
61. Boe K, Angelidaki I (2012) Pilot-scale application of an online VFA sensor for monitoring and control of a manure digester. *Water Sci Technol* 66:2496–2503
62. Madsen M, Holm-Nielsen JB, Esbensen KH (2011) Monitoring of anaerobic digestion processes: a review perspective. *Renew Sust Energ Rev* 15:3141–3155
63. Falk HM, Reichling P, Andersen C, Benz R (2015) Online monitoring of concentration and dynamics of volatile fatty acids in anaerobic digestion processes with mid-infrared spectroscopy. *Bioprocess Biosyst Eng* 38:237–249
64. Jonsson S, Borén H (2002) Analysis of mono- and diesters of o-phthalic acid by solid-phase extractions with polystyrene-divinylbenzene-based polymers. *J Chromatogr A* 963:393–400
65. Lützhøft H-CH, Boe K, Fang C, Angelidaki I (2014) Comparison of vfa titration procedures used for monitoring the biogas process. *Water Res* 54:262–272
66. Hansen TL, Schmidt JE, Angelidaki I, Marca E, Jansen JC, Mosbæk H, Christensen TH (2004) Method for determination of methane potentials of solid organic waste. *Waste Manag* 24:393–400

67. Vahlberg C, Nordell E, Wiberg L, Schnürer A (2013) Method for correction of vfa loss in determination of dry matter in biomass. Swedish Gas Technology Centre: Malmö, 1102–7371
68. Zupancic GD, Ros M (2012) Determination of chemical oxygen demand in substrates from anaerobic treatment of solid organic waste. *Waste Biomass Valor* 3:89–98
69. Agger J, Nilsen P, Eijssink VH, Horn S (2014) On the determination of water content in biomass processing. *Bioenergy Res* 7:442–449
70. Vannecke TPW, Lampens DRA, Ekarna GA, Volcke EIP (2014) Evaluation of the 5 and 8 ph point titration methods for monitoring anaerobic digesters treating solid waste. *Environ Technol* 36:861–869
71. Esposito G, Frunzo L, Giordano A, Liotta F, Panico A, Pirozzi F (2012) Anaerobic co-digestion of organic wastes. *Rev Environ Sci Biotechnol* 11:325–341
72. Liu DW, Zeng RJ, Angelidaki I (2008) Effects of ph and hydraulic retention time on hydrogen production versus methanogenesis during anaerobic fermentation of organic household solid waste under extreme-thermophilic temperature (70 degrees c). *Biotechnol Bioeng* 100:1108–1114
73. Zhai N, Zhang T, Dongxue Y, Yang G, Wang X, Ren G, Feng Y (2015) Effect of initial ph on anaerobic co-digestion of kitchen waste and cow manure. *Waste Manag* 38:126–131
74. Jiang J, Zhang Y, Li K, Wang Q, Gong C, Li M (2013) Volatile fatty acids production from food waste: effects of ph, temperature, and organic loading rate. *Bioresour Technol* 143:525–530
75. Ripley LE, Boyle WC, Converse JC (1986) Improved alkalimetric monitoring for anaerobic digestion of high-strength wastes. *J Water Pollut Control Fed* 58(5):406–411
76. Lahav O, Morgan BE (2004) Titration methodologies for monitoring of anaerobic digestion in developing countries - a review. *J Chem Technol Biotechnol* 79:1331–1341
77. Martín-González L, Font X, Vincent T (2013) Alkalinity ratios to identify process imbalances in anaerobic digesters treating source-sorted organic fraction of municipal wastes. *Biochem Eng J* 76:1–5
78. Karlsson A, Ejlertsson J (2012) Addition of HCL as a means to improve biogas production from protein-rich food industry waste. *Biochem Eng J* 61:43–48
79. Kleyböcker A, Liebrich M, Verstraete W, Kraume M, Würdemann H (2012) Early warning indicators for process failure due to organic overloading by rapeseed oil in one-stage continuously stirred tank reactor, sewage sludge and waste digesters. *Bioresour Technol* 123:534–541
80. Capri MG, Marais GVR (1975) Ph adjustment in anaerobic digestion. *Water Res* 9:307–313
81. McInerney MJ, Struchtemeyer CG, Sieber J, Mouttaki H, Stams AJ, Schink B, Rohlin L, Gunsalus RP (2008) Physiology, ecology, phylogeny, and genomics of microorganisms capable of syntrophic metabolism. *Ann N Y Acad Sci* 1125:58
82. Palatsi J, Laurenzi M, Andrés MV, Flotats X, Nielsen HB, Angelidaki I (2009) Strategies for recovering inhibition caused by long chain fatty acids on anaerobic thermophilic biogas reactors. *Bioresour Technol* 100:4588–4596
83. Silva SA, Cavaleiro AJ, Pereira MA, Stams AJM, Alves MM, Sousa DZ (2014) Long-term acclimation of anaerobic sludges for high-rate methanogenesis from LCFA. *Biomass Bioenergy* 67:297–303
84. Cavaleiro AJ, Salvador AF, Alves JI, Alves M (2009) Continuous high rate anaerobic treatment of oleic acid based wastewater is possible after a step feeding start-up. *Environ Sci Technol* 43:2931–2936
85. Marchaum U, Krause C (1993) Propionic to acetic acid ratios in overloaded anaerobic digestion. *Bioresour Technol* 43:195–203
86. Browne JD, Allen E, Murphy JD (2014) Assessing the variability in biomethane production from the organic fraction of municipal solid waste in batch and continuous operation. *Appl Energy* 128:307–314
87. Lebuhn M, Liu F, Heuwinkel H, Gronauer A (2008) Biogas production from monodigestion of maize silage-long-term process stability and requirements. *Water Sci Technol* 58:1645–1651
88. Gustavsson J, Svensson BH, Karlsson A (2011) The feasibility of trace element supplementation for stable operation of wheat stillage-fed biogas tank reactors. *Water Sci Technol* 64:320–325
89. Schattauer A, Abdoun E, Weiland P, Plöchl M, Heiermann M (2011) Abundance of trace elements in demonstration biogas plants. *Bio-syst Eng* 108:57–65
90. Gustavsson J, Yekta SS, Karlsson A, Skjellberg U, Svensson BH (2013) Potential bioavailability and chemical forms of co and ni in the biogas process-an evaluation based on sequential and acid volatile sulfide extractions. *Eng Life Sci* 13(6):572–579

91. Oleszkiewicz JA, Sharma VK (1990) Stimulation and inhibition of anaerobic processes by heavy metals: a review. *Biol Wastes* 31:45–67
92. Facchin V, Cavinato C, Fatone F, Pavan P, Cecchi F, Bolzonella D (2013) Effect of trace element supplementation on the mesophilic anaerobic digestion of foodwaste in batch trials: the influence of inoculum origin. *Biochem Eng J* 70:71–77
93. Ortner M, Rachbauer L, Somitsch W, Fuchs W (2014) Can bioavailability of trace nutrients be measured in anaerobic digestion? *Appl Energy* 126:190–198
94. Karlsson A, Einarsson P, Schnürer A, Sundberg C, Ejlertsson J, Svensson BH (2012) Impact of trace element addition on degradation efficiency of volatile fatty acids, oleic acid and phenyl acetate and on microbial populations in a biogas digester. *J Biosci Bioeng* 114:446–452
95. Moestedt J (2015) Biogas production from thin stillage - exploring the microbial response to sulphate and ammonia. Swedish University of Agricultural Sciences, Uppsala
96. Stams AJM, Oude Elferink SJWH, Westermann P (2003) Metabolic interactions between methanogenic consortia and anaerobic respiring bacteria. *Adv Biochem Eng Biotechnol* 81:31–56
97. Raposo F, Fernandez-Cegri V, De la Rubia MA, Borja R, Beline F, Cavinato C, Demirer G, Fernandez B, Fernandez-Polanco M, Frigon JC et al (2011) Biochemical methane potential (bmp) of solid organic substrates: Evaluation of anaerobic biodegradability using data from an international interlaboratory study. *J Chem Technol Biotechnol* 86:1088–1098
98. Koch K, Bajón Fernández Y, Drewes JE (2015) Influence of headspace flushing on methane production in biochemical methane potential (bmp) tests. *Bioresour Technol* 186:173–178
99. Wellinger A, Murphy J, Baxter D (2013) *Biogas handbook: science, production and application*, vol 52. Woodhead Publishing Limited, Cambridge
100. Naegele H-J, Mönch-Tegeder M, Haag NL, Oechsner H (2014) Effect of substrate pretreatment on particle size distribution in a full-scale research biogas plant. *Bioresour Technol* 172:396–402
101. Behera S, Arora R, Nandhagopal N, Kumar S (2014) Importance of chemical pretreatment for bioconversion of lignocellulosic biomass. *Renew Sust Energ Rev* 36:91–106
102. Montgomery LFR, Bochmann G (2014) Pretreatment of feedstock for enhanced biogas production. IEA Bioenergy Task 37, Technical brochure
103. Chen Y, Cheng JJ, Creamer KS (2008) Inhibition of anaerobic digestion process: a review. *Bioresour Technol* 99:4044–4064
104. Hansen KH, Angelidaki I, Ahring BK (1998) Anaerobic digestion of swine manure: inhibition by ammonia. *Water Res* 32:5–12
105. Yenigün O, Demirel B (2013) Ammonia inhibition in anaerobic digestion: a review. *Process Biochem* 48:901–911
106. de Baere LA, Devocht M, van Assche P, Verstraete W (1984) Influence of high NaCl and NH<sub>4</sub>Cl salt levels on methanogenic associations. *Water Res* 18:543–548
107. Hashimoto AG (1986) Ammonia inhibition of methanogenesis from cattle wastes. *Agric Wastes* 17:241–261
108. van Velsen AFM (1979) Adaption of methanogenic sludge to high ammonia-nitrogen concentrations. *Water Residue* 13:995–999
109. Sun L, Müller B, Westerholm M, Schnürer A (2014) Syntrophic acetate oxidation in industrial CSTR biogas digesters. *J Biotechnol* 171:39–44
110. Rosenfeld JS (2002) Functional redundancy in ecology and conservation. *Oikos* 98:156–162
111. De Vrieze J, Gildemyn S, Vilchez-Vargas R, Jáuregui R, Pieper D, Verstraete W, Boon N (2015) Inoculum selection is crucial to ensure operational stability in anaerobic digestion. *Appl Microbiol Biotechnol* 99:189–199
112. Gu Y, Chen X, Liu Z, Zhou X, Zhang Y (2014) Effect of inoculum sources on the anaerobic digestion of rice straw. *Bioresour Technol* 158:149–155
113. Nuchdan S, Khemkhao M, Techkarnjanaruk S, Phalakornkule C (2015) Comparative biochemical methane potential of paragrass using an unacclimated and an acclimated microbial consortium. *Bioresour Technol* 183:111–119
114. Labatut RA, Angenent LT, Scott NR (2011) Biochemical methane potential and biodegradability of complex organic substrates. *Bioresour Technol* 102:2255–2264
115. Labatut RA, Angenent LT, Scott NR (2014) Conventional mesophilic vs. thermophilic anaerobic digestion: a trade-off between performance and stability? *Water Res* 53:249–258
116. Moset V, Bertolini E, Cerisuelo A, Cambra M, Olmos A, Cambra-López M (2014) Start-up strategies for thermophilic anaerobic digestion of pig manure. *Energy* 74:389–395
117. Golkowska K, Greger M (2013) Anaerobic digestion of maize and cellulose under

- thermophilic and mesophilic conditions - a comparative study. *Biomass Bioenergy* 56:545–554
118. Bagge E, Sahlström L, Albiñ A (2005) The effect of hygienic treatment on the microbial flora of biowaste at biogas plants. *Water Res* 39:4879–4886
  119. Brambilla M, Romano E, Cutini M, Pari L, Bisaglia C (2013) Rheological properties of manure/biomass mixtures and pumping strategies to improve ingestate formulation: a review. *Trans ASABE* 56:1905–1920
  120. Leven L, Nyberg K, Schnürer A (2013) Conversion of phenols during anaerobic digestion of organic solid waste—a review of important microorganisms and impact of temperature. *J Environ Manage* 95(Suppl):S99–S103
  121. Lindorfer H, Waltenberg R, Köller K, Braun R, Kirchmayr R (2008) New data on temperature optimum and temperature changes in energy crop digesters. *Bioresour Technol* 99:7011–7019
  122. Ziembinska-Buczynska A, Banach A, Bacza T, Pieczykolan M (2014) Diversity and variability of methanogens during the shift from mesophilic to thermophilic conditions while biogas production. *World J Microbiol Biotechnol* 30:3047–3053
  123. Dinsdale RM, Hawkes FR, Hawkes DL (1997) Comparison of mesophilic and thermophilic upflow anaerobic sludge blanket reactors treating instant coffee production wastewater. *Water Res* 31:163–169
  124. Lindmark J, Thorin E, Fdhila RB, Dahlquist E (2014) Effects of mixing on the result of anaerobic digestion: review. *Renew Sust Energy Rev* 40:1030–1047
  125. Li C, Champagne P, Anderson BC (2013) Biogas production performance of mesophilic and thermophilic anaerobic co-digestion with fat, oil, and grease in semi-continuous flow digesters: Effects of temperature, hydraulic retention time, and organic loading rate. *Environ Technol* 34:2125–2133
  126. Mauky E, Jacobi HF, Liebetrau J, Nelles M (2015) Flexible biogas production for demand-driven energy supply – feeding strategies and types of substrates. *Bioresour Technol* 178:262–269
  127. De Vrieze J, Verstraete W, Boon N (2013) Repeated pulse feeding induces functional stability in anaerobic digestion. *Microb Biotechnol* 6:414–424
  128. Lv Z, Leite AF, Harms H, Richnow HH, Liebetrau J, Nikolauz M (2014) Influences of the substrate feeding regime on methanogenic activity in biogas reactors approached by molecular and stable isotope methods. *Anaerobe* 29:91–99
  129. Moestedt J, Nilsson Pålédal S, Schnürer A, Nordell E (2013) Biogas production from thin stillage on an industrial scale—experience and optimisation. *Energies* 6:5642–5655
  130. Boe K, Batstone DJ, Steyer J-P, Angelidaki I (2010) State indicators for monitoring the anaerobic digestion process. *Water Res* 44:5973–5980
  131. van der Veen A, Feroso FG, Lens PNL (2007) Bonding form of metals and sulfur fractionation in methanol-grown anaerobic granular sludge. *Eng Life Sci* 7:480–489
  132. Ek A, Hallin S, Vallin L, Schnürer A, Karlsson M (2011) Slaughterhouse waste co-digestion - experiences from 15 years of full-scale operation. In: *Proceedings of World Renewable Energy Congress*. Linköping
  133. Van der Zee F, Villaverde S, Garcia PA, Fdz-Polanco M (2007) Sulfide removal by moderate oxygenation of anaerobic sludge environments. *Bioresour Technol* 98:518–524
  134. Ramirez M, Fernandez M, Granada C, Le Borgne S, Gomez JM, Cantero D (2011) Biofiltration of reduced sulphur compounds and community analysis of sulphur-oxidizing bacteria. *Bioresour Technol* 102:4047–4053
  135. Ruile S, Schmitz S, Mönch-Tegeder M, Oechsner H (2015) Degradation efficiency of agricultural biogas plants – a full-scale study. *Bioresour Technol* 178:341–349
  136. Romero-Güiza MS, Vila J, Mata-Alvarez M, Chimenos JM, Aстал S (2016) The role of additives on anaerobic digestion: a review. *Renew Sustain Energy Rev* 58:1486–1499
  137. Choong YY, Norli I, Abdullah AZ, Yhaya MF (2016) Impacts of trace element supplementation on the performance of anaerobic digestion process: a critical review. *Biores Technol* 209:369–379

# Protocols for the Isolation and Preliminary Characterization of Bacteria for Biodesulfurization and Biotenitrogenation of Petroleum-Derived Fuels

Marcia Morales and Sylvie Le Borgne

## Abstract

The use of microorganisms to improve fuel quality has been proposed, and in this chapter we describe basic experimental procedures for the isolation and characterization of bacteria for biodesulfurization and biotenyitrogenation with dibenzothiophene and carbazole as model compounds for each application, respectively. The presented protocols should be considered as a starting point and adapted to other problematic compounds and conditions. Basic protocols for the evaluation of the treatment of real oil fractions are also presented.

**Keywords:** 4S pathway, Biodegradation, Biotenyitrogenation, Biodesulfurization, Carbazole, Dibenzothiophene, Heteroatom, Nitrogen, Sulfur

---

## 1 Introduction

The use of microorganisms to improve the refining of problematic petroleum feedstocks has been proposed [1]. The main target has been the precombustion removal of sulfur (desulfurization) in diesel oils in a process called biodesulfurization (BDS) [2]. Hydrodesulfurization (HDS) is the technology currently used in refineries for the precombustion desulfurization of fuels. It involves the use of metallic catalysts at high pressures and temperatures to remove organic sulfur compounds from petroleum fractions. Precombustion removal of sulfur-containing compounds is important in order to limit SO<sub>x</sub> emissions into the atmosphere during the combustion of petroleum-derived fuels and therefore avoid the formation of acid rain. Stringent restrictions on the levels of sulfur in transportation fuels now exist in most countries [1]. Dibenzothiophene (DBT) and DBT with alkyl substituents in the 4- and 6-position flanking the sulfur atom (Fig. 1) are more resistant to the HDS treatment than mercaptans and sulfides [3]. DBT is the model

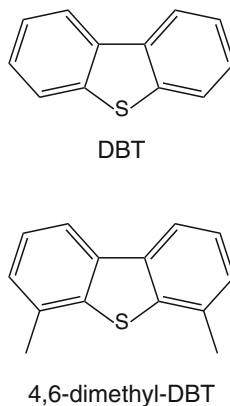


**Fig. 1** Dibenzothiophenes

compound of polyaromatic sulfur heterocyclic compounds. A significant portion of the hydrocarbon present in diesel oil is DBT and its derivatives; it is therefore important that hydrocarbons associated to sulfur are not lost during desulfurization [4]. It has been possible to isolate aerobic bacteria able to selectively extract the sulfur atom from DBT and its derivatives through the 4S pathway (Fig. 2) [5]. These bacteria use DBT as sole source of sulfur but not as source of carbon. DBT is not degraded in the process but only desulfurized by specific cleavage of its C–S bonds, leading to the formation of 2-hydroxybiphenyl (2-HBP) which partitions to the hydrocarbon phase (the fuel), while the sulfur is eliminated as inorganic sulfate in the aqueous phase containing the biocatalyst. This transformation does not destroy the hydrocarbon skeleton and the thermal value of fuels is conserved. A number of “desulfurizing” bacteria have been described as *Rhodococcus erythropolis* IGTS8 [6], *Rhodococcus* sp. [7–9], *Gordonia* sp. [10], *Nocardia* sp. [11], *Sphingomonas* sp. [12], *Pantoea agglomerans* [13], *Stenotrophomonas* sp. [14], *Sphingomonas subarctica* [15], *Brevibacillus invocatus* [16] and the moderate thermophiles or thermotolerant *Paenibacillus* sp. [17], *Bacillus subtilis* [18], *Mycobacterium* sp. [19], and *Klebsiella* sp. [20]. Mesophilic and moderately thermophilic desulfurizing microorganisms operate at 30 and 45–60°C, respectively. Mining of genomic databases indicates that potential “desulfurizing” bacteria from different genera are still to be isolated [21].

The higher the sulfur content in petroleum fractions, the higher is the nitrogen content [22]. So another proposed application has been the bionitrogenation (BDN) of fuels. Carbazole (CAR) and its alkylated derivatives (Fig. 3) typically comprise 70–75% of the total nitrogen in crude oils [23]. These non-basic nitrogen compounds can be converted into basic compounds during the catalytic cracking process, which are strong inhibitors of

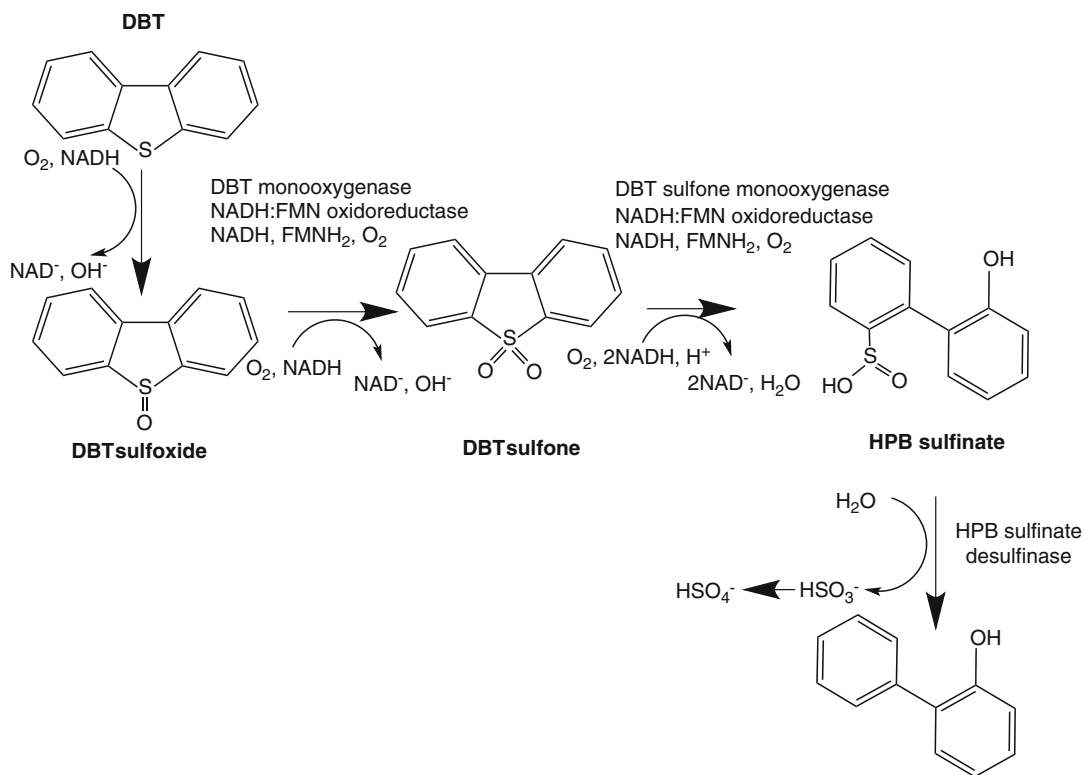


**Fig. 2** 4S pathway for DBT desulfurization

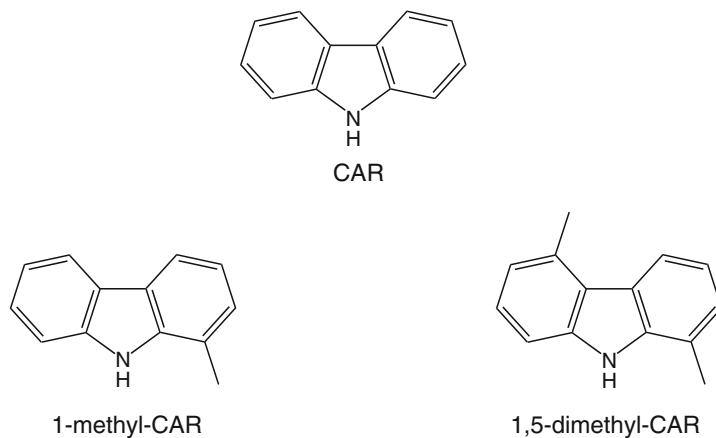


**Fig. 3** Carbazoles

hydrodesulfurization (HDS) catalysts. It is therefore important to remove CAR-like compounds before HDS in order to obtain high yields of desulfurized transportation fuels and reduce NO<sub>x</sub> emissions after combustion. No microorganisms able to selectively extract the nitrogen atom from CARs have been isolated till now

[24]. The removal of the nitrogen atom from CAR leads to the complete degradation of the carbon skeleton leading to the loss of fuel value [25]. Some of the most studied CAR-utilizing microorganisms are *Pseudomonas* [26–33], *Xanthomonas*, *Bacillus*, *Ralstonia* [34], *Klebsiella* [35], *Alteromonas*, *Neptunomonas*, *Cycloclasticus* [36], *Janthinobacterium* [37], *Acinetobacter* [38], *Marinobacterium*, *Achromobacter*, *Nocardioidea* [39], *Burkholderia* [40, 41], *Sphingomonas* [42–44], *Stenotrophomonas*, *Gordonia* [45], *Enterobacter* [46], and *Methylobacterium* [47]. The biodegradation of mono- and dimethyl-CAR is influenced by the positions of the methyl substitutions [28]. Monomethyl-CARs are degraded more easily than CAR and dimethyl-CARs (Fig. 3). Dimethyl-CAR isomers with substitutions on the same benzo-nucleus are more susceptible to degradation especially when harboring one substitution in position 1. The 1-methyl CAR and the 1,5-dimethyl-CAR are the most susceptible and recalcitrant isomers, respectively [28]. In the case of physicochemical catalysis, it has been shown that a higher energy is required to break C–N bonds as compared to C–S bonds and that nitrogen removal requires the hydrogenation of aromatic rings prior to the attack of the C–N bonds [48]. In microbiological catalysis (Fig. 4), CAR is first dihydroxylated by angular dioxygenation before the C–N bond is broken and the nitrogen atom liberated after extensive degradation of the aromatic rings. In contrast, the sulfur atom in DBT has a lower electronegativity compared to the nitrogen atom in CAR [49] and is first oxidized before the C–S bond is broken to liberate sulfate without aromatic ring degradation.

Here, the basic techniques for the isolation and characterization of microorganisms for BDS and BDN applications are presented. For BDS, the isolation of microorganisms able to selectively extract the sulfur atom from DBT-like compounds without C–C bond cleavage is described. The enrichment and isolation procedure is based on the use of DBT as unique source of sulfur, and the culture medium is supplemented with glycerol as a carbon source (see **Notes 1** and **2**). For BDN, the isolation of microorganisms able to degrade CAR-like compounds is described with CAR being used as sole source of carbon and nitrogen for the enrichment and isolation procedure (see **Note 3**). The procedures used to characterize the metabolites produced during BDS and BDN reactions are included, and basic protocols for the evaluation of the treatment of diesel oil and gas oil are also presented. Diesel oil and gas oil are middle-distillate fractions that are well suited for microbial treatment since they concentrate significant amounts of organosulfur compounds and problematic basic nitrogen compounds as mentioned above.

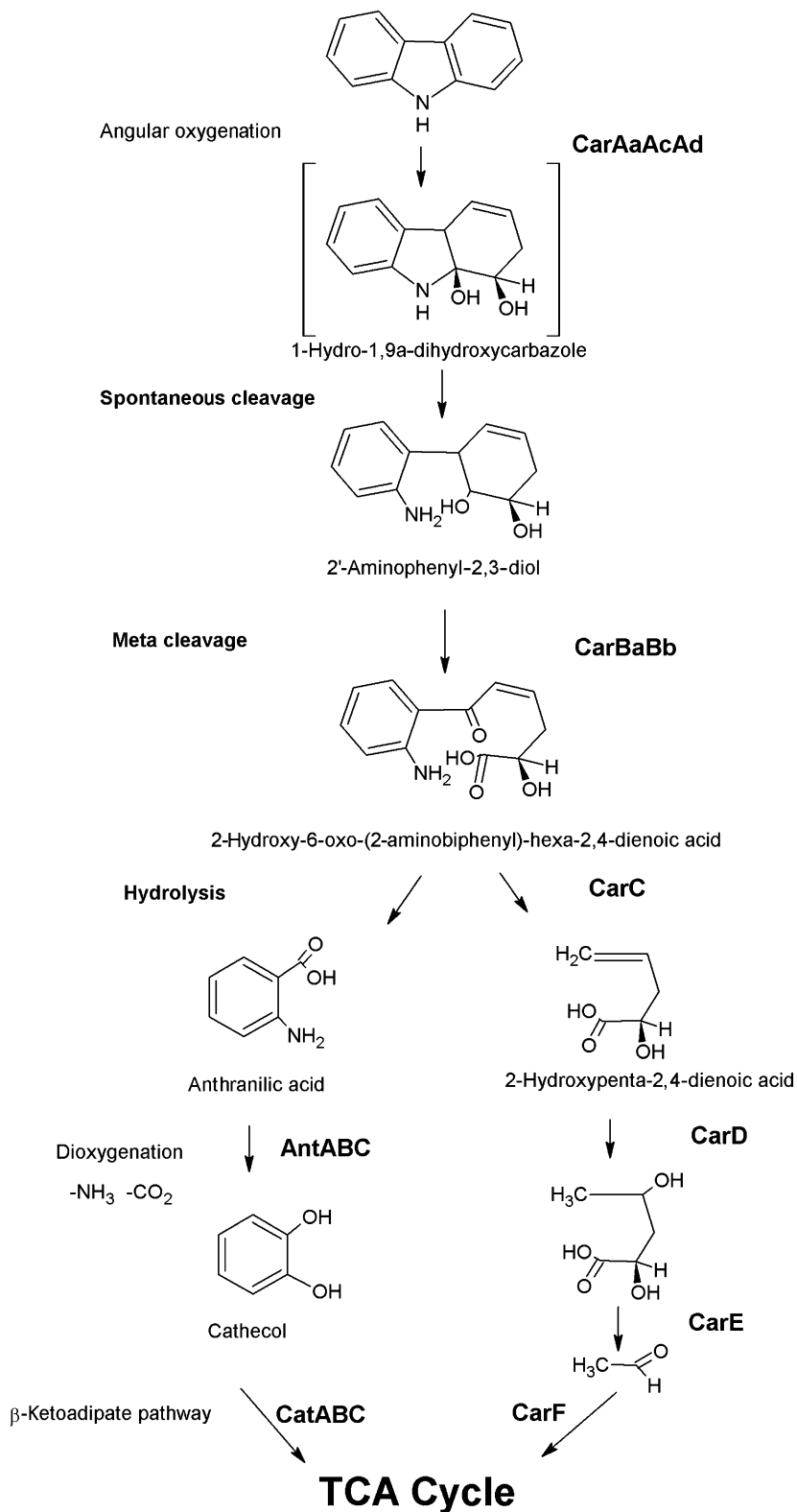


**Fig. 4** Pathway for CAR degradation by *Pseudomonas* sp. CarA: carbazole 1,9a dioxygenase; CarB: 2'-aminophenyl-2,3-diol,1,2-dioxygenase; CarC: 2-hydroxy-6-oxo-6-(20amino.phenyl) hexa 2,4-dienoic acid hydroxylase. Taken from Morales et al. [24]

## 2 Biodesulfurization

### 2.1 Materials and Equipment

#### 2.1.1 Isolation and Identification of Bacteria

1. Minimal salt medium (MSM): 4.33 g of  $\text{Na}_2\text{HPO}_4$ , 2.65 g of  $\text{KH}_2\text{PO}_4$ , 2 g of  $\text{NH}_4\text{Cl}$ , and 0.64 g of  $\text{MgCl}_2 \times 6\text{H}_2\text{O}$  in 1 L of dd $\text{H}_2\text{O}$  [50]. Autoclave at 121°C for 20 min. Add 200  $\mu\text{L}$  of vitamin mixture and 5 mL of metal solution per liter of MSM medium after autoclaving [51].
2. Vitamin mixture: 400 mg of calcium pantothenate, 200 mg of inositol, 400 mg of niacin, 400 mg of pyridoxine hydrochloride, 200 mg of *p*-aminobenzoic acid, and 0.5 mg of cyanocobalamin in 1 L dd $\text{H}_2\text{O}$ . Sterilize by filtration with a cellulose acetate membrane filters with a 0.45  $\mu\text{m}$  pore size.
3. Metal solution: 0.5 g of  $\text{ZnCl}_2$ , 0.5 g of  $\text{FeCl}_2$ , 0.5 g of  $\text{MnCl}_2 \times 4\text{H}_2\text{O}$ , 0.1 g of  $\text{Na}_2\text{MoO}_4 \times 2\text{H}_2\text{O}$ , 0.05 g of  $\text{CuCl}_2 \times 2\text{H}_2\text{O}$ , and 0.05 g of  $\text{Na}_2\text{WO}_4 \times 2\text{H}_2\text{O}$  in 1 L of 100 mM HCl prepared in dd $\text{H}_2\text{O}$ . Sterilize by filtration with a cellulose acetate membrane filter with a 0.45  $\mu\text{m}$  pore size.
4. MSM liquid medium with glycerol as carbon source (Gly-MSM): add 10 g  $\text{L}^{-1}$  of glycerol as an autoclaved concentrated solution to the MSM.
5. Gly-MSM liquid medium with DBT (DBT-Gly-MSM): add 1.5 mM of DBT to the Gly-MSM from a 50 mM stock solution prepared in hexane. The hexane is then allowed to evaporate in the laminar flow hood.
6. DBT-Gly-MSM solid medium: add 15 g  $\text{L}^{-1}$  of Difco Noble agar to the MSM before autoclaving. The vitamin mixture, metal solution, and glycerol are added after autoclaving as described below. The DBT is spread on the solidified medium using sterile glass beads (3 mm diameter) that are shaken on top of the medium to evenly spread the DBT solution on the top of the agar. 1 mL of DBT stock solution is used for a 90 mm diameter petri dish. The hexane is then allowed to evaporate in the laminar flow hood.
7.  $\text{NaHCO}_3$  1 M (pH 8.0): 84 g of  $\text{NaHCO}_3$  in 1 L dd $\text{H}_2\text{O}$ .
8. Gibbs reagent (2,6-dichloroquinone-4-chloroimide, Fluka 35620): freshly prepared by dissolving 20 mg of reagent in 1 mL of ethanol.
9. Materials, reagents, and thermal cycler for polymerase chain reaction (PCR) including standard Taq DNA polymerase and 10 $\times$  buffer containing 15 mM  $\text{MgCl}_2$ , dNTPs, and the Bac8f (5'-AGA GTT TGA TCC TGG CTC AG-3') and 1492r (5'-GGT TAC CTT GTT ACG ACT T-3') primers specific to the 16S rRNA genes from bacteria [52, 53].

10. Materials, reagents, and apparatus for ion-exchange high-performance liquid chromatography (HPLC) including a 250 × 4.5 mm IonoSpher A anion-exchange column (Varian), a photodiode array detector (PDAD), a potassium hydrogen phthalate buffer (40 mM, pH 4), and sulfate standards prepared in MSM to generate a standard curve with concentrations under 10 mM.

**2.1.2 Analysis of Organosulfur Compounds and Metabolites**

1. DBT-Gly-MSM liquid medium.
2. 50 mL Oak Ridge Teflon centrifuge tubes (Nalgene), centrifuge, and rotor capable of spinning up to 10,000g.
3. Materials, reagents, and apparatus for gas chromatography (GC) including a GC chromatograph coupled to mass spectrometry (MS) with a 30 m × 250 μm × 0.25 μm 5% phenylmethyl polysiloxane nonpolar capillary column (Hewlett-Packard), helium as carrier gas (*see Note 4*), and a flame ionization detector (FID) (*see Note 5*) to detect hydrocarbon-containing molecules, DBT sulfoxide, DBT sulfone, and 2-hydroxybiphenyl (2-HBP) (*see Note 6*) standards (0.2–1.2 mg mL<sup>-1</sup>) prepared in heptane, naphthalene as internal standard.

**2.1.3 BDS of a Diesel Oil**

1. DBT-Gly-MSM liquid medium.
2. NaCl 0.85% (wt/v) prepared in dd H<sub>2</sub>O and autoclaved at 121°C for 20 min.
3. MSM salts: MSM without vitamin mixture and metal solution.
4. Anhydrous Na<sub>2</sub>SO<sub>4</sub> (reagent grade).
5. Materials, reagents, and apparatus for GC including an FID and a sulfur chemiluminescence detector (SCD) (*see Note 7*) and a dimethylsiloxane column (30 m × 320 μm × 0.25 μm) (Hewlett-Packard).
6. Materials, reagents, and apparatus for sulfur-in-oil analysis including a sulfur-in-oil analyzer and corresponding commercial sulfur standard (Horiba) (*see Note 8*), reagent grade commercial mineral oil, or low sulfur content isooctane.

**2.2 Methods**

**2.2.1 Isolation and Identification of Bacteria**

1. Inoculate 100 mL of DBT-Gly-MSM with 10 g of a soil sample collected in an area contaminated with heavy crude oil in a 500 mL Erlenmeyer flask. Grow for 14 days at 30°C (*see Note 9*) in an orbital shaker with an agitation of 200 rpm.
2. Use 10 mL of this culture (let the soil settle before sampling the culture) to inoculate 100 mL of the same medium in a 500 mL Erlenmeyer flask. Grow for 14 days at 30°C in an orbital shaker with an agitation of 200 rpm.
3. Repeat the same procedure twice.

4. Spread 150  $\mu\text{L}$  of serial dilutions of the obtained culture on DBT-Gly-MSM plates. Grow until visible colonies are obtained.
  5. At this stage, several different microorganisms can be observed based on colony morphology.
  6. Purify the obtained colonies by repeated streaking on DBT-Gly-MSM plates.
  7. Inoculate individual purified colonies in 5 mL of DBT-Gly-MSM in screw-capped 25 mL culture tubes. Grow for 7 days or until significant growth is observed at 30°C in an orbital shaker with an agitation of 200 rpm.
  8. Centrifuge 1.5 mL of the obtained cultures and save the rest of the culture at +4°C. Recover the supernatants, filter through 0.45  $\mu\text{m}$  nylon filters, transfer to new tubes, and store at -20°C for further analysis (*see* Sect. 2.2.2. Analysis of organosulfur compounds and metabolites).
  9. Transfer 1 mL of the filtered supernatant to a glass tube containing 200  $\mu\text{L}$  of  $\text{NaHCO}_3$  (1 M) and vortex to mix. Add 100  $\mu\text{L}$  of the Gibbs reagent and incubate for 1 h at 30°C under agitation. The Gibbs reagent reacts with aromatic hydroxyl groups (phenolic compounds) such as 2-HBP to form a blue to purple-colored complex (*see* **Note 10**) [54]. Use 1 mL of non-inoculated DBT-Gly-MSM as negative control. At this stage, cultures developing a blue to purple color are considered positive for further analysis.
  10. Determine the release of sulfur in the form of sulfate in the positive culture supernatants by ion-exchange HPLC using a PDAD at 308 nm and elution with potassium hydrogen phthalate buffer at 0.8 mL  $\text{min}^{-1}$ . Inject the filtered culture supernatant obtained in step 8 and use the DBT-Gly-MSM as negative control. At this stage, cultures that both developed a blue color and released sulfate in the culture medium are considered positive for further analyses.
  11. Identify the isolates by sequencing the 16S rRNA gene using the Bac8f and Univ1492r bacterial primers (*see* **Note 11**) under standard reaction conditions with the following amplification conditions: one cycle of 2 min at 95°C; 35 cycles of 45 s at 94°C, 30 s at 56°C, and 1 min at 72°C; and one cycle of final extension at 72°C for 5 min.
  12. Store the cultures at +4°C in DBT-Gly-MSM agar slants or at -80°C in the presence of 25% (v/v) of sterile glycerol.
1. Inoculate 25 mL of DBT-Gly-MSM with 2.5 mL of a previous positive culture and grow for 7 days at 30°C in an orbital shaker with an agitation of 200 rpm.

2. Acidify the cultures to pH 2 with concentrated HCl.
3. Extract three times with an equal volume of toluene, discard the aqueous phase, and filter the extracts through a 0.45  $\mu\text{m}$  nylon membrane. Dry by passing the obtained solution through a column of anhydrous  $\text{Na}_2\text{SO}_4$  and concentrate by evaporation with a rotavapor.
4. Analyze the sulfur compounds (DBT) and the produced metabolites (DBT sulfoxide and DBT sulfone) by GC-MS. Program the injector temperature at 250°C and the FID at 250°C. For DBT and its metabolites, program the oven temperature at 100°C (initial temperature) for 2 min, then increase the temperature from 100 to 200°C at a rate of 10°C  $\text{min}^{-1}$ , and finally hold for 2 min at 200°C. For quantification of DBT, alkylated DBTs, and their metabolites, prepare 0.2–1.2 mg  $\text{mL}^{-1}$  standard curves and use naphthalene as internal standard. Determine the molecular structure of the metabolites produced from DBT alkylated derivatives by MS by comparing the obtained spectrographs with mass spectrograph libraries data prepared from known standard compounds.

### 2.2.3 BDS of a Diesel Oil

1. Culture the microorganisms as described above in DBT-Gly-MSM liquid medium, harvest the cells in mid-exponential phase of growth, wash twice with NaCl 0.85%, and suspend the cells in MSM salts.
2. Prepare 100 mL of Gly-MSM in a 500 mL Erlenmeyer flask and add 10% (v/v) of diesel oil. Inoculate with the suspended biomass in order to achieve a wet biomass concentration of 5 g  $\text{L}^{-1}$ . Incubate for 7 days at 30°C in an orbital shaker with an agitation of 200 rpm. Prepare control diesel oil without biomass and incubate under the same conditions.
3. Separate the oil by centrifugation at 10,000g for 10 min and dry over anhydrous  $\text{Na}_2\text{SO}_4$  to eliminate all the residual water.
4. Analyze the quantity and distribution of total hydrocarbons and organosulfur compounds in treated and non-treated diesel oil by GC coupled to an FID and an SCD. Set the injector and detector temperatures to 280 and 300°C, respectively. Figure 5 shows an example of the distribution of hydrocarbons in diesel oil submitted to BDS [9].
5. Analyze the total sulfur content of the treated and non-treated oil with a sulfur-in-oil analyzer. If required, the samples can be diluted with commercial mineral oil or isooctane with low sulfur content. The sulfur content of the diluent must also be analyzed.

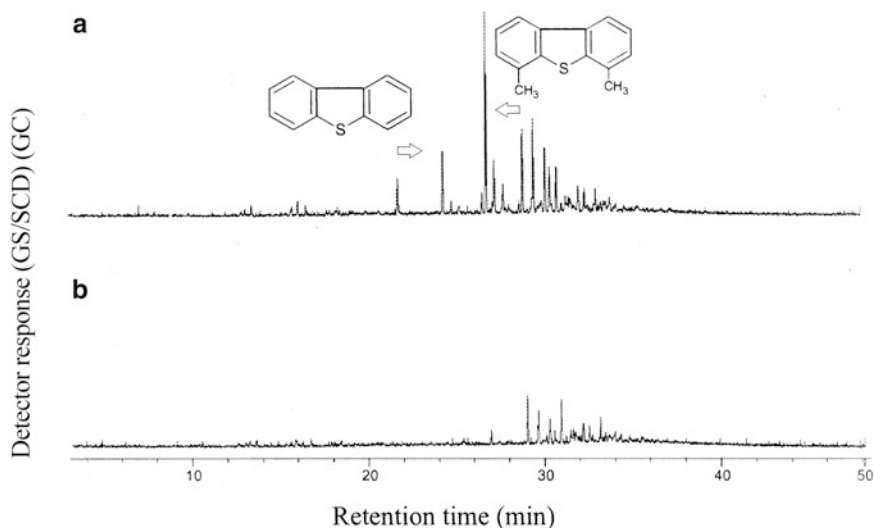


**Fig. 5** GC-SCD chromatographs of diesel oil (a) before and (b) after BDS treatment with strain *Rhodococcus* sp. IMP-S02. The DBT and 4,6-DMDBT peaks are indicated by arrows. Taken from Castorena et al. [9]. Reproduced with the permission of the publisher, “John Wiley and Sons”

### 3 Biodenitrogenation

#### 3.1 Materials and Equipment

##### 3.1.1 Isolation and Identification of Bacteria

1. Minimal medium (MM) (*see Note 12*): 2.2 g of  $\text{Na}_2\text{HPO}_4 \times 12\text{H}_2\text{O}$ , 0.8 g of  $\text{KH}_2\text{PO}_4$ , 0.015 g of  $\text{FeSO}_4 \times 7\text{H}_2\text{O}$ , 0.015 g of  $\text{CaCl}_2 \times 2\text{H}_2\text{O}$ , 0.015 g of  $\text{MgSO}_4 \times 7\text{H}_2\text{O}$ , and 0.025 g of yeast extract [26] in 1 L of  $\text{ddH}_2\text{O}$ .
2. MM liquid medium with CAR as carbon source (CAR-MM): add 0.1% of CAR (wt/v) to the MM after autoclaving from a  $10 \text{ mg mL}^{-1}$  stock solution prepared in dimethyl sulfoxide and sterilized by filtration with a  $0.2 \mu\text{m}$  pore-size PTFE membrane filter.
3. CAR-MM solid medium: add  $15 \text{ g L}^{-1}$  of Difco Noble agar to the MM before autoclaving. After autoclaving, cool the medium to about  $60^\circ\text{C}$  before adding the CAR at a final concentration of 0.1% (wt/v) and pour into 90 mm diameter petri dishes.
4. Materials and reagents for polymerase chain reaction (PCR) as described above (Sect. 2.1.1).
5. Materials, reagents, and apparatus for HPLC including a C-18 column ( $4.6 \times 150 \text{ mm}$ , Hewlett-Packard) and a photodiode array detector (PDAD), a mobile phase of (86:14) (v/v) methanol–water mixture, and CAR standards prepared in acetonitrile (ACN) with CAR concentrations under 2 mM.

### 3.1.2 Analysis of Organonitrogen Compounds and Metabolites

1. CAR-MM liquid medium.
2. 50 mL Oak Ridge Teflon centrifuge tubes, centrifuge, and rotor capable of spinning up to 10,000*g*.
3. Materials, reagents, and apparatus for GC including a 30 m × 250 μm × 0.25 μm nonpolar capillary column such as 5% phenylmethyl polysiloxane or a 100% dimethylpolysiloxane column (Hewlett-Packard) [55], CAR and alkylated CAR standards prepared in isooctane (0–1 mg mL<sup>-1</sup>), and *N*-phenyl-CAR as internal standard.

### 3.1.3 BDN of a Gas Oil

1. CAR-MM.
2. NaCl 0.85% (wt/v).
3. MM salts: MM without yeast extract.
4. Oak Ridge Teflon centrifuge tubes, centrifuge, and rotor capable of spinning up to 10,000*g*.
5. Materials, reagents, and apparatus for GC including a GC chromatograph coupled to an FID and MS and a dimethylsiloxane column (30 m × 320 μm × 0.25 μm) (Hewlett-Packard).
6. Materials, reagents, and apparatus for nitrogen-in-oil analysis including a ThermoQuest Trace 2000 GC (ThermoQuest) equipped with a nitrogen phosphorous detector (NPD) (*see Note 13*) [41], an (30 m × 320 μm × 0.20 μm) Alltech TM10 column, and quinoline as external standard (Fig. 6).

## 3.2 Methods

### 3.2.1 Isolation and Identification of Bacteria

1. Inoculate 100 mL of CAR-MM with 10 g of a soil sample collected in an area contaminated with heavy crude oil in a 500 mL Erlenmeyer flask and grow for 14 days at 30°C in an orbital shaker with an agitation of 200 rpm.
2. Use 10 mL of this culture (let the soil settle before sampling the culture) to inoculate 100 mL of fresh medium in a 500 mL Erlenmeyer flask and grow for 14 days at 30°C in an orbital shaker with an agitation of 200 rpm.
3. Repeat the same procedure three times.
4. Spread 150 μL of serial dilutions of the obtained culture on CAR-MM solid medium and grow at 30°C until visible colonies are obtained.
5. At this stage, several different microorganisms can be observed based on colony morphology. Colonies surrounded by a clear zone, as a result of CAR degradation, are considered positive.
6. Purify the obtained colonies by repeated streaking on CAR-MM solid medium.

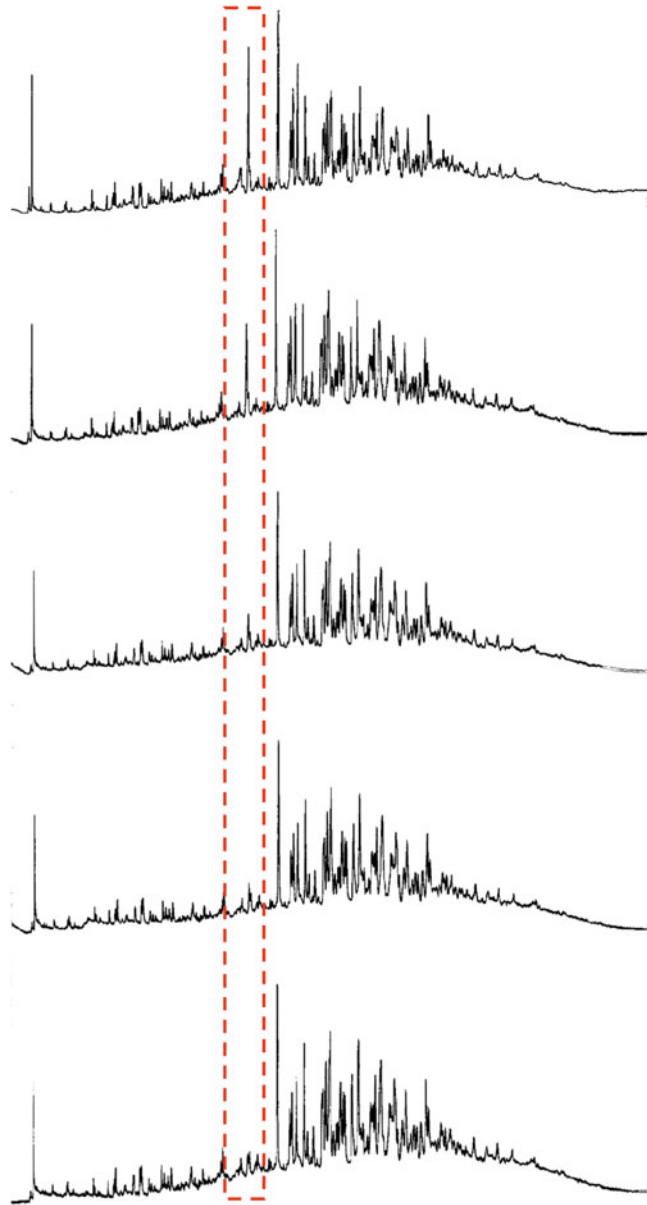


**Fig. 6** GC-NPD chromatograms of gas oil: light cycle oil (85:15) during BDN treatment. The first chromatogram corresponds to the sample before treatment, while the other chromatograms correspond to samples treated with a *Pseudomonas* sp. The CAR peak is marked in *dashed line* (unpublished data)

7. Inoculate individual purified colonies in 5 mL of CAR-MM in screw-capped 25 mL culture tubes and grow for 7 days or until significant growth is observed at 30°C in an orbital shaker with an agitation of 200 rpm.

8. Re-inoculate the 5 mL in 50 mL of the same medium in a 250 mL Erlenmeyer flask. Grow for 7 days at 30°C in an orbital shaker with an agitation of 200 rpm.
9. Acidify the cultures to pH 2 with 4 N H<sub>2</sub>SO<sub>4</sub> [56].
10. Extract 25 mL of the culture with an equal volume of ACN and save the rest of the culture at +4°C. Filter the extract through a 0.2 µm PTFE filter.
11. Analyze the degradation of CAR by reverse phase HPLC using a PDAD at 230 nm and an elution flow rate of 0.5 mL min<sup>-1</sup>. Inject the filtered culture supernatant obtained in step 10 and use an extract of CAR-MM as negative control.
12. At this stage, cultures that both show the halo zone in solid medium and present a decrease of the CAR peak in HPLC are considered positive for further analysis.
13. Identify the isolates by sequencing the 16S rRNA gene as described below (Sect. 2.2.1).
14. Store the cultures at +4°C in CAR-MM agar slants or at -80°C in the presence of 25% (v/v) of glycerol.

3.2.2 Analysis of  
Organonitrogen  
Compounds and  
Metabolites

1. Inoculate 25 mL of CAR-MM with 2.5 mL of a previous positive culture and grow for 7 days at 30°C in an orbital shaker with an agitation of 200 rpm.
2. Extract the culture three times with an equal volume of ethyl acetate, discard the aqueous phase, and filter the extracts through a 0.2 µm PTFE membrane. Dry over anhydrous Na<sub>2</sub>SO<sub>4</sub> and concentrate by evaporation.
3. Analyze the nitrogen compounds and the produced metabolites by GC-MS. Program the column temperature from 50 (held 3 min) to 220°C with an increasing rate of 10°C min<sup>-1</sup>. Set the injector, detector, and oven temperatures at 200, 220, and 100°C, respectively. CAR metabolites include 1-hydro-1,9a-dihydroxycarbazole, 2-hydroxy-6-oxo-(2aminobiphenyl)-hexa-2,4 dienoic acid, anthranilic acid, 2-hydroxypenta-2,4 dienoic acid, and catechol (Fig. 4) [24]. For quantification of CAR and alkylated CARs, prepare 0-1 mg mL<sup>-1</sup> standard curves and use *N*-phenylCAR as internal standard. The molecular structure of the metabolites produced from CAR alkylated derivatives can be determined by MS by comparing the obtained spectrographs with mass spectrograph libraries data prepared from known standard compounds.

3.2.3 *BDN of a Gas Oil*

1. Culture the microorganisms as described above in CAR-MM liquid medium, harvest the cells in mid-exponential phase of growth, wash twice with NaCl (0.85%), and suspend the cells in MM salts.
2. Prepare 100 mL of MM in a 500 mL Erlenmeyer flask and add an equal volume of gas oil. Inoculate with the suspended biomass in order to achieve a concentration of  $2 \text{ g L}^{-1}$  of biomass and incubate for 7 days at  $30^\circ\text{C}$  in an orbital shaker with an agitation of 200 rpm. Prepare control gas oil without biomass and incubate under the same conditions.
3. Separate the oil by centrifugation at  $10,000g$  for 10 min and dry over anhydrous  $\text{Na}_2\text{SO}_4$  to eliminate all the residual water.
4. Analyze the quantity and distribution of total hydrocarbons in treated and non-treated gas oil by GC coupled to FID. Set the injector and detector temperatures to  $280$  and  $300^\circ\text{C}$ .
5. Analyze the quantity and distribution of organonitrogen compounds in treated and non-treated gas oil using a ThermoQuest Trace 2000 GC equipped with an NPD (*see Note 13*) [41]. Set the injector temperature at  $250^\circ\text{C}$  and the detector temperature at  $275^\circ\text{C}$ . Keep the oven temperature at  $100^\circ\text{C}$  for 1 min, increase the temperature up to  $156^\circ\text{C}$  at a rate of  $4^\circ\text{C min}^{-1}$ , increase the temperature up to  $198^\circ\text{C}$  at a rate of  $2^\circ\text{C min}^{-1}$ , and finally increase the temperature up to  $250^\circ\text{C}$  at a rate of  $4^\circ\text{C min}^{-1}$ . Set the airflow at  $50 \text{ mL min}^{-1}$ , the  $\text{H}_2$  flow at  $2 \text{ mL min}^{-1}$ , and the makeup flow ( $\text{N}_2$ ) at  $10 \text{ mL min}^{-1}$ .
6. Analyze the total nitrogen content of the treated and non-treated gas oil using the ASTM D4649 method (*see Note 14*) [23].<sup>1</sup>

---

## 4 Notes

1. Alkylated derivatives of DBT may also be used and are in fact recommended if heavier fractions are to be treated; these compounds will be more abundant in fractions derived from heavy oils.
2. The isolation of microorganisms able to selectively cleave C–S bonds within alkyl chains and release sulfate by using the synthetic compound bis-(3-pentafluorophenylpropyl)-sulfide as sole source of sulfur has been reported [57].

---

<sup>1</sup> ASTM D4629-08 Standard test method for trace nitrogen in liquid petroleum hydrocarbons by syringe/inlet oxidative combustion and chemiluminescence detection

3. Alkylated derivatives of CAR may also be used and are in fact recommended if heavier fractions are to be treated; these compounds will be more abundant in fractions derived from heavy oils.
4. HPLC can be used when DBT is the substrate. In this case, the cultures are extracted with an equal volume of acetonitrile (ACN), filtered and injected onto a C18 reverse phase column. Elution is performed at  $1 \text{ mL min}^{-1}$  with a 80/20 (v/v) ACN/water mobile phase, and detection is realized with an UV detector at 225 nm. DBT and 2-HBP standards are prepared in ACN to generate a standard curve for concentrations between  $0.02$  and  $0.10 \text{ mg mL}^{-1}$ .
5. FIDs are used to detect total hydrocarbons (not only sulfur-containing hydrocarbons). So both the organosulfur compounds and their desulfurized metabolites will be detected.
6. Different temperature conditions must be used for the analysis of alkylated DBT derivatives and their metabolites.
7. The SCD is a sulfur-specific detector in which the sulfur-containing compounds are burned at a very high temperature ( $>1,800^\circ\text{C}$ ) to form sulfur monoxide (SO). A photomultiplier tube detects the light produced by the chemiluminescent reaction of SO with ozone.
8. For low sulfur levels (5–20 ppm), the detection is performed by X-ray fluorescence. For ultralow sulfur levels (30 ppb), the detection can be performed through combustion ultraviolet fluorescence.
9. If thermophilic desulfurizing microorganisms are targeted, a higher temperature should be used.
10. DBT alkylated derivatives may produce a purple rather than blue color.
11. If thermophilic microorganisms were targeted, the archaeal primers PRA46f and PREA1100r may be used as described by [58].
12. Other similar or more concentrated mineral medium compositions have been used [27, 40].
13. The NPD (also called thermionic detector) is a very sensitive detector that responds almost exclusively to nitrogen and phosphorus compounds. Nitrogen- or phosphorus-containing molecules exiting the column collide with a hot rubidium or cesium silicate glass bead located near the FID and undergo a catalytic surface chemistry reaction. The resulting ions are attracted to a collector electrode and amplified.
14. Briefly, fuel samples are injected into a high-temperature combustion tube where the fuel is vaporized and organically bound

nitrogen is converted to nitric oxide (NO) in an oxygen-rich atmosphere. The water produced during the sample combustion is removed, and the sample combustion gases are then exposed to ultraviolet (UV) light. The NO contacts ozone and is converted to excited nitrogen oxide (NO<sub>2</sub>). The light is emitted as the excited NO<sub>2</sub> decays and a photomultiplier tube detects it and the resulting signal is a measure of the nitrogen contained in the sample. CAR or pyridine can be used as standard.

## References

- Morales M, Ayala M, Vazquez-Duhalt R, Le Borgne S (2010) Application of microorganisms to the processing and upgrading of crude oil and fractions. In: Timmis KN, McGenity TJ, Meer JR, de Lorenzo V (eds) Consequences of microbial interactions with hydrocarbons, oils and lipids, vol 4, Handbook of hydrocarbon and lipid microbiology. Springer, Berlin, pp 2768–2785
- Mohebbi G, Ball AS (2008) Biocatalytic desulfurization (BDS) of petrodiesel fuels. *Microbiology* 154:2169–2183
- Kabe T, Akamatsu K, Ishihara A, Otsuki S, Godo M, Zhang Q, Qian W (1997) Deep hydrodesulfurization of light gas oil. 1. Kinetics and mechanisms of dibenzothiophene hydrodesulfurization. *Ind Eng Chem Res* 36:5146–5152
- Monticello DJ, Finnerty WR (1985) Microbial desulfurization of fossil fuels. *Annu Rev Microbiol* 39:371–389
- Le Borgne S, Ayala M (2010) Microorganisms utilizing sulfur-containing hydrocarbons. In: Timmis KN, McGenity TJ, Meer JR, de Lorenzo V (eds) Microbes and communities utilizing hydrocarbons, oils and lipids, vol 3, Handbook of hydrocarbon and lipid microbiology. Springer, Berlin, pp 2130–2141
- Kilbane JJ (1992) Mutant microorganisms useful for cleavage of organic C-S bonds. US Patent No. 5,104,801
- Denis-Larose C, Labbe D, Bergeron H, Jones AM, Creer CW, Al-Hawari J, Grossman MJ, Sankey BM, Lau PCK (1997) Conservation of plasmid-encoded dibenzothiophene desulfurization genes in several *Rhodococci*. *Appl Environ Microbiol* 63:2915–2919
- Izumi Y, Ohshiro T, Ogino H, Hine Y, Shimao M (1994) Selective desulphurization of dibenzothiophene by *Rhodococcus erythropolis* D-1. *Appl Environ Microbiol* 60:223–226
- Castorena G, Suárez C, Valdez I, Amador G, Fernández L, Le Borgne S (2002) Sulfur-selective desulfurization of dibenzothiophene and diesel oil by newly isolated *Rhodococcus* sp. strains. *FEMS Microbiol Lett* 215:157–161
- Rhee SK, Chang JH, Chang YK, Chang HN (1998) Desulfurization of dibenzothiophene and diesel oils by a newly isolated *Gordonia* strain, CYKS1. *Appl Environ Microbiol* 64:2327–2331
- Chang JH, Rhee SK, Chang YK, Chang HN (1998) Desulfurization of diesel oils by a newly isolated dibenzothiophene-degrading *Nocardia* sp. strain CYKS2. *Biotechnol Prog* 14:851–855
- Darzins A, Mrachko GT (2000) *Sphingomonas* biodesulfurization catalyst. US Patent No. 6,133,016
- Bhatia S, Sharma DK (2010) Biodesulfurization of dibenzothiophene, its alkylated derivatives and crude oil by a newly isolated strain *Pantoea agglomerans* D23W3. *Biochem Eng J* 50:104–109
- Papizadeh M, Ardakani MR, Motamedi H, Rasouli I, Zarei M (2011) C-S targeted biodegradation of dibenzothiophene by *Stenotrophomonas* sp. NISOC-04. *Appl Biochem Biotechnol* 165:938–948
- Gunam IB, Yamamura K, Sujaya IN, Antara NS, Aryanta WR, Tanaka M, Tomita F, Sone T, Asano K (2013) Biodesulfurization of dibenzothiophene and its derivatives using resting and immobilized cells of *Sphingomonas subarctica* T7b. *J Microbiol Biotechnol* 23:473–482
- Nassar HN, El-Gendy NS, Abo-State MA, Mostafa YM, Mahdy HM, El-Temtamy SA (2013) Desulfurization of dibenzothiophene by a novel strain *Brevibacillus invocatus* C19 isolated from Egyptian coke. *Biosci Biotechnol Res Asia* 10:29–46
- Konishi J, Ishii Y, Onaka T, Okumura K, Suzuki M (1997) Thermophilic carbon-sulfur-bond-targeted biodesulfurization. *Appl Environ Microbiol* 63:3164–3169

18. Kirimura K, Furuya T, Nishii Y, Ishii Y, Kino K, Usami S (2001) Biodesulfurization of dibenzothiophene and its derivatives through the selective cleavage of carbon-sulfur bonds by a moderately thermophilic bacterium *Bacillus subtilis* WU-S2B. *J Biosci Bioeng* 91:262–266
19. Furuya T, Kirimura K, Kino K, Usami S (2001) Thermophilic biodesulfurization of dibenzothiophene and its derivatives by *Mycobacterium phlei* WU-F1. *FEMS Microbiol Lett* 204:129–133
20. Bhatia S, Sharma DK (2012) Thermophilic desulfurization of dibenzothiophene and different petroleum oils by *Klebsiella* sp. 13T. *Environ Sci Pollut Res Int* 19:3491–3497
21. Bhatia S, Sharma DK (2010) Mining of genomic databases to identify novel biodesulfurizing microorganisms. *J Ind Microbiol Biotechnol* 37:425–429
22. Éigenson AS, Ivchenko EG (1977) Distribution of sulfur and nitrogen in fractions from crude oil and residues. *Chem Technol Fuels Oils* 13:542–544
23. Laredo GC, Leyva S, Alvarez R, Mares MT, Castillo JJ, Cano JL (2002) Nitrogen compounds characterization in atmospheric gas oil and light cycle oil from a blend of Mexican crudes. *Fuel* 81:1341–1350
24. Morales M, Le Borgne S (2010) Microorganisms utilizing nitrogen-containing hydrocarbons. In: Timmis KN, McGenity TJ, Meer JR, de Lorenzo V (eds) *Microbes and communities utilizing hydrocarbons, oils and lipids*, vol 3, *Handbook of hydrocarbon and lipid microbiology*. Springer, Berlin, pp 4554–4562
25. Yu B, Xu P, Zhu S, Cai X, Wang Y, Li L, Li F, Liu X, Ma C (2006) Selective biodegradation of S and N heterocycles by a recombinant *Rhodococcus erythropolis* strain containing carbazole dioxygenase. *Appl Environ Microbiol* 72:2235–2238
26. Ouchiyama N, Zhang Y, Omori T, Kodama T (1993) Biodegradation of carbazole by *Pseudomonas* spp. CA06 and CA10. *Biosci Biotechnol Biochem* 57:455–460
27. Hisatsuka K, Sato M (1994) Microbial transformation of carbazole to anthranilic acid by *Pseudomonas stutzeri*. *Biosci Biotechnol Biochem* 58:213–214
28. Li L, Li Q, Li F, Shi Q, Yu B, Liu F, Xu P (2006) Degradation of carbazole and its derivatives by a *Pseudomonas* sp. *Appl Microbiol Biotechnol* 73:941–948
29. Larentis AL, Sampaio HCC, Carneiro CC, Martins OB, Alves TLM (2011) Evaluation of growth, carbazole biodegradation and anthranilic acid production by *Pseudomonas stutzeri*. *Braz J Chem Eng* 28(01):37–44
30. Singh GB, Srivastava A, Saigal A, Aggarwal S, Bisht S, Gupta S, Srivastava S, Gupta N (2011) Biodegradation of carbazole and dibenzothiophene by bacteria isolated from petroleum-contaminated sites. *Biorem J* 15(4):189–195
31. Zhao C, Zhang Y, Li X, Wen D, Tang X (2011) Biodegradation of carbazole by the seven *Pseudomonas* sp. strains and their denitrification potential. *J Haz Mat* 190:253–259
32. Nojiri H (2012) Structural and molecular genetic analyses of bacterial carbazole degradation system. *Biosci Biotechnol Biochem* 76:1–18
33. Singh GB, Gupta S, Gupta N (2013) Carbazole degradation and biosurfactant production by newly isolated *Pseudomonas* sp. strain GBS.5. *Int Biodeterior Biodegradation* 84:35–43
34. Schneider J, Grosser RJ, Jayasimhulu K, Xue W, Kinkle B, Warshawsky D (2000) Biodegradation of carbazole by *Ralstonia* sp. RJGII.123 isolated from hydrocarbon contaminated soil. *Can J Microbiol* 46:269–277
35. Li YW, Li WL, Huang JX, Xiong XCH, Gao HSH, Xing JM, Liu HZ (2008) Biodegradation of carbazole in oil/water biphasic system by a newly isolated bacterium *Klebsiella* sp. LSSE-H2. *Biochem Eng J* 41:166–170
36. Fuse H, Takimura O, Murakami K, Inoue H, Yamaoka Y (2003) Degradation of chlorinated biphenyl, dibenzofuran, and dibenzo-p-dioxin by marine bacteria that degrade biphenyl, carbazole, or dibenzofuran. *Biosci Biotechnol Biochem* 67:1121–1125
37. Yamazoe A, Yagi O, Oyaizu H (2004) Bio-transformation of fluorene, diphenyl ether, dibenzo-p-dioxin and carbazole by *Janibacter* sp. *Biotechnol Lett* 26:479–486
38. Singh GB, Gupta S, Srivastava S, Gupta N (2011) Biodegradation of carbazole by newly isolated *Acinetobacter* spp. *Bull Environ Contam Toxicol* 87:522–526
39. Inoue K, Habe H, Yamane H, Omori T, Nojiri H (2005) Diversity of carbazole-degrading bacteria having the car gene cluster: isolation of a novel gram-positive carbazole-degrading bacterium. *FEMS Microbiol Lett* 245:145–153
40. Castorena G, Múgica V, Le Borgne S, Acuña ME, Bustos- Jaimes I, Aburto J (2006) Carbazole biodegradation in gas oil/water biphasic media by a new isolated bacterium *Burkholderia* sp. strain IMP5GC. *J Appl Microbiol* 100:739–745

41. Castorena G, Acuña MA, Aburto J, Bustos-Jaimes I (2008) Semi-continuous biodegradation of carbazole in fuels by biofilm-immobilised cells of *Burkholderia* sp. strain IMP5GC. *Process Biochem* 43:1318–1321
42. Habe H, Ashikawa Y, Saiki Y, Yoshida T, Nojiri H, Omori T (2002) *Sphingomonas* sp. strain KA1, carrying a carbazole dioxygenase gene homologue, degrades chlorinated dibenzo-p-dioxins in soil. *FEMS Microbiol Lett* 211:43–49
43. Kilbane JJ II, Daram A, Abbasian J, Kayser KJ (2002) Isolation and characterization of *Sphingomonas* sp. GTIN11 capable of carbazole metabolism in petroleum. *Biochem Biophys Res Commun* 297:242–248
44. Shepherd JM, Lloyd-Jones G (1998) Novel carbazole degradation genes of *Sphingomonas* CB3: sequence analysis, transcription, and molecular ecology. *Biochem Biophys Res Commun* 247:129–135
45. Santos SC, Alviano DS, Alviano CS, Padula M, Leitao AC, Martins OB, Ribeiro CM, Sasaki MY, Matta CP, Bevilacqua J, Sebastian GV, Seldin L (2006) Characterization of *Gordonia* sp. strain F.5.25.8 capable of dibenzothiophene desulfurization and carbazole utilization. *Appl Microbiol Biotechnol* 71:355–362
46. Singh GB, Srivastava S, Gupta S, Gupta N (2011) Evaluation of carbazole degradation by *Enterobacter* sp. isolated from hydrocarbon contaminated soil. *Recent Res Sci Technol* 3:44–48
47. Pasternak G, Kolwzan B (2013) Surface tension and toxicity changes during biodegradation of carbazole by newly isolated methylotrophic strain *Methylobacterium* sp. GPE1. *Int Biodeterior Biodegradation* 84:143–149
48. Szymanska A, Lewandowski M, Sayag C, Djega- Mariadassou G (2003) Kinetic study of the hydrodenitrogenation of carbazole over bulk molybdenum carbide. *J Catal* 218:24–31
49. Bressler DC, Fedorak PM (2000) Bacterial metabolism of fluorene, dibenzofuran, dibenzothiophene, and carbazole. *Can J Microbiol* 46:397–409
50. Oldfield C (1998) Microorganisms which can desulphurise benzothiophenes. Patent WO/1998/004678
51. Li FL, Xu P, Ma CQ, Luo LL, Wang XS (2003) Deep desulfurization of hydrodesulfurization treated diesel oil by a facultative Thermophilic bacterium *Mycobacterium* sp. X7B. *FEMS Microbiol Lett* 223:301–307
52. Johnson JL (1994) Similarity analysis of rRNAs. In: Gerhardt P, Murray RGE, Wood WA, Krieg NR (eds) *Methods for general and molecular microbiology*. ASM Press, Washington, pp 683–700
53. Baker GC, Smith JJ, Cowan DA (2003) Review and re-analysis of domain-specific 16S primers. *J Microbiol Methods* 55:541–555
54. Kayser KJ, Bielaga-Jones BA, Jackowski K, Odusan O, Kilbane JJ (1993) Utilization of organosulfur compounds by axenic and mixed cultures of *Rhodococcus rhodochrous* IGTS8. *J Gen Microbiol* 139:3123–3129
55. Kirimura K, Nakagawa H, Tsuji K, Matsuda K, Kurane R, Usami S (1999) Selective and continuous degradation of carbazole contained in petroleum oil by resting cells of *Sphingomonas* sp. CDH-7. *Biosci Biotechnol Biochem* 63:1563–1568
56. Gieg L, Otter A, Fedorak P (1996) Carbazole degradation by *Pseudomonas* sp. LD2: metabolic characteristics and the identification of some metabolites. *Environ Sci Technol* 30:575–585
57. Van Hamme JD, Fedorak PM, Foght JM, Gray MR, Dettman HD (2004) Use of a novel fluorinated organosulfur compound to isolate bacteria capable of carbon-sulfur bond cleavage. *Appl Environ Microbiol* 70:1487–1493
58. Ovreas SL, Forney L, Daae FL, Torsvik V (1997) Distribution of bacterioplankton in meromictic Lake Saelenvannet, as determined by denaturing gradient gel electrophoresis of PCR-amplified gene fragments coding for 16S rRNA. *Appl Environ Microbiol* 63:3367–3373

# Protocol for the Application of Bioluminescence Full-Cell Bioreporters for Monitoring of Terrestrial Bioremediation

Sarah B. Sinebe, Ogonnaya I. Iroakasi, and Graeme I. Paton

## Abstract

Microbial full-scale bioreporters are associated with a variety of names that include biosensors, bio-indicators and bio-reactive agents. The role of such microbial agents is to respond to the bioavailable fraction of a given analyte under “near environmental conditions”. Making use of appropriate assays with relevant and biologically compatible extraction procedures means that such techniques can be applied to develop site specific risk and hazard assessments, an appraisal of constraints inhibiting biodegradation and a prediction of potential for biodegradation. The effectiveness of an assay requires: (1) the comprehensive characterisation of the marker gene (the reporter gene) and the isolate, (2) the collection of an environmentally relevant sample in a suitable matrix and (3) a technique to integrate the bioreporters with the sample to generate focussed and relevant data. This technology is ideally placed for high throughput, rapid screening of samples from a range of environmental matrices.

**Keywords:** Bioassay, Bioavailability, Biodegradability, Bioreporters, Degradation, Fingerprint, Hydrocarbon, Non-exhaustive extraction techniques (NEETs)

---

## 1 Introduction

When exhaustive extraction techniques are applied to hydrocarbon contaminated matrices, the measured value reflects what is often referred to as the “total concentration”. This can be fractionated to more fairly represent the component parts present in the matrix. Although risk assessment models can be used to relate this “total value” to relevant ecological and human exposure values, it is not a direct measure of “bioavailability”. The development of “non-exhaustive extraction techniques” (NEETs) enables the user to determine the portion of hydrocarbons that could be termed “bio-available”. A confusing point is that “bioavailable” has been used both to define toxicity and biodegradation. Regardless of this, microbial bioreporters enable a quantitative assessment of the bioavailable fraction if appropriate extractions are conducted and the microbial/environmental interface is appropriate [1]. In this

chapter, the term bioavailability represents the fraction of the chemical that is toxic to the bioreporter and/or the fraction that is degradable.

Many of the earliest manuscripts that championed the use of bioreporters acknowledged both the speed of application and their relatively low cost of deployment [1]. Yet as chromatographic techniques have evolved to offer more automated and low cost analysis, this point is less relevant, and the true value of the bioreporter is based on its status as a biological agent. Examples of their successful use include monitoring bioremediation of hydrocarbon [2, 3], toxicity measurement of chlorophenols in soil water extract [4], bioavailability assessments of chlorinated solvents [5], measurement of toxicity of TPH during bioremediation [6] and measurement of the extractable fraction of naphthalene [7]. There are, however, few examples of researchers having made use of more than a single bioreporter when interrogating an environmental matrix.

The extraction of the bioavailable fraction of hydrocarbons through the use of NEETs has made use of reagents such as Tenax, hydroxypropyl- $\beta$ -cyclodextrin (HPCD), ethanol, methanol and butanol. The fractions extracted by HPCD [8–10], ethanol [11], methanol [9, 12] and Tenax [13] have been correlated with the bioavailable or biodegradable fraction in a broad range of soils. NEETs have also been used to derive an estimation of bioaccessibility [14]. Recently, to complement the array of synthetic extraction solvents deployed, the use of biosurfactants has been proposed because of their ease of application, low toxicity and ability to work within biological systems [15].

It is pertinent to consider the integration of bioreporters and NEETs. In an early study of such an approach, five soils were amended with naphthalene and incubated for 2 days. The soil was extracted with Amberlite XAD-4 and HPCD. The response of the biosensor *Pseudomonas fluorescens* HK44 (pUTK21) to the naphthalene in the soil solution was linear [7] enabling an estimation of the concentration of the bioavailable fraction to be made. Later work confirmed that if optimal bioremediation techniques were deployed, this integrated approach could diagnose a remediation end-point [9]. In practice, remedial constraints imposed by the physiochemical environment can be overcome through the use of appropriate irrigation regimes and some osmotic buffering. The addition of nutrients and the augmentation of samples with a characterised degrader inoculum also serve to remove biological and physiological constraints. This leaves the variable of bioavailability to be considered. It has been proposed that microbial bioreporters can underpin our understanding of bioavailability and the environmental parameters that regulates this [16, 17].

Bioavailability studies have confirmed that hydrocarbon degradation is rarely enhanced by microbial inoculation intimating that the indigenous population is often composed of active degraders

[3, 6, 18]. Such studies can be routinely monitored through the measurement of the response of a combination of constitutive and hydrocarbon induced sensors using appropriate NEETs [3, 6, 18]. Such analysis has been performed across laboratory amended and field collected samples from a wide variety of international sources with matrices impacted by a broad suite of hydrocarbons [6]. If the technology is to be successful, then the response must aid in fulfilling the successful management of a bioremediation programme mainly:

1. Monitor the microbial performance of the indigenous or augmented population
2. Assess the physiochemical environment
3. Determine pollutant/hydrocarbon bioavailability

In this case study, the constitutively marked bioreporters *Escherichia coli* HB101 (pUCD607) and *Pseudomonas putida* F1Tn5 which are “lights off” system [19] and four hydrocarbon induced marked bioreporters that are “lights on” system [19] *P. fluorescens* OS8(pDNdmpRlux), *P. putida* TVA8, *P. fluorescens* HK44 (pUTK21) and *E. coli* HMS174 (pOS25) were used to monitor changes in the bioavailable fraction of a Libyan crude oil (and inferred toxicity) to samples undergoing control and nutrient amended treatments during a biodegradation period of 42 days.

---

## 2 Materials

### 2.1 Antibiotics

1. Tetracycline hydrochloride (Sigma: <http://www.sigmaaldrich.com>): prepare in 100% ethanol. Light sensitive. Store below 0°C. Stock concentration of 50 mg l<sup>-1</sup>.
2. Kanamycin sulphate (Sigma: <http://www.sigmaaldrich.com>): prepare in water. Store between 2 and 8°C. Stock concentration of 50 mg l<sup>-1</sup>.
3. Ampicillin sodium salt (Sigma: <http://www.sigmaaldrich.com>): prepare in water. Store between 2 and 8°C. Stock concentration of 30 and 14 mg l<sup>-1</sup>.

### 2.2 Bacteria Strain: Biosensor

### 2.3 Equipment

1. Spectrophotometer – Camspec M107
2. Shaking incubator – Gallenkamp
3. Jouan MR1822 centrifuge
4. Jade luminometer (Labtech International, Uckfield)
5. LB 962 CentroLIApc (Berhold Technologies) microtitre plate luminometer

## 2.4 Media

A great deal of the optimisation work in managing the bioreporters is to refine and optimise both the growth characteristics and media. Being able to grow a range of bioreporters on the same medium makes procedures simpler and easier to execute but this could be at the expense of sensitivity and responsiveness to target analytes. This has been the focus of two decades of work in Aberdeen and it is acknowledged that the adopted methods are often different to those in published manuscripts detailing construction.

### 2.4.1 *Luria-Bertani (Lennox) Growth Media*

These may be purchased from any supplier of common bacterial growth medium components or pre-prepared media. In our lab, we use products of Sigma: (<http://www.sigmaaldrich.com>) 10 g/l tryptone, 5 g/l yeast extract and 5 g/l NaCl prepared in water.

### 2.4.2 *Nutrient Broth Growth Media*

These may be purchased from any supplier of common bacterial growth medium components or pre-prepared media. In our lab, we use products of Sigma: (<http://www.sigmaaldrich.com>) 1 g/l D (+)-glucose, 15 g/l peptone, 6 g/l NaCl and 3 g/l yeast extract prepared in water.

To prepare solid media, Bacteriological Agar No. 1 (Oxoid) at the final concentration of 15 g/l was added to the solutions. Following the autoclaving, the media were supplemented with antibiotics (*see* Table 1).

## 2.5 *Non-Exhaustive Extraction Techniques*

Many authors are very critical about the excessive use of plastics in routine procedures for hydrocarbon analysis. Plastic can sorb key hydrocarbon fractions and components may also dissolve into aggressive solvents causing considerable artefacts. For this study, the objective is to achieve a high level of replication with a considerably large sample throughput and glass vials with Teflon-lined screw caps were used. The selected NEETs were:

1. Water (double reverse osmosis)
2. HPCD (<http://www.sigmaaldrich.com>) (25 mM). Dissolved in water
3. Methanol (100%)
4. Purified biosurfactants of *Bacillus licheniformis*. (Overnight cultures of the isolate were grown in nutrient broth for 16 h at 30°C and 180 rpm. The cells were harvested by centrifugation in 50 ml Corning centrifuge tubes at 2,500 × g (Jouan MR1822) and 4°C for 30 min. The supernatant was collected in sterile 500 ml Duran bottles and acidified to a pH of 2.0 ± 0.2 with 1 M HCl and then kept at 4°C overnight. The acidified supernatant was centrifuged at 2,500 × g and the supernatant discarded. The resultant pellet was re-suspended in sterile reverse osmosis water and the pH adjusted to 7.0 ± 0.2 with 1 M NaOH. The final volume of the extract

**Table 1**  
**Construction properties of bioreporters used in this study**

Bioreporter	Sensing analyte	Antibiotic ( $\mu\text{g l}^{-1}$ )	Induction time (min)	Optical density (550 nm) <sup>a</sup>	Linear defined control (mg/l) <sup>b</sup>	Construction references	Application references
<i>Pseudomonas putida</i> F1Tn5	Constitutive	NR	15–20	2.34	NA	[20]	[6]
<i>Escherichia coli</i> HB101 (pUCD607)	Constitutive	50 Amp	15–20	3.88	NA	[21]	[3, 17]
<i>P. fluorescens</i> OS8 (pDNDmprlux)	Phenolic compounds	30 Tet	240	1.64	10	[22]	[22]
<i>P. fluorescens</i> HK44 (pUTK21)	Naphthalene	14 Tet	60	4.69	15	[23]	[7]
<i>Escherichia coli</i> HMS174 (POS25)	Alkylbenzenes, alkanes, chlorinated solvents and naphthalene	50 Kan	120	1.25	5	[24]	[6]
<i>Pseudomonas putida</i> (F1) TVA8	BTEX	50 Kan	240	2.24	5	[25]	[5, 17]

*Amp* ampicillin, *Kan* kanamycin, *Tet* tetracycline, *NA* not applicable, *NR* not required

<sup>a</sup>This is the measure of O.D. of the preculture. The required dilutions are laboratory specific and cannot be translated meaningfully (approximate your values to two digits)

<sup>b</sup>Linear defined control is the range in which the response of the assay is linear

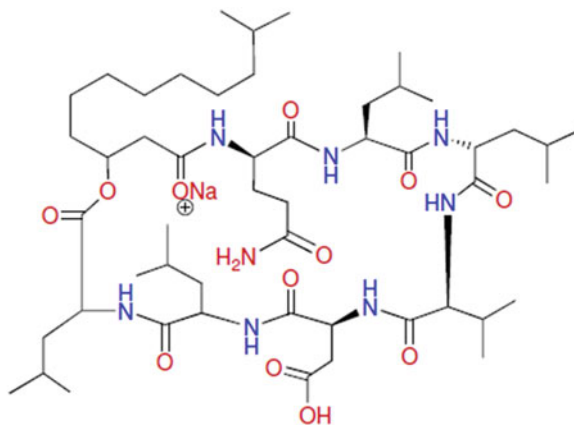


**Fig. 1** C<sub>13</sub>-lichenysin A. Chemical formula: C<sub>51</sub>H<sub>90</sub>N<sub>8</sub>NaO<sub>12</sub>. Exact mass: 1029.657. The actual composition of the biosurfactant used in the assay was confirmed to be a mixture of C<sub>13</sub>-lichenysin A, C<sub>14</sub>-lichenysin A and C<sub>15</sub>-lichenysin A

was 10% of the starting culture volume. Surface tension measurements of the extract were 27 mN m<sup>-1</sup>. Surfactin from Sigma-Aldrich was used as the calibration standard

To initially validate purity performance of the procedure and resultant analyte, high resolution mass spectral data were obtained from a Thermo Instruments ESI-MS system (LTQ XL/ LTQ Orbitrap Discovery) coupled to a Thermo Instruments HPLC system (Accela PDA detector, Accela PDA autosampler and Accela Pump). The following conditions were used: capillary voltage 45 V, capillary temperature 260°C, auxiliary gas flow rate 10–20 arbitrary units, sheath gas flow rate 40–50 arbitrary units, spray voltage 4.5 kV, mass range 100–2,000 amu (maximum resolution 30,000). HPLC separations were carried out using a Phenomenex reversed-phase (C18, 250 10 mm, L i.d.) column connected to an Agilent 1100 series binary pump and monitored using an Agilent photodiode array detector. Surfactin and C<sub>13</sub>-lichenysin A (Fig. 1) was identified in the exogenous biosurfactants extracted from the *Bacillus* species. Analysis by LC-MS confirmed that C<sub>13</sub>-lichenysin A is structurally similar to surfactin but with a higher surfactant power [26].

### 3 Methods

#### 3.1 Analytical Extraction

1. Weigh 0.25 g of soil and add 0.75 ml of the NEETs (see Sect. 2.5) in a microcentrifuge tube and vortexed for 4 min. This is routinely done as three independent replicates.
2. Place the mixture in an over-end-over shaker for 1 h.

3. Sonicate in a water bath for 15 min.
4. Place the mixture in an over-end-over shaker for a further 1 h.
5. Centrifuge at  $1,734 \times g$  for 30 s.
6. Remove supernatant carefully by pipetting into 4 ml glass vials to await assay. Perform a tenfold (v/v) dilution of the methanol extract with water before conducting the bioassay.

### 3.2 Lyophilization of Cells

Batch cultures of the biosensors were grown in 100 ml LB medium with appropriate antibiotics in 250 ml Erlenmeyer flasks. The biosensors were harvested at the mid-exponential phase. The concentration of biosensors in the media was estimated by OD and confirmed by plate count (CFU). The harvested biosensors were centrifuged in 50 ml Corning sterile centrifuge tubes at  $1,734 \times g$  at 4°C for 30 min (Jouan GR422 refrigerated floor centrifuge). Mist Dessicans was prepared by mixing freshly defrosted 100 ml horse serum (Oxoid) and 15 ml of 0.66 g of LB and 18 ml of 10 g glucose.

The supernatant was decanted and the pellets re-suspended in Mist Dessicans. Using a Distriman pipette, 1 ml aliquot of cell suspension was aseptically transferred to 5 ml glass freeze-drying vials; this was loosely closed with rubber stoppers and placed in liquid nitrogen for 90 min. The glass vials were then transferred to a freeze-dryer (Edwards Modulyo EF4 freeze-dryer) at pressure 0.1 mmHg, -70°C overnight (between 16 and 18 h). After freeze-drying, the stoppers were closed under vacuum and labeled before storing at -20°C. Quality control was confirmed by selecting 5 vials randomly for CFU and their bioluminescence response to Cu and Zn measured.

### 3.3 Activation of Bioreporter

1. Many of the constitutive bioreporters can be lyophilised and this allows resuscitation and activation with a high level of consistency. However some induced bioreporters perform poorly after preservation and are best used in batch cultures despite the associated time constraints that this imposes. Detailed growth curves will have been established for each bioreporter, for the given medium at defined growth condition. Light emission (on activation), colony forming units and optical density (550 nm) will have been established and confirmed.
2. A suspension of sensors can be generated from either growth of an overnight culture from a single colony [to the pre-defined optical density (as specified in Table 1)]. This will typically require a colony of the biosensor cultured on a media plate transferred to a 10 ml medium with 10 µl of specified antibiotic as required (Table 1). Incubate the culture using an orbital shaking incubator at 25°C [*P. putida* F1Tn5, *P. fluorescens* OS8 (pDNDmpflux), *P. fluorescens* HK44 (pUTK21) and *P. putida*

(F1) TVA8] or 30°C [*E. coli* HB101 (pUCD607) and *E. coli* HMS174 (POS25)] for 14–16 h (overnight), aseptically transfer 1 ml of the homogenised overnight culture into a 100 ml medium with 100 µl of antibiotic (when necessary) and incubate at the same temperature as the overnight.

Lyophilised *E. coli* HB101 (pUCD607) biosensors are resuscitated by re-suspending the cells in sterile 10 ml of 0.1 M KCl in a 30 ml Universal bottle, incubated for 1 h in a rotary incubator and then used for the bioassay. Lyophilised *P. putida* F1Tn5 was resuscitated by re-suspending the cells in sterile 10 ml of *Luria-Bertani* media for 1 h in a rotary incubator, cells are washed, pellet re-suspended sterile 10 ml of 0.1 M KCl in a 30 ml Universal bottle and then used for the bioassay.

### **3.4 Performing the Bioassay with the Bioreporter**

1. Both microtitre and single cuvettes can be used. The former has high throughput capabilities but can suffer both from edge effects, high surface area sorption and evaporation during longer incubation periods. Regardless of which device is used there should be one part of bioreporters cell suspension to nine parts of test medium. So for the microtitre plate reader, this is typically 20 µl of suspension to 180 µl of test solution. For the standard glass or polypropylene cuvette (with a maximum capacity of 4 ml), this would be 100 µl of cell suspension and 900 µl of test solution.
2. Positive (spiked) and negative controls should be established for each of the bioreporters. The negative control is deionised water. A second control, an environmental negative control, composed of either a non-contaminated soil extract or an osmotically matched sample is required. These are required for both constitutive and induced bioreporters. The induced bioreporters also require the use of a positive control, a concentration of a relevant analyte that causes a predictable amount of induction. In Table 1, the “linear defined control” is the concentration used for the positive control.
3. The suspension of bioreporters must be aliquoted into the microtitre plate or cuvette at a pre-defined time interval to allow equal exposure duration for all samples and controls.
4. Bioluminescence measurements are measured in relative light units (RLU).
5. The user can select to study the response of the bioreporters across a pre-defined temporal period should data processing capabilities be available.

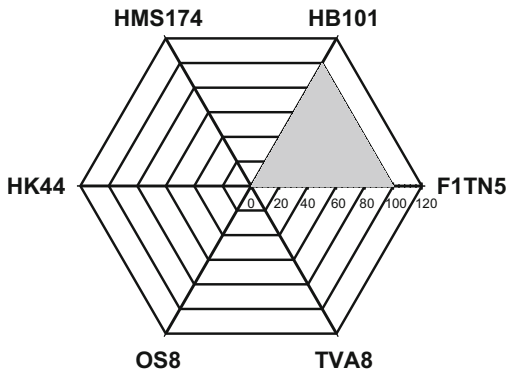
### **3.5 Calculation of Bioluminescence**

Bioluminescence of the constitutively marked bioreporters is calculated as a percentage of negative controls (reverse osmosis water with no pollutant or equivalent), while for inducible marked

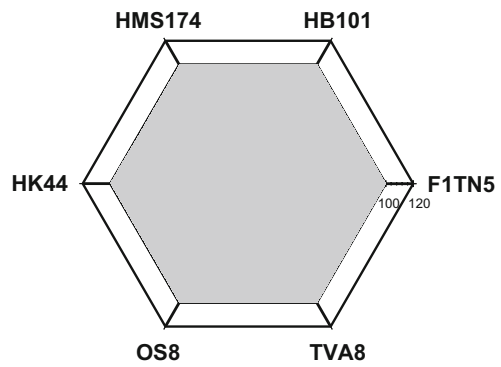
bioreporters, it is calculated as a percentage of positive control (the response of bioluminescence to the pre-defined concentration).

**3.6 Data Processing and Results**

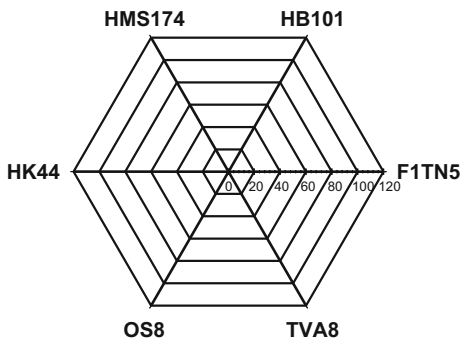
A key aspect of the use of bioreporters is that they generate a considerable amount of data. It is not uncommon to be overwhelmed with data if a microtitre plate has undergone dozens of readings and the data compilation seems unclear. To this end, it is essential that the user has an expectation of what the results may be and this is particularly important for induced bioreporters where the optimal time response may vary considerably between bioreporters. The use of web-graphs (Fig. 2) enables a rapid appraisal of the response of the different types of sensors allowing the user to rapidly view trend. In this example, using Libyan soils, only a single temporal response of the individual bioreporters has been recorded but it should be acknowledged that each of the four inducible responses varied by up to 90 min (Figs. 3 and 4).



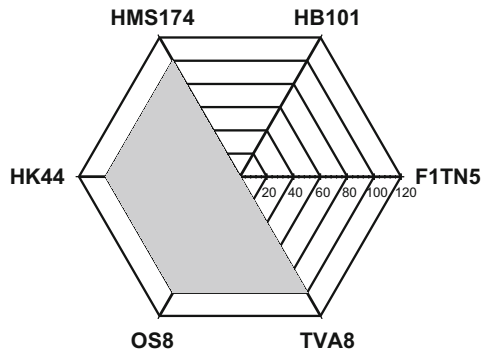
**Low toxicity and low induction**



**Low toxicity and high induction**



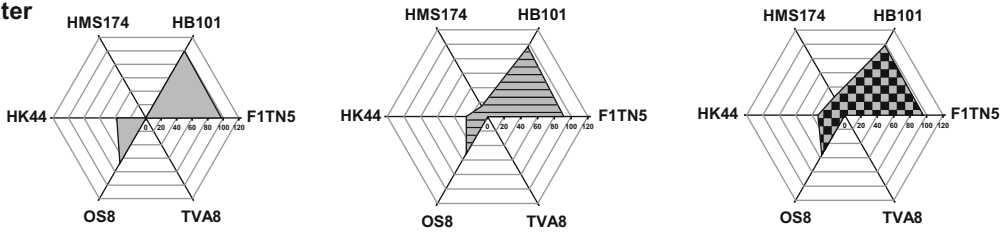
**High toxicity and low induction**



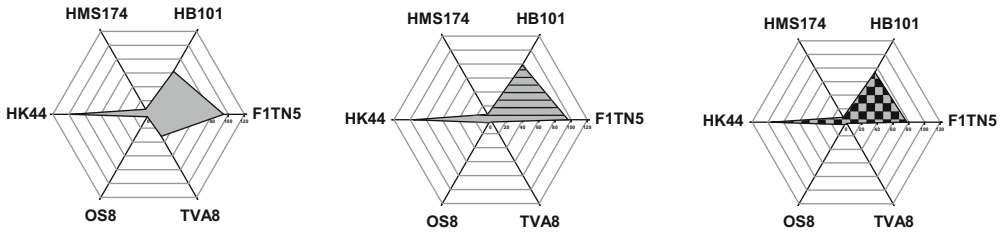
**High toxicity and high induction**

**Fig. 2** Web-graphs for data generated using multiple bioreporters: theoretical interpretation of data (percentage)

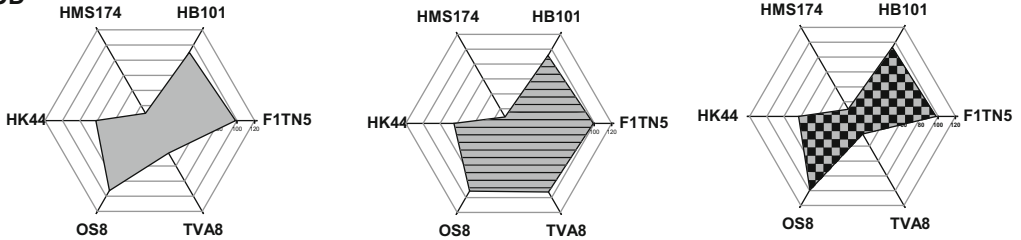
**Water**



**Methanol**



**HPCD**



**B. licheniformis**

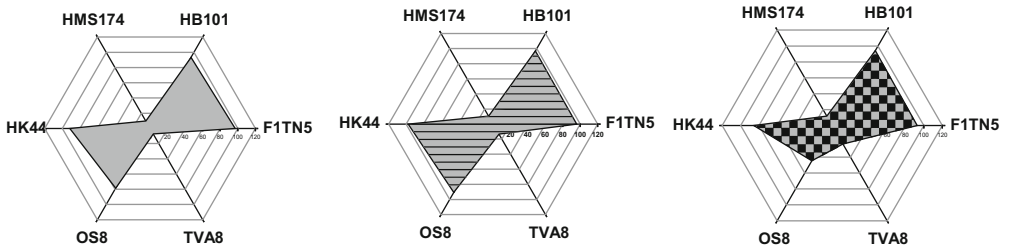


**Fig. 3** Response (percentage of control) of six different bioreporters to Libyan soils undergoing control treatment (only incubation) sampled at days 5 (*left column*), 20 (*central column*) and 42 (*right column*). The NEETs that were performed were water, methanol (with 1:10 dilution), HPCD and biosurfactants derived from *Bacillus licheniformis*

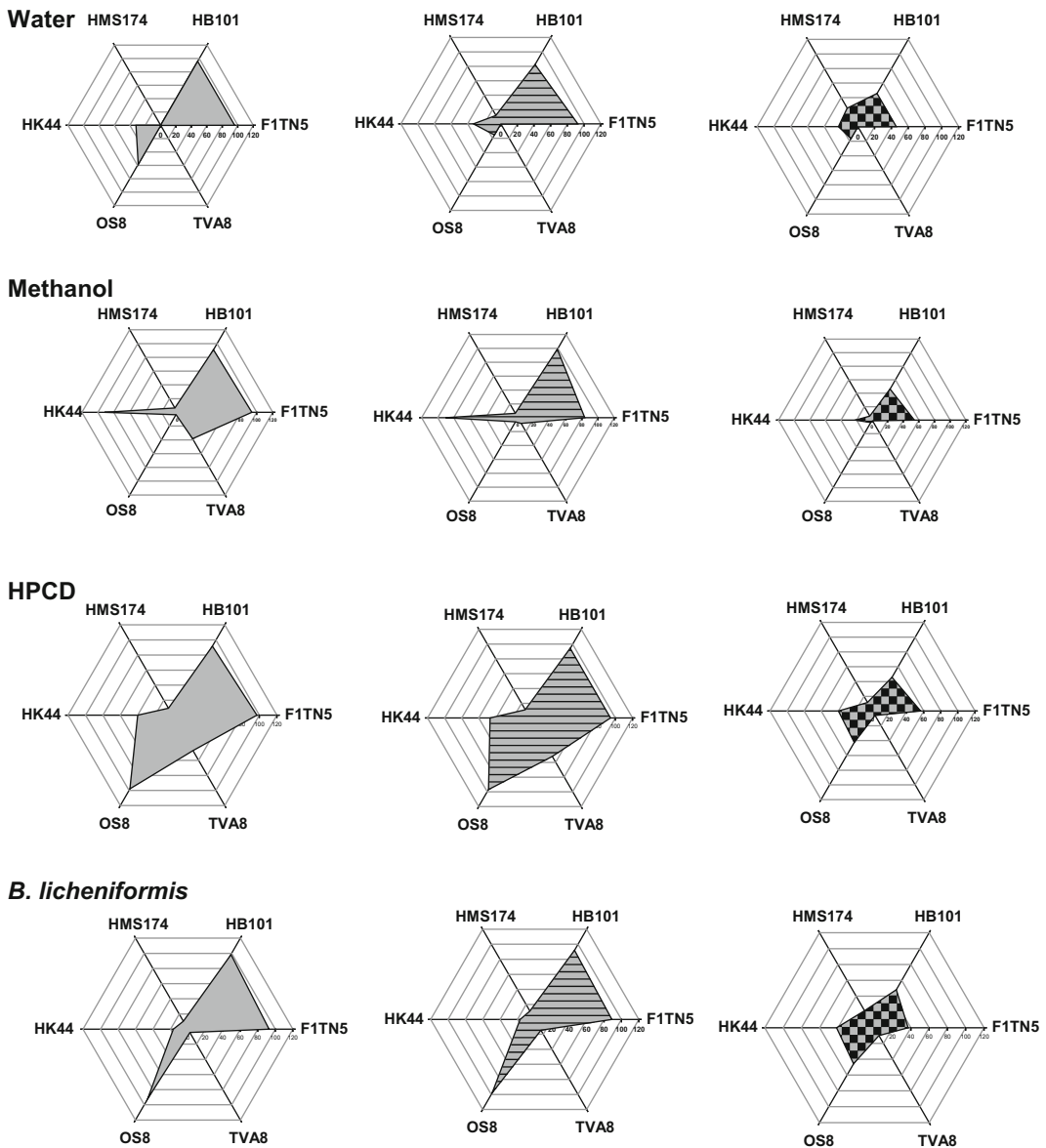


**Fig. 4** Response (percentage of control) of six different bioreporters to Libyan soils undergoing a treatment with nutrient amendments (for every 100 parts hydrocarbon present 10 parts of N (as ammonium nitrate) and 1 part P (as potassium orthophosphate) were added and sampled at days 5 (*left column*), 20 (*central column*) and 42 (*right column*). The NEETs that were performed were water, methanol (with 1:10 dilution), HPCD and biosurfactants derived from *B. licheniformis*

## References

- Xu TT, Close DM, Sayler GS, Ripp S (2013) Genetically modified whole-cell bioreporters for environmental assessment. *Ecol Indic* 28:125–141
- Dawson JJC, Godsiffe EJ, Thompson IP, Ralebitso-Senior TK, Killham KS, Paton GI (2007) Application of biological indicators to assess recovery of hydrocarbon impacted soils. *Soil Biol Biochem* 39(1):164–177
- Bundy JG, Campbell CD, Paton GI (2001) Comparison of response of six different luminescent bacterial bioassays to bioremediation of five contrasting oils. *J Environ Monit* 3 (4):404–410
- Tiensing T, Strachan N, Paton GI (2002) Evaluation of interactive toxicity of chlorophenols in water and soil using *lux*-marked biosensors. *J Environ Monit* 4(4):482–489
- Bhattacharyya J, Read D, Amos S, Dooley S, Killham K, Paton GI (2005) Biosensor-based diagnostics of contaminated groundwater: assessment and remediation strategy. *Environ Pollut* 134(3):485–492
- Diplock EE, Mardlin DP, Killham KS, Paton GI (2009) Predicting bioremediation of hydrocarbons: laboratory to field scale. *Environ Pollut* 157(6):1831–1840
- Patterson CJ, Semple KT, Paton GI (2004) Non-exhaustive extraction techniques (NEETs) for the prediction of naphthalene mineralisation in soil. *FEMS Microbiol Lett* 241(2):215–220
- Doick KJ, Dew NM, Semple KT (2005) Linking catabolism to cyclodextrin extractability: determination of the microbial availability of PAHs in soil. *Environ Sci Tech* 39 (22):8858–8864
- Paton GI, Reid BJ, Semple KT (2009) Application of a luminescence-based biosensor for assessing naphthalene biodegradation in soils from a manufactured gas plant. *Environ Pollut* 157(5):1643–1648
- Dandie CE, Weber J, Aler S, Adetutu EM, Ball AS, Juhasz AL (2010) Assessment of five bioaccessibility assays for predicting the efficacy of petroleum hydrocarbon biodegradation in aged contaminated soils. *Chemosphere* 81 (9):1061–1068
- Kilbane JJ II (1998) Extractability and subsequent biodegradation of PAHs from contaminated soil. *Water Air Soil Pollut* 104 (3–4):285–304
- Puglisi E, Patterson CJ, Paton GI (2003) Non-exhaustive extraction techniques (NEETs) for bioavailability assessment of organic hydrophobic compounds in soils. *J Agron* 23 (8):755–756
- Bernhardt C, Derz K, Kördel W, Terytze K (2013) Applicability of non-exhaustive extraction procedures with Tenax and HPCD. *J Hazard Mater* 261:711–717
- Oleszczuk P (2009) Application of three methods used for the evaluation of polycyclic aromatic hydrocarbons (PAHs) bioaccessibility for sewage sludge composting. *Bioresour Technol* 100(1):413–420
- Sinebe BS (2015) Application of microbial biosensors for groundwater and wastewater monitoring. PhD thesis, University of Aberdeen
- Bundy JG, Maciel H, Cronin MTD, Paton GI (2003) Limitations of a cosolvent for ecotoxicity testing of hydrophobic compounds. *Bull Environ Contam Toxicol* 70(1):1–8
- Dawson JJC, Iroegbu CO, Maciel H, Paton GI (2008) Application of luminescent biosensors for monitoring the degradation and toxicity of BTEX compounds in soils. *J Appl Microbiol* 104(1):141–151
- Sousa S, Duffy C, Weitz H, Glover LA, Bär E, Henkler R, Killham K (1998) Use of a *lux*-modified bacterial biosensor to identify constraints to bioremediation of btx-contaminated sites. *Environ Toxicol Chem* 17 (6):1039–1045
- van der Meer JR, Belkin S (2010) Where microbiology meets microengineering: design and applications of reporter bacteria. *Nat Rev Microbiol* 8:511–522
- Weitz HJ, Ritchie JM, Bailey DA, Horsburgh AM, Killham K, Glover LA (2001) Construction of a modified mini-Tn5 *luxCDABE* transposon for the development of bacterial biosensors for ecotoxicity testing. *FEMS Microbiol Lett* 197(2):159–165
- Ratray EA, Prosser JI, Killham K, Glover LA (1990) Luminescence-based nonextractive technique for in situ detection of *Escherichia coli* in soil. *Appl Environ Microbiol* 56 (11):3368–3374
- Leedjäv A, Ivask A, Virta M, Kahru A (2006) Analysis of bioavailable phenols from natural samples by recombinant luminescent bacterial sensors. *Chemosphere* 64(11):1910–1919
- King JMH, Digrazia PM, Applegate B, Burlage R, Sanseverino J, Dunbar P, Larimer F, Sayler GS (1990) Rapid, sensitive bioluminescent reporter technology for naphthalene exposure

- and biodegradation. *Science* 249 (4970):778–781
24. Selifonova OV, Eaton RW (1996) Use of an *ipb-lux* fusion to study regulation of the isopropylbenzene catabolism operon of *Pseudomonas putida* RE204 and to detect hydrophobic pollutants in the environment. *Appl Environ Microbiol* 62(3):778–783
25. Applegate BM, Kehrmeyer SR, Saylor GS (1998) A chromosomally based *tod-lux*-CDABE whole-cell reporter for benzene, toluene, ethylbenzene, and xylene (BTEX) sensing. *Appl Environ Microbiol* 64(7):2730–2735
26. Grangemard I, Wallach J, Maget-Dana R, Peypoux F (2001) Lichenysin: A more efficient cation chelator than surfactin. *Appl Biochem Biotechnol* 90(3):199–210

# Protocols for the Use of Gut Models to Study the Potential Contribution of the Gut Microbiota to Human Nutrition Through the Production of Short-Chain Fatty Acids

Andrew J McBain, Ruth Ledder, and Gavin Humphreys

## Abstract

The colonic microbiota influences human energy status through the metabolic activity of the taxonomically diverse prokaryotic residents that number up to  $10^{12}$  cells per gram. The principal means by which this happens is probably via short-chain fatty acids (SCFAs) (mainly acetate, propionate and butyrate), which are continually produced by fermentation of dietary fibre, absorbed through the colonic epithelium, transported via the hepatic portal vein to the liver and then converted to glucose and other lipids. SCFAs may also regulate appetite via G protein-coupled receptor (GPR43) activation and signalling. Since the colonic microbiota is inaccessible for routine investigation, microbiologists have used human faeces as a surrogate for intestinal contents, animal models and various in vitro systems. These range in complexity from batch cultures of isolated gut bacteria through defined consortia grown in batch and continuous culture to multistage continuous culture models that reproduce features of the proximal and distal colons. Such systems have been used to investigate the metabolism of gut bacteria for several decades and can be adopted for studies specifically focussing on SCFA production in the context of nutrition/obesity. SCFAs generated by bacterial fermentation can be analysed using gas chromatography, or more inclusive data can be obtained via metabonomics/metabolomics. Whilst culture and FISH provide a useful means of bacteriological analysis, next-generation sequencing (NGS) has facilitated major advances in our understanding of this complex ecosystem. The following protocol details the establishment of a three-stage continuous culture microcosm of the human colon and outlines options for bacteriological and metabolite analyses.

**Keywords:** Gas chromatography, Gut model, Short-chain fatty acid (SCFA) fermentation

---

## 1 Introduction

The human large bowel hosts a complex bacterial microbiota (or microbiome) estimated to comprise up to  $10^{12}$  cells per gram [1]. The functions of this bacterial community are diverse, and it is now believed to play a significant role in immune modulation (as reviewed in [2]), intestinal epithelial repair/development [3] and the breakdown of indigestible dietary substrates, such as resistant starches and fibre [4].

### **1.1 The Gut Microbiome and Obesity**

The deep sequencing of samples representative of the distal regions of the gut has shown ca. 90% of the bacterial phylotypes residing at this site are represented by two phyla: the Firmicutes and the Bacteroidetes [5]. Recent research indicates that an imbalance in these phyla may be associated with the development of metabolic disorders, in particular obesity, in which the gut microbiome of obese individuals has been shown to exhibit marked differences in bacterial composition when compared to lean individuals. Pioneering studies in genetically obese mice, carrying a mutation in the leptin gene (*ob/ob*), were the first to propose an obesity-associated microbiota, characterised by a reduction in Bacteroidetes abundance in comparison to lean kin (*ob/+* and *+/+*) [6]. Further studies suggest that this effect was transmissible, i.e. the transfer of gut microbiota from *ob/ob* mice to germ-free wild-type mice resulted in increased fat accumulation and subsequent development of the obesity phenotype [7]. In a separate investigation, differences in body composition were shown to correlate with increased intestinal short-chain fatty acid production in lean animals, in contrast to obese mice, which exhibited increased production of branched chain amino acids by the gut microbiota which principally results from bacterial protein degradation [8]. Surprisingly, the cohousing of obese and lean mice resulted in protection against obesity, possibly due to increased Bacteroidetes abundance in the *ob* gut microbiota following coprophagy [9].

The apparent association of gut microbiome composition and obesity has not been limited to animal studies. Similar observations have been made in human volunteers, in particular profiling studies of lean/obese twins, in which a shift in favour of Firmicutes abundance has been associated with the obese phenotype [10]. Similarly, in infants under 1 year of age, Kalliomäki et al. [11] reported that the composition of the gut microbiome was predictive for obesity. Despite purported associations between obesity and microbiome, the topic remains controversial, and the exact role of bacteria in the pathophysiology of metabolic disease, assuming this putative association is real, remains unclear. It has however been hypothesised that certain shifts in microbiome composition could be associated with an increased capacity to harvest energy from ingested food stuffs and that SCFA may regulate host metabolic physiology.

### **1.2 Bacterial Fermentation and Short-Chain Fatty Acid Production**

The fermentation of dietary fibre by the gut microbiome is a complex process that results in the production of SCFAs, predominantly acetate, propionate and butyrate. In individuals consuming a “Western” diet, these products have been estimated to account for up to 10% of the body’s total calorific daily requirement [12]. Butyrate is an essential source of energy for colonocytes, whilst propionate is principally involved in gluconeogenesis in hepatocytes [13]. SCFAs have also been shown to be ligands for G protein-coupled receptors (e.g. GPR41 as a receptor for butyrate and

isobutyrate) which occur in the distal regions of the gastrointestinal tract [14]. Importantly, GPR41 may be associated with leptin expression and subsequent effects on appetite mediated by anorectic hormone production [15]. In this study, GPR41-deficient mice were characterised by reduced expression of peptide YY and reduced gut motility [15]. Oral dosing with an inulin-propionate ester in overweight human volunteers ( $n = 60$ ) was shown to cause increased circulating levels of glucagon-like peptide 1 and peptide YY and reduced energy intake [16]. In the longer term (24 weeks), increasing colonic concentrations of this SCFA through dietary supplementation reportedly reduced weight gain and intrahepato-cellular lipid content. Interestingly, Frost et al. recently demonstrated intraperitoneal acetate to have similar effects on appetite suppression, potentially as a result of altered expression of regulatory neuropeptide profiles [17].

### **1.3 In Vitro Models for Gut Microbiome Investigations**

Investigations of the human gut microbiome are complicated by inaccessibility and ethical considerations associated with any direct means of access. Faeces are commonly used as a substitute for intestinal contents, but investigations into the effects of interventions on bacterial metabolism can be most readily achieved using in vitro models. Considerable knowledge has previously been gleaned through the use of such systems into activities including protein degradation [8], breakdown of complex carbohydrates [18], gas metabolism [19], biofilm formation [20, 21], bile acid metabolism and capacity to produce mutagens [22]. Such models can be as simple as batch incubations of faecal slurries in serum or Universal bottles through to various stirred systems and models that utilise pH control with continuous culture. Gut microbial processes can be modelled in a reductionist manner, utilising pure cultures and relatively simple media, which is often the best approach where the aim is to elucidate mechanisms, or alternatively, models can be used to broadly simulate the microbial and substrate complexity of the large bowel. Such microcosms are generally inoculated with freshly voided human faeces and utilise growth medium that is compositionally similar to digesta that enters the large bowel. All model systems have inherent advantages and disadvantages, and much of the challenge associated with their use is selecting the best model for a particular application (reviewed in [23]). For example, multiple Universal bottle batch cultures can run at the same time, enabling replication and the testing of multiple variables independently. However, since pH is uncontrolled, nutrients may be rapidly depleted (often in under 24 h) and metabolic products accumulate, so such systems are not compositionally stable over time and are probably less representative of the in situ conditions than continuous culture models.

Whilst mucous, sloughed cells and other potential bacterial growth substrates are endogenous to the colon, the majority of substrates enter the large bowel via the small intestine and then

transit through the lumen to the rectum where they are voided. From a microbial perspective, the colon therefore functions in a manner similar to a continuous culture system [24]. Thus, chemostats, which have proved so useful for general microbial physiology studies are also a useful tool for the gut microbiologist since steady states can be established, nutrient availability and growth rate can be controlled and pH can be varied. In order to reproduce the sequential depletion of nutrients that occurs with transit of digesta through the colon, however, multiple vessel continuous culture models have proven utility. Such systems are fed from a medium reservoir into the primary vessel which functions as an independent fermentation vessel and then, with continuous feeding, spent culture fluid transits into further vessel(s). The most common configuration for such systems involves three vessels [25, 26] (Fig. 1), but dual vessel systems have also been used to good effect [27] as have models comprising up to five vessels [26]. Investigations on gut contents from humans [28] have enabled the validity of such systems to be confirmed.

In this chapter we describe protocols associated with establishing a continuous culture model of the human large intestine and options for SCFA and NGS analyses.

---

## 2 Materials

### 2.1 *In Vitro* Gut Model

1. Fermentation vessels (chemostat type) with water jackets (Fig. 1a). Volume can be varied but commonly 280 ml (vessel 1), 280 ml (vessel 2) and 320 ml (vessel 3).
2. pH controllers 3× (Fig. 1b). For example, pH 1,000 pH system (New Brunswick Scientific, St. Albans, Herts., UK) coupled to CW711/EXT/250 pH electrodes (Thermo-Russell, Auchterarder, UK).
3. NaOH (1.0 M) for pH controllers (Fig. 1c).
4. Recirculating incubating water pump (Fig. 1d; e.g. Haake B3).
5. Peristaltic medium pump (Fig. 1e).
6. Stands for fermentation vessels (3×).
7. Peristaltic pump tubing.
8. Gas tubing for sparging gas.
9. Gas filters (0.2 µm).
10. Magnetic stirrers and stir bars (4×).
11. Medium (Fig. 1f) and waste (Fig. 1g) reservoirs (10 L) with drilled silicon rubber bungs.
12. Growth medium (Fig. 1h) (*see* Table 1).
13. Oxygen-free nitrogen gas.
14. Freshly voided human faeces (inoculum; *see* Note 2).

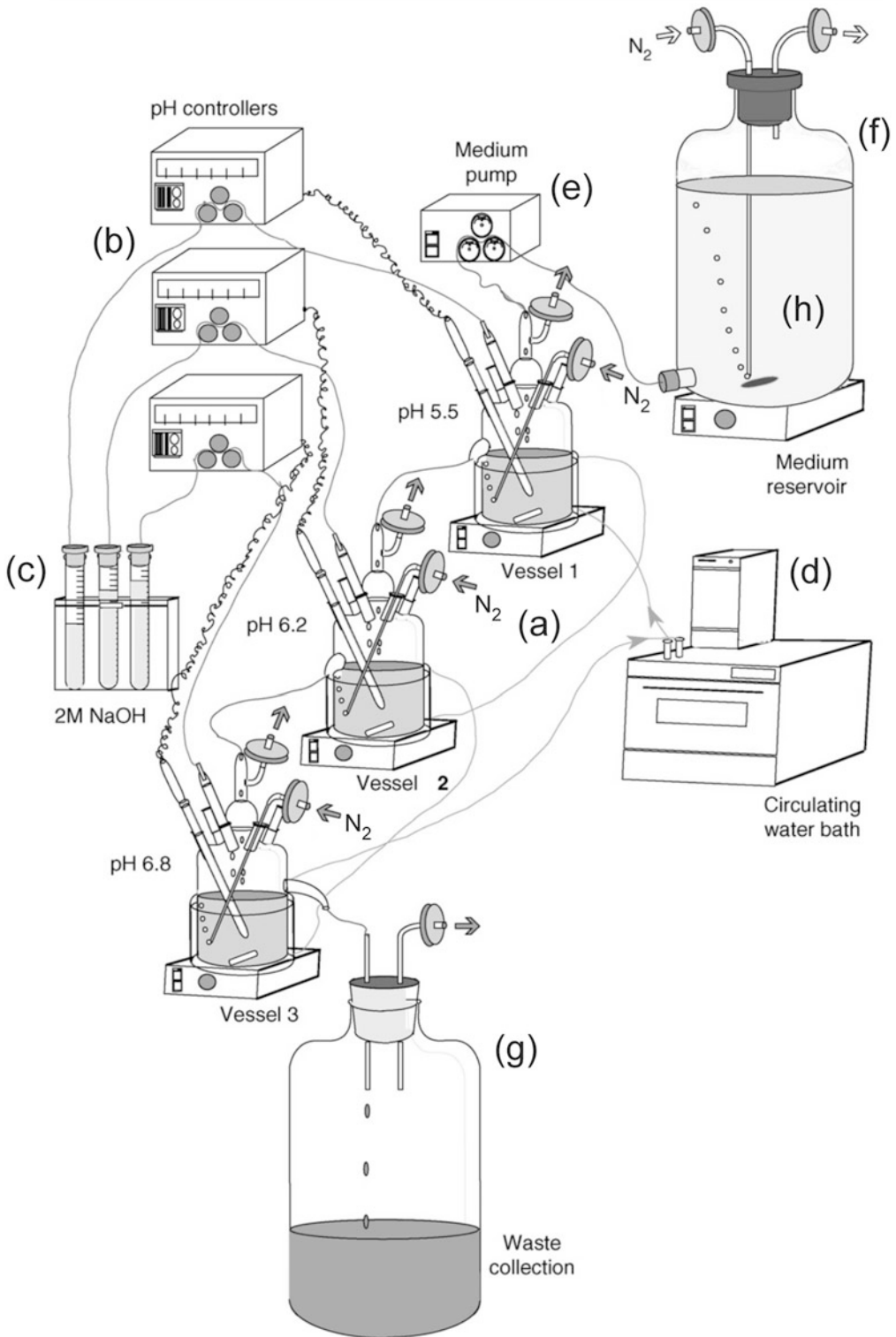


**Fig. 1** A three-stage continuous culture simulator of the human large intestine. Since all three vessels are inoculated with human faecal material and a large proportion of the bacterial diversity present establishes in

**Table 1**  
**Growth medium (see Note 1)**

Component	Quantity (g/L)
Pectin	0.6
Xylan	0.6
Arabinogalactan	0.6
Inulin	0.6
Lintner's starch	5.0
Guar gum	0.6
Casein	3.0
Peptone water	3.0
Yeast extract	2.5
Mucin (porcine type 111)	5.0
Tryptone	3.0
K <sub>2</sub> HPO <sub>4</sub>	2.0
NaHCO <sub>3</sub>	0.2
NaCl	4.5
MgSO <sub>4</sub> ·7H <sub>2</sub> O	0.5
CaCl <sub>2</sub> ·2H <sub>2</sub> O	0.45
Cysteine	0.40
FeSO <sub>4</sub> ·7H <sub>2</sub> O	0.005
Hemin	0.01
Bile salts	0.05

Composition of medium can be varied depending on requirements. pH should be between 6.8 and 7.0. Reagents can be obtained from Sigma-Aldrich (<http://www.sigmaaldrich.com>)

## 2.2 Eubacterial Profiling by Next-Generation Sequencing

### 2.2.1 Isolation and Quantification of Faecal Genomic DNA

1. Genomic DNA extraction kit – MoBio PowerSoil<sup>®</sup>-htp 96 well soil DNA isolation kit
2. FastPrep 120 cell disrupter system (Thermo Savant) or equivalent device
3. Nanodrop Spectrophotometer (Thermo Scientific) or Qubit<sup>®</sup> 2.0 or 3.0 fluorometer (Invitrogen)

**Fig. 1** (continued) the system, nutrients are depleted as medium transits through the system. Thus, vessel 1 is broadly analogous to the caecum (proximal colon), vessel 2 to the transverse colon and the final vessel to the distal colon/rectum. The types of substrate utilisation and pH gradients which establish in the model have been documented in samples taken from the human large bowel [28]. Details of parts labelled **a–h** are given in Sect. 2.1. Image courtesy of GT Macfarlane, University of Dundee, UK

### 2.2.2 Construction of MiSeq Sequencing Libraries

1. Standard desalting purified oligonucleotide primers containing additional Illumina adaptor overhang nucleotide sequences (italicised): F515 (5'-*TCG TCG GCA GCG TCA GAT GTG TAT AAG AGA CAG* GTG CCA GCM GCC GCG GTA A - 3') and R806 (5'-*GTC TCG TGG GCT CGG AGA TGT GTA TAA GAG ACA GGG* ACT ACH VGG GTW TCT AAT - 3') [29]. Prepare 5 µM primer stocks for use in PCR master mix using nuclease-free, PCR grade water (*see Note 3*).
2. MyTaq™ HS Mix DNA polymerase (BioLine).
3. Agencourt AMPure XP PCR purification kit (Beckman Coulter). Other methodologies, such as the QIAquick PCR purification kit (Qiagen), offer an alternative methodology with comparable DNA yields post clean-up.
4. Nextera XT Index kit (Illumina).
5. Qubit® 2.0 or 3.0 fluorometer (Invitrogen).
6. Illumina MiSeq system (Illumina, available commercially and via sequencing core facilities).

---

## 3 Methods

### 3.1 In Vitro Gut Model

1. Construct the model as outlined in Fig. 1 such that vessel 1 is placed above vessel 2 and vessel 2 above vessel 3. Connect the vessels with a minimal length of marprene tubing, the medium reservoir to vessel 1 and vessel 3 to the waste vessel. Add a magnetic stir bar to each fermentation vessel and to the empty medium reservoir.
2. Calibrate the pH controllers and connect to pH probes placed in each fermentation vessel and to the 1 M NaOH vessel. Set pH controllers such that vessels 1, 2 and 3 are maintained at pH 5.5, 6.2 and 6.8, respectively.
3. Sterilise the vessels and probes by autoclaving at 121°C for 15 min. Add sufficient distilled water to the vessels such that the pH probe tips are immersed during autoclaving.
4. Connect the oxygen-free nitrogen to the three fermentation vessels and the medium reservoirs through the air filters as indicated in Fig. 1.
5. Prepare the growth medium (normally 10 L) by adding the ingredients listed in Table 1 to ca. 9 L of deionised water in the 10 L medium reservoir vessel. Sterilise by autoclaving for 15 min. for volumes of less than 1 L. The holding time should be increased for larger volumes (*see Note 1*).

6. Taking precautions due to risks associated with hot medium, cool medium under a headspace of oxygen-free nitrogen (achieved by sparging at 2 L/h).
7. Connect medium via peristaltic tubing to the peristaltic pump and fill all three vessels to approximately half capacity with sterile growth medium.
8. Sparge (2 L/h) the fermentation vessels with oxygen-free nitrogen.
9. Switch on magnetic stirrers and incubating water pump to regulate temperature at 37°C.
10. Inoculate each fermentation vessel twice using 30 ml volumes of a 40% w/v slurry prepared from freshly voided faeces from a healthy donor with an interval of 48 h between (*see Note 4*).
11. For the first 2 days, maintain anaerobic conditions by continuous sparging with oxygen-free nitrogen (2 L/h). Thereafter, the system can be run without external gassing.
12. Pump sterile medium continuously into vessel 1, which sequentially feeds the other two vessels via a series of weirs, to give a total system retention time of between 30 and 60 h.
13. Dynamic states are achieved after several total system turnovers (approximately nine).
14. Remove samples at appropriate intervals depending on the experimental design using a sterile pipette, directly from the fermentation vessels.

### 3.2 SCFA/Metabolite Analyses

Samples should be collected directly from the fermenter vessels immediately spun down and supernatants should rapidly be frozen at  $-80^{\circ}\text{C}$  prior to analyses (pelleted cells can be separately processed and stored for other analyses). Submit samples to analytical facility to quantify SCFAs by LC–UV, as described in [30], NMR [31], GC [32] or GC–MS [33].

---

## 4 Eubacterial Profiling by Next-Generation Sequencing

### 4.1 Isolation and Quantification of Genomic DNA

1. Thoroughly clean all surfaces in order to remove potential sources of DNA contaminants (*see Note 5*).
2. Perform DNA extraction using the MoBio PowerSoil<sup>®</sup>-htp 96 well soil DNA isolation kit as described in DNA extraction protocol (Version 4\_13) of the Earth Microbiome Project (<http://www.earthmicrobiome.org>).
3. Quantify the DNA yield (ng/ $\mu\text{l}$ ) using a NanoDrop Spectrophotometer or Qubit fluorometer prior to preparation of PCR reaction mixtures.

## 4.2 MiSeq Sequencing Analysis

1. This methodology is based on the 16S metagenomics protocol described by Illumina (<http://support.illumina.com>) (*see Note 6*).
2. Set up a PCR reaction mixture stock so that each reaction comprises the following: 12.5 ng extracted DNA, 1  $\mu$ l forward and reverse primer stock and 25  $\mu$ l Hot Start ready mix taq. Adjust to a final volume of 50  $\mu$ l using PCR grade water.
3. Perform PCR amplification reactions in triplicate using the following programme settings: 95°C (3 min) followed by 30 cycles of 95°C (30 s), 55°C (30 s) and 72°C (30 s). The final cycle should incorporate a 5 min chain elongation step (72°C).
4. Pool PCR reactions by sample name and investigate the quality and quantity of amplified 16S rDNA through electrophoresis on a 0.8 % agarose gel. For large sample sizes, a random selection of 12 samples may be used.
5. Purify the amplified 16S rDNA using the AMPure XP PCR purification kit according to the manufacturer's protocol. Whilst this PCR clean-up methodology is recommended by Illumina, the QIAquick PCR purification kit (Qiagen) may be applied at this stage and offers comparable DNA yields for this amplicon length (<800 bp).
6. Attach Illumina sequencing adapters and dual indices using the Nextera XT Index kit (Illumina, Inc.) according to the manufacturer's instructions.
7. Perform a second PCR clean-up using the AMPure XP PCR purification kit. Perform the purification process according to the manufacturer's protocol.
8. Quantify the concentration of DNA per sample (ng/ $\mu$ l) using the Qubit fluorometer.
9. Proceed to follow the MiSeq 16S metagenomics protocol in order to perform library normalisation and sample pooling (*see Note 7*).
10. Sequence the purified samples using the MiSeq system by paired end sequencing. This system is typically available at any core or commercial sequencing facility.

## 4.3 Processing Next-Generation Sequencing Data

1. Sequencing results are typically provided in a compressed format (fastq.gz).
2. Analyse the metagenome files using a dedicated high-throughput software package. Numerous software packages are available for the interpretation of metagenome files. For the inexperienced user, MG-RAST (<https://metagenomics.anl.gov>) and the ribosomal database project (<https://pyro.cme.msu.edu>) offer online pipelines for the analysis of

sequencing data. Alternatively, for the experienced users, QIIME (Quantitative insights into microbial ecology) and MOTHUR are open-source software packages for the in-depth analysis of next-generation sequencing data (*see* **Note 8**).

---

## 5 Notes

1. Prepare in a 10 L vessel. Add 5 L deionised water and add ingredients sequentially with magnetic stirring, make to final volume and ensure that it is well mixed before autoclaving and that the mucin is fully dispersed in the growth medium.
2. The inoculum comprises slurries (40% [wt/vol]) prepared using faeces stored at room temperature and processed within 1 h of defecation by homogenising in a stomacher bag in anaerobic phosphate-buffered saline (0.1 M; pH 6.8). Slurries should then be passed through a 500 µm mesh sieve to remove large food particles and used immediately.
3. Illumina recommend standard desalting purification. Primers can be ordered from an online supplier of custom nucleic acids (e.g. Integrated DNA Technologies ([www.idtdna.com](http://www.idtdna.com))).
4. Human faecal samples will contain human tissue, and as such, ethical approval may be required from a local research ethics committee prior to sample collection. Further information is available from the health research authority (NHS) or institutional ethics committee.
5. Appropriate measures should be taken to reduce contamination of the samples with exogenous DNA which can lead to an overestimation of species diversity. DNA away<sup>TM</sup> surface decontaminant or 10% bleach solution is suitable for this purpose.
6. The protocol outlined describes use of primers specific for the V4 region of the 16S rRNA gene, whilst the Illumina protocol generates a greater amplicon length, targeting V3-V4. Despite compromising on amplicon length, amplification of the V4 region offers greater overlap between R1 and R2 sequences and reduced error when performing the merging of mate pairs.
7. A total of 96 samples can be multiplexed per MiSeq run using this methodology. However, this is at the discretion of the user and should be assessed following validation runs.
8. Extensive tutorials for QIIME ([qiime.org/tutorials/index.html](http://qiime.org/tutorials/index.html)) and MOTHUR ([http://www.mothur.org/wiki/Main\\_Page](http://www.mothur.org/wiki/Main_Page)) are available for these software packages from the developer's website.

## Acknowledgement

AJM gratefully acknowledges Professor George Tennant Macfarlane (1958–2015) for permission to use his designs and diagrams in this article, for inspiration and insight and for his significant contributions to intestinal microbiology over more than 30 years.

## References

1. Leser TD, Molbak L (2009) Better living through microbial action: the benefits of the mammalian gastrointestinal microbiota on the host. *Environ Microbiol* 11(9):2194–2206. doi:[10.1111/j.1462-2920.2009.01941.x](https://doi.org/10.1111/j.1462-2920.2009.01941.x)
2. Kau AL, Ahern PP, Griffin NW, Goodman AL, Gordon JI (2011) Human nutrition, the gut microbiome and the immune system. *Nature* 474:327–336. doi:[10.1038/nature10213](https://doi.org/10.1038/nature10213)
3. Stappenbeck TS, Hooper LV, Gordon JI (2002) Developmental regulation of intestinal angiogenesis by indigenous microbes via Paneth cells. *Proc Natl Acad Sci U S A* 99:15451–15455. doi:[10.1073/pnas.202604299202604299](https://doi.org/10.1073/pnas.202604299202604299)
4. Macfarlane GT, Englyst HN (1986) Starch utilization by the human large intestinal microflora. *J Appl Bacteriol* 60(3):195–201
5. Arumugam M, Raes J, Pelletier E, Le Paslier D, Yamada T, Mende DR, Fernandes GR, Tap J, Bruls T, Batto JM, Bertalan M, Borruel N, Casellas F, Fernandez L, Gautier L, Hansen T, Hattori M, Hayashi T, Kleerebezem M, Kurokawa K, Leclerc M, Levenez F, Manichanh C, Nielsen HB, Nielsen T, Pons N, Poulain J, Qin J, Sicheritz-Ponten T, Tims S, Torrents D, Ugarte E, Zoetendal EG, Wang J, Guarner F, Pedersen O, de Vos WM, Brunak S, Dore J, Meta HITC, Antolin M, Artiguenave F, Blottiere HM, Almeida M, Brechot C, Cara C, Chervaux C, Cultrone A, Delorme C, Denariuz G, Dervyn R, Foerstner KU, Friss C, van de Guchte M, Guedon E, Haimet F, Huber W, van Hylckama-Vlieg J, Jamet A, Juste C, Kaci G, Knol J, Lakhdari O, Layec S, Le Roux K, Maguin E, Merieux A, Melo Minardi R, M'Rini C, Muller J, Oozeer R, Parkhill J, Renault P, Rescigno M, Sanchez N, Sunagawa S, Torrejon A, Turner K, Vandemeulebrouck G, Varela E, Winogradsky Y, Zeller G, Weisenbach J, Ehrlich SD, Bork P (2011) Enterotypes of the human gut microbiome. *Nature* 473(7346):174–180. doi:[10.1038/nature09944](https://doi.org/10.1038/nature09944)
6. Ley RE, Backhed F, Turnbaugh P, Lozupone CA, Knight RD, Gordon JI (2005) Obesity alters gut microbial ecology. *Proc Natl Acad Sci U S A* 102(31):11070–11075. doi:[10.1073/pnas.0504978102](https://doi.org/10.1073/pnas.0504978102)
7. Turnbaugh PJ, Ley RE, Mahowald MA, Magrini V, Mardis ER, Gordon JI (2006) An obesity-associated gut microbiome with increased capacity for energy harvest. *Nature* 444(7122):1027–1031. doi:[10.1038/nature05414](https://doi.org/10.1038/nature05414)
8. Macfarlane GT, Cummings JH, Allison C (1986) Protein degradation by human intestinal bacteria. *J Gen Microbiol* 132(6):1647–1656
9. Ridaura VK, Faith JJ, Rey FE, Cheng J, Duncan AE, Kau AL, Griffin NW, Lombard V, Henrissat B, Bain JR, Muehlbauer MJ, Ilkayeva O, Semenkovich CF, Funai K, Hayashi DK, Lyle BJ, Martini MC, Ursell LK, Clemente JC, Van Treuren W, Walters WA, Knight R, Newgard CB, Heath AC, Gordon JI (2013) Gut microbiota from twins discordant for obesity modulate metabolism in mice. *Science* 341(6150):1241214. doi:[10.1126/science.1241214](https://doi.org/10.1126/science.1241214)
10. Turnbaugh PJ, Hamady M, Yatsunenkov T, Cantarel BL, Duncan A, Ley RE, Sogin ML, Jones WJ, Roe BA, Affourtit JP, Egholm M, Henrissat B, Heath AC, Knight R, Gordon JI (2009) A core gut microbiome in obese and lean twins. *Nature* 457(7228):480–484. doi:[10.1038/nature07540](https://doi.org/10.1038/nature07540)
11. Kalliomäki M, Collado MC, Salminen S, Isolauri E (2008) Early differences in fecal microbiota composition in children may predict overweight. *Am J Clin Nutr* 87(3):534–538
12. Bergman EN (1990) Energy contributions of volatile fatty acids from the gastrointestinal tract in various species. *Physiol Rev* 70(2):567–590
13. Bloemen JG, Venema K, van de Poll MC, Olde Damink SW, Buurman WA, Dejong CH

- (2009) Short chain fatty acids exchange across the gut and liver in humans measured at surgery. *Clin Nutr* 28(6):657–661. doi:[10.1016/j.clnu.2009.05.011](https://doi.org/10.1016/j.clnu.2009.05.011)
14. Le Poul E, Loison C, Struyf S, Springael JY, Lannoy V, Decobecq ME, Brezillon S, Dupriez V, Vassart G, Van Damme J, Parmentier M, Detheux M (2003) Functional characterization of human receptors for short chain fatty acids and their role in polymorphonuclear cell activation. *J Biol Chem* 278(28):25481–25489. doi:[10.1074/jbc.M301403200](https://doi.org/10.1074/jbc.M301403200)
  15. Engelstoft MS, Egerod KL, Holst B, Schwartz TW (2008) A gut feeling for obesity: 7TM sensors on enteroendocrine cells. *Cell Metab* 8(6):447–449. doi:[10.1016/j.cmet.2008.11.004](https://doi.org/10.1016/j.cmet.2008.11.004)
  16. Chambers ES, Viardot A, Psichas A, Morrison DJ, Murphy KG, Zac-Varghese SE, MacDougall K, Preston T, Tedford C, Finlayson GS, Blundell JE, Bell JD, Thomas EL, Mt-Isa S, Ashby D, Gibson GR, Kolida S, Dhillo WS, Bloom SR, Morley W, Clegg S, Frost G (2014) Effects of targeted delivery of propionate to the human colon on appetite regulation, body weight maintenance and adiposity in overweight adults. *Gut*. doi:[10.1136/gutjnl-2014-307913](https://doi.org/10.1136/gutjnl-2014-307913)
  17. Frost G, Sleeth ML, Sahuri-Arisoylu M, Lizarbe B, Cerdan S, Brody L, Anastasovska J, Ghourab S, Hankir M, Zhang S, Carling D, Swann JR, Gibson G, Viardot A, Morrison D, Louise Thomas E, Bell JD (2014) The short-chain fatty acid acetate reduces appetite via a central homeostatic mechanism. *Nat Commun* 5:3611. doi:[10.1038/ncomms4611](https://doi.org/10.1038/ncomms4611)
  18. Degan BA, Macfarlane S, Quigley ME, Macfarlane GT (1997) Starch utilization by *Bacteroides ovatus* isolated from the human large intestine. *Curr Microbiol* 34(5):290–296
  19. Gibson GR, Cummings JH, Macfarlane GT (1988) Competition for hydrogen between sulphate-reducing bacteria and methanogenic bacteria from the human large intestine. *J Appl Bacteriol* 65(3):241–247
  20. Macfarlane S, McBain AJ, Macfarlane GT (1997) Consequences of biofilm and sessile growth in the large intestine. *Adv Dent Res* 11(1):59–68
  21. Macfarlane S, Woodmansey EJ, Macfarlane GT (2005) Colonization of mucin by human intestinal bacteria and establishment of biofilm communities in a two-stage continuous culture system. *Appl Environ Microbiol* 71(11):7483–7492. doi:[10.1128/AEM.71.11.7483-7492.2005](https://doi.org/10.1128/AEM.71.11.7483-7492.2005)
  22. McBain AJ, Macfarlane GT (2001) Modulation of genotoxic enzyme activities by non-digestible oligosaccharide metabolism in in-vitro human gut bacterial ecosystems. *J Med Microbiol* 50(9):833–842
  23. McBain AJ (2009) Chapter 4: in vitro biofilm models: an overview. *Adv Appl Microbiol* 69:99–132
  24. Macfarlane GT, Macfarlane S (2007) Models for intestinal fermentation: association between food components, delivery systems, bioavailability and functional interactions in the gut. *Curr Opin Biotechnol* 18(2):156–162. doi:[10.1016/j.copbio.2007.01.011](https://doi.org/10.1016/j.copbio.2007.01.011)
  25. Gibson GR, Cummings JH, Macfarlane GT (1988) Use of a three-stage continuous culture system to study the effect of mucin on dissimilatory sulfate reduction and methanogenesis by mixed populations of human gut bacteria. *Appl Environ Microbiol* 54(11):2750–2755
  26. Allison C, McFarlan C, Macfarlane GT (1989) Studies on mixed populations of human intestinal bacteria grown in single-stage and multi-stage continuous culture systems. *Appl Environ Microbiol* 55(3):672–678
  27. Macfarlane GT, Gibson GR (1991) Co-utilization of polymerized carbon sources by *Bacteroides ovatus* grown in a two-stage continuous culture system. *Appl Environ Microbiol* 57(1):1–6
  28. Macfarlane GT, Gibson GR, Cummings JH (1992) Comparison of fermentation reactions in different regions of the human colon. *J Appl Bacteriol* 72(1):57–64
  29. Caporaso JG, Lauber CL, Walters WA, Berg-Lyons D, Lozupone CA, Turnbaugh PJ, Fierer N, Knight R (2011) Global patterns of 16S rRNA diversity at a depth of millions of sequences per sample. *Proc Natl Acad Sci U S A* 108(Suppl 1):4516–4522. doi:[10.1073/pnas.1000080107](https://doi.org/10.1073/pnas.1000080107)
  30. Huda-Faujan N, Abdulmir AS, Fatimah AB, Anas OM, Shuhaimi M, Yazid AM, Loong YY (2010) The impact of the level of the intestinal short chain Fatty acids in inflammatory bowel disease patients versus healthy subjects. *Open Biochem J* 4:53–58
  31. Furusawa Y, Obata Y, Fukuda S, Endo TA, Nakato G, Takahashi D, Nakanishi Y, Uetake C, Kato K, Kato T, Takahashi M, Fukuda NN, Murakami S, Miyachi E, Hino S, Atarashi K, Onawa S, Fujimura Y, Lockett T, Clarke JM, Topping DL, Tomita M, Hori S, Ohara O, Morita T, Koseki H, Kikuchi J, Honda K, Hase K, Ohno H (2013) Commensal

- microbe-derived butyrate induces the differentiation of colonic regulatory T cells. *Nature* 504(7480):446–450. doi:[10.1038/nature12721](https://doi.org/10.1038/nature12721)
32. Bourriaud C, Robins RJ, Martin L, Kozlowski F, Tenailleau E, Cherbut C, Michel C (2005) Lactate is mainly fermented to butyrate by human intestinal microfloras but inter-individual variation is evident. *J Appl Microbiol* 99(1):201–212. doi:[10.1111/j.1365-2672.2005.02605.x](https://doi.org/10.1111/j.1365-2672.2005.02605.x)
33. Zheng X, Qiu Y, Zhong W, Baxter S, Su M, Li Q, Xie G, Ore BM, Qiao S, Spencer MD, Zeisel SH, Zhou Z, Zhao A, Jia W (2013) A targeted metabolomic protocol for short-chain fatty acids and branched-chain amino acids. *Metabolomics* 9(4):818–827. doi:[10.1007/s11306-013-0500-6](https://doi.org/10.1007/s11306-013-0500-6)